

Copyright is owned by the Author of the thesis. Permission is given for a copy to be downloaded by an individual for the purpose of research and private study only. The thesis may not be reproduced elsewhere without the permission of the Author.

Structural Aspects of β -Lactoglobulin during Self-assembly into Amyloid-like Fibrils

A thesis presented in partial fulfilment of the
requirements for the degree of

Doctor of Philosophy
in
Food Technology

at
Riddet Institute, Massey University,
Palmerston North
New Zealand.

Anant Chandrakant Dave

2014



Abstract

This study explores the structural characteristics of β -lactoglobulin (β -Lg) during its self-assembly into long amyloid-like fibrils on heating at low pH and low ionic strength. β -Lg (1%, w/v) was heated at 80°C, pH 2 and low ionic strength and the different processes occurring during self-assembly were characterized using a variety of techniques including circular dichroism spectroscopy, sodium dodecyl sulfate polyacrylamide gel electrophoresis, and mass spectrometry.

The results of this study indicate that fibril formation from β -Lg self-assembly consists of four processes: 1) protein unfolding; 2) heat- and acid- induced protein hydrolysis 3) nuclei formation and; 4) growth of nuclei into mature fibrils by peptide self-assembly. It was found that the heat-induced unfolding of β -Lg and its acid hydrolysis promoted self-assembly by removing structural constraints and generating assembly-capable peptides. The peptides from the N-terminal region (1-53) of β -Lg were found to play an important role during nucleation and may form the core of the fibrils. The characterization of fibril composition strongly indicated the presence of disulfide bonding in fibrils and the native disulfide bond Cys66-Cys160 in β -Lg appeared to be conserved during fibril formation.

The substitution of amino acid residues in β -Lg variants A, B and C did not significantly affect the kinetics of different self-assembly processes. The fibrils from β -Lg A, B and C had similar morphology, but were slightly different in their peptide compositions. The latter may be explained on the basis of sites of genetic substitutions, in particular, the Asp64 of β -Lg A that is Gly in variants B and C. In comparison, glucosylation and lactosylation of β -Lg strongly inhibited fibril formation primarily by inhibition of peptide self-assembly due to the steric conformational

Abstract

restrictions. The inhibitory effect of glycation varied with the type of sugar and the degree of glycation. Lactosylation produced a stronger effect than glucosylation, but glycation with either sugar did not appear to have any effect on the morphology of fibrils.

The modification of the aqueous phase composition by glycerol and sorbitol (0-50 % w/v) greatly decreased the rate of β -Lg self-assembly and the effect of glycerol and sorbitol on β -Lg self-assembly was concentration-dependent. Sorbitol inhibited the self-assembly by stabilizing β -Lg against unfolding and acid-hydrolysis, resulting in fewer fibril-forming peptides, whereas glycerol inhibited peptide self-assembly without affecting unfolding and acid-hydrolysis. Although, both polyols increased the viscosity of the solutions, viscosity did not affect the self-assembly of peptides, indicating that, under these conditions, the self-assembly was not diffusion-limited.

The effects of β -casein on β -Lg self-assembly were investigated by heating β -Lg- β -casein mixtures (molar ratios 1:0.0625 to 1:1). Heating under fibril-forming conditions resulted in acid hydrolysis of both proteins at approximately equal rate. β -Casein produced a small but consistent effect in inhibiting β -Lg self-assembly in heated β -Lg- β -casein mixtures. The transmission electron microscopy images of solutions showed irregular, coiled and ribbon-like structures co-existing with the β -Lg fibrils. These aggregates were absent in respective heated control samples of either protein indicating that β -Lg assembly-competent peptides have alternate competing pathway during self-assembly. The limited effect of β -casein on β -Lg self-assembly may be explained by the aggregation of β -casein peptides by a separate alternate pathway which competed with their interaction with β -Lg peptides.

Overall, the findings of this study have advanced our understanding of the mechanisms of self-assembly of globular proteins and provided insights into the ways to decouple self-assembly processes. This may help to design protocols for the control of globular protein self-assembly and extend the functionality and applications of protein fibrils.

Acknowledgements

The journey of my Ph.D. studies has been extremely special for me since pursuing research was a long-held dream that I shared with many people. This work has come to be from the contribution of time, resources and expertise of a number of people who have placed their faith in me and allowed me to pursue my dream. I express my deepest sense of gratitude to everyone who has contributed to the successful completion of this work.

It is with great pleasure that I express my immense gratitude to Distinguished Professor Harjinder Singh for supervising my research. His constant guidance and encouragement have been a huge source of motivation and inspired me to work harder. I appreciate the opportunity to study at the Riddet Institute, and the freedom to explore my own ideas.

I thank Dr. Simon Loveday, my co-supervisor, for introducing me to research, in helping me take my first steps and inspiring me all through this journey. His patience, especially during my writing phase has been a learning that I will be carrying with me wherever I go.

I also wish to extend my deepest and sincerest thanks to my co-supervisor, Dr. Skelte Anema (Fonterra Research and Development Centre, Palmerston North). His critical evaluation, advice and suggestions for my work during the planning, execution and writing phases of my research have been instrumental in the success of my research. His continued support and encouragement have been one of the main driving forces for maintaining the standard of my work.

Acknowledgements

I thank Professor Geoffrey Jameson, Institute of Fundamental Sciences (IFS), Massey University for his useful advice and guidance for protein unfolding studies. His valuable critical suggestions for my studies and assistance in interpreting and summarising the findings of the studies in the publications have been invaluable. I acknowledge his earnest interest in my wellbeing and in helping me to evolve as a researcher. I also thank Dr. Gillian Norris (IFS) for her valuable guidance in the peptide sequencing studies. Working at her laboratory has personally helped me immensely and added a completely different dimension to my work. I am grateful to Mr. Trevor Loo for the stimulating discussions on proteomics research and his useful advice regarding the protein unfolding and mass spectrometry studies. Working with him has helped me immensely in developing and sharpening my general laboratory skills.

I also wish to acknowledge the following specific contributions from:

- Nutrition laboratory Institute of Food, Nutrition and Human Health, Massey University for proximate analysis of the protein used in the study.
- Mr. Mallesh Peram for introducing and familiarizing me with the electrophoresis techniques.
- Ms. Leiza Turnbull for lyophilisation of all my samples.
- Dr. Simon Loveday for writing the SigmaPlot software codes for curve fitting.
- Dr. Skelte Anema for providing the purified genetic variants of the protein β -lactoglobulin.
- Dr. Geoff Jones (IFS) for his valuable guidance with statistical analysis.
- Mr. Doug Hopcroft and Ms. Jordan Taylor for their assistance with transmission electron microscopy of samples.

Acknowledgements

- Mr. Trevor Loo (IFS) and Ms. Diana Carne (Centre for Protein Research, University of Otago) for running the samples on the mass spectrometer and analysis of the mass spectrometry data.
- Mr. Manu Singh for his skillful assistance in standardization of protocols for circular dichroism spectroscopy and mass spectrometry.
- The referees of my peer-reviewed publications for providing critical feedback and appreciating my work in the submitted manuscripts.
- Dr. Gareth Rowlands (Institute of Fundamental Sciences, Massey University, Palmersto North, New Zealand) and the staff of The Graduate Research School, Massey University, Palmerston North, New Zealand, for facilitating my thesis examination process.
- Prof. Edward Allen Foegeding (North Carolina State University, USA), Dr. Nigel Larsen (Plant & Food Research, Lincoln, New Zealand) and Dr. Alistair Carr (Institute of Food, Nutrition and Human Health, Massey University, Palmersto North, New Zealand) for reviewing the work in this thesis and being my PhD thesis examiners.

I wish to acknowledge the financial support provided by the Riddet Institute, in the form of Riddet Institute Scholarship and travel grant for attending international conference in Australia. I also thank Fonterra Cooperative Ltd. and the New Zealand Foundation for Research Science and Technology (contract number DRIX0701) for funding my research.

I am grateful to Distinguished Professor Paul Moughan for his concern for my wellbeing and constant encouragement throughout my research. I gratefully acknowledge the contribution of the Riddet Institute administration and information

Acknowledgements

technology team who have worked tirelessly to facilitate my research. A big thank you to Ms. Ansley Te Hiwi, Ms. Terri Palmer, Ms. Felicia Stibbards, Ms. Paula McCool, Mr. John Henley-King and Mr. Matt Levin. I also wish to thank Ms. Willi Stevenson-Wright and Dr. Shantanu Das, who were with the Riddet Institute for a major duration of this work, for their constant encouragement and motivation.

I thank the Riddet Institute researchers Dr. Shane Rutherford, Dr. Jaspreet Singh, Dr. Carlos Montaya, Dr. Aiqien Ye, Dr. Ashling Ellis, Dr. Lovedeep Kaur, Dr Sharon Henare and Dr. Xiang-Qian Zhu for promoting a stimulating atmosphere that has greatly facilitated the flow of ideas during my research work. The 'epicentre' of the experimental work in this research was the Riddet Institute laboratory. I wish to extend my heartfelt thanks to Ms. Janiene Gilliland and Mr. Chris Hall for maintaining the 'epicentre'. I acknowledge the constant support from the Riddet Institute staff including, Mr. Russell Richardson, Ms. Chanapha Sawatdeenaruenat, Ms. Namrata Taneja, Mr. Amit Taneja and Mr Jian Cui. Their support and encouragement helped me to maintain a positive attitude when the experiments did not work as planned.

I am equally thankful to all my past and present lab-mates with whom I have spent several hours here. My heartfelt thanks to Mr. Mallesh Peram, Mr. Qing Guo, Mr. Vikas Mittal, Ms. Lakshmi Dave, Ms. Natascha Stroebinger, Mr. Shakti Singh and Mr. Devastotra Poddar for creating a conducive, friendly atmosphere that made working in the lab all the more enjoyable.

I acknowledge the emotional support of close friends who have contributed to this work by facilitating my stay in Palmerston North. Thanks to all my friends including Mr. Sebastian Riedle, Mr. Rajesh Deshpande, Mr. Pankaj Sharma, Ms. Nancy Taneja, Ms. Jinita Das, Ms. Wibha Desai and the members of the Indian Gujarati community

Acknowledgements

in Palmerston North, for making my stay in Palmerston North comfortable and for being there when the pangs of going back home struck! I wish to acknowledge the constant support and encouragement from Dr. Anwesha Sarkar (University of Leeds, Leeds, UK). Over the the last decade she has been a source of constant motivation and supported me like an elder sister. I thank her for all the valuable advice she has offered and, in particular, for inspiring me to embark on this journey.

This endeavour could only be successful because of the unconditional love and constant support from my family. I acknowledge the endless support from my father Dr. Chandrakant J. Dave, my mother Mrs. Hemlata Dave, my sister Ms. Priyanka Dave and my parents-in-law Dr. A.V.R.L Narasimhacharya and Mrs. Vani Acharya who have shared my dream, stood like strong pillars providing a solid emotional foundation and inspired me to complete my research. I thank them for their blessings and am extremely grateful for their sacrifices that they have made in order to allow me to complete this work.

Finally, I wish to acknowledge the contribution of my best friend, who has stood besides me unconditionally for the last 10 years. A special friend who has been extremely patient, understading and caring throughout this journey as I realized this dream. A friend who has celebrated all the successes and milestones of this project with me, and supported me firmly when I found this journey challenging. A big thank you to my wife Lakshmi Dave for being there always, from taking care of home while I was busy with experiments or thesis writing to being the first to correct the drafts of the manuscripts or thesis chapters.

Contents

Abstract	I
Acknowledgements	V
List of Figures	XVII
List of Tables	XXXI
List of Publications	XXXIII
1. Introduction	1
2. Review of literature	7
2.1. Amyloid fibrils	8
2.1.1. Defining characteristics of amyloid fibrils	11
2.1.1.1. Characteristic cross β -structure	11
2.1.1.2. Nucleation-dependent polymerization	12
2.1.2. Structural basis for self-assembly.....	13
2.1.2.1. Role of amyloidogenic sequences	13
2.1.2.2. Role of protein structure.....	16
2.1.3. Factors affecting the self-assembly of proteins	18
2.1.3.1. Factors promoting protein self-assembly	18
2.1.3.2. Factors inhibiting protein self-assembly	20
2.2. β -Lactoglobulin	23
2.2.1. Native structure	23
2.2.2. Genetic variants of β -Lg.....	27
2.2.3. Heat-induced unfolding of β -Lg.....	29
2.2.4. Heat-induced aggregation of β -Lg	31
2.2.5. Factors affecting thermal aggregation of β -Lg.....	33
2.2.5.1. Genetic variation	34
2.2.5.2. Effects of polyols	35
2.2.5.3. Glycation	36
2.2.5.4. Chaperone-like properties of β -casein.....	38

Contents

2.3.	Self-assembly of β -Lg into amyloid-like fibrils	42
2.3.1.	Conditions of β -Lg self-assembly.....	42
2.3.2.	Mechanism of β -Lg self-assembly at low pH.....	44
2.3.3.	Heat-induced acid hydrolysis	46
2.3.4.	Characteristics of β -Lg fibrils.....	50
2.3.5.	Sequences present in fibrils	53
2.3.6.	Factors affecting kinetics of self-assembly	54
2.3.6.1.	Temperature.....	54
2.3.6.2.	pH and ionic strength	55
2.3.6.3.	Cations.....	56
2.3.6.4.	Seeding	56
2.3.6.5.	Shear	57
2.3.7.	Stability of β -Lg fibrils	58
2.4.	Objectives	59
2.4.1.	Experimental Approach.....	59
2.4.2.	Experimental techniques.....	60
3.	Materials and Methods.....	61
3.1.	Materials	61
3.1.1.	Water	61
3.1.2.	Whey protein isolate	61
3.1.3.	Trypsin.....	62
3.1.4.	β -Lg variants A, B and C.....	62
3.1.5.	Bovine β -casein	62
3.1.6.	Chemicals	62
3.2.	Instruments	65
3.2.1.	Centrifuges.....	65
3.2.2.	Waterbath.....	66
3.2.3.	Spectrofluorometer	66
3.2.4.	Spectrophotometer.....	66
3.2.5.	pH meter	66
3.2.6.	Circular dichroism spectrometer	67
3.2.7.	High performance liquid chromatography system	67

3.2.8. Mass spectrometers	67
3.2.9. Transmission electron microscope	67
3.2.10. Other instruments	67
3.2.11. General consumables	68
3.3. Methods	68
3.3.1. Isolation of β -lactoglobulin	68
3.3.2. Preparation of fibrils	69
3.3.3. Thioflavin T assay for detection of fibrils	69
3.3.4. Separation of fibrils using ultracentrifugation	74
3.3.5. Polyacrylamide gel electrophoresis (PAGE)	76
3.3.5.1. Native non-denaturing PAGE	78
3.3.5.2. Glycine SDS-PAGE	79
3.3.5.3. Tricine SDS-PAGE	80
3.3.5.4. Running, staining and imaging of gels	81
3.3.5.5. 2-Dimensional nonreducing-reducing (2D NR-R) SDS-PAGE	82
3.3.5.6. Densitometry	82
3.3.6. CD spectroscopy	83
3.3.6.1. Introduction	83
3.3.6.2. Sample preparation	85
3.3.6.3. Recording scans	86
3.3.7. Mass Spectrometry	88
3.3.7.1. Introduction	88
3.3.7.2. Determination of molecular weights	91
3.3.7.3. Sequence characterization by MALDI-TOF MS/MS	92
3.3.7.4. Characterization of sequences in fibrils by ESI- MS/MS	93
3.3.8. Transmission electron microscopy	95
3.4. Software packages	96

4. Characterization of β-Lactoglobulin self-assembly: Structural changes in early stages and disulfide bonding in fibrils	97
4.1. Abstract	97
4.2. Introduction	99
4.3. Materials and Methods	101
4.4. Results	102
4.4.1. Characterization of β -Lg isolated from WPI	102
4.4.2. Self-assembly of β -Lg	105
4.4.3. Hydrolysis of β -Lg in heated samples	106
4.4.4. Structural transitions in the lag phase	108
4.4.4.1. Hydrolysis of β -Lg	108
4.4.4.2. Unfolding of β -Lg during heating	110
4.4.5. Characterization of fibril composition	115
4.4.5.1. Composition of fibrils after different heating times ...	115
4.4.5.2. Disulfide bonding in fibrils	120
4.4.5.3. Characterization of sequences of fibril peptides	122
4.5. Discussion	138
5. Self-assembly from β-Lg A, B and C	147
5.1. Abstract	147
5.2. Introduction	149
5.3. Materials and Methods	150
5.4. Results	151
5.4.1. Characterization of β -Lg variants	151
5.4.2. Unfolding of β -Lg	153
5.4.3. SDS-PAGE of heated samples	156
5.4.4. Self-assembly of β -Lg A, B and C	159
5.4.5. Morphology of fibrils	160
5.4.6. Composition of fibrils	162
5.5. Discussion	163

6. Glycation as a tool to probe the mechanism of β-lactoglobulin self-assembly	171
6.1. Abstract	171
6.2. Introduction	173
6.3. Materials and methods	175
6.3.1. Preparation of glycosylated β -Lg	176
6.4. Results	177
6.4.1. Preliminary experiments	177
6.4.2. Characterization of glycosylated β -Lg for self-assembly studies	180
6.4.3. Unfolding behavior of glycosylated β -Lg	183
6.4.4. Heat-induced acid hydrolysis	187
6.4.5. Self-assembly from glycosylated β -Lg	191
6.4.6. Morphology of fibrils	196
6.5. Discussion	199
7. Modulating β-Lg self-assembly using polyols glycerol and sorbitol	203
7.1. Abstract	203
7.2. Introduction	205
7.3. Materials and Methods	207
7.3.1. Preparation of fibrils	208
7.3.2. Effect of polyols on ThT assay	208
7.4. Results	209
7.4.1. Effect of polyols on the rate of β -Lg self-assembly	209
7.4.2. Effects of polyols on pre- self-assembly processes	213
7.4.2.1. Heat-induced acid hydrolysis	213
7.4.2.2. Unfolding behavior of β -Lg in presence of polyols	218
7.4.3. Morphology of fibrils in presence of glycerol and sorbitol	224
7.5. Discussion	227

Contents

8. Interactions of β-Lactoglobulin and β-casein during self-assembly	233
8.1. Abstract	233
8.2. Introduction	235
8.3. Materials and Methods	237
8.3.1. Preparation of β -casein	237
8.3.2. Preparation of samples for self-assembly	238
8.4. Results	240
8.4.1. Self-assembly from β -Lg in the presence of β -casein	240
8.4.2. Heat-induced acid hydrolysis of β -Lg and β -casein	241
8.4.3. Composition of aggregates in the heated solutions	250
8.4.4. Morphology of aggregates	251
8.5. Discussion	253
9. Overall discussion and avenues for future work.....	263
9.1. Summary	263
9.1.1. Unfolding of β -Lg.....	264
9.1.2. Heat-induced acid hydrolysis	264
9.1.3. Self-assembly.....	265
9.1.4. Fibril composition and amyloidogenic sequences.....	267
9.1.5. Morphology of fibrils	268
9.2. Overall discussion	271
9.3. Applications.....	281
9.4. Avenues for Further Work	283
10. References	287
11. Annexures	322
12. DRC 16 forms: Statement of contribution to doctoral thesis	
containing publications.....	349

List of Figures

Figure 1.1 Overview of following thesis chapters.	6
Figure 2.1 Schematic representation of characteristic X-ray fibre diffraction arising from the cross- β structure of fibrils. The distance between two β -strands is approximately 4.8 Å, while between the anti-parallel arrangements of β -strands is 9.6 Å. The distance between two β -sheets is 10-11 Å. Adapted from Serpell (2000).....	12
Figure 2.2 Free energy landscape of protein aggregation. The area in the pink region represents different transitional states during aggregation. Adapted from Hartl et al. (2009).....	17
Figure 2.3 Aggregation pathways for misfolded proteins. N, I and U represent native, intermediate and unfolded polypeptide conformation states of the protein. Adapted from Dobson (2003a).	18
Figure 2.4 Sequence of β -Lg A (Variant B shows presence of glycine instead of aspartic acid at residue 64 and alanine instead of valine at residue 118) adapted from the Protein Data Bank [©] (PDB ID 1BSO) (Qin et al., 1998a). Dotted lines indicate disulfide bonding. Solid arrows indicate β -strands; waveforms indicate helices and arches indicate loops.	24
Figure 2.5 pH-dependent reversible association behavior of β -Lg. Adapted from Cheison et al. (2011).	27
Figure 2.6 Proposed mechanism of acid hydrolysis of proteins. Adapted from Blackburn et al. (1954).....	47

List of Figures

- Figure 2.7** Characteristics of β -Lg fibrils (A) wide angle X-ray diffraction pattern of β -Lg fibrils, adapted from Bromley et al. (2005); (B) TEM and (C) AFM image of β -Lg fibrils, adapted from Adamcik et al. (2010); (D) Distribution of proto-filaments in β -Lg fibrils, numbers indicate number of protofilaments, adapted from Lara et al. (2011)..... 52
- Figure 2.8** Comparison of sequences found in β -Lg fibrils reported by (i) Akkermans et al. (2008b) and (ii) Hettiarachchi et al. (2012). The numbers on the top show the locations of aspartic acid residues in the sequence, based on the sequence of β -Lg A. (A) and (B) show the peptides from β -Lg A and B..... 54
- Figure 3.1** (A) Structure of Thioflavin T molecule and (B) orientation of ThT molecules bound to fibrils. The ThT molecules align themselves in the channels formed by the ordered arrangement of side-chain residues in cross- β sheets of fibrils. Adapted from Krebs et al. (2005). 71
- Figure 3.2** Residual Thioflavin T intensities of supernatants obtained by ultracentrifugation at different speeds for 30 and 60 minutes (20 °C). β -Lg 1% (w/v) was heated at 80 °C at pH 2 for 12 h. Sample intensities were corrected by subtracting the intensity of the blank containing ThT solution without any sample. 75
- Figure 3.3** Components of circularly polarized light (A) without absorption and (B) after absorption by chiral component. Adapted from Kelly et al. (2005). 84
- Figure 3.4** Schematic representation of mass spectrometer. 89

Figure 4.1 Native PAGE pattern of β -Lg isolated from WPI by salt precipitation.....	103
Figure 4.2 SDS-PAGE (with or without reducing agent) patterns of β -Lg isolated from WPI by salt precipitation method. I represents interface of stacking and resolving gel. For description of bands 1 to 4, see text.....	104
Figure 4.3 Deconvoluted MS spectrum of the isolated β -Lg.....	105
Figure 4.4 Thioflavin T (ThT) fluorescence intensity (empty circles) at 486 nm for 1% β -Lg at pH 2 heated at 80 °C. Error bars show standard deviations for triplicate measurements for three separate samples and the solid line show fit of Equation 3.1. Filled circles represent normalized intensity of the SDS-PAGE band corresponding to intact monomer. Error bars show standard deviations from three separate samples while the solid line shows fit of Equation 3.8.	106
Figure 4.5 Reduced SDS-PAGE of β -Lg heated at 80 °C and pH 2 for different times. M_0 , Molecular mass marker in kDa; 0, unheated sample, numbers above the lanes indicate the heating times in hours.	107
Figure 4.6 Reduced SDS-PAGE of β -Lg (1% w/v) heated at 80 °C and pH 2 during the lag phase. M_0 , Molecular mass marker (kDa); 0, unheated sample; Numbers above the lanes indicate the heating time in minutes. For description of bands A-E, M and N, see text.	110
Figure 4.7 CD spectra of β -Lg at pH 2 and 80 °C. (A) Near-UV scans, (10 mg/mL). (B) Far-UV spectra (0.01 mg/mL). Conditions for data collection were: path length 10 mm, temperature 80 °C and scans were averaged at 2-minute intervals each.	113

List of Figures

- Figure 4.8** Relative change in ellipticity at (A) 293 nm representing the loss of tertiary structure, and (B) 208 nm representing change in secondary structure, calculated from data shown in Figure 4.7. Solid lines are for visual reference. 114
- Figure 4.9** High-tension (HT) curves of circular dichroism scans shown in Figure 4.7 (B) showing high absorption by the sample between 180 and 200 nm. 115
- Figure 4.10** Thioflavin T fluorescence intensities at 486 nm in heated β -Lg (1%) samples (filled circles) and supernatants in (empty circles) obtained after centrifugation at 2.4×10^5 g for 60 minutes. The pellets were used for SDS-PAGE analysis shown in Figure 4.12. Solid line shows the fit of Equation 3.1. 116
- Figure 4.11** Comparison of reduced SDS-PAGE profiles of centrifuged samples at different heating times. M_0 , Molecular mass marker, weights in kDa; 0, unheated sample; U, heated and uncentrifuged; S, supernatant; P, pellet. Numbers above the lanes indicate heating times in hours. Uncentrifuged sample and supernatants were diluted 1:10 with the PAGE sample buffer. Surface-washed pellets were suspended in the loading buffer without dilution. For description of bands M, N and A to E see text. 117
- Figure 4.12** SDS-PAGE profiles of pellets obtained after centrifugation of heated samples (1% β -Lg) at different stages of self-assembly. Pellets were obtained by ultracentrifugation and were complete-washed (see Chapter 3 for details). The washed pellets were suspended in PAGE loading buffer with 4% SDS and 100 mM DTT

-
- and allowed to dissolve for 7 days 20 °C. Samples were run on tricine SDS-PAGE gels prepared in house. M₀: Molecular weight marker (weights in kDa); U: unheated; numbers above the lanes indicate heating times in h. For description of bands A to E, M and N see text..... 119
- Figure 4.13** SDS-PAGE comparison of peptide bands in fibrils under reducing and non-reducing conditions. Complete-washed pellets obtained after ultracentrifugation for 12 h. M₀, Molecular mass marker (weights in kDa); 0, unheated sample; U, heated and uncentrifuged sample; P_R, complete-washed pellet suspended in reducing PAGE buffer; P_{NR}, complete-washed pellet suspended in non-reducing PAGE buffer. For description of bands C, D and E, see text..... 121
- Figure 4.14** 2D SDS-PAGE of the pellet obtained from a sample heated for 12 h. Complete-washed pellet suspended in buffer containing 4% SDS and run under non-reducing conditions in 1D. The target gel lane was excised, reduced and run in the 2nd dimension. P_R: reduced sample obtained from the same sample..... 122
- Figure 4.15** Typical MS/MS spectra of showing ions with assigned masses for peptide SLAMAASDISLLDAQSAPLR (with oxidation of methionine) from band C in Table 4.2 with a cut-off ion score of 100 (expect value 6.3×10^{-7})..... 130
- Figure 4.16** Schematic representation of regions found in peptides from in-gel digestion ESI-MS/MS and MALDI-TOF MS/MS. The dark blocks in the sequence show location of aspartic acid residues indicating potential sites of acid hydrolysis of β -Lg. Sequence of β -Lg variant
-

List of Figures

- A is shown. Variant B has glycine instead of aspartic acid at residue 64 and alanine instead of valine at residue 118. 137
- Figure 4.17** Schematic illustration of how disulfide-bonded peptides come to be present in fibrils. Red colored regions indicate the N- terminal region (1-53) of the β -Lg sequence. 141
- Figure 5.1** Native non-denaturing PAGE of β -Lg A, B and C. 151
- Figure 5.2** De-convoluted MS spectra of β -Lg variants. (A) β -Lg A, (B) β -Lg B and (C) β -Lg C. 152
- Figure 5.3** Spectra of native β -Lg A, B and C at pH 2. (A) NUV spectra (1 mg/mL) and (B) FUV spectra (0.01 mg/mL). 154
- Figure 5.4** Unfolding of the β -Lg A, B and C upon heating at 80 °C. The NUV scans in (A), (C) and (D) show effect of heating on the tertiary structure, while FUV scans in (B), (D) and (E) show the effect of heating on the secondary structure of β -Lg A, B and C respectively. The concentration of β -Lg was 1 mg/mL for the NUV scans, and 0.01 mg/mL for the FUV scans. 155
- Figure 5.5** Relative losses of ellipticities at (A) 293 nm and (B) 208 nm calculated from Equations 3.11 and 3.12. Solid lines are for visual reference. 156
- Figure 5.6** Reducing tricine SDS-PAGE profiles of control and heated samples after heating for 12 and 24 h at 80 °C. M_0 Molecular weight marker; molecular weights are in kDa. For description of band Q, see text. 157
- Figure 5.7** Residual intensities of β -Lg band at different heating times. Each value represents an average of two separate experiments. Solid lines

indicate fit of Equation 3.8. Thick solid lines represent β -Lg A; dots, β -Lg B; and dashes, β -Lg C.	158
Figure 5.8 ThT fluorescence intensities at 486 nm in heated samples of β -Lg A, B and C (1% w/v) at 80 °C and pH 2. Error bars represents standard error of measurements from two experiments with two replicates in each. Solid lines indicate fit to Equation 3.1. Thick solid lines represent β -Lg A; dots, β -Lg B; and dashes, β -Lg C.	159
Figure 5.9 TEM images of fibrils from β -Lg A, B and C after 24 h at 80 °C.....	161
Figure 5.10 Reducing tricine SDS-PAGE of fibrils formed after heating at 80 °C for 12 h and separated by ultracentrifugation. M ₀ , Molecular weight marker; S, supernatant; P pellet containing fibrils. Molecular weights in kDa; for descriptions of (i), bands A to E and R, see text. ...	162
Figure 6.1 De-convoluted MS spectra of glucosylated β -Lg (A) 8 h, (B) 16 h and (C) 36 h. Numbers in the figure represent the number of glucose residues attached on the β -Lg variant A.....	178
Figure 6.2 De-convoluted MS spectra of lactosylated β -Lg (A) 3 days, (B) 5 days and (C) 7 days. Numbers in the figure represent the number of lactose residues attached on the β -Lg variant A.....	179
Figure 6.3 De-convoluted MS spectra of glucosylated (A) LowGlu β -Lg and (B) HighGlu β -Lg. Peak labels show the number of attached glucose residues.....	181
Figure 6.4 De-convoluted MS spectra of lactosylated (A) LowLac β -Lg and (B) HighLac β -Lg. Peak labels show the number of attached lactose residues.....	182

List of Figures

- Figure 6.5** Comparison of CD spectra of β -Lg glycosylated with glucose and lactose (A) NUV (10 mg/mL β -Lg) and (B) FUV (0.01 mg/mL β -Lg) region..... 184
- Figure 6.6** CD spectra of LowGlu β -Lg in the (A) NUV region (10 mg/mL β -Lg) and (B) in the FUV region (0.01 mg/mL β -Lg). The numbers in the figures indicate heating time in minutes..... 185
- Figure 6.7** Relative change in ellipticity at (A) 293 nm in the NUV region and (B) 208 nm in the FUV region. Solid lines are for visual reference. For details of x and y-axes see Section 3.3.6.3, Chapter 3..... 186
- Figure 6.8** Tricine SDS-PAGE profiles of control and glycosylated samples after heating for 12 h at 80 °C, at pH 2. M_0 , Molecular weight markers in kDa; C, heated control..... 187
- Figure 6.9** The normalized band intensities of the un-hydrolyzed β -Lg band at different times in glycosylated samples. Each value is an average of quantifications from two sets of independent experiments. The solid lines represent fits to the first-order exponential decay model of Equation 3.8..... 188
- Figure 6.10** The normalized band intensities of the un-hydrolyzed β -Lg band at different times in the controls with no sugar added. Each value is an average of quantifications from two sets of independent experiments. The solid lines represent fits the first-order exponential decay model in Equation 3.8. 190
- Figure 6.11** (A) ThT fluorescence intensity of control and glycosylated β -Lg (1% w/v) during heating at pH 2 and 80 °C. Each data point is an average of triplicates from two independent experiments, and error bars are

standard deviations. Solid lines indicate the fit to Equation 3.1. (B) Normalized parameters of self-assembly calculated from Equations 3.2 and 3.4. The kinetic parameters of individual samples were normalized by those of control sample.	192
Figure 6.12 Self-assembly from β -Lg (1% w/v) without sugars used as control during glycation and treated similarly to the glycated samples. Error bars represent standard error of triplicate measurements in samples. Each value represents an average of triplicate values. Solid lines indicate fits to Equation 3.1.....	194
Figure 6.13 Tricine SDS-PAGE profiles of centrifugally separated fibrils made by heating glycated β -Lg at 80 °C for 24 h. M_0 , Molecular weight markers in kDa; C, control fibrils made from the same heat treatment.....	195
Figure 6.14 Residual ThT intensities in supernatants obtained for upon ultra centrifugation. Heated β -Lg solutions obtained after heating at 80°C for 24 h were ultracentrifuged. The pellets obtained after ultracentrifugation were used for SDS-PAGE (Figure 6.13).....	196
Figure 6.15 TEM images of fibrils from glycated β -Lg after heating for 24 h at 80 °C. (A) LowGlu β -Lg; (B) HighGlu β -Lg.....	197
Figure 6.16 TEM images of fibrils from glycated β -Lg after heating for 24 h at 80 °C. (A) LowLac β -Lg; (B) HighLac β -Lg.....	198
Figure 6.17 Proposed mechanism of inhibition of self-assembly of glycated β -Lg by the steric effect of the sugar adduct.	201
Figure 7.1 Thioflavin T (ThT) fluorescence intensity at 486 nm for β -Lg (1%, w/v) heated at 80 °C and pH 2 in presence of different levels (%,	

List of Figures

- w/v) of (A) glycerol and (B) sorbitol. Solid lines indicate the fit using Equation 3.1. Error bars represent the standard errors of measurements from two separate experiments with three replicates in each..... 210
- Figure 7.2** Normalized ThT fluorescence intensities β -Lg sample containing fibrils diluted using different levels of polyols (0-50% w/v, used for self-assembly studies). The ThT fluorescence intensity in the undiluted sample was 920 fluorescence units. The intensity of the sample diluted using water (pH 2) was used for normalization. A value close to 1 indicates that the fluorescence intensity in samples diluted with water or polyols were similar. 213
- Figure 7.3** Reduced SDS-PAGE of samples heated at 80 °C for 12 h in the presence of different concentrations of (A) glycerol or (B) sorbitol. (M_0) Molecular weight marker in kDa; (U) unheated sample. Numbers above the lanes indicate polyol concentrations (% w/v)..... 214
- Figure 7.4** Normalized β -Lg band intensities from SDS-PAGE gels of samples containing different concentrations of (A) glycerol and (B) sorbitol. Values are the average of two independent experiments. Solid lines indicate fit to Equation 3.8. 215
- Figure 7.5** Effect of glycerol (A) and sorbitol (B) on the normalized kinetic parameters of hydrolysis and self-assembly..... 217
- Figure 7.6** CD spectra of β -Lg at 20 °C in presence of different levels of (A) and (C) glycerol and (B) and (D) sorbitol. For the NUV scans (A) and (B), the concentration of β -Lg was 1 mg/mL, while that for FUV

-
-
- spectra (C) and (D) was 0.01mg/mL. The sample scans were corrected by subtracting the baseline scans and smoothed. 220
- Figure 7.7** NUV (A, B) or FUV (C,D) circular dichroism spectra of β -Lg during heating at 80 °C and pH 2 with 30% glycerol (A,C) or 30% sorbitol (B,D). Numbers indicate the heating time in minutes. 221
- Figure 7.8** Relative loss of ellipticity at 293 nm in β -Lg solutions during heating at 80 °C with 0-50% glycerol (A) or sorbitol (B) calculated from Equations 3.13 and 3.14. For details of the notations of Y axis see Section 3.3.6.3 in Chapter 3. The same symbols representing glycerol concentrations in (A) apply for sorbitol concentrations in (B). Solid lines are a visual guide only. 222
- Figure 7.9** Normalized ellipticities in the samples at 293 nm at the end of 10 minutes at 80 °C. Absolute ellipticities in the samples with different levels of polyols (θ_{polyol}) were normalized by the ellipticity of the control sample without any polyols (θ_{control}). Values >1 indicates a higher residual signal in the sample and hence the stabilized state of β -Lg. Solids lines are a visual guide. 223
- Figure 7.10** High tension curves for FUV scans of β -Lg in presence of 30% w/v of (A) glycerol and (B) sorbitol during heating at 80 °C. The data in A and B represent the high tension (HT) values for the same scans shown in Figure 7.7 C and D. Solid lines are a guide and are not fitted with any mathematical model. 223
- Figure 7.11** Transmission electron microscopy images of β -Lg fibrils separated from heated solutions. (A) Without any polyol; (B) With 20%

List of Figures

- glycerol; and (C) With 20% sorbitol. Samples heated at 80 °C, pH 2 and 24 h. 225
- Figure 7.12** Transmission electron microscopy images of β -Lg fibrils separated from β -Lg samples heated at 80 °C, pH 2 and 24 h in the presence of (A) 50% (w/v) glycerol and (B) 50% (w/v) sorbitol at 80 °C, pH 2 and 24 h. 226
- Figure 7.13** Schematic illustration of how β -Lg fibril assembly is affected by sorbitol (slowing unfolding) and glycerol (slowing assembly of peptides). 228
- Figure 7.14** Viscosity of polyol solutions at 80 °C at a shear rate of 1 s⁻¹. Polyol solutions were made in Milli Q water without pH adjustment. Measurements were carried out on an AR-G2 rheometer (TA Instruments, New Castle, DE) using a double gap measuring system equilibrated at 80 °C for two minutes prior to measurements. 230
- Figure 8.1** ThT fluorescence intensities at 486 nm in samples of heated β -Lg- β -casein mixtures. The control sample contained β -Lg alone. Error bars show the standard errors of measurements from two separate experiments with two replicates for each data point. Solid lines indicate fit of Equation 3.1. 240
- Figure 8.2** Reduced SDS-PAGE of β -Lg and β -casein mixtures heated at 80 °C for (A) 12 h and (B) 24 h. M₀ molecular weight marker (kDa); C, control. Lanes marked 1 to 5 represent β -Lg and β -casein mixtures at different molar ratios. Lane marked 1 represents a molar ratio 1:0.0625; 2, 1:0.125; 3, 1:0.250; 4, 1:0.50; 5, 1:1. 242

-
-
- Figure 8.3** Reduced SDS-PAGE of β -casein controls heated at 80 °C for (A) 12 h and (B) 24 h. M_0 molecular weight marker (kDa); Lanes marked 1 to 5 represent the same β -casein concentrations as used in β -Lg- β -casein mixtures of Figure 8.4. 243
- Figure 8.4** Peptide compositions of heated solutions after 12 h at 80 °C. M_0 molecular weight marker (kDa); C, control β -Lg (without β -casein); 1, β -Lg and β -casein mixture (molar ratio 1:1) and 2, control β -casein (without β -Lg) at same concentration as in 1. For description of band F to J, see text. All samples analyzed under reducing conditions. 245
- Figure 8.5** Residual SDS-PAGE monomeric band intensities of (A) β -Lg and (B) β -casein in heated β -Lg- β -casein mixtures. Symbols in (B) represent the same β -casein concentrations as used in (A). Values are an average of two separate estimations. Solid lines indicate fit of Equation 3.8. 248
- Figure 8.6** Composition of aggregates formed from the heated and ultracentrifuged samples containing β -Lg (1%, w/v) with (0.65% w/v, molar ratio 1:0.5) or without β -casein. Samples were heated at 80 °C for 12 h. M_0 represents molecular weight markers (kDa); H, heated solution; S, supernatant and P, Pellet. Supernatants were diluted 1:10 in reducing PAGE sample buffer, while the pellets were suspended in 1.2 ml PAGE sample buffer without further dilution. 250
- Figure 8.7** TEM images of β -Lg samples heated (A) without, and (B to D) with β -casein at molar ratios of 1:0.5 (B and C) or 1:1 (D and E). Samples

List of Figures

heated at 80 °C for 24 h selected for TEM analysis. For description of white arrows see text.....	252
Figure 8.8 TEM images of β -casein samples heated at 80 °C for 24 h without β -Lg. The β -casein concentration was equivalent to that in mixed solutions at molar ratio of 1:0.5.....	253
Figure 8.9 Charge distribution on β -casein polypeptide at pH (A) 6.7 and (B) 2.6. Adapted with permission from Moitzi et al. (2008), Copyright 2008 American Chemical Society.....	254
Figure 8.10 Overview of the hydrophobicity (pH 7) of β -casein peptides G to J of Figure 8.4 calculated using the method of Kyte et al. (1982). At pH 2, the hydrophobicity of the peptides is likely to be higher due to protonation of carboxylic groups of Asp and Glu (Kuhn et al., 1995). Bands G (A), I (D) and J (E) contain phosphate groups bound to serine residues.	257
Figure 8.11 Proposed mechanism for the effect of β -casein on β -Lg self-assembly. (i), (ii) and (iii) represent aggregation pathways.....	259
Figure 9.1 Mechanism of β -Lg self-assembly at 80 °C, pH 2 at low concentrations (<3% w/v).	266
Figure 9.2 Strategies to decouple acid hydrolysis from self-assembly by modifying (A) glycation of β -Lg or (B) composition of aqueous solution by glycerol.	277

List of Tables

Table 2.1 Human diseases associated with amyloid fibrils.....	9
Table 2.2 Sites of differences in β -Lg A, B and C.	28
Table 2.3 Non-native conditions promoting fibril formation from β -Lg.	43
Table 2.4 Overview of experimental techniques used in this study.	60
Table 3.1 List of chemicals and reagents used and their vendors.	63
Table 3.2 Composition of native and SDS-PAGE gels.....	79
Table 3.3 Composition of resolving and stacking gels for tricine SDS-PAGE analysis.....	81
Table 4.1 Proximate composition of extracted β -Lg.....	103
Table 4.2 Peptides from β -Lg hydrolysis present in fibrils analyzed by MALDI- TOF MS/MS.....	123
Table 4.3 Peptide sequences of peptide bands A to E (Figure 4.12) in the pellet (12 h) analyzed by ESI-MS/MS after extraction following in-gel digestion with trypsin.....	125
Table 4.4 MS/MS data from Mascot search showing masses of the assigned ion peaks shown in Figure 4.16.....	131
Table 4.5 Peptides obtained by in-gel digestion of unheated β -Lg followed by ESI-MS/MS. β -Lg loaded on to SDS-PAGE gel (resolving gel concentration 20%). After running, the β -Lg band was excised and processed along with the peptide bands A-E which have been characterized in Table 4.3.	133
Table 4.6 Possible sequences of peptides present in SDS-PAGE bands of fibrils..	144
Table 5.1 Rate constants of monomer hydrolysis calculated from Equation 3.8....	158

List of Figures

Table 5.2 Kinetic parameters of self-assembly calculated from Equations 3.2 to 3.4.....	160
Table 5.3 Possible sequences present in the peptide bands of fibrils of β -Lg A, B and C, shown in Figure 5.10.....	165
Table 6.1 Rate constants of acid hydrolysis of glycated β -Lg calculated from data in Figure 6.9 and Equation 3.8.....	189
Table 6.2 Rate constants of acid hydrolysis of β -Lg used as glycation control calculated from the data in Figure 6.10 and Equation 3.8.....	190
Table 6.3 Kinetic parameters describing β -Lg self-assembly calculated using Equations 3.2 to 3.4.....	193
Table 6.4 Kinetic parameters describing self-assembly calculated from Equations 3.1-3.4 for β -Lg samples used as controls during glycation experiments. The ThT fluorescence intensities are shown in Figure 6.12 above.....	194
Table 7.1 Kinetic parameters from Equation (3.2-3.4) showing effect of glycerol and sorbitol on β -Lg self-assembly.....	211
Table 7.2 Fit parameters from Equation 3.8 describing the kinetics of acid hydrolysis of β -Lg during heating under fibril forming conditions.....	216
Table 8.1 Composition of β -Lg- β -casein mixtures.....	239
Table 8.2 Kinetic parameters of self-assembly calculated from Equations 3.2-3.4.....	241
Table 8.3 Predicted sequences of β -casein peptides shown in Figure 8.6.....	246
Table 8.4 Rate constants of acid hydrolysis of β -Lg and β -casein in heated β -Lg- β -casein mixtures during heating at 80 °C.....	249
Table 9.1 Summary of the results from Chapters 5-8.....	269

List of Publications

- Dave, A. C., Loveday, S. M., Anema, S. G., Loo, T. S., Norris, G. E., Jameson, G. B., & Singh, H. (2013). β -Lactoglobulin self-assembly: Structural changes in early stages and disulfide bonding in fibrils. *Journal of Agricultural and Food Chemistry*, 61(32), 7817-7828.
- Dave, A. C., Loveday, S. M., Anema, S. G., Jameson, G. B., & Singh, H. (2014). Modulating β -lactoglobulin self-assembly into nanofibrils at pH 2 using polyols. *Biomacromolecules*, 15(1), 95-103.
- Dave, A. C., Loveday, S. M., Anema, S. G., Jameson, G. B., & Singh, H. (2014). Glycation as a tool to probe the mechanism of β -lactoglobulin self-assembly. *Journal of Agricultural and Food Chemistry*. 62(14), 3269-3278.
- Dave, A. C., Loveday, S. M., Anema, S. G., Jameson, G. B., & Singh, H. ***In press***. Formation of nano-fibrils from the A, B and C variants of β -lactoglobulin. *International Dairy Journal*.

Chapter 1

1. Introduction

Protein engineering to develop self-assembled amyloid-like fibrils with novel functionalities has recently emerged as an exciting area of scientific research. Protein-based amyloid-like fibrils present themselves as smart, designer biomaterials with a range of potential applications across different disciplines (Raynes et al., 2012) from biotechnology (Raynes et al., 2011; Waterhouse et al., 2004) to nanoelectronics (Bolisetty et al., 2012; Scheibel et al., 2003). In addition, fibrils have unique properties that modulate the solvent properties, pointing towards their potential applications in food systems as thickening or gelling agents (Veerman et al., 2003a) or as stabilizers and emulsifiers (Ruhs et al., 2012).

Recently, fibril-forming properties of a number of food proteins including α -lactalbumin, bovine serum albumin (Veerman et al., 2003c), β -lactoglobulin (Akkermans et al., 2008b; Lara et al., 2011), whey protein isolate (Bolder et al., 2006; Loveday et al., 2012b), κ -casein (Thorn et al., 2005), ovalbumin (Veerman et al., 2003b), soy glycinin and soy protein isolate (Akkermans et al., 2007) have been investigated in detail. Amongst these sources, the self-assembly of β -Lg has been widely studied, perhaps due to its abundant availability, its relative ease of purification and its ability to form fibrils rapidly at low pH in a crude protein mixture (WPI). Besides, a large volume of information about the native structure and its unfolding, and aggregation mechanism of β -Lg allows a detailed understanding of the underlying mechanisms of its self-assembly.

Chapter 1. Introduction

β -Lg self-assembles into long, semi-flexible fibrils when heated above its denaturation temperature at low pH; and under these conditions, the kinetics of β -Lg self-assembly follows the nucleation-dependent polymerization model (Bolder et al., 2007a; Bromley et al., 2005; Clark et al., 2001). These fibrils demonstrate typical characteristics of amyloid fibrils found *in vivo* (Adamcik et al., 2010; Bromley et al., 2005). The mechanism of self-assembly has been a subject of several investigations. Studies published prior to the 2008 considered β -Lg fibrils to consist of intact monomers (Bolder et al., 2007c; Ikeda et al., 2002; Rogers et al., 2005). In 2008, Akkermans et al. (2008b) showed that the building blocks of fibrils formed after prolonged heating time were primarily peptides released by the acid-induced cleavage of β -Lg.

In addition, other studies reported the effects of heating temperature (Kroes-Nijboer et al., 2011; Loveday et al., 2012c), mode of heating (Hettiarachchi et al., 2012), pH (Loveday et al., 2011b) and ionic strength (Arnaudov et al., 2006; Loveday et al., 2011a; Loveday et al., 2011b) on β -Lg self-assembly. These studies provided important insights into the mechanisms involved during self-assembly of β -Lg.

In spite of these attempts, the exact mechanism of β -Lg self-assembly has not been understood in detail and several aspects of self-assembly remain unexplored. In particular, the structural changes in β -Lg prior to self-assembly in the lag phase and the composition of growth-promoting nuclei have not received much attention. This is perhaps due to the fact that most of the recent studies (after 2008) investigating self-assembly have used shear during heating, which is known to speed up self-assembly by secondary nucleation (Dunstan et al., 2009; Hill et al., 2006).

Although heat-induced acid hydrolysis of β -Lg monomers during self-assembly is now well known, the extent to which hydrolysis is rate-limiting is not yet understood. Similarly, the exact role of acid hydrolysis during self-assembly has remained as a subject of debate especially after the report of Hettiarachchi et al. (2012) who showed that extensive hydrolysis of β -Lg was not necessary for fibril formation during microwave heating. Besides, the possibility that fibrils could undergo acid hydrolysis during heating or whether fibrils contain any disulfide bonding has not been investigated.

This work seeks to address the above questions and understand the mechanism of β -Lg self-assembly by characterizing the different processes occurring during fibril formation. The interrelationships between these processes have also been investigated in detail by perturbing the conditions of self-assembly using two different approaches described below:

1. Investigating how self-assembly is affected by altering the nature of β -Lg using:
 - Purified β -Lg variants A, B and C
 - Glucosylated and lactosylated β -Lg
2. Investigating the effects of change in aqueous environmental conditions using two types of cosolutes:
 - Neutral cosolutes, polyols
 - β -Casein, which possesses chaperone-like activity

Chapter 4 compares the kinetics of unfolding, acid hydrolysis and self-assembly and seeks to understand their roles at different stages of self-assembly. This study also investigates to what extent each of these steps was rate-limiting and explores some

Chapter 1. Introduction

important aspects about the mechanism of self-assembly, including amyloidogenic sequences in β -Lg and their specific roles during nucleation and growth, composition of fibrils at different stages of self-assembly and disulfide bonding in fibrils.

The self-assembly from genetic variants of β -Lg A, B and C has been investigated in Chapter 5. These variants of β -Lg have minor substitutions at sites that have been previously found on assembly-capable peptides of fibrils. These sites, being in the different regions of the primary structure, present a previously unexplored opportunity to investigate the amyloidogenicity of peptides originating from these regions. Under conditions of β -Lg self-assembly, the substitution Asp64 in β -Lg A, may provide an additional site of acid hydrolysis, similarly, Val118 (β -Lg A) may increase the propensity of this region to form fibrils. Similarly, the substitution of His59 in β -Lg C would increase the net positive charge on the monomer at pH 2. The objective of this study was to determine whether the net effect of these substitutions manifests in a change in the kinetics of self-assembly or morphology of fibrils. The study in Chapter 5 summarizes the effect of site substitutions in β -Lg A, B and C on different self-assembly processes, morphology and the composition of fibrils.

Recently Liu et al. (2013a) used lactosylated WPI to prepare fibrils with enhanced functional properties. The authors noted that the kinetics of fibril formation from glycosylated WPI remained unaffected but glycation reduced the yield of fibrils. However, information about the mechanism of β -Lg self-assembly could not be derived due to the complexity of starting material resulting from a composite mixture of proteins, as well as the harsh conditions of glycation. The effects of non-native structural constraints introduced by glycation or its consequent effect on self-assembly processes were not considered in that study.

Glycation of β -Lg not only affects its thermal unfolding but also its aggregation characteristics. Chapter 6 explores the self-assembly from glucosylated and lactosylated β -Lg. The objective of this study is to perturb self-assembly by introducing non-native constraints on the β -Lg molecule without affecting its native structure. The high specificity of lysine residues to undergo glycation during the initial stages was exploited to investigate the possible roles of amyloidogenic sequences during β -Lg self-assembly. This study compared the effect of glucosylation and lactosylation on the native structure and its unfolding, the kinetics of acid hydrolysis and self-assembly at two different degrees of glycation.

Chapters 7 and 8 investigate the effect of perturbing the aqueous environment composition on β -Lg self-assembly. Two types of co-solutes have been used to modify solution compositions: polyols, which have largely non-specific effects on proteins due to their influence on water structure, and β -casein, which exhibits chaperone-like activity. The study in Chapter 7 aims to investigate conditions that slow-down self-assembly by using polyols and allows for the decoupling of the self-assembly processes. This would allow a greater understanding about the underlying mechanisms and inter-relationships between these processes. Chapter 8 investigates how self-assembly was perturbed by the chaperone-like properties of β -casein. This study provides information about the alternative pathways available to the assembly-competent building blocks during their self-assembly. The schematic in Figure 1.1 gives a brief overview of the thesis chapters.

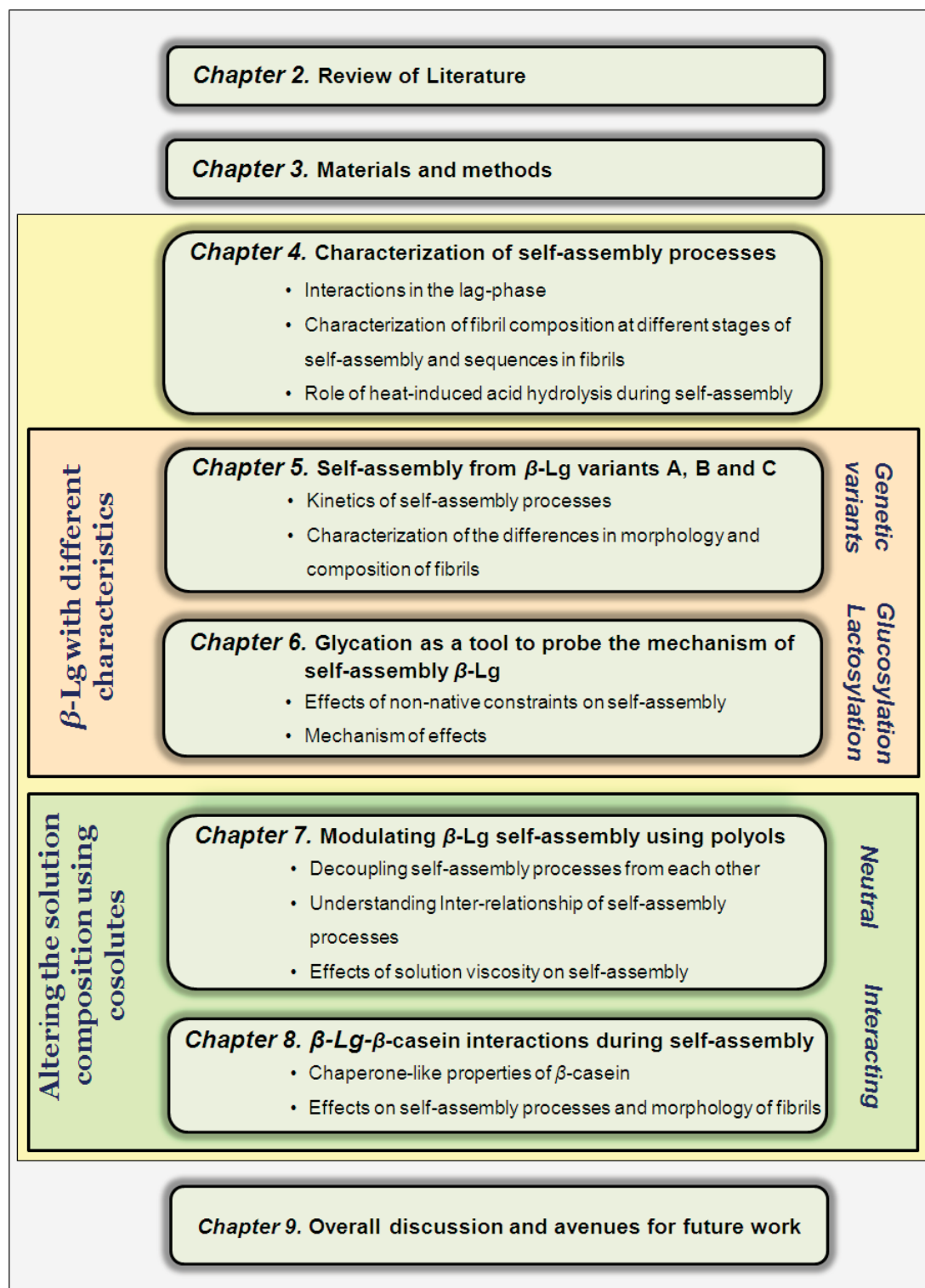


Figure 1.1 Overview of following thesis chapters.

Chapter 2

2. Review of literature

Bovine β -Lactoglobulin (β -Lg) is a major globular protein present in milk at concentrations of approximately 0.18 to 0.5% (w/v) (Sawyer, 2003). It has a molecular weight of 18.4 kDa and 162 amino acid residues in its primary structure. It has a well defined, secondary structure with nine anti-parallel strands and a three turn α -helix (Manderson et al., 1999; Molinari et al., 1996; Qi et al., 1997). The unique arrangement of β -strands forms a barrel-like structure (Jameson et al., 2002; Molinari et al., 1996; Uhrinova et al., 2000) resulting in a well defined tertiary structure which is stabilized by two disulfide bonds, between Cys66-Cys160 and Cys106-Cys119 (Brownlow et al., 1997; Qin et al., 1998a). β -Lg has a free thiol group at Cys121 which participates in inter-molecular thiol-disulfide exchange reactions responsible for the heat-induced aggregation of β -Lg at neutral pH (Hoffmann et al., 1997). β -Lg exhibits a pH-dependent reversible association behavior and is primarily monomeric at the extremes of pH (McKenzie et al., 1967; Townend et al., 1969; Townend et al., 1960).

The tertiary structure of β -Lg is extremely sensitive to heat-induced unfolding (Manderson et al., 1999) and heating results in partially unfolded monomers with a high proportion of secondary structure also termed as molten-globule like unfolded monomers (Cairolì et al., 1994; Iametti et al., 1996). At extremes of pH, the partially unfolded monomers aggregate into fibrillar aggregates upon continued heating (Langton et al., 1992). The fine-stranded fibrillar aggregates of β -Lg formed at low pH demonstrate typical characteristics of the amyloid fibrils formed *in vivo*, these

Chapter 2. Review of Literature

include, nucleation-dependent polymerization kinetics, characteristic X-ray diffraction pattern and ability to bind to amyloid-specific dyes like Congo Red and thioflavin T (Adamcik et al., 2010; Bromley et al., 2005).

This chapter is divided into three sections; the first section summarizes the general principles of amyloid formation and its inhibition. The important themes of investigations and underlying mechanisms have been discussed and these themes have been chosen to perturb the conditions of self-assembly in Chapters 5-8. The second part of this review discusses the native structure of β -Lg, heat-induced unfolding and aggregation processes. The studies based on the selected themes of the first section that investigate the properties of β -Lg have been specifically considered to gain possible insights into the effects on β -Lg self-assembly. Finally the current understanding of β -Lg self-assembly at pH 2, factors affecting self-assembly and the morphology of fibrils have been discussed in the third section.

2.1. Amyloid fibrils

The term “amyloid” was first used by Rudolph Virchow in 1858 to describe tissue deposits of cerebral corpora amylacea. These aggregates gave a positive iodine test leading to the conclusion that these deposits were structurally similar to starch. However, subsequent research showed that the amyloid deposits found by Virchow were primarily protein in nature (Cohen, 1986) and since then protein based fibrils have been implicated in a number of diseases in humans (Table 2.1) (Chiti et al., 2006). For diagnostic purposes, the International Society of Amyloidosis, defined amyloids as "extracellular deposition of protein fibrils with characteristic appearance in electron microscope images, typical X-ray diffraction patterns and an affinity for Congo red with concomitant green birefringence" (Westermarck et al., 2005).

Table 2.1 Human diseases associated with amyloid fibrils

Disease	Aggregating protein
<i>Neurodegenerative diseases</i>	
Alzheimer's disease	Amyloid β -peptide
Spongiform encephalopathies	Prion proteins and fragments
Parkinson's disease	α -synuclein
Dementia with Lewy bodies	α -synuclein
Frontotemporal dementia with Parkinson's disease	Tau
Huntington's disease	Huntington with polyQ expansion
<i>Nonneuropathic systemic amyloidosis</i>	
AL Amyloidosis	Immunoglobulin light chains or fragments
AA Amyloidosis	Serum amyloid fragments
Lysozyme amyloidosis	Mutants of lysozyme
Fibrinogen amyloidosis	Variants of fibrinogen α -chain
<i>Nonneuropathic localized diseases</i>	
Type II diabetes	Amylin
Cataract	γ -crystallins
Hereditary cerebral hemorrhage with amyloidosis	Mutants of amyloid- β peptide
Inclusion-body myotonia	Amyloid- β -peptide
Cutaneous lichen amyloidosis	Keratins

Adapted from Chiti et al. (2006).

Chapter 2. Review of Literature

As the biological processes of living organisms of different orders were understood in more detail, it became clear that different proteins that had no association with pathological conditions could form functionally active fibrillar aggregates. The important biological functions of fibrils include cell adhesion (Chapman et al., 2002), silk production (Iconomidou et al., 2000) and melanin production (Berson et al., 2003). In addition, structurally similar fibrils can be synthesized by the *in vitro* self-assembly of numerous proteins including those consumed as foods by humans. Thus, these findings prompted the idea that the ability to form ordered fibrillar structures may be a generic property of the polypeptide chain (Dobson, 1999).

To include these proteins, a structure based nomenclature was proposed by Nilsson (2004). According to this framework, in order to be classified as amyloid fibrils, aggregates must have fibrillar morphology and must exhibit two or more additional features which include seeded kinetics of formation, a high proportion of β -sheets, and ability to bind dyes thioflavin T (ThT), thioflavin S (ThS) or Congo Red (CR).

Interestingly, this framework also considers the properties of fibrils, including their ability to form three dimensional gel networks, solubility in denaturants and resistance to proteases (Nilsson, 2004). However, Fandrich (2007) defined amyloid fibrils solely on the basis of their characteristic structure. He stated that amyloid fibrils are aggregates with “ β -sheets ordered to an extent so that they give rise to a fibrillar overall organization” (Fandrich, 2007). The definition of Nilsson (2004) describing key features of amyloid fibrils has been widely accepted and has been routinely used to classify aggregates as 'amyloid fibrils'.

In the subsequent discussion, the term fibril refers to filamentous protein aggregates with a high proportion of anti-parallel cross- β structure. To allow differentiation, the

term 'amyloid proteins' or 'amyloids' refers to proteins whose fibrils have been implicated in pathological conditions and the term 'amyloid fibrils' refers exclusively to their fibrils. The fibrils from other proteins are referred to as 'amyloid-like' and the process of formation of amyloid or amyloid-like fibrils is referred to as 'self-assembly' or 'fibril formation'.

2.1.1. Defining characteristics of amyloid fibrils

Despite the differences in the type, or origin of the misfolded protein or the nature of system in which fibrils form, amyloid and amyloid-like fibrils have certain common characteristics. These characteristics have also been included in the definition of amyloid fibrils by Nilsson (2004).

2.1.1.1. Characteristic cross β -structure

Both amyloid and amyloid-like fibrils exhibit a remarkable similarity in their structure and display unique X-ray diffraction patterns with reflections at 4.7 to 4.8 Å (Figure 2.1, meridional direction) in the region parallel to fibril-axis, arising from the inter-chain spacing, and at 9 to 11 Å in the equatorial direction, arising from the inter-sheet spacing in the fibrils (Serpell, 2000). This distinctive diffraction pattern was first used to describe the arrangement of cross- β strands in silk fibres (Geddes et al., 1968) and has since been used to define the similar structure of fibrils in which β -sheets run perpendicular to the axis of the fibrils (Nelson et al., 2005; Sunde et al., 1997). The arrangement of side-chain residues in the anti-parallel β -sheets results in a repeated "cross-strand ladder" arrangement (Biancalana et al., 2010; Krebs et al., 2005) which facilitates the binding of amyloid-specific dyes, such as ThT, ThS and CR.

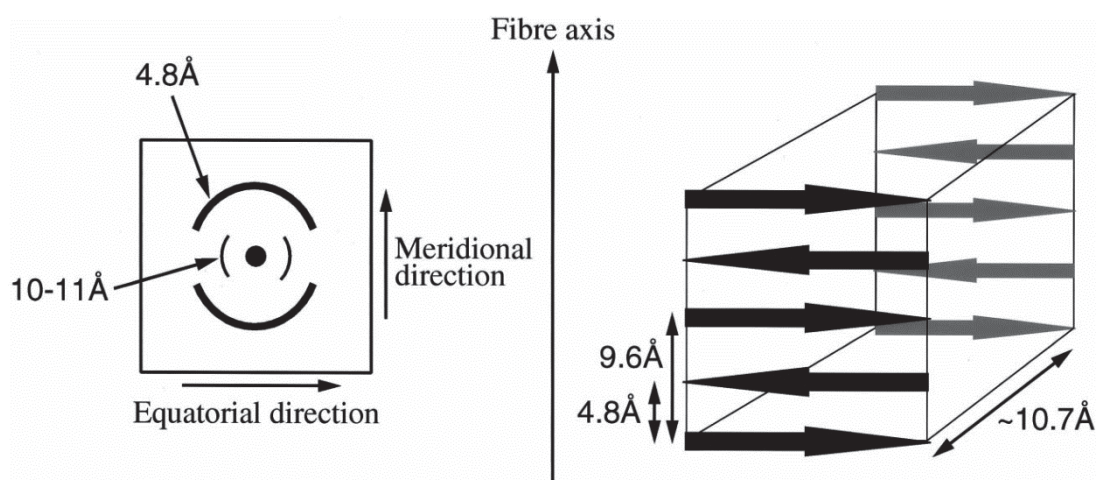


Figure 2.1 Schematic representation of characteristic X-ray fibre diffraction arising from the cross- β structure of fibrils. The distance between two β -strands is approximately 4.8 Å, while between the anti-parallel arrangements of β -strands is 9.6 Å. The distance between two β -sheets is 10-11 Å. Adapted from Serpell (2000).

2.1.1.2. Nucleation-dependent polymerization

The kinetics of protein self-assembly follows nucleation-dependent polymerization evident by a distinct initial lag phase followed by a period of exponential growth (Bromley et al., 2005; Chiti et al., 2006; Hamada et al., 2002). In order to self-assemble into fibrils, the protein must overcome the forces stabilizing its native structure and adopt either unfolded or misfolded conformation states. It must then diffuse to another unfolded molecule in the vicinity to form an intermediate capable of growth, referred to as a nucleus. The time required for the formation of nuclei is represented by the lag phase (Chiti et al., 2006). Jarrett et al. (1993) defined the lag phase as the duration for which the supersaturated solution of the protein remains kinetically soluble. The lag time can be drastically reduced by introducing mature fibrils which act as nuclei and promote self-assembly (Bolder et al., 2007a; Krebs et

al., 2004; Tanaka et al., 2005) or by altering the conditions of fibril formation (Mishra et al., 2007; Munishkina et al., 2008; Ow et al., 2013).

2.1.2. Structural basis for self-assembly

Under a given set of conditions, the amyloidogenicity of proteins shows wide variations, and proteins with very different native structures yield structurally similar fibrils. The intriguing question has been what causes proteins to form fibrils spontaneously? A number of approaches have been used to understand the factors that promote protein self-assembly. In this section, the major themes of relevant investigations will be discussed.

2.1.2.1. Role of amyloidogenic sequences

The structure of a protein is a manifestation of the sequential arrangement of the combination of the same 20 amino acids, and their properties. This led to the hypothesis that specific amino acid residues may have a tendency to promote fibril formation by their ability to facilitate the formation of β -sheets. Street et al. (1999) correlated the β -sheet formation propensity of amino acid residues with their side-chain composition. Residues with side-chains whose interaction with the polypeptide backbone was unfavorable promoted self-assembly. Amongst the different residues studied by these authors, branched (Ile, Val and Thr) and aromatic residues (Phe and Tyr) had a higher propensity to form β -sheets (Street et al., 1999). It should be noted that Pro residues in the sequence inhibit the formation of β -sheets and hence are frequently excluded from β -sheets domains of the proteins (MacArthur et al., 1991).

Another theme has been to understand the possible role of aromatic residues in promoting fibril formation (Azriel et al., 2001; Reches et al., 2003). Gazit (2002) compared short amyloidogenic sequences of unrelated proteins and noted that these

Chapter 2. Review of Literature

sequences had aromatic residues in their sequence. It was hypothesized that the π - π stacking involving aromatic residues plays an important role in molecular recognition and formation of ordered β -sheets in fibrils (Gazit, 2002; Kim et al., 2006; Makin et al., 2005). Further, a number of structurally similar small molecules consisting of aromatic ring structures, such as polyphenols (Porat et al., 2006), Congo red (Lorenzo et al., 1994; Pratim Bose et al., 2010) and the antibiotic drug tetracycline (Cosentino et al., 2005) inhibit the self-assembly of proteins into fibrils indicating an important role of aromatic residues in protein self-assembly.

However, Tracz et al. (2004) noted that the presence of aromatic residues is not necessary for self-assembly. In their study, the substitution of Phe by Leu in peptides of human amylin did not affect its ability to form fibrils. These authors concluded that the amyloidogenicity of a sequence not only depends on the composition of its residues but also on the size and hydrophobicity of the residues. Their hypothesis found support from a number of other studies (Armstrong et al., 2011; Bowerman et al., 2009; Cukalevski et al., 2012), that noted that aromatic residues were not necessary for fibril formation.

Another hypothesis was that the sequences showing an alternating pattern of polar and non-polar residues are particularly susceptible to fibril formation (Broome et al., 2000; West et al., 1999; Xiong et al., 1995). The blocks of residues within these sequences collectively contributed to the propensity to form fibrils. Tjernberg et al. (2002) proposed that the fibril-forming ability of proteins results from the propensity of short sequences capable of promoting β -sheet formation. Also, Hamada et al. (2009) reported that fragments of β -lactoglobulin (β -Lg) could self-assemble into fibrils and promote self-assembly of full-length β -Lg supporting this hypothesis. Substitutions within these assembly-promoting sequences may affect the kinetics of

self-assembly without affecting the ability of the sequence to form fibrils, e.g. substitutions Phe19Leu and Phe20Leu in amyloid β -peptide greatly affected the kinetics of self-assembly (Cukalevski et al., 2012).

Over the past decade, numerous attempts have been made to develop models for predicting sequences capable of forming fibrils. These models incorporate different orders of complexity of the systems, such as protein structure or solution conditions. Some examples of these models are, PASTA (Trovato et al., 2007), AMYLPRED (Frousios et al., 2009), Betascan (Bryan Jr et al., 2009) and FoldAmyloid (Garbuzynskiy et al., 2010). In spite of these attempts, no single universally accepted model capable of accurately predicting the amyloidogenicity of proteins exists, and the mechanisms of self-assembly still remain an intriguing area for researchers.

From the above discussion, it appears that the aromatic residues in the primary sequence favour but are not necessary for self-assembly. The substitution of residues in the amyloidogenic sequences may affect their propensity to form fibrils or affect assembly kinetics. This implies that genetic variants of the protein or polypeptides with engineered mutations may have varying propensities to form fibrils. Indeed, minor substitutions in the primary sequence of human lysozyme made it more prone to form amyloid fibrils (Pepys et al., 1993). The prediction of the ability of a given polypeptide sequence to form fibrils is extremely complex, and both short and long sequences of the same polypeptide may form structurally similar fibrils. Similarly, the prediction of fibril forming propensity in large proteins is difficult, since other factors such as the impact of its three-dimensional structure and its stability under the varying aqueous conditions need to be considered.

2.1.2.2. Role of protein structure

The conformation that a polypeptide adopts under a given set of conditions depends on thermodynamics governing protein folding. The stability of a given protein conformation is governed by the Gibbs free energy (ΔG). Under the given conditions of temperature and the nature of solution surrounding the protein, the polypeptide tends to assume conformations that minimize its ΔG . The ΔG of the native structure is minimum resulting in the most stable conformational state (Dobson, 1999; Dobson et al., 2001; Hartl et al., 2009). The structural stability of the native state is a net result of the equilibrium between attractive and repulsive forces. When this delicate balance is altered, the protein unfolds or folds into non-native transitional structures to compensate for the change in equilibrium. The transition from native to unfolded and then to aggregated states continues until the equilibrium is reached again and an aggregated state with a minimum ΔG is formed. It is possible to construct a free energy landscape of these transitions during protein folding, as shown in Figure 2.2.

Thus, in order to form fibrils the protein requires at least a partial destabilization of its native structure (Chiti et al., 2006; Dobson et al., 2001; Rochet et al., 2000; Uversky et al., 2004). This is particularly applicable to globular proteins in which potential amyloidogenic sequences may be buried in the interior of the native structure (Uversky et al., 2004). Experimental evidence for a number of globular proteins, including chicken egg white lysozyme (Mishra et al., 2007), bovine serum albumin (BSA) (Veerman et al., 2003c), β -Lg (Hamada et al., 2002) and α -lactalbumin (Goers et al., 2002) shows that these proteins require destabilization of the native structure for fibril formation.

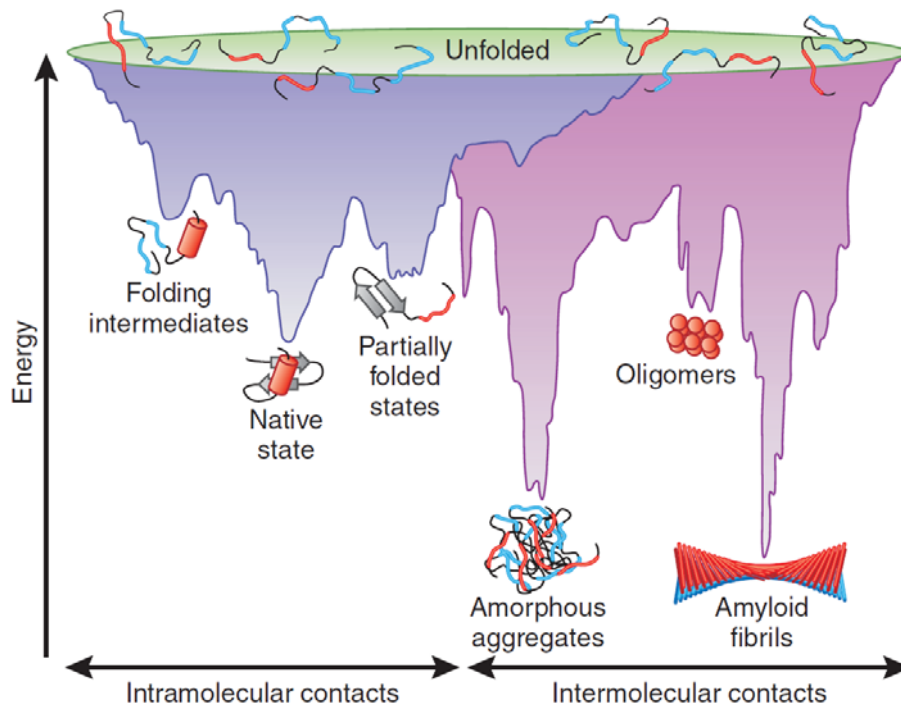


Figure 2.2 Free energy landscape of protein aggregation. The area in the pink region represents different transitional states during aggregation. Adapted from Hartl et al. (2009).

The free energy landscape in Figure 2.2 indicates that the transition from the misfolded state to the final aggregated state is complex and may involve a series of intermediates. In addition, the meta-stable intermediates have a number of competing aggregation pathways available for further growth (Dobson, 1999). These pathways are represented in Figure 2.3. In Section 2.1.3, the principles governing the choice of the self-assembly pathway have been discussed.

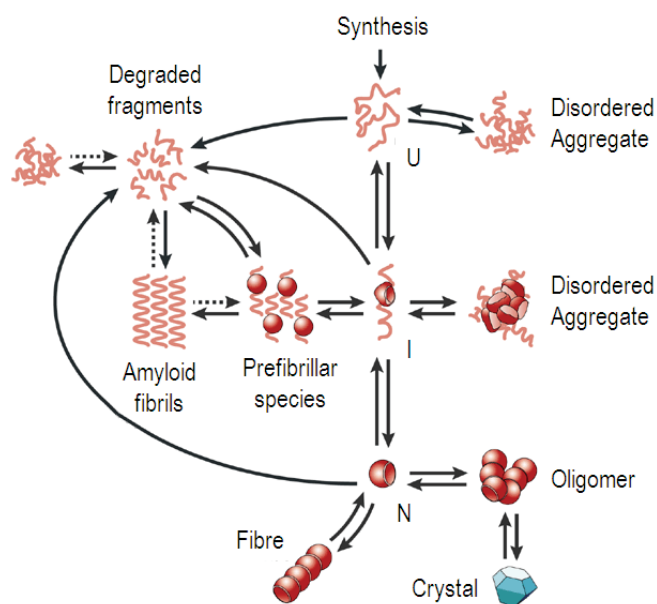


Figure 2.3 Aggregation pathways for misfolded proteins. *N*, *I* and *U* represent native, intermediate and unfolded polypeptide conformation states of the protein. Adapted from Dobson (2003a).

2.1.3. Factors affecting the self-assembly of proteins

The choice of aggregation via fibril formation over other pathways is governed by factors such as protein modification and prevailing aqueous conditions surrounding the destabilized protein molecule. For the ease of discussion, the factors affecting protein self-assembly have been grouped into those that promote self-assembly and those that inhibit self-assembly.

2.1.3.1. Factors promoting protein self-assembly

Protein modification has been reported to promote self-assembly, both *in vivo* and *in vitro*. Advanced glycation end products (AGE)-linked amyloid deposits have been isolated from affected tissues of patients suffering from Alzheimer's disease (Reddy et al., 2002). Glycation promoted self-assembly in bovine serum albumin (Bouma et al., 2003; Obrenovich et al., 2004) by AGE-induced protein cross-links. Similar

effects of protein modification have been reported for the *in vitro* self-assembly of amyloid- β peptide and tau (Loske et al., 2000). By comparison, the modification of the free amine groups of amyloidogenic proteins α -synuclein (Lee et al., 2009) and insulin (Oliveira et al., 2011) by the reactive dicarbonyl compounds (glyoxal and methylglyoxal) slowed their assembly into fibrils *in vitro*. It is hypothesized that the altered flexibility of the modified polypeptide backbone contributed to the inhibition of self-assembly of these proteins (Bouma et al., 2003; Lee et al., 2009).

Another important principle governing protein self-assembly is the effect of cosolutes in the aqueous medium. Proteins *in vivo* co-exist with a number of other bio-molecules and may collectively account for up to 40% of the total volume of the cell-fluid (Ellis, 2001; Zimmerman et al., 1993). In such a system, no single molecule has a distinctly high concentration and hence such systems are termed as “crowded” rather than “concentrated” (Minton, 1997). Molecular crowding affects protein self-assembly by the volume exclusion principle (Minton, 1997). The volume exclusion effect is defined as the repulsive steric effect arising from the crowded environment, forcing protein molecules to adopt folded states that minimize the opposing effect (Minton, 1997; Ralston, 1990).

Crowding by inert macromolecules accelerated the *in vitro* self-assembly of a number of proteins including bovine core histone proteins, α -synuclein, S-carboxymethylated α -lactalbumin (Munishkina et al., 2008), tau (Qian et al., 2012), β -Lg (Ma et al., 2013) and MET-16 (Sukenik et al., 2012; Sukenik et al., 2011). By comparison, an opposite effect was noted for insulin for which molecular crowding delayed self-assembly (Munishkina et al., 2008). It has to be noted that structurally similar fibrillar aggregates could be produced from the same protein by different pathways (Bromley et al., 2005; Hamada et al., 2002).

Chapter 2. Review of Literature

Thus, composition of the aqueous medium plays a decisive role during protein self-assembly but the mechanism of this effect is complex and not yet fully understood.

To counter the effects of stress conditions, there are several mechanisms *in vivo* that ensure correct folding and stability of the native protein structure.

2.1.3.2. Factors inhibiting protein self-assembly

To prevent extensive *in vivo* protein misfolding, Nature has designed protective mechanisms which stabilize the proteins against misfolding and their aggregation. In this section, two important mechanisms: role of structure-stabilizing cosolutes and molecular chaperones have been considered. The structure-stabilizing cosolutes are small molecules which include amino acids (Arakawa et al., 1983), salts (Arakawa et al., 1982a; Boye et al., 1996), and polyols and sugars (Anuradha et al., 2008; Arakawa et al., 1982b; Back et al., 1979; Cioci, 1996; Gekko et al., 1981b; Gerlsma, 1968, 1970; Kaushik et al., 1998). In this review, the discussion is restricted to the effect of polyols, which formed a major part of experimental work (Chapter 7).

Polyols are polyhydroxy sugar-alcohols and form miscible solutions with water. The mechanism of protein stabilization by polyols can be explained by the phenomena of preferential exclusion (McClements, 2002; Timasheff, 1993). Polyols remain excluded from the surface of the protein, resulting in a zone of exclusion around the protein in which only water molecules are permitted. At a molecular level, the preferential exclusion of polyols arises from two phenomena: a) steric exclusion and b) differential exclusion (McClements, 2002; Timasheff, 1993). Steric exclusion is a non-specific effect that results from polyol molecules being larger than water molecules. The second effect is related to the strong affinity of polyols for hydrogen-bonded water molecules, a moderate affinity for protein polar groups and a strong phobia towards protein nonpolar groups. These interactions of polyols with protein

and water molecules are collectively termed as differential interactions (McClements, 2002; Timasheff, 1993).

Another effect contributing to the protein stabilization by polyols is the increase in the surface tension of the aqueous solutions brought about by polyols (Chanasattru et al., 2008; Kaushik et al., 1998). However, this effect is not applicable universally since glycerol decreases the surface tension of aqueous solutions and yet stabilizes protein structure (Gekko et al., 1981a; Timasheff, 1998). Glycerol may partly penetrate into the solvation layer surrounding the proteins, especially at higher concentrations because of its relatively small size and slightly amphiphilic character (Gekko et al., 1981a, 1981b; Vagenende et al., 2009). The contact of the nonpolar residues in the unfolded protein with aqueous solution containing polyols is thermodynamically unfavorable and hence folded polypeptide conformation states which minimize this contact are favored (Kamiyama et al., 1999; Timasheff, 1998).

The effect of polyols varies with the type of protein and the stage of self-assembly. Glycerol stabilized the native structure of insulin, and thereby delayed nucleation for the fibril formation (Grudzielanek et al., 2005). Both glycerol and sorbitol had similar effects on a synthetic β -hairpin peptide MET16, but they also increased the final yield of fibrils (Sukenic et al., 2012; Sukenic et al., 2011). Using glycerol and sorbitol these authors noted that the self-assembly of peptide MET16 was not diffusion-limited. For amyloid- β peptide, glycerol accelerated the transition from random coil to β -sheet-rich structures, thereby stimulating fibril formation (Yang et al., 1999). The effects of polyols on the self-assembly of β -Lg is not known.

In addition to the small molecule osmolytes, another mechanism which prevents self-assembly of proteins *in vivo* is chaperone-mediated protein folding. In cells, there are

Chapter 2. Review of Literature

specific functional proteins whose primary role is to identify aggregation-prone conformations of other proteins and ensure their correct folding (Ellis, 1988; Hartl et al., 2002). These proteins are termed as molecular chaperones. Molecular chaperones are defined as a “class of cellular proteins whose function is to ensure that the folding of certain other polypeptide chains and their assembly into oligomeric structures occur correctly” (Ellis, 1988). In order to be classified as a molecular chaperone, the chaperone protein must be necessary for the correct folding or assembly of the target protein but must not be a component of the assembled protein structure (Ellis, 1993).

Thus, during chaperone-assisted protein folding the number of accessible aggregated states on the free energy landscape of Figure 2.2 are minimized and the protein folding is funnelled towards the correctly folded state with minimum free energy (Jahn et al., 2005). In biological systems, the proteins which function as molecular chaperones include small heat shock proteins (sHsps) (Muchowski et al., 2005) and clusterin (Carver et al., 2003; Humphreys et al., 1999).

2.2. β -Lactoglobulin

Bovine β -Lactoglobulin (β -Lg) is a major globular protein present in milk at concentrations of approximately 0.18 to 0.5% (w/v) (Sawyer, 2003). The exact biological role of β -Lg is not known but it belongs to a large group of proteins known as lipocalins that are capable of binding hydrophobic ligands (Perez et al., 1989), such as retinol or retinoic acid (Kontopidis et al., 2002) or 12-bromododecanoic acid (Qin et al., 1998a). β -Lg has remained a protein of interest to food scientists due to its effect on physicochemical properties of milk and milk products. Its interaction with κ -casein results in delayed rennet clotting time (Dalgleish, 1990), and the proximity of its denaturation temperature to that employed for thermal treatments has made it an indicator protein for milk processing conditions (Dannenberg et al., 1988).

2.2.1. Native structure

Bovine β -Lg has a molecular weight of 18400 Da and a monomer-diameter of approximately 18 Å (Green et al., 1979; Verheul et al., 1999). It has 162 residues consisting of all the 20 amino acids in its primary sequence (Sawyer, 2003), and shows substantial homology with the sequence of lipocalins involved in the transport of hydrophobic ligands (Pervaiz et al., 1985). β -Lg has a free thiol group at Cys121 and two disulfide bonds, between Cys66-Cys160 and Cys106-Cys119 (Brownlow et al., 1997; Qin et al., 1998a).

β -Lg has a high proportion of β -sheets in its secondary structure comprising up to 50% of the protein conformation, the rest being 10% α -helix and 35% random coils determined from its far-UV (FUV) circular dichroism spectroscopy spectra (Qi et al., 1997). The β -sheets are primarily found on the 9 anti-parallel β -strands designated as

Chapter 2. Review of Literature

strands A to I, and their arrangement results in a three dimensional barrel-like structure also called the β -barrel or the β -calyx (Brownlow et al., 1997). The three-turn α -helix is located between β -strands H and E on the outside of the β -barrel in the C-terminal region of β -Lg. The random coils are mostly found on the structure-stabilizing flexible loops connecting the different β -strands in the structure (Jameson et al., 2002). The locations of the different elements of the tertiary structure are shown in Figure 2.4.

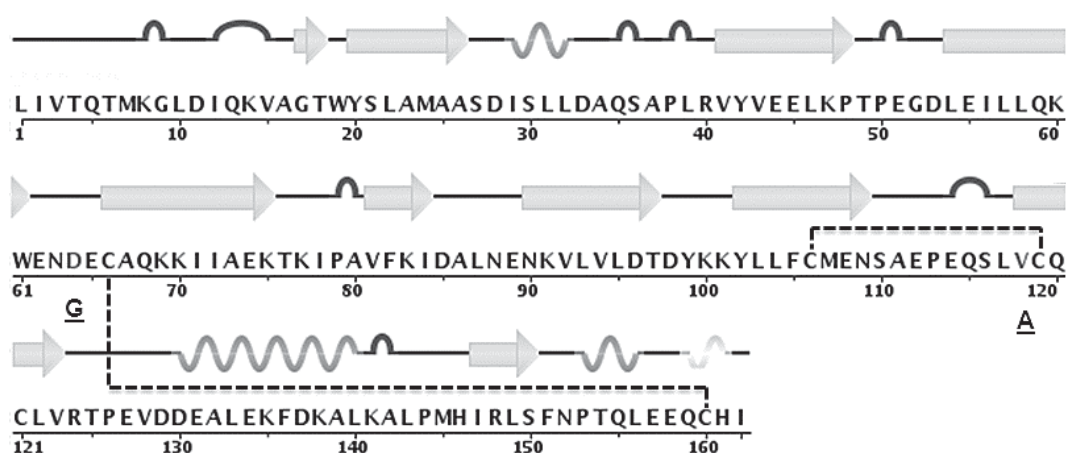


Figure 2.4 Sequence of β -Lg A (Variant B shows presence of glycine instead of aspartic acid at residue 64 and alanine instead of valine at residue 118) adapted from the Protein Data Bank[®] (PDB ID 1BSO) (Qin et al., 1998a). Dotted lines indicate disulfide bonding. Solid arrows indicate β -strands; waveforms indicate helices and arches indicate loops.

The tertiary structure of β -Lg has been characterized in fine detail by different methods, including CD and NMR spectroscopy and X-ray crystallography. The near UV (NUV) CD spectrum of β -Lg is characterized by two sharp troughs at about 286 and 293 nm that are due to Trp19 (Manderson et al., 1999). Small troughs observed in the region between 262 and 269 nm are attributed to Phe residues (Strickland, 1974; Woody, 1978). The tertiary structure is stabilized by the two disulfide bonds between, Cys66-Cys160 linking the flexible CD loop to the outside of the β -barrel in

the C-terminal region, and Cys106-Cys119 linking the strands G and H (Brownlow et al., 1997; Qin et al., 1998a).

The free Cys121 residue is located on strand H and is hidden between strand H and the α -helix in the native β -Lg structure (Brownlow et al., 1997; Qin et al., 1998a). The reduction of the native disulfide bonds does not affect the native structure of β -Lg (Burova et al., 1998), however the effect of reduction followed by modification of cysteine residues in β -Lg depends on the modifying agent used (Iametti et al., 1996; Sakai et al., 2000). The modification of Cys121 in the native β -Lg alters its association properties (Iametti et al., 1996).

The stability of the native structure is a net result of the equilibrium between forces that stabilize the native structure e.g. hydrophobic interactions, hydrogen bonds or van der Waals interactions and those that oppose folding e.g. steric effects of side chain residues (Creighton, 1993; Damodaran, 1996). The hydrophobic non-polar residues remain buried inside the native structure (Tanford, 1991) which minimizes their thermodynamically unfavorable contact with the aqueous solution (Privalov et al., 1993). The polar residues are retained on the surface in contact with the aqueous solution stabilizing the globular structure (Damodaran, 1996).

β -Lg exhibits pH-dependent reversible structural transitions in its tertiary and quaternary structures. One of the most important changes in the tertiary structure occurs between pH 6 and 8 and is called the Tanford transition. This reversible transition in the native structure is characterized by a low sedimentation coefficient of β -Lg (Pedersen, 1936), an increase in optical levo-rotation (Groves et al., 1951) and change in the titration behavior of β -Lg (Tanford et al., 1959). Qin et al. (1998b) proposed that these changes resulted from the pH-dependent transitions of loop EF

Chapter 2. Review of Literature

(residues 85-90). At acidic pH, the EF loop is placed over the calyx, but rearranges itself by moving aside to expose the calyx at alkaline pH (Qin et al., 1998b). These authors hypothesized that this pH-dependent structural transition may have a role to play in protecting the ligands bound in the calyx from the acidic conditions of stomach (Qin et al., 1998b) since native β -Lg remains largely undigested by the proteolytic enzyme pepsin (Peram et al., 2013). The structural changes in the native structure of β -Lg at pH >8 are irreversible (Groves et al., 1951; Taulier et al., 2001).

The quaternary structure of β -Lg also exhibits a pH-dependent association behavior. At low ionic strengths and neutral pH, β -Lg exists as stable non-covalently-linked dimer (Uhrinova et al., 2000) stabilized by hydrophobic interactions (Mercadante et al., 2012). Between pH 5.5 and 3.5, dimers associate to form octamers (Casal et al., 1988; McKenzie et al., 1967). Below pH 3.5 (Townend et al., 1969; Townend et al., 1960), and above 7.5 (McKenzie et al., 1967) the dimers dissociate and β -Lg primarily exists as monomers due to high electrostatic repulsion (Aymard et al., 1996; Mercadante et al., 2012; Molinari et al., 1996). These pH-dependent transitions in the quaternary structure are represented in Figure 2.5.

The factors affecting pH-dependent association of β -Lg include protein concentration (McKenzie, 1971; Verheul et al., 1999), genetic variation (Thresher et al., 1997), ionic strength of the medium (Aymard et al., 1996; Renard et al., 1998; Sakurai et al., 2001; Verheul et al., 1999) and temperature (Aymard et al., 1996; Verheul et al., 1999). Reduction of disulfide bonds, followed by their thiolation, produced β -Lg with modified properties. Thiolated β -Lg retained a native-like structure at acidic pH, but became partially unfolded at neutral pH (Sakai et al., 2000).

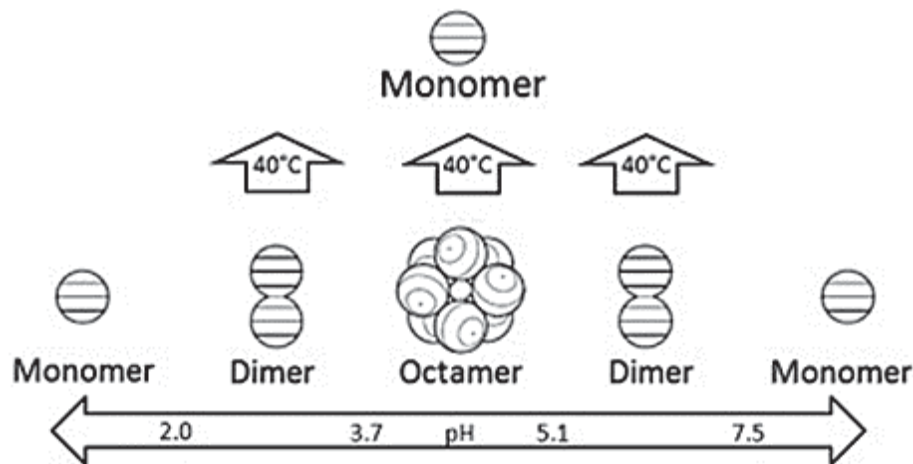


Figure 2.5 pH-dependent reversible association behavior of β -Lg. Adapted from Cheison et al. (2011).

At pH below its isoelectric point, the native structure of β -Lg shows high resemblance to that at neutral pH (Belloque et al., 1998; Casal et al., 1988; Matsuura et al., 1994; Uhrinova et al., 2000). The native structure of β -Lg is comparatively rigid at low pH imparting high structural stability (Boye et al., 1997; Jameson et al., 2002). Under these conditions, β -Lg retains the proportion of different elements of the secondary structures (Casal et al., 1988) and the three dimensional β -barrel fold (Ragona et al., 1997). However, minor transitions in the secondary structure of β -Lg have been noted at very low pH (< 2.0) (Taulier et al., 2001).

2.2.2. Genetic variants of β -Lg

Around 13 variants of β -Lg have been isolated from bovine milk (Sawyer, 2003), but β -Lg commonly exists as a mixture of polymorphic forms A and B (Creamer et al., 1997). β -Lg C, although found less commonly in milk, has been extensively used to compare its properties with that of variants A and B. For the purpose of this review and subsequent work, the discussion will be restricted to β -Lg A, B and C. β -Lg A has Asp at position 64 and Val at 118 instead of Gly and Ala in β -Lg B and C respectively, while β -Lg C has His at position 59 instead of Gln in β -Lg B (Bell et

Chapter 2. Review of Literature

al., 1968; Bewley et al., 1997; Kalan et al., 1965). Table 2.2 summarizes the differences between β -Lg A, B and C.

Table 2.2 Sites of differences in β -Lg A, B and C.

Residue	β -Lg A	β -Lg B	β -Lg C
64	Asp	Gly	Gly
118	Val	Ala	Ala
59	Gln	Gln	His

The substitutions of amino-acids in β -Lg A, B and C do not affect their secondary (Manderson, 1998) and tertiary structures (Bewley et al., 1997; Monaco et al., 1987), although they have a marked effect on a number of physicochemical properties e.g. monomer-dimer dissociation (Thresher et al., 1997; Verheul et al., 1999), the heat stability (Boye et al., 2004; Boye et al., 1997; Gough et al., 1962; Huang et al., 1994a; Huang et al., 1994b; Imafidon et al., 1991; Manderson et al., 1999; McSwiney et al., 1994; Nielsen et al., 1996; Qin et al., 1999) and properties of aggregates formed upon heating at neutral pH (Manderson et al., 1999).

2.2.3. Heat-induced unfolding of β -Lg

Destabilization or the unfolding of the native structure requires a shift in the equilibrium of forces stabilizing the native structure to overcome the constraints that oppose unfolding. The Gibbs free energy of unfolding of globular proteins decreases with an increase in temperature and becomes negative above the denaturation temperature resulting in spontaneous unfolding of the protein structure (Privalov et al., 1993).

The thermal stability of the native structure of β -Lg is strongly dependent on the pH of the solution. At pH 7 and at 20 °C, β -Lg exists as a dimer which dissociates into monomers when the temperature reaches 60 °C. In this temperature range, heating results in the swelling of the β -Lg monomers and a slight increase in the surface hydrophobicity (Cairolì et al., 1994), but these modifications in the tertiary structure at <60 °C are reversible (Cairolì et al., 1994; Iametti et al., 1996; Mills, 1976). Heating beyond 60 °C results in rapid irreversible loss of tertiary structure (Cairolì et al., 1994; Iametti et al., 1996; Prabakaran et al., 1997).

The secondary structure of β -Lg exhibits remarkable thermal stability and remains unaffected until the temperature reaches 60 °C (Casal et al., 1988; Prabakaran et al., 1997). Heating at temperatures >60 °C resulted in slight decrease (up to 18%) in the β -sheet content (Casal et al., 1988; Prabakaran et al., 1997; Qi et al., 1997). Prabakaran et al. (1997) found that the loss of β -sheets at 60 to 65 °C coincided with the appearance of disulfide-linked aggregates at this temperature. The enhanced reactivity of the free Cys121 at this temperature along with the reduction of β -sheet content indicate that the changes in the secondary structure were restricted to the β -strand H containing the free Cys121, and nearby β -strands E-G (Prabakaran et al.,

Chapter 2. Review of Literature

1997). At temperatures of 60-75 °C, the exposed α -helix in the β -Lg monomers unfolds, while continued heating above 75 °C results in the melting of the β -calyx (Belloque et al., 1998; Euston et al., 2007; Qi et al., 1997).

A few studies have investigated the role of native disulfide bonds and the free Cys121 residue on heat-induced unfolding of native structure. The reduction of disulfide bonds does not affect the denaturation temperature of β -Lg (Belloque et al., 1998; Harwalkar et al., 1992). Similarly, Beringhelli et al. (2002) found no major difference in the kinetics of unfolding when disulfide bonds were reduced. However, modification of Cys121 by iodoacetamide protected β -Lg against thermal unfolding at 70 °C (Iametti et al., 1996).

β -Lg exists as a monomer at pH 2 and its native structure is comparatively more resistant to thermal (Kella et al., 1988) as well as non-thermal unfolding (Sakai et al., 2000) than the native structure at neutral pH. Under these conditions, a relatively high temperature (>78 °C) is necessary for destabilization of the native structure (Bryant et al., 1998) as the native structure is stabilized by flexibility of loops (Jameson et al., 2002) and disulfide bonds (Papiz et al., 1986). The unfolded β -Lg monomers are more compact than their counterparts at neutral pH and retain a significant proportion of their secondary structure upon unfolding (Boye et al., 1996). Modification of Cys121 resulted in a slight decrease (of 5 to 7 °C) in thermal denaturation temperature at pH 2 (Burova et al., 1998).

The heat-induced disruption of the tertiary structure exposes the hydrophobic interior of the β -Lg molecule. The partially unfolded structure of the β -Lg monomer that retains a large proportion of secondary structure is referred to as molten globule-like

(Cairolì et al., 1994; Iametti et al., 1996; Qi et al., 1997). This structure is extremely prone to aggregation (Cairolì et al., 1994; Casal et al., 1988; Iametti et al., 1996).

2.2.4. Heat-induced aggregation of β -Lg

At >70 °C, the highly reactive molten-globule state can aggregate by a number of different pathways (Gerrard, 2002). At neutral pH, the primary pathway for the heat-induced aggregation of β -Lg is by intermolecular thiol-disulfide exchange leading to polymers of β -Lg (Schokker et al., 1999) especially at lower temperatures (<70 °C) (Hoffmann et al., 1997; Roefs et al., 1994). The interaction of the exposed thiol group (Cys121) in the molten-globule with Cys66-Cys160 or Cys109-Cys119 of the same molecule is sterically unfavorable (Gezimati et al., 1997). In order for aggregation to proceed, the exposed thiol group of one unfolded β -Lg monomer should be in the close vicinity of the disulfide bond of another unfolded monomer which would thermodynamically facilitate their interaction (Gezimati et al., 1997). However, several studies have subsequently provided evidence of intramolecular thiol-disulfide exchange reactions, leading to re-distribution of disulfide bonds in β -Lg, formed during heat treatment (Manderson et al., 1998; Morgan et al., 1997; Schokker et al., 1999). Modification of Cys121 inhibited formation of disulfide-linked polymers (Iametti et al., 1998; Iconomidou et al., 2008).

Heating results in the formation of non-native monomers, disulfide-linked dimers, trimers and tetramers linked by both disulfide and non-covalent interactions (Bauer et al., 2000; Iametti et al., 1996; Manderson et al., 1998; Prabakaran et al., 1997; Schokker et al., 1999; Zuniga et al., 2010). During the inter-molecular disulfide exchange reactions, the aggregates have more than one free reactive thiol groups which promote aggregation by complex aggregation pathways (Schokker et al.,

Chapter 2. Review of Literature

1999). Schokker et al. (1999) proposed that the interactions of monomers, dimers and tetramers with the aggregates are more favorable than interactions with another of the same species, resulting in rapid aggregation. A few studies have noted that the disulfide-linked non-native dimers play an important role in formation of large polymers (Bauer et al., 2000; Manderson et al., 1998; Prabakaran et al., 1997).

Apart from thiol-disulfide exchange reactions, non-covalent interactions have been reported to play an important role during β -Lg aggregation (Galani et al., 1999; Gezimati et al., 1997; Hoffman et al., 1999; Hoffmann et al., 1997; Manderson et al., 1998; Schokker et al., 1999). The contribution of non-covalent interactions becomes particularly significant at higher temperatures (90 to 100 °C) (Galani et al., 1999). Shimada et al. (1989) proposed that heat-induced aggregation of β -Lg occurs in two stages: the first stage consists of aggregation via thiol-disulfide exchange reactions and is completed within the first few minutes of heating. The second stage is the formation of intermolecular hydrophobic linkages resulting in a three-dimensional network (Shimada et al., 1989).

In comparison, the native structure of β -Lg is highly stable to heat at low pH (Boye et al., 1997; Kella et al., 1988). Once the β -Lg monomers are unfolded, the low pH has a profound effect on their aggregation properties. At low pH, β -Lg has a net positive charge (+20 at pH 2) which results in a high electrostatic repulsion (Aymard et al., 1999). In addition, at low pH the thiol group of the free cysteine residue in β -Lg remains protonated and hence the likelihood of intermolecular thiol-disulfide formation is greatly reduced (Alting et al., 2002; Otte et al., 2000). Aggregation under such conditions primarily proceeds via non-covalent interactions (Shimada et al., 1989). Another important phenomenon occurring during heating proteins at low pH is their heat-induced acid hydrolysis (Inglis, 1983). The mechanism of heat-

induced acid hydrolysis and studies noting acid hydrolysis of β -Lg during heating at low pH are discussed in Section 2.3.

2.2.5. Factors affecting thermal aggregation of β -Lg

The aggregation kinetics and the characteristics of the aggregates strongly depend on factors, such as protein concentration (Elofsson et al., 1996) and ionic strength of the aqueous medium (Renard et al., 1998). High protein concentrations affect the heat stability of β -Lg (Nielsen et al., 1996), favor formation of intermolecular disulfide bonds (Iametti et al., 1995), increase aggregate size (Hoffmann et al., 1997), alter the microstructure of gels (Langton et al., 1992) and their rheological characteristics (McSwiney et al., 1994).

The structure of β -Lg is stable to changes in ionic strength at room temperature (Boye et al., 1996). High salt concentration at neutral pH stabilizes β -Lg against thermal unfolding (Haug et al., 2009) reduces its critical gelation concentration (Baussay et al., 2004) and alters the microstructure of gels (Renard et al., 1992). Increasing ionic strength screens the charges on β -Lg monomers and this facilitates their aggregation (Schokker et al., 1999). Similar effects of ionic strength on the aggregation kinetics have been reported for β -Lg aggregation at low pH, and these have been discussed in detail later in Section 2.3.

2.2.5.1. Genetic variation

A number of studies have reported differences in the heat stability and the aggregation propensities of β -Lg A, B and C. These studies could be divided into two groups, based on the findings of Nielsen et al. (1996). The first group of studies use β -Lg (<5%, w/v) and report that the heat stability of β -Lg variants (concentration < 5%, w/v) follows the order: β -Lg C > β -Lg A > β -Lg B (Bikker et al., 2000; Gough et al., 1962; Manderson et al., 1999; Nielsen et al., 1996; Qin et al., 1998b). In contrast, Huang et al. (1994b) have noted a reverse trend for β -Lg A and B (stability of B > A) at low concentrations (2% w/v). The second group used β -Lg concentration in excess of 5% w/v and report that the order of stability was β -Lg C > β -Lg B > β -Lg A (Imafidon et al., 1991; McSwiney et al., 1994; Nielsen et al., 1996).

The differences in the heat stabilities of β -Lg A, B and C have been attributed to the differences in their primary sequences (Qin et al., 1998b). These authors proposed that a salt bridge between residues Glu44 and His59 in β -Lg C imparts higher structural stability to β -Lg C as compared to β -Lg A and B. Similarly, the substitution of Ala118 with Val in β -Lg A improves the hydrophobic packing around the site of substitution which imparts better conformational stability to the monomer (Qin et al., 1998b). In addition, the Asp64 is located on an exposed loop between β -strands C and D and this may enhance the possibility of its interaction via salt bridge (McSwiney et al., 1994; Qin et al., 1999). However, the differences in the heat stability of β -Lg reported in different studies may also be attributed to the diversity in the experimental conditions used such as the analysis method used to measure denaturation, buffer conditions, pH, ionic strength used in those studies (Boye et al., 2004; Huang et al., 1994b; Nielsen et al., 1996).

The substitutions in β -Lg A, B and C greatly affect the properties of the aggregates of these proteins. Using a combination of electrophoresis techniques, Manderson et al. (1998) reported that the aggregates of β -Lg A contained a higher proportion of unfolded monomers linked by non-covalent interactions. Similarly, Boye et al. (2004) found that although β -Lg B was more heat-stable than β -Lg A, its stability to chaotropes was slightly lower than that of β -Lg A.

2.2.5.2. Effects of polyols

The mechanism of protein stabilization by polyols is discussed in Section 2.1.3.2. Polyols affect the heat-induced aggregation of β -Lg by stabilizing the protein structure against unfolding or indirectly by their effects on the properties of the medium surrounding the protein. Experimental studies have shown that at neutral pH sucrose increased the thermal denaturation temperature (T_m) of WPI by 8 °C (40% w/v) (Kulmyrzaev et al., 2000a), and sorbitol increased T_m by approximately 10 °C (Chanasattru et al., 2007a). The increase in the stability brought about by these osmolytes was attributed to a strong steric exclusion effect arising from their larger size (Chanasattru et al., 2007a; Kulmyrzaev et al., 2000a). In comparison, glycerol does not affect the T_m of β -Lg which has been attributed to its smaller size (Chanasattru et al., 2007a, 2008; Tiwari et al., 2006), and its weaker differential interaction effects (Baier et al., 2004; Chanasattru et al., 2008). Studies using other globular proteins including bovine serum albumin (Baier et al., 2004; Baier et al., 2003), lysozyme (Back et al., 1979) and ovalbumin (Back et al., 1979), show a similar trend indicating a stronger effect of sorbitol or sucrose on thermal unfolding than that of glycerol. Interestingly, Anuradha et al. (2008) did not find any difference in the heat stability of β -Lg in presence of the sucrose and sorbitol (0-

Chapter 2. Review of Literature

40%, w/v) at pH 7.9 but glycerol at the same concentrations increased the T_m by approximately 10 °C. The reason for this apparent discrepancy is not known.

After unfolding of protein molecules, polyols may modulate the aggregation propensity of β -Lg and the properties of the aggregates by two possible mechanisms. Due to their ability to stabilize hydrophobic interactions by extensive hydrogen bonding around the protein, polyols promote the formation of associated states that minimize the exposure of hydrophobic groups to the polyols. In addition, polyols increase the viscosity of the aqueous solutions which may have a detrimental effect on diffusion-limited reactions and limit the frequency of protein-protein interactions (Kulmyrzaev et al., 2000a). However, it is difficult to decouple these two effects, i.e. the decoupling their effects on diffusion-limited reactions from that of the creation of aggregation-prone species.

2.2.5.3. Glycation

Glycation or non-enzymatic browning of β -Lg by the Maillard reaction involves the interaction of the reactive side-chain amine groups with the free carbonyl groups of the reducing sugars. The details of the various steps involved in Maillard reaction of milk proteins and their mechanism have been a subject of extensive reviews (Gras et al., 2008; Waterhouse et al., 2004) and will not be considered here. Chemical modification of β -Lg by the Maillard reaction has been used as a tool to modify its functional properties (Chevalier et al., 2001b; Medrano et al., 2009; Nacka et al., 1998).

β -Lg has 19 free amine groups (15 from lysine and 3 from arginine residues and the N-terminal amine group) that can participate in the Maillard reaction. Glycation of these residues takes place sequentially exhibiting a marked specificity. Studies using

lactosylated β -Lg have noted that lysines at residues 47, 91 and 100 are glycosylated first followed by the glycosylation of other lysines and the N-terminal amine group and finally the amine groups of arginines (Fenaille et al., 2004; Fogliano et al., 1998; Morgan et al., 1998; Morgan et al., 1999a; Morgan et al., 1999b). This site-specificity of lysine glycosylation has been attributed to a higher exposure of these residues to the solvent and location of another positively charged lysine in their vicinity (Fogliano et al., 1998).

Glycosylation of β -Lg can be achieved by incubating the protein-sugar mixture at pH 7 under controlled conditions in the dry state or aqueous state (Chevalier et al., 2001a; Morgan et al., 1999a). Dry glycosylation or solid-state glycosylation of β -Lg is much faster than aqueous glycosylation, and retains all the native-like characteristics, including its structure (Morgan et al., 1999a; Morgan et al., 1999b; van Teeffelen et al., 2005) and its association tendency (Morgan et al., 1999b). Dry glycosylation of β -Lg yields a heterogeneous mixture of glycoforms that differ in the degree and sites of glycosylation (Morgan et al., 1997). In contrast, aqueous glycosylation induces significant changes in the native β -Lg structure (Chevalier et al., 2002; Morgan et al., 1999b) and leads to sugar-induced protein cross-linking (Da Silva Pinto et al., 2012; Morgan et al., 1998; Morgan et al., 1999b). Subsequent discussion has been restricted to solid state-glycosylation with simple sugars.

Glycosylation of β -Lg improves its heat stability and the thermal denaturation temperature of β -Lg by about 5-8 °C (Broersen et al., 2004; Liu et al., 2013b; Medrano et al., 2009; Mulsow et al., 2009; van Teeffelen et al., 2005). Although glycosylation of β -Lg increased its T_m by 5 °C, it reduced the Gibbs free energy of unfolding by 20% and heat capacity (ΔC_p) by approximately 60% as compared to that of unglycosylated β -Lg (van Teeffelen et al., 2005). These authors attributed the

Chapter 2. Review of Literature

marked decrease in the ΔC_p to the differences in the hydration of non-polar residues and the interactions of bound sugars that protected the non-polar groups from aqueous solvent phase. Broersen et al. (2004) noted that the glycation was more effective in stabilizing the native β -Lg secondary structure than the tertiary structure.

Glycation of β -Lg lowers its isoelectric point (Broersen et al., 2007; Liu et al., 2013b) decreases its surface hydrophobicity (Medrano et al., 2009; Mulsow et al., 2009) and hence decreases the chances of protein-protein encounters via hydrophobic interactions (Broersen et al., 2004). In addition, the large sugar residues exhibit a significant steric effect and inhibit inter-molecular protein aggregation (Liu et al., 2013b; Mulsow et al., 2009).

2.2.5.4. Chaperone-like properties of β -casein

A number of properties of caseins are similar to those of small heat-shock proteins (Morgan et al., 2005; Yong et al., 2010). These include similar molecular weights, the ability to form oligomers and the ability to preferentially bind to the unfolded protein by non-covalent interactions (Kehoe et al., 2011; O'Kennedy et al., 2006). The casein fractions possessing chaperone-like activity include α_{s1} -, β - and κ -casein (Bhattacharyya et al., 1999; Morgan et al., 2005). However, all caseins, except β -casein, lose their activity at high temperatures (>75 °C) (Kehoe et al., 2011; Yong et al., 2008). For the purpose of this review and experimental studies, only the interactions of β -casein have been discussed.

After α_{s1} -casein, β -casein is the major casein fraction in milk and has a molecular weight of approximately 24.0 kDa with 209 residues in its primary structure (Swaisgood, 1993). It is sensitive to calcium and accounts for approximately 34% (w/v) of the total casein (Schmidt, 1982). It has high proportion of proline and

glutamine residues in its primary structure and is devoid of any cysteine residues (Ribadeau Dumas et al., 1972). β -Casein does not have a defined tertiary structure (Bhattacharyya et al., 1999) and has only a small proportion of secondary structure (Byler et al., 1988; Farrell Jr et al., 2001; Qi et al., 2004). β -Casein has been classified as an intrinsically unstructured protein (IUP) (Tompa, 2002), while Holt et al. (1993) termed the highly flexible and mobile structure of β -casein as “rheomorphic”.

The amino acid composition and the distribution of amino acids in the β -casein polypeptide chain impart unique properties to the β -casein molecule. The N-terminal region (1-47) of β -casein contains all of the serine residues with negatively charged phosphate groups, while the C-terminal end predominantly contains hydrophobic residues. This results in an amphiphilic di-block copolymer-like character (Horne, 2002; Leclerc et al., 1997a). This has important implications on its functional properties, including its ability to behave as a surfactant or emulsifying agent (Dalglish, 1997), micellization (Arima et al., 1979; Gangnard et al., 2007; Mikheeva et al., 2003; O'Connell et al., 2003; Sullivan et al., 1955; Takase et al., 1980) and chaperone-like properties (Yousefi et al., 2009).

The unique amphiphilic character of β -casein monomers facilitates their reversible association into three-dimensional structures referred to as micelles (Horne, 2002). During micelle formation, the β -casein monomers associate via their C-terminal region primarily by hydrophobic bonding forming a dense core (Leclerc et al., 1997b). The micelle structure is stabilized by the steric effects, and electrostatic interactions arising from the charged phosphoserine residues on the N-terminal region (Horne, 2002; O'Connell et al., 2003). The most widely accepted model explaining the monomer-micelle equilibrium is the “shell model” (Kegeles, 1979,

Chapter 2. Review of Literature

1992). In this model, the β -casein micelles remain in equilibrium with β -casein monomers and the micelles grow by the addition of β -casein monomers. The critical size that a micelle can attain is limited by the steric effect and the electrostatic interactions of the phosphoserine residues of the N-terminal regions (O'Connell et al., 2003).

The association of β -casein into micelles is an endothermic process (Mikheeva et al., 2003) and exhibits a highly temperature-dependent behavior (Buchheim et al., 1979; de Kruif et al., 2002; Mikheeva et al., 2003; Moitzi et al., 2008; O'Connell et al., 2003; Takase et al., 1980). At a given temperature, there exists a certain minimum concentration of β -casein required for micelle formation, termed as the critical micelle concentration (CMC) (Arima et al., 1979; Buchheim et al., 1979; Kegeles, 1979, 1992), which has a negative correlation with temperature (Arima et al., 1979; de Kruif et al., 2002; Leclerc et al., 1997b; Moitzi et al., 2008; Portnaya et al., 2006). The shielding of charges at high ionic strength decreases the CMC (Portnaya et al., 2006) while the presence of cosolutes, like urea or ethanol, in the aqueous medium increase the CMC (Mikheeva et al., 2003).

At low temperature (≤ 4 °C) β -casein exists as a monomer (Arima et al., 1979; de Kruif et al., 2002; Payens et al., 1963; Schmidt et al., 1972; Takase et al., 1980). As the temperature is raised to 20 °C (pH 7), there is an increase in the number of surface accessible hydrophobic groups of β -casein (O'Connell et al., 2003). Within this temperature range, the number of β -casein monomers forming the micelles (N_{agg}) increases (O'Connell et al., 2003; Portnaya et al., 2006). Continued heating beyond 25 °C (≤ 45 °C) does not affect the CMC and micelle characteristics appreciably (de Kruif et al., 2002; Moitzi et al., 2008; O'Connell et al., 2003; Portnaya et al., 2006). The micelle characteristics at >40 °C are not known with

certainty but an increase in N_{agg} (to 73) during heating to 70 °C at neutral pH has been reported (Leclerc et al., 1997a).

When acting as a molecular chaperone, β -casein does not affect the unfolding of the target protein (Kaushik et al., 1998; Kehoe et al., 2011), but its subsequent interaction with the unfolded protein inhibits further interactions (Ghahghaei et al., 2011; O'Kennedy et al., 2006; Yong et al., 2008; Zhang et al., 2005). The active β -casein species responsible for chaperone-like activity is the β -casein monomer (Yousefi et al., 2009). During its chaperone-like activity, the highly hydrophobic C-terminal region of β -casein preferentially interacts with the hydrophobic patches on the unfolded protein (Ghahghaei et al., 2011). The negatively charged phosphoserine residues of β -casein in the N-terminal region then stabilize the complex by a combination of steric hindrance and electrostatic repulsion (Koudelka et al., 2009; Yousefi et al., 2009). The chaperone-like activity of β -casein decreases with an increase in ionic strength or when pH is lowered from 6.5 to 5.8 (Kehoe et al., 2011). Its activity at pH below its isoelectric point (5.3 to 5.5) has not yet been investigated.

Different whey proteins for which β -casein displays a significant chaperone-like activity include whey protein mixtures in whey protein isolate (O'Kennedy et al., 2006) bovine serum albumin (Kehoe et al., 2011), α -lactalbumin (Kehoe et al., 2011), and β -lactoglobulin (Kehoe et al., 2011; Yong et al., 2008).

2.3. Self-assembly of β -Lg into amyloid-like fibrils

The self-assembly of β -Lg into amyloid-like fibrils has been extensively investigated, partly due to its abundant availability and the immense volume of information available about its structural stability. Due to their high aspect ratio, β -Lg fibrils can form networks by entangling with each other, thereby increasing the viscosity of the matrix (Veerman et al., 2003a). Their unique properties have been used to design food thickeners (Veerman et al., 2003a), encapsulating systems (Sagis et al., 2008), stabilize emulsions (Ruhs et al., 2012), develop magnetic-responsive sensors (Bolisetty et al., 2013) and nanowires (Bolisetty et al., 2012).

2.3.1. Conditions of β -Lg self-assembly

β -Lg self-assembles into amyloid-like fibrils under a variety of denaturing conditions, including incubation with solvents (Gosal et al., 2002), heating in the presence of urea (Hamada et al., 2002) or heating above its denaturation temperature at low pH (Arnaudov et al., 2003; Durand et al., 2002; Gosal et al., 2002; Huang et al., 1994b; Rogers et al., 2005; Veerman et al., 2002). The common underlying feature of these conditions is the nucleation-dependent kinetics (Bromley et al., 2005; Hamada et al., 2002). All of these conditions are known to destabilize the native β -Lg structure, indicating that self-assembly proceeds from unfolded monomers of the protein. Table 2.3 compares the different conditions of β -Lg self-assembly.

The most widely studied condition for β -Lg self-assembly is heating at low pH. Heating produces rapid denaturation, and low pH (typically pH 2-3) inhibits random aggregation by enhancing electrostatic repulsion and inhibiting disulphide bonding. In the subsequent sections, only the studies investigating β -Lg self-assembly at low

pH have been considered for discussion and henceforth unless stated otherwise, the conditions of self-assembly would imply heating at low pH.

Table 2.3 *Non-native conditions promoting fibril formation from β -Lg.*

Composition of the aqueous solution	Time required for the fibrils to appear	Fibril characteristics	Selected Reference
5 to 7 M urea, pH 7, 37 °C	~10 days	Long, $\geq 1 \mu\text{M}$ and 8 to 10 nm in diameter	Hamada et al. (2002)
50% v/v 2, 2, 2-trifluoroethanol, ethanol, methanol and propan-2-ol water mixtures, pH 2 and pH 7, 80 °C, 4% w/v	3 days to 5 weeks	Short, curved and worm-like fibrils, 150-500 nm in length, 7.5 nm in diameter	Gosal et al. (2002)
Enzyme hydrolysate of β -Lg (AspN Endoproteinase for 24 h pH 8) heated at pH 2, 37 °C	24 h	1 μm long	Akkermans et al. (2008a)
pH 2, 80 °C, $\geq 1\%$ w/v	24 h	$\geq 1 \mu\text{m}$ long and 4 nm in diameter	Arnaudov et al. (2003)

2.3.2. Mechanism of β -Lg self-assembly at low pH

β -Lg self-assembly on heating at low pH follows the classic nucleation-dependent model of amyloid self-assembly (Bolder et al., 2007a; Bromley et al., 2005; Chiti et al., 2006; Clark et al., 2001) and self-assembly follows a sigmoid curve with the characteristic lag, growth and stationary phases. During self-assembly, the lag phase is the initial period that is characterized by the absence of fibrils and is a rate-limiting step for β -Lg self-assembly (Aymard et al., 1999). The key phenomena occurring during the lag phase include activation of β -Lg monomers followed by the formation of nuclei (Bolder et al., 2007a).

The activation step referred to by Bolder et al. (2007a) is likely to be a form of structural transition in native β -Lg monomers since heating results in unfolding of tertiary structure (Section 2.2.3 and 2.2.4). However, heating temperature above the denaturation temperature of β -Lg is not necessary for its self-assembly. Fibril formation from β -Lg has been reported at temperatures as low as 60 °C (pH 2.5, 4% w/v β -Lg) (Bromley et al., 2005). In addition, incubation of enzyme hydrolysed β -Lg resulted in fibrils upon incubation at 37 °C (Akkermans et al., 2008a). The temperatures employed for heating in these studies are too low to cause any substantial irreversible structural changes; moreover, it is not known as to what degree of unfolding is rate-limiting during self-assembly.

Once activated, nuclei form by intermolecular interactions of the building blocks. Light scattering studies have shown that the formation of nuclei is initially reversible but the nuclei can disintegrate into constituent building blocks upon cooling (Arnaudov et al., 2003; Aymard et al., 1999). It is hypothesized that the nuclei must attain a certain critical size (C^*) beyond which the self-assembly becomes

irreversible (Arnaudov et al., 2003; Aymard et al., 1999) due to formation of intermolecular β -sheets (Bolder et al., 2007a; Kavanagh et al., 2000). At low protein concentrations, the rate limiting step during self-assembly is the formation of nuclei (Aymard et al., 1999). The time required to attain C^* marks the end of the lag phase and the beginning of the growth phase.

Once in the growth phase, the nuclei grow by addition of building blocks at both ends resulting in mature fibrils. The high temperature of heating facilitates the formation of hydrophobic interactions (Schellman, 1997) between the building blocks (Akkermans et al., 2008b) while the high electrostatic repulsion at low pH and low ionic strength induces formation of long fibrils (Aymard et al., 1999; Kavanagh et al., 2000; Langton et al., 1992). Other whey proteins do not form fibrils under the low pH, low ionic strength and high temperature conditions that are favorable for β -Lg self-assembly (Bolder et al., 2007c).

Upon prolonged heating, the amount of fibrils plateaus, and no further fibril formation occurs. Two possible mechanisms have been proposed for the decline in the rate of self-assembly. After prolonged heating, the fibrils may lose the ability to allow further addition of building blocks or the constituent building blocks undergo irreversible change that inhibits their addition onto the growing fibrils (Bolder et al., 2007a). It is also likely that the supply of building blocks may cease upon prolonged heating, but experimental evidence of this hypothesis is yet to be elucidated. The yield of fibrils reported in previous studies range from 28 to 68%, w/w (Akkermans et al., 2008b; Hettiarachchi et al., 2012; Veerman et al., 2002) when purified β -Lg was used and between 5 to 44% when WPI (Bolder et al., 2007b; Bolder et al., 2007c) was used. The wide variation in the reported yields of fibrils may be

attributed to the varying initial protein concentrations, conditions of self-assembly and the method used for estimation of yield.

2.3.3. Heat-induced acid hydrolysis

Most of the earlier studies (prior to 2008) investigating β -Lg self-assembly assumed that the constituent building blocks in fibrils were partially unfolded monomers joined head-to-tail (Arnaudov et al., 2006; Arnaudov et al., 2003; Aymard et al., 1999; Bolder et al., 2007a; Bolder et al., 2007c; Rogers et al., 2005). However, the experimental techniques used in these studies examined mostly the characteristics of intact aggregates. Bolder et al. (2007c) were the first to analyze the composition of fibrils and heated WPI solutions by disintegrating the aggregates. These authors concluded that the acid hydrolysis of β -Lg during heating limited the growth of fibrils. Subsequently, Akkermans et al. (2008b) characterized the building blocks of β -Lg fibrils by mass spectrometry and noted that fibrils were made up of selected peptides released from the acid hydrolysis of intact monomers. Since then several other studies have noted acid hydrolysis of β -Lg monomers during fibril formation (Bateman et al., 2010; Hettiarachchi et al., 2012; Kroes-Nijboer et al., 2011; Lara et al., 2011; Mudgal et al., 2011; Oboroceanu et al., 2010).

Acid hydrolysis of proteins during heating at low pH occurs by the preferential cleavage of peptide bonds involving aspartic acid (Asp, D) residues (Inglis, 1983). The first step in acid hydrolysis involves an interaction of the free carboxylic acid group of aspartic acid residue with the polypeptide backbone on either side of the Asp residue (pathways 'a' and 'b' in Figure 2.6). The resulting unstable intermediate produces two separate products on either side of the peptide bond (Blackburn et al.,

1954). It was also found that the formation of intermediate ring structures is greatly accelerated at high temperatures (Blackburn et al., 1954).

Leach (1956) noted that the preferential cleavage of peptide bonds depended on the spatial arrangement of the free $-\text{COOH}$ group rather than the H^+ ion concentration. He suggested that the free $-\text{COOH}$ closer to the polypeptide backbone may render the peptide bond more prone to hydrolysis implying that peptide bonds involving Asp residues were more prone to hydrolysis than Glu (glutamic acid) residues (Leach, 1956). Nevertheless, the low-pH conditions during heating do promote the cleavage of peptide bonds involving Glu residues (Harris et al., 1956; Partridge et al., 1950) although at a much slower rate (Blackburn et al., 1954). Similarly, the deamidation of asparagine (Asn) did not affect the rates of acid hydrolysis significantly (Blackburn et al., 1954; Tsung et al., 1965).

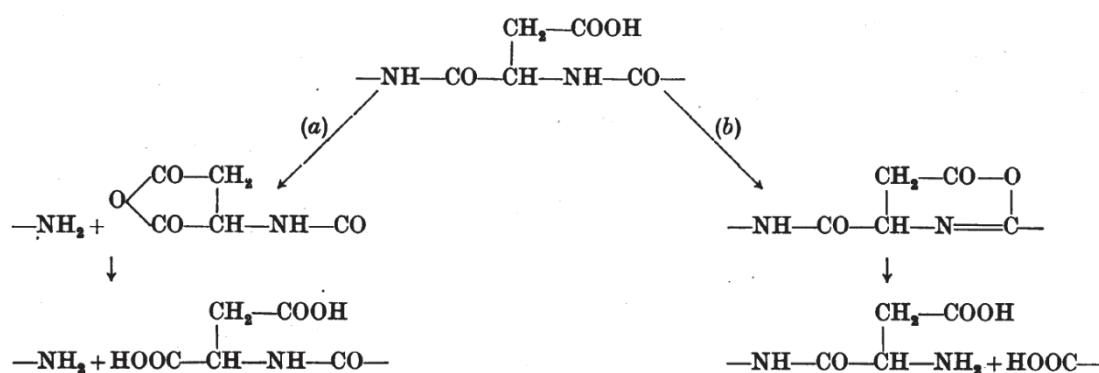


Figure 2.6 Proposed mechanism of acid hydrolysis of proteins. Adapted from Blackburn et al. (1954).

Acid hydrolysis of labile peptide bonds follows first-order exponential kinetics (Oliyai et al., 1993; Tsung et al., 1965) and is unaffected by the type of acid used (Inglis, 1983) or the ionic strength of the medium (Blackburn et al., 1954). Using dipeptide systems, Syngé (1945) reported that the branched chain residues, or a positively charged residue immediately adjacent to a labile peptide bond inhibited its

Chapter 2. Review of Literature

cleavage, however the latter could not be confirmed in large polypeptides (Inglis, 1983). Wu et al. (1992) compared the kinetics of acid hydrolysis using two different heating methods and concluded that the rate of hydrolysis was much faster during microwave heating.

Thus, it is important to incorporate the phenomenon of acid hydrolysis in the mechanism of self-assembly. Kroes-Nijboer et al. (2011) noted that acid hydrolysis of β -Lg during self-assembly was faster at higher temperatures and its dependence on temperature could be explained by the Arrhenius equation. The faster kinetics of hydrolysis in this study coincided with the faster kinetics of self-assembly and these authors concluded that hydrolysis probably promoted self-assembly. Similarly Lara et al. (2011) proposed a common mechanism for the self-assembly of globular proteins with hydrolysis playing an important role during self-assembly, but this study does not address certain important questions such as: what is the role of hydrolysis during self-assembly? What degree of acid hydrolysis is required for self-assembly?

The prediction of the possible role of acid hydrolysis during self-assembly was further complicated by the finding that β -Lg fibrils could be prepared from the unfolded monomers without significant hydrolysis in a protocol using microwave heating (Hettiarachchi et al., 2012). Therefore, whether the hydrolysis of β -Lg monomers occurs as a mere consequence of heating at low pH or has a specific role in assisting fibril formation remains to be established.

Another question which has remained unaddressed is whether or not fibrils themselves undergo acid-hydrolysis. Loveday et al. (2012c) proposed a model in which acid hydrolysis and self-assembly are seen as competing reactions, analogous

to the model of lysozyme fibril assembly proposed by (Mishra et al., 2007). As per this model, fibrils can be formed from short peptides or long peptides depending on conditions, and fibrils consisting of large peptides undergo a gradual process of “trimming” during continued heating, with more mobile and solvent-exposed regions being trimmed off (Loveday et al., 2012c). Previous studies (Akkermans et al., 2008b; Hettiarachchi et al., 2012) characterizing the composition of fibrils have noted that fibrils consisted primarily of peptides, but these analyses were carried out only at a single time-point and the possibility that fibrils undergo acid hydrolysis themselves as proposed by Bolder et al. (2007a) still remains unresolved.

The kinetics of β -Lg self-assembly with a slow continuous nucleation, followed by fast autocatalytic growth has been described by the Finke-Watzky model (Morris et al., 2008; Watzky et al., 1997). This model suggests that the end-product or fibrils are capable of promoting self-assembly, and are treated as kinetically equivalent to the nuclei formed in the early stages of self-assembly (Morris et al., 2009). The mathematical expression representing the model is as described as under (Morris et al., 2008).

$$f_t = \alpha - \frac{\frac{\beta + \alpha}{\gamma}}{1 + \frac{\beta}{\alpha\gamma} \exp[t(\beta + \alpha\gamma)]} \dots\dots\dots(2.1)$$

where f_t roughly represents the concentration of fibrils and α , β and γ are empirical constants. The above expression was fitted to the ThT data in Chapters 4 to 8. Loveday et al. (2010) used the above mathematical expression to derive kinetic parameters of self-assembly: the time for the lag phase t_{lag} , the time required for attaining half of the maximum fluorescence value $t_{1/2 \max}$ and the maximum rate of fluorescence $(df/dt)_{\max}$.

$$t_{lag} = \frac{1}{\beta + \alpha\gamma} \left(\ln \left(\frac{\alpha\gamma}{\beta} \right) - 4 \frac{\alpha\gamma}{\beta + \alpha\gamma} + 2 \right) \dots\dots\dots (2.2)$$

$$t_{\frac{1}{2}max} = \frac{\ln \left(2 + \frac{\alpha\gamma}{\beta} \right)}{(\beta + \alpha\gamma)} \dots\dots\dots (2.3)$$

$$\left(\frac{df}{dt} \right)_{max} = \frac{\left(\frac{\beta}{\gamma} + \alpha \right) (\beta + \alpha\gamma)}{4} \dots\dots\dots (2.4)$$

2.3.4. Characteristics of β -Lg fibrils

β -Lg fibrils show typical characteristics of amyloid fibrils, such as a high proportion of β -sheets (Lara et al., 2011) arranged in typical anti-parallel cross- β arrangement, and the ability to bind amyloid fibril-specific dyes such as CR and ThT (Bromley et al., 2005; Hettiarachchi et al., 2012), although the X-ray diffraction patterns obtained from β -Lg fibrils are not very distinct (Figure 2.7, A) (Bromley et al., 2005). At low ionic strengths, the persistence length of these fibrils, an indicator of their flexibility, is of the same order as their lengths and hence these fibrils are classified as semi-flexible (Nicolai et al., 2013).

The morphology of fibrils has been investigated extensively using TEM and atomic force microscopy (AFM). Wang (2009) followed the morphology of fibrils at different stages of self-assembly using TEM. β -Lg fibrils at short heating times (3 h) appeared short up to 200 to 300 nm in length, but increased in length with continued heating (Wang, 2009). Mature fibrils at low ionic strengths appear straight and unbranched with lengths of up to 1 to 10 μ m (Figure 2.7, B) (Akkermans et al., 2008b; Aymard et al., 1999; Hettiarachchi et al., 2012; Liu et al., 2013a; Loveday et al., 2010; Veerman et al., 2002) and 5 to 10 nm in diameter (Hettiarachchi et al., 2012; Liu et al., 2013a; Loveday et al., 2010; Veerman et al., 2002).

When observed under AFM, fibrils appear to have a periodicity in their height suggesting that fibrils may have helical twists (Figure 2.7, C) (Adamcik et al., 2010; Arnaudov et al., 2003; Lara et al., 2011; Loveday et al., 2010). Adamcik et al. (2010) proposed that the helical twists may facilitate the arrangement of mutually-repulsive positively charged residues close to each other. Lara et al. (2011) noted that β -Lg fibrils consist of proto-fibrils ranging from 1 to 16 in number.

Ikeda et al. (2002) compared the morphology of fibrils from purified β -Lg and WPI and reported that fibrils of WPI appeared slightly thicker in diameter. The fibrils in this study were prepared in the presence of 0.1 M NaCl. α -Lactalbumin (Goers et al., 2002) and bovine serum albumin (Veerman et al., 2003c) are known to self-assemble into fibrillar aggregates under conditions similar to those of β -Lg self-assembly and in presence of salt. It is possible that these proteins along with β -Lg participated in the formation of fibrils, thus explaining the thicker fibrils of WPI. By comparison at low ionic strength these proteins do not form fibrils (Bolder et al., 2007c).

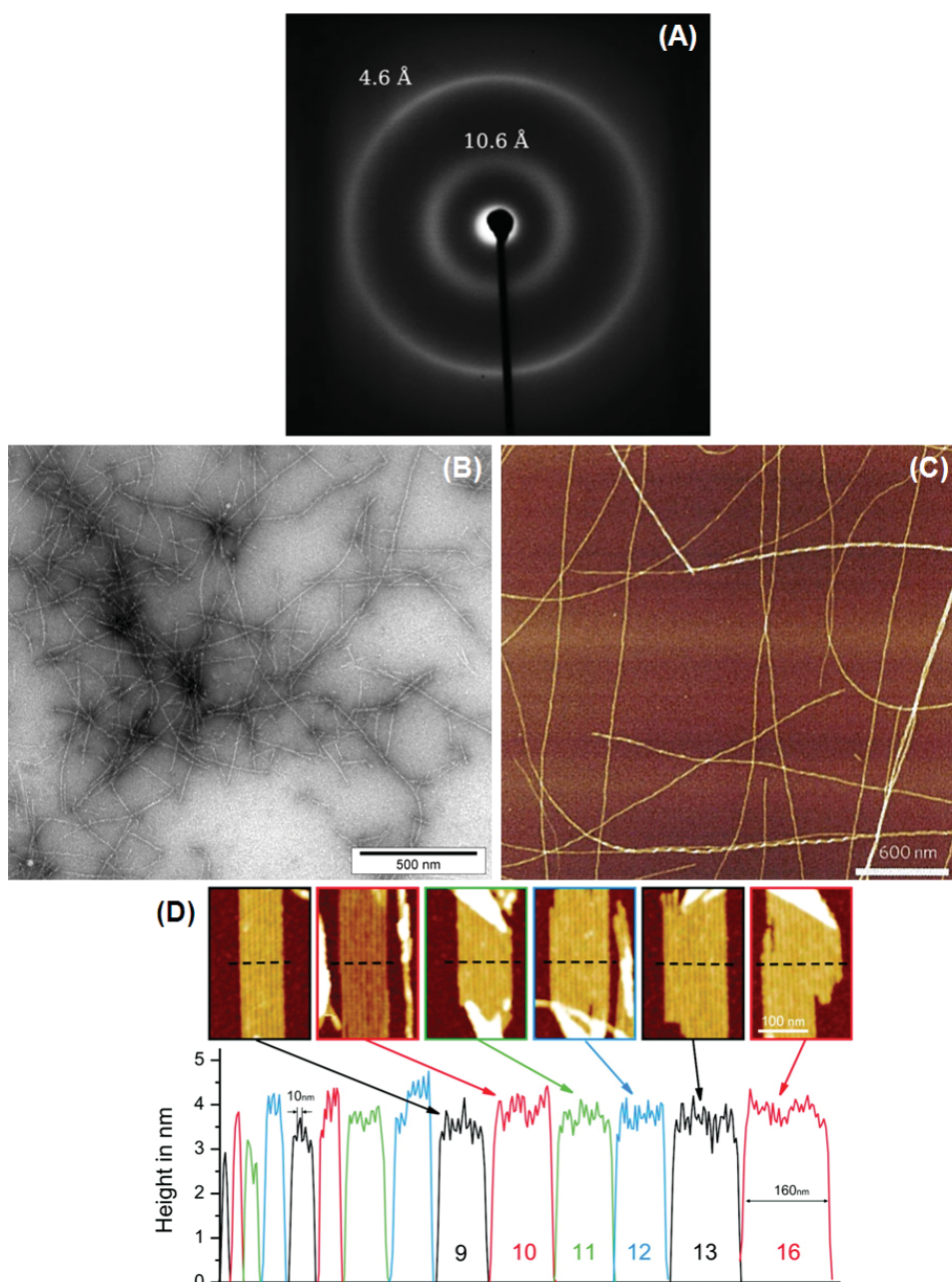


Figure 2.7 Characteristics of β -Lg fibrils (A) wide angle X-ray diffraction pattern of β -Lg fibrils, adapted from Bromley et al. (2005); (B) TEM and (C) AFM image of β -Lg fibrils, adapted from Adamcik et al. (2010); (D) Distribution of proto-filaments in β -Lg fibrils, numbers indicate number of protofilaments, adapted from Lara et al. (2011).

2.3.5. Sequences present in fibrils

The composition of fibrils has not received much attention in comparison to the other aspects of self-assembly. Akkermans et al. (2008b) analyzed the composition of fibrils formed at 85 °C for 20 h (3%, w/v) and under constant shear. These authors noted that fibrils consisted of only few preferentially accumulated peptides primarily from the N-terminal region (1 to 64) (Figure 2.8, i). By comparison Hettiarachchi et al. (2012) analyzed fibrils prepared by heating at 80 °C for 18 h (1.5%, w/v) and without shear. These authors found peptides belonging to the middle region of β -Lg (34-85) in the fibrils. The reason for the difference in the reported sequences in these two studies is not known and may be attributed to the differences in conditions of self-assembly, the type of MS method used for analysis or interpretation of the MS data in these studies. Nevertheless, both the methods also showed evidence of sequences from the two opposite ends of the β -Lg primary sequence.

The presence of the peptide from the C-terminal region is significant since this region consists of the Cys160 residue which is connected to Cys66 by a disulfide bond in the native structure. Similarly, the sequence 99-129 in fibrils in the study of (Akkermans et al., 2008b) contains the other native disulphide bond Cys106-Cys119 and the free Cys121. The disulfide bonding in β -Lg fibrils has not yet been explored, perhaps because the disulfide bonds and free thiol group in the native structure remain stable at low pH. In addition, it is not known whether the sequences from different regions of the β -Lg have any role during different stages of self-assembly.

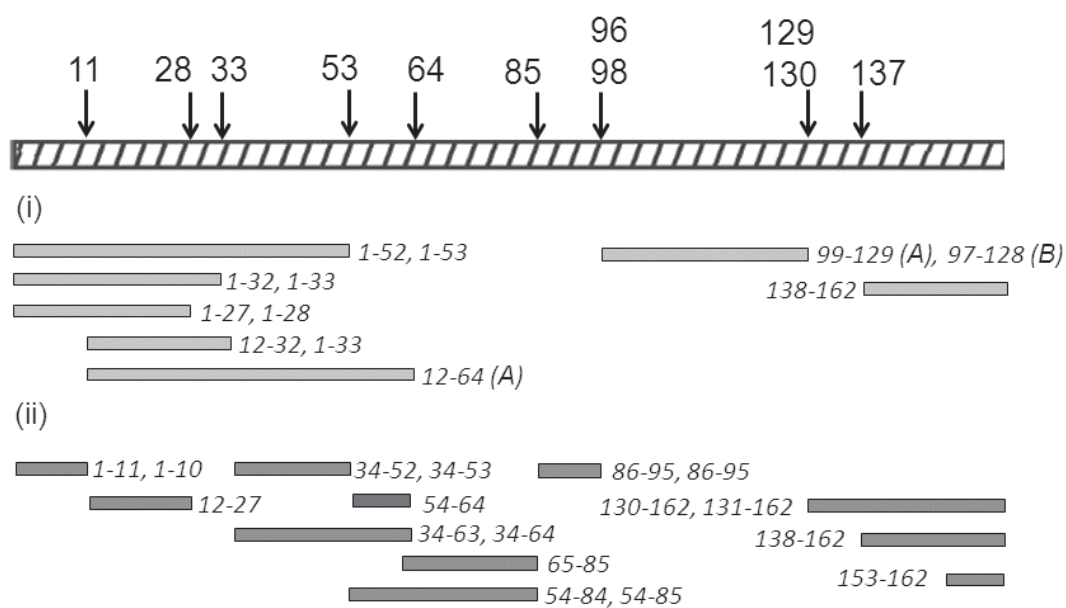


Figure 2.8 Comparison of sequences found in β -Lg fibrils reported by (i) Akkermans *et al.* (2008b) and (ii) Hettiarachchi *et al.* (2012). The numbers on the top show the locations of aspartic acid residues in the sequence, based on the sequence of β -Lg A. (A) and (B) show the peptides from β -Lg A and B.

2.3.6. Factors affecting kinetics of self-assembly

2.3.6.1. Temperature

A higher heating temperature would facilitate faster unfolding (Harwalkar, 1980) decrease the viscosity of the aqueous solutions and increase the frequency of collisions between fibril building blocks (Loveday *et al.*, 2012c). The net effect of these reactions would be faster fibril assembly kinetics. Kroes-Nijboer *et al.* (2011) noted that high temperature promoted the acid hydrolysis of monomers. Collectively these effects translate into faster kinetics of self-assembly both during the lag as well as the growth phases (Kroes-Nijboer *et al.*, 2011; Loveday *et al.*, 2012c). Shearing or stirring during heating eliminates the lag phase (Kroes-Nijboer *et al.*, 2011), and in unstirred solutions the t_{lag} is shortened at higher heating temperatures (Loveday *et al.*, 2012c).

2.3.6.2. pH and ionic strength

At pH 2, β -Lg has a net positive charge of +20 which would be distributed on the peptides released by the acid hydrolysis of monomers. The net positive charge on the resulting peptides is likely to result in high electrostatic repulsion between peptides. Loveday et al. (2010) compared the kinetics of self-assembly between pH 1.6 to 2.4. These authors noted that a decrease in pH <2 did not affect the t_{lag} significantly, but increasing the pH >2 increased the t_{lag} slightly (Loveday et al., 2010). Within this pH range (1.6 to 2.4), there was little effect of pH on the morphology of fibrils (Loveday et al., 2010) but above pH 3 only short fibril-like aggregates were observed (Kavanagh et al., 2000; Langton et al., 1992; Mudgal et al., 2009).

Ionic strength affects both the kinetics of self-assembly and the fibril morphology. At higher ionic strength, the anions of the salt would interact with the positive charges on the peptides, screening the electrostatic repulsion and facilitating their interactions (Schokker et al., 2000). Aymard et al. (1999) and Arnaudov et al. (2006) noted that an increase in NaCl concentration decreased the C^* . At up to 100 mM NaCl, this did not translate into a shortened lag phase, but NaCl did increase the $(df/dt)_{max}$ in the growth phase (Loveday et al., 2010).

Ionic strength has a profound effect on the morphology of β -Lg fibrils. At high ionic strengths, the fibrils appear short, un-branched, curly and worm-like (Aymard et al., 1999; Durand et al., 2002; Kavanagh et al., 2000; Loveday et al., 2012a; Loveday et al., 2010; Veerman et al., 2002). There is no apparent effect of the type of salt on the morphology of fibrils (Loveday et al., 2012a) which have low persistence lengths (Loveday et al., 2010) and hence have been classified as “flexible” (Storm et al., 2005).

2.3.6.3. Cations

The type of cations has a major effect on the kinetics of β -Lg self-assembly (Loveday et al., 2011a, 2012a; Loveday et al., 2010; Zappone et al., 2013). Loveday et al. (2012a) proposed that in addition to non-specific charge-screening effects, cations may affect β -Lg self-assembly by two possible mechanisms: bridging interactions with the building blocks and preferential cation-water interactions that compete with protein-water interactions.

At equal Cl^- concentrations, CaCl_2 shortened t_{lag} more effectively than NaCl , but NaCl and CaCl_2 increased $(df/dt)_{\text{max}}$ to approximately the same extent (Loveday et al., 2010). These authors proposed that Ca^{2+} may facilitate nucleation via specific cation- π interactions with the aromatic (Phe, Tyr and Trp) residues in the sequences of assembly-competent peptides (Loveday et al., 2010).

Ca^{2+} or Na^+ in the aqueous medium greatly modified the morphology of fibrils and the proportion of curly fibrils increased at $\text{CaCl}_2 \geq 33$ mM or $\text{NaCl} \geq 60$ mM (Loveday et al., 2010). Similar effects on fibril morphology were noted for other group IA and IIA cations (Loveday et al., 2012a). By comparison, the Cu^{2+} ions had no effect on fibril morphology (Zappone et al., 2013).

2.3.6.4. Seeding

Addition of preformed fibrils prior to heating accelerates the self-assembly kinetics by acting as nuclei, thus abolishing the lag phase (Bolder et al., 2007a; Loveday et al., 2012b). Loveday et al. (2012b) investigated the effect of seeding of curly fibrils produced at high ionic strengths in promoting the fibril formation under conditions which aid the formation of long fibrils. These authors noted that the curly fibrils upon seeding promoted the growth of only straight and long fibrils but not curly

fibrils (Loveday et al., 2012b). This suggests that during β -Lg self-assembly, the morphology of fibrils was primarily determined by the ionic strength of the solution and curly fibrils resulted strictly from the lower electrostatic repulsions at high ionic strength. However, an experimental study exploring such an effect using long semi-flexible fibrils for seeding in systems which promote curly fibrils has not yet been reported. A slight increase in the yield of β -Lg fibrils has been reported upon seeding (Bolder et al., 2007a), but this study used shearing during heating of the samples and hence the effects of seeding alone without stirring were not investigated in this study.

2.3.6.5. Shear

Application of shear, controlled or variable, greatly accelerates self-assembly (Dunstan et al., 2009; Hill et al., 2006) through its effect on the formation of nuclei (Bolder et al., 2007a; Hill et al., 2006). In addition, application of shear is likely to enhance the diffusion of building blocks facilitating their frequency of collisions (Bolder et al., 2007a). Enhanced nucleation can result from shear-induced structural transitions in the protein's native structure (Morinaga et al., 2010) and/or by shear-induced fragmentation of protofibrils, whose fragments act as nuclei and promote self-assembly (Dunstan et al., 2009; Hill et al., 2006). The lag times decreased at high shear rates (Hill et al., 2006) and the duration of shear does not have an effect on self-assembly kinetics (Akkermans et al., 2006). Also, the effects of shear and seeding were not additive (Bolder et al., 2007a). Loveday et al. (2012c) noted that heating at 85-120 °C without stirring gave a lower yield of fibrils in comparison to a previous study (Kroes-Nijboer et al., 2009) that used shear at the same temperatures and concluded that shear may have a role to play in increasing the yield of fibrils.

2.3.7. Stability of β -Lg fibrils

β -Lg fibrils may aggregate or fracture due to changes in pH or during unit operations such as freeze drying (Loveday et al., 2011a, 2012b). Loveday et al. (2011a) investigated the stability of β -Lg fibrils prepared by heating WPI, to electrostatic aggregation. Fibrils precipitated between pH 4.0 and 6.0 but appeared to be stable at the extremes of pH (Kroes-Nijboer et al., 2012; Loveday et al., 2011a). Ca^{2+} ions in the aqueous medium resulted in calcium-induced precipitation of fibrils at pH >6.0 (Loveday et al., 2011a). The morphology of fibrils remained largely unaffected when pH was raised to 8 (Kroes-Nijboer et al., 2012).

The long stiff fibrils prepared at low ionic strength were prone to fracture during freezing (Loveday et al., 2012b) and elongational flow (Kroes-Nijboer et al., 2010). Loveday et al. (2012c) found that long semi-flexible fibrils formed at 120 °C after short heating times fractured into smaller fibrils upon prolonged incubation. In comparison, the curly worm-like fibrils produced at high ionic strength were more stable during freeze drying due to their enhanced flexibility (Loveday et al., 2012b).

The primary forces involved in the formation of β -Lg fibrils are non-covalent in nature (Schokker et al., 2000) and hence fibrils can be easily dissociated by denaturants such as SDS (Kroes-Nijboer et al., 2011; Lara et al., 2011; Oboroceanu et al., 2010) or guanidine hydrochloride (Akkermans et al., 2008b; Hettiarachchi et al., 2012); although, at very low concentrations the SDS molecules align themselves in head to tail conformations around the fibrils improving their stability against pH (Jung et al., 2008).

2.4. Objectives

The main objective of this work was to characterize the different processes occurring during the formation of fibrils and determine their inter-relationships. The experiments in this work were also aimed at understanding the interactions of different types of cosolutes with β -Lg during its self-assembly.

2.4.1. Experimental Approach

The experimental studies in this work have been divided into three parts:

1. Characterization of self-assembly processes:
 - The different structural changes in β -Lg prior to and, leading to, the formation of fibrils have been characterized.
 - The composition of fibrils at different stages of self-assembly was compared.
 - The amyloidogenic sequences in β -Lg fibrils have been characterized.
2. Investigation of self-assembly from β -Lg with different chemical properties:
 - Purified β -Lg variants A, B and C
 - Glucosylated and lactosylated β -Lg
3. Investigation of the change in aqueous environment using cosolutes:
 - Polyols: Glycerol and sorbitol
 - β -Casein, which possesses chaperone-like activity.

For each of the treatments of 2 and 3, the effects on different self-assembly processes, and morphology of fibrils have been compared to predict interrelationships between self-assembly processes.

2.4.2. Experimental techniques

Table 2.4 below provides a brief overview of different experimental techniques used in this study.

Table 2.4 Overview of experimental techniques used in this study.

Study	Technique
Characterization of β -Lg	Native and sodium dodecyl sulfate (SDS) polyacrylamide gel electrophoresis (PAGE) Electro spray ionization Mass spectrometry (ESI/MS)
Native structure and its unfolding	Circular dichroism spectroscopy with <i>in situ</i> heating
Self-assembly of β -Lg	Thioflavin T assay
Acid hydrolysis of β -Lg during heating	SDS-PAGE
Composition of fibrils	SDS-PAGE In-gel digestion ESI-MS/MS Matrix assisted laser desorption ionisation time of flight (MALDI-TOF MS/MS)
Disulfide bonding in fibrils	1 D and 2D reducing and non reducing SDS-PAGE
Morphology of fibrils	Transmission electron microscopy

Chapter 3

3. Materials and Methods

This chapter lists the major materials, equipments and protocols used extensively in this work. For the ease of clarity, any modifications of these protocols or other specific protocols used specifically have been described at the beginning of the respective chapter.

3.1. Materials

3.1.1. Water

Unless mentioned otherwise, all reagents were made in Milli Q water. The quality of the Milli Q water was tested by the in-built conductivity meter and the instrument was flushed using a cleaning cycle recommended by the manufacturer when the conductivity of the water increased above 18 M Ω .

For preparing HPLC grade water, the Milli Q water was passed through a C₁₈ cartridge. Mass Spectrometry grade water was purchased from Sigma and was used without any further treatment.

3.1.2. Whey protein isolate

Whey protein isolate (WPI) 8855 was provided by Fonterra Cooperative Ltd. Auckland, New Zealand. The composition of WPI was: total protein 93.5 % w/w (as is basis); moisture 4.7 %w/w; ash 0.3 %w/w the rest being carbohydrate and fat. This WPI was the starting material from which β -Lg was purified.

3.1.3. Trypsin

The trypsin used for digestion in mass spectrometry (MS) analysis work (Chapter 4) was purchased from Promega Corporation, USA (Trypsin Gold, VS5280).

3.1.4. β -Lg variants A, B and C

The β -Lg variants A, B and C used in Chapter 5 were provided by Fonterra Cooperative Ltd. Auckland, New Zealand. The purity of these variants, determined by spectrophotometry, was approximately 75%. The identity of these variants was further characterized by MS analysis.

3.1.5. Bovine β -casein

Bovine β -casein was purchased from Sigma Aldrich Ltd. St. Louis, USA (cat. # C6905) and had purity $\geq 98\%$ by PAGE (manufacturer).

3.1.6. Chemicals

Unless otherwise mentioned, all chemicals were of analytical grade and the purity of the chemicals was at least 99%. The different chemicals used in the experimental chapters are listed in Table 3.1 along with their product codes for retrieving further information.

Table 3.1 List of chemicals and reagents used and their vendors.

Sr. No.	Chemical/Reagent	Vendor reference code ^a
1	Sodium chloride (NaCl)	S7653
2	Tris(hydroxymethyl)aminomethane (tris)	252859
3	Sodium dodecyl sulfate (SDS), grade: elite	L3771
4	Tricine	T0377
5	Glycine	G8898
6	Acrylamide	8887
7	N,N'-methylene-bis-acrylamide	146072
8	Bromophenol blue	B0126
9	Coomassie brilliant blue G-250	B7920
10	Coomassie brilliant blue R-250	B0770
11	Ammonium persulphate (APS)	A3678
12	N,N,N',N'-tetramethylethylenediamine (TEMED)	T9281
13	Dithiothreitol (1 M solution)	43816
14	2-propanol	1.09634.5000 ^b

Chapter 3. Materials and Methods

15	Glacial acetic acid	1.00063.2500 ^b
16	Molecular weight markers for SDS-PAGE ^c	
	10 kDa to 250 kDa	1610363
	1.4 kDa to 26.6 kDa	1610326
16	Guanidine hydrochloride	BP178.500 ^d
17	Acetonitrile (MeCN)	1.00030.4000 ^b
18	Trifluoroacetic acid (TFA)	A116-50 ^d
19	Formic acid	14265
20	Glycerol	G6279
21	D-sorbitol	240850
22	Hydrochloric acid (HCl)	1.00317.100 ^b
22	Potassium bromide	P0838
23	D-(+)-glucose	G7528
24	α -lactose monohydrate	L8783
25	D-(-)-arabinose	10850
26	Thioflavin T (dye content 65 to 70%)	T3516
27	Potassium phosphate monobasic	P5655
28	Potassium phosphate dibasic	P3786

a: Unless, mentioned otherwise, the chemicals were purchased from Sigma-Aldrich Ltd., St. Louis, USA

b: Merck KGaA, Darmstadt, Germany

c: Bio-Rad Laboratories, CA, USA

d: Fisher Scientific, Pittsburgh, USA.

3.2. Instruments

In this section, the details of the different instruments used in the experimental protocols are described.

3.2.1. Centrifuges

The centrifugation of samples at speeds $<5,000\text{ g}$ was undertaken using a table top centrifuge (Thermo Scientific, Langensfeld, Germany). For speeds, 5,000 to 50,000 g a Sorvall Evolution RC (Thermo Scientific, USA) centrifuge with a fixed angle rotor (SS-34) was used. This equipment was equipped with temperature control mechanism for maintaining temperature during runs. All samples were centrifuged at $20\text{ }^{\circ}\text{C}$.

For ultracentrifugation, the samples were filled in Nalgene[®] Oak Ridge centrifuge tubes with sealing cap and ultracentrifuged (Kendro Laboratory Products, USA) using a T-890 rotor. The ultracentrifuge had a speed control of $\pm 10\text{ rpm}$, a temperature control of $\pm 0.5\text{ }^{\circ}\text{C}$ and vacuum was maintained during the runs.

3.2.2. Waterbath

All samples were heated in a temperature-controlled waterbath (Jeio Tech, Seoul, South Korea). The accuracy of the temperature display was ± 0.1 °C. The temperature of the waterbath during use was checked manually at least once during the experiment using a glass thermometer or a hand-held digital thermometer.

3.2.3. Spectrofluorometer

Fluorescence measurements were carried out on a spectrofluorometer (FP-6200, Jasco, Tokyo, Japan). The functioning of the fluorometer was tested periodically by measuring the Raman spectra of water and the position of the focus mirrors in the instruments was adjusted to achieve the same standard maxima as in the Raman spectra. During the course of the experimental work for the project, the measurements were compared with another instrument available at Massey University (Shimadzu, Kyoto, Japan). The measurements recorded using the two instruments were found to be similar.

3.2.4. Spectrophotometer

The spectrophotometer used in this work was Ultraspec 2000 (Pharmacia Biotech, Cambridge, UK.). The measurements were made at ambient temperature using a glass cuvette (Starna Pty Ltd. NSW, Australia). The instrument was calibrated before each run.

3.2.5. pH meter

For all pH measurements, the same pH meter (Oakton Instruments, Vernon Hills, USA) was used. All pH measurements were carried out at 20 °C. The pH meter was calibrated using a 2-point calibration protocol at pH 4 and pH 7 (20 °C) before each

set of measurements. Additionally, a 3-point calibration including a calibration at pH 10 was followed for solutions with higher pH.

3.2.6. Circular dichroism spectrometer

The circular dichroism (CD) studies were done on a Chirascan CD spectrometer (Applied Photophysics Ltd., UK). The instrument had a temperature control unit with an accuracy of ± 0.01 °C. Scans were recorded in Quartz Suprasil[®] cuvettes (Hellma GmbH & Co. Müllheim, Germany).

3.2.7. High performance liquid chromatography system

The HPLC system was from Agilent Technologies, USA. For RP-HPLC a C₁₈ column (Jupiter, Torrance, CA, USA) was used the UV detector.

3.2.8. Mass spectrometers

The MS analyses were carried out on an LC-ESI MS system (Agilent 6520 Q-TOF, Agilent Technologies, Hanover, Germany), and a MALDI-TOF/TOF MS (4800 MALDI TOF analyzer, Applied Biosystems, MA). The MALDI sample plate was opti-TOF 384-well plate (Applied Biosystems, MA, USA).

3.2.9. Transmission electron microscope

The imaging of the grids was done on a Phillips CM10 transmission electron microscope (Eindhoven, Netherlands) operating at 80 kV.

3.2.10. Other instruments

For all polyacrylamide gel electrophoresis work, the MiniProtean III system supplied by Bio-Rad Laboratories (Hercules, CA) was used. Samples for MS analysis were concentrated with a Savant centrifuge (SpeedVac SC100, Holbrook, NY, USA),

connected to a vacuum pump (Varian DS 102, Varian Vacuum Technologies, Torino, Italy).

3.2.11. General consumables

Polypropylene tubes 1 mL and 0.5 mL used for heating experiments and all general sample preparations were purchased from Eppendorf AG (Hamburg, Germany), and Kimax[®] glass tubes were purchased from Schott (Elmsford, NY, USA). Samples were filtered with 0.2 μm syringe filters (Minisart CE, Sartorius Stedim Biotech GmbH, Goettingen, Germany) and disposable Terumo[®] syringes (Terumo Medical Corporation, Elkton, USA). The centrifugal filters (Amicon[®] Ultra, EMD Millipore, MA, USA) used for separating fibrils were made up of regenerated cellulose.

3.3. Methods

3.3.1. Isolation of β -lactoglobulin

β -Lactoglobulin (β -Lg) was isolated from whey protein isolate (WPI) 8855 (Fonterra Cooperative Ltd. Auckland, New Zealand) using a modification of the method described previously Manderson et al. (1998) and originally proposed by Mailliar et al. (1988) .

The salt precipitation was carried out as per the protocol described by Manderson (1998) but at 20 °C instead of 50 °C to avoid the risk of any heat-induced structural modifications. The precipitation and dialysis steps were carried out at pH 2 instead of pH 4, because this was found to improve the solubility of β -Lg. The final precipitate obtained from the salt precipitation was dissolved in water at pH 2 and dialyzed for 48 h at 4 °C followed by freeze-drying. The freeze-dried β -Lg was always stored at -18 °C and used for experiments without further purification. The

total protein content of β -Lg was 97% (Leco, total combustion method, AOAC 968.06). Purified β -Lg was also analyzed by native non-denaturing PAGE and SDS-PAGE under reducing and non-reducing conditions. CD spectroscopy was used to investigate the native structure of purified β -Lg. Small working batches (10 g) were separated from the larger stock for the experimental work of different chapters to avoid contamination.

3.3.2. Preparation of fibrils

β -Lg powder was dissolved in Milli Q water at pH 2 and stirred at 4 °C for at least 8 h to allow complete hydration of the protein. The hydrated protein solution was centrifuged at 44,000 g for 30 minutes at 20 °C and the supernatant was filtered (pore size 0.2 μ m syringe filter) to remove any insoluble material. Water was added to achieve a final β -Lg concentration of 1% (w/v) and then pH was readjusted to 2.00 \pm 0.02 using 6 M HCl. Concentrations of β -Lg were determined by measuring the absorbance at 278 nm and applying an extinction coefficient of 0.94 cm²/mg (Swaisgood, 1982b). The samples were transferred to 1.5 mL polypropylene tubes (sample volume 1 mL) or 10 mL Kimax[®] glass tubes (sample volume 10 mL) and then heated in a temperature-controlled water bath maintained at 80 \pm 0.2 °C in triplicates without shaking/stirring. Samples were taken at different holding times and quenched by rapid cooling in an ice bath. The cooled samples were analyzed by the Thioflavin T assay at 20 °C with a maximum delay of 1 hour after their removal. Samples intended for SDS-PAGE were frozen and stored at -18 °C until analysis.

3.3.3. Thioflavin T assay for detection of fibrils

The benzothiole dye thioflavin T (ThT) preferentially binds to amyloid fibrils, resulting in characteristic fluorescence at 482 nm (LeVine III, 1993; Naiki et al.,

Chapter 3. Materials and Methods

1989). The structure of ThT molecule (Figure 3.1) contains benzylamine and benzathiol rings which have rotational freedom around the carbon atoms linking these two rings. This rapidly quenches any excited states resulting in low fluorescence. During their binding to the fibrils, these rings are immobilized by their interactions with the side chain residues of the β -sheets, and their inability to rotate freely increases the net fluorescence intensity (Biancalana et al., 2010).

The mechanism of interaction of ThT with fibrils can be explained by the channel binding model (Krebs et al., 2005). The unique cross- β structure present in fibrils results in an ordered arrangement of side-chain residues referred to as "cross-strand ladders" or channels (Biancalana et al., 2008; Krebs et al., 2005). During their interaction with fibrils, the ThT molecules align in these channels resulting in a fluorescent complex. The schematic showing the alignment of the dye molecules in channels parallel to the axis of the fibrils is shown in Figure 3.1. In addition, other mechanisms proposed for ThT binding to fibrils include hydrophobic interactions between fibrils and ThT micelles (Khurana et al., 2005) or with ThT dimers (Groenning et al., 2007), but these are not widely accepted and fail to explain the specific binding pattern explained by the first model (Biancalana et al., 2010).

The use of ThT for investigating amyloid self-assembly was first proposed by Vassar et al. (1959) and since then has been extensively used as a standard probe for studying protein self-assembly. It has a preferential affinity for binding fibrils formed *in vivo* and *in vitro* including from synthetic polypeptides (LeVine III, 1993; Naiki et al., 1989). This finding has supported the hypothesis that fibrils from different proteins have similar molecular structure (Biancalana et al., 2010). The fluorometric detection of fibril-ThT complexes offers better sensitivity than Congo Red and does not affect the kinetics of self-assembly (Khurana et al., 2005).

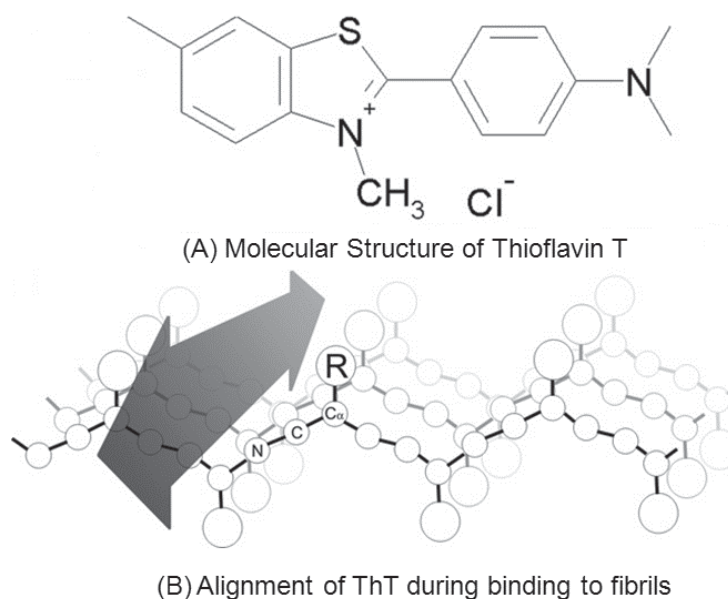


Figure 3.1 (A) Structure of Thioflavin T molecule and (B) orientation of ThT molecules bound to fibrils. The ThT molecules align themselves in the channels formed by the ordered arrangement of side-chain residues in cross- β sheets of fibrils. Adapted from Krebs et al. (2005).

Bolder et al. (2007b) found strong linear correlation ($R^2=0.93$) between the increase in ThT fluorescence intensities and yield of fibrils. The conditions of the ThT assay and fibril formation (WPI 2%w/v, 80 °C and pH 2) used in that study were similar to those used here. Based on this finding and those of others discussed above indicating high specificity of ThT for amyloid or amyloid-like fibrils, the quantitation of fibrils with ThT fluorescence was a valid approach and other methods were not considered.

For the ThT assay, a protocol described previously by Loveday et al. (2010) was used. A stock solution of ThT was prepared by dissolving ThT dye in 10 mM phosphate buffer containing 150 mM NaCl (pH 7), and the solution was sonicated for 10 minutes to allow complete dissolution of the dye. The final concentration of the dye was 0.96 mg/mL. The solution was then filtered using a 0.2 μ m syringe filter and stored in either amber colored bottles or containers covered with aluminum foil at 4 °C. Fresh stock solution was prepared for each block of experiments and no

Chapter 3. Materials and Methods

solution stored for more than two weeks was used for preparing the working solutions. The working solution of ThT was prepared by diluting the stock solution 50 times using 10 mM phosphate buffer containing 150 mM NaCl (pH 7). The working solution was held in glass containers covered with aluminum foil during the assay. Fresh working solutions were prepared for each experiment and the solutions were stored at 4 °C in case of prolonged delays between two successive assay times e.g. 12 h and 24 h.

The fluorescence intensity was recorded by mixing 3 mL of the working solution with 100 μ L of the sample. Fluorescence intensities were read after a minimum delay of 60 s on a spectrofluorometer using an excitation wavelength of 440 nm and emission wavelength of 486 nm, band widths 10 nm in the fixed wavelength measurement mode.

The fluorescence intensity of the ThT solution alone was always between 65 and 80 and was auto-corrected from the recorded sample intensities. All sample intensities were recorded as average values of triplicate measurements. The intensity of an unheated control was subtracted from all samples to obtain net fluorescence intensities, which were then plotted against heating time.

The ThT fluorescence intensities were fitted using the same Equation (3.1) used to characterize β -Lg self-assembly (Loveday et al., 2010) and originally proposed by Morris et al. (2008) in which f_i denotes fluorescence at time t (h), while α , β and γ are constants.

$$f_t = \alpha - \frac{\frac{\beta}{\gamma} + \alpha}{1 + \frac{\beta}{\alpha\gamma} \exp[t(\beta + \alpha\gamma)]} \dots\dots\dots (3.1)$$

The time for the lag phase t_{lag} , and the time required for attaining half of the maximum fluorescence value $t_{1/2 \max}$ and the maximum rate of fluorescence increase $(df/dt)_{max}$, were calculated using Equations 3.2 to 3.4 respectively.

$$t_{lag} = \frac{1}{\beta + \alpha\gamma} \left(\ln \left(\frac{\alpha\gamma}{\beta} \right) - 4 \frac{\alpha\gamma}{\beta + \alpha\gamma} + 2 \right) \dots\dots\dots (3.2)$$

$$t_{\frac{1}{2} \max} = \frac{\ln \left(2 + \frac{\alpha\gamma}{\beta} \right)}{(\beta + \alpha\gamma)} \dots\dots\dots (3.3)$$

$$\left(\frac{df}{dt} \right)_{max} = \frac{\left(\frac{\beta}{\gamma} + \alpha \right) (\beta + \alpha\gamma)}{4} \dots\dots\dots (3.4)$$

The value of the empirical constant α represented the value of f_{max} , the maximum fluorescence in the stationary phase.

The standard deviations of kinetic parameters were calculated using variances of α , β , and γ , whose variances were obtained from the nonlinear regression calculation (SigmaPlot). The variances in the functions $f(\alpha, \beta, \gamma)$ of equations 3.1 to 3.3 were calculated as under

$$X \equiv [\alpha \quad \beta \quad \gamma] \dots\dots\dots (3.5)$$

$$V(f(X)) = (f')^T V(X) f' \dots\dots\dots (3.6)$$

where $f' = \left[\frac{\partial f}{\partial \alpha} \quad \frac{\partial f}{\partial \beta} \quad \frac{\partial f}{\partial \gamma} \right]$ and the covariance matrix

$$V(X) = \begin{bmatrix} \sigma_{\alpha}^2 & \sigma_{\alpha\beta} & \sigma_{\alpha\gamma} \\ \sigma_{\alpha\beta} & \sigma_{\beta}^2 & \sigma_{\beta\gamma} \\ \sigma_{\alpha\gamma} & \sigma_{\beta\gamma} & \sigma_{\gamma}^2 \end{bmatrix} \dots\dots\dots(3.7)$$

All calculations were done in Microsoft Excel, and variances were converted to standard deviations by taking the square root of $V(X)$ for calculation of partial derivatives see Annexure 11.1

3.3.4. Separation of fibrils using ultracentrifugation

Heated and quenched β -Lg solutions (9 mL) were ultracentrifuged using a Sorvall[®] T-890 fixed angle rotor at different centrifugation speeds ranging from $1.1 \times 10^5 g$ to $2.9 \times 10^5 g$ for either 30 or 60 minutes. The extent of separation of fibrils from the heated solution into the pellet was determined by measuring the residual ThT intensity of the supernatants (Figure 3.2). Complete separation of fibrils was achieved at $2.4 \times 10^5 g$ for 60 minutes and under these conditions, the unheated β -Lg did not form a pellet. The TEM of the supernatant obtained after ultracentrifugation of β -Lg heated for 12 h, using the method described in Section 3.3.9, did not show the presence of any fibrils (results not shown), indicating complete separation.

Bolder et al. (2007c) used centrifugal filters with molecular weight cut off of 100 kDa to separate the fibrils from the heated solution. The efficiency of separation of fibrils using filters is dependent on the shape of the particles being separated. In addition, the separation of filters may be limited by concentration of fibrils in the samples and the sample volume. For example, Bolder et al. (2007c), diluted the heated samples to a final protein concentration of 0.1% w/v and used 2 mL of the diluted solution for filtration. In comparison, the ultracentrifugation method separates the fibrils irrespective of their size or shape. This method allows complete

separation of fibrils from the heated solutions, allowing characterization of fibrils and unassembled material after separation.

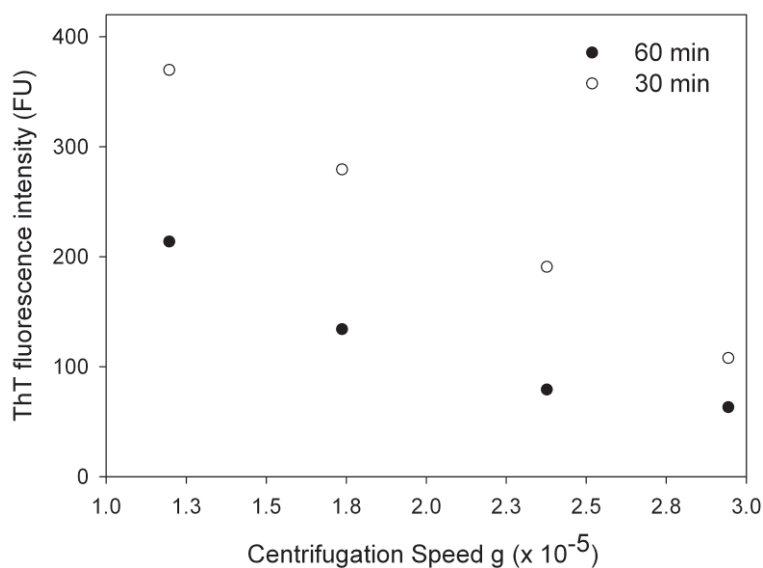


Figure 3.2 Residual Thioflavin T intensities of supernatants obtained by ultracentrifugation at different speeds for 30 and 60 minutes (20 °C). β -Lg 1% (w/v) was heated at 80 °C at pH 2 for 12 h. Sample intensities were corrected by subtracting the intensity of the blank containing ThT solution without any sample.

Based on the above results, the ultracentrifugation speed equivalent to a centrifugal force of 2.4×10^5 g for 60 minutes was adopted for the separation of fibrils in all subsequent work. After centrifugation, the supernatant was collected, and the pellet was washed twice with 2 mL of water (pH 2, no re-dispersion), to remove any residual supernatant. This pellet will be referred to here as the ‘surface-washed pellet’. The supernatant and surface-washed pellets from heated solutions were used for further analysis.

To remove any loosely adhering peptides entrapped in the pellet, the surface washed pellet was suspended in water (pH 2) and vortexed. The volume of the sample in the tube was adjusted to 9 mL with pH 2 water and the samples were ultracentrifuged.

The above procedure of centrifugation and vortexing was repeated three times to produce the final sample for analysis. To differentiate the pellet washed using the method from the surface-washed pellet, it has been referred to as the ‘complete-washed pellet’ in Chapter 4. For experiments in Chapters 5, 6 and 8, unless otherwise stated, complete-washed pellet was used for analysis.

3.3.5. Polyacrylamide gel electrophoresis (PAGE)

The PAGE analysis is a powerful protein analysis technique working on the principle that when proteins are exposed to an electric field, they migrate at different rates depending upon their characteristics, such as charge density or molecular weight. The polypeptide mixture is mixed with a suitable sample or loading buffer and loaded on to the PAGE gels. The proteins are separated on a porous gel matrix consisting of polymerized acrylamide and a cross-linking agent. The separation of proteins can be improved by careful selection of the acrylamide concentration (%T) and that of the cross-linker (%C, expressed as % of total acrylamide concentration) (Dunn, 1993b). At a given acrylamide concentration, the optimum %C for achieving minimum pore size of the gel is approximately 5% (Gordon, 1975). Two main types of PAGE methodologies have been used in this work: the native non-denaturing PAGE and sodium dodecyl sulfate PAGE (SDS-PAGE). In both these systems, the sample is diluted in a PAGE sample buffer and the composition of the loading buffer determines the separation characteristics.

In the native non-denaturing PAGE, the native protein conformation state is conserved and the proteins are separated based on their charge density and their structure. The native structure of the protein is largely conserved during the analysis and hence this method is widely used as a purification step e.g. for purification of

enzymes. Native PAGE can also be used for determining the purity of the proteins extracted from a mixture, or for studying the aggregation of proteins in combination with SDS-PAGE.

In comparison, the separation of proteins in SDS-PAGE is primarily based on their molecular weights (Weber et al., 1969). To eliminate the effects of charge density, the sample is mixed with PAGE buffer containing an anionic surfactant, SDS which binds to the protein at a ratio of 1.4 g SDS per gram of protein and imparts a high net-negative charge on the protein (Reynolds et al., 1970). The SDS also disrupts all non-covalent interactions disrupting the native protein structure. Thus, with the charge on protein neutralized and its structure disrupted, the separation of the proteins is primarily based on their molecular weights (Weber et al., 1969).

SDS-PAGE has been widely used for investigating aggregation or hydrolysis of the proteins. Often a reducing agent, usually β -mercaptoethanol (β -ME) or dithiothreitol (DTT), in the sample buffer is needed to reduce the disulfide bonds in the sample (Dunn, 1993a). The combination of non-reducing and reducing SDS-PAGE provides useful information on protein aggregation and the nature of interactions involved in their formation.

The polypeptide bands are stained using different dyes. In this work two major staining techniques have been used for staining: staining by Coomassie Blue as well silver staining. The staining of polypeptide bands by Coomassie blue detects proteins in the concentration range of 5 to 20 ng/mm² (Diezel et al., 1972) and is achieved by placing the gels immersed in an acidic solution of the dye. Tal et al. (1985) reported that the binding of the dye to the proteins was related to the number of positively charged residues i.e. lysine, arginine, histidine and the N-terminal amine group. The

Chapter 3. Materials and Methods

dye binding occurs at the rate of 1.5 to 3 dye molecules per charged residue (Tal et al., 1985). The polypeptide bands appear blue in color after destaining of the gels.

In silver staining, the gels are first immersed in a solution containing silver ions (Ag^+). During this time the Ag^+ ions migrate into the gels and bind to the polypeptide bands of the sample. The color of the polypeptide bands in the gel is developed by adding a reducing agent which acts on the silver ions. The polypeptides catalyze this reduction of silver resulting in intense brown colored bands. The silver staining technique is extremely sensitive and can detect 0.01 ng/mm^2 protein in the sample (Merril et al., 1981).

3.3.5.1. Native non-denaturing PAGE

For the native non-denaturing PAGE, the protocol described by Manderson et al. (1998) was used. The samples were diluted to a final concentration of 0.5 to 1 mg/mL and 5 to 10 μg of protein was loaded onto the gels. The sample buffer contained 62.5 mM Tris, 40% v/v glycerol, and 0.01% w/v bromophenol blue. The typical preparations of resolving gel and stacking gel mixtures is listed in Table 3.2. The acrylamide (30% T, 2.6% C) solution was prepared by dissolving 29.2 g acrylamide and 0.8 g of N,N'-methylene-bis-acrylamide in water. The resolving gel (1.5 M Tris-HCl, pH 8.8) and stacking gel (0.5 M Tris-HCl, pH 6.8) buffers were prepared in Milli Q water while the pH of the buffers was adjusted using 6 M HCl. The running buffer contained 2.5 mM Tris and 19.1 mM glycine. The native PAGE analysis protocol described here was used for checking the purity of WPI and β -Lg extracts in Chapter 4 and that of β -Lg A, B and C in Chapter 5.

Table 3.2 *Composition of native and SDS-PAGE gels.*

Constituents ^a	Native	SDS-PAGE
Resolving gel concentration	15%	16%
Milli-Q water	2.5 mL	2.02 mL
1.5 M Tris-HCl buffer (pH 8.8)	2.5 mL	3.75 mL
Acrylamide (30%)	5 mL	7.95 ml
10% SDS	-	100 μ L
TEMED	5 μ L	5 μ L
10% APS	50 μ L	50 μ L
Stacking gel concentration	4%	4%
Milli-Q water	3.10 mL	3.05 mL
0.5 M Tris-HCl buffer	1.25 mL	1.25 mL
Acrylamide (30%)	0.65 mL	0.65 mL
10% SDS	-	100 μ L
TEMED	5 μ L	5 μ L
10% APS	50 μ L	50 μ L

^aThe recipe listed here is for preparation of two gels.

3.3.5.2. Glycine SDS-PAGE

For SDS-PAGE, the same acrylamide solution as above was used to prepare the gels. The samples intended for SDS-PAGE analysis were diluted to a final protein concentration of 1 mg/mL using the PAGE sample buffer and 10 μ L sample (10 μ g) sample was loaded on to the gels. When protein concentration in the sample was not

Chapter 3. Materials and Methods

known, the samples were diluted 1:10 using PAGE buffer. For non-reducing conditions, the sample buffer contained 62.5 mM Tris, 25% v/v glycerol, 2% SDS and 0.01% w/v bromophenol blue. For the analysis of reduced samples, the sample buffer additionally contained either 5% β -ME solution or 100 mM DTT. These samples were heated at 95 °C for 5 minutes for samples with β -ME and 56 °C for 15 minutes for samples with DTT. The running buffer contained 1.2 mM Tris, 10 mM glycine and 0.05% w/v SDS. The glycine SDS-PAGE was primarily used for checking the purity of WPI and β -Lg extracts in Chapter 4, and that of β -casein in Chapter 8.

3.3.5.3. Tricine SDS-PAGE

Tricine SDS-PAGE was based on the methods described previously (Schagger et al., 1987; Stryer, 1995). The solutions were diluted 1:10 with reducing PAGE sample buffer containing 2 or 4% w/v SDS and 100 mM dithiothreitol (DTT). For centrifuged samples, 100 μ L aliquots of supernatant solutions were diluted while the pellets were suspended in the PAGE sample buffer without further dilution.

The fibrils present in complete washed pellets were analyzed for disulfide bonding by comparing the non-reducing and reducing PAGE profiles. For this, the final pellet obtained was dispersed in non-reducing SDS-PAGE sample buffer containing 4% w/v SDS and dissolved with constant agitation at 20 °C over 7 days. The sample was then divided in two and 1 M DTT solution was added to one half (final concentration 100 mM), while a volume of water equivalent to that of DTT was mixed with the other half. The results of this analysis are discussed in Chapter 4. For all subsequent analysis of the pellets by SDS-PAGE in Chapters 5, 6, and 8, the complete-washed pellet was suspended in reducing PAGE sample buffer.

About 5-10 μL samples were loaded onto an SDS PAGE gel with a resolving gel concentration of 16% (49.5% T, 3% C). The components of the resolving and stacking gels are listed in Table 3.3. The thickness of all the gels was 0.75 mm and all gels were prepared in-house.

Table 3.3 *Composition of resolving and stacking gels for tricine SDS-PAGE analysis.*

Constituents ^a	Resolving Gel	Stacking gel
Concentration	16%	4%
Milli-Q water	2.96 mL	4.15 mL
3M Tris-HCl buffer (pH 8.45)	3 mL	1.5 mL
Glycerol (90%)	1 g	-
Acrylamide (49.5%)	3.25 mL	0.5 mL
10% APS	50 μL	50 μL
TEMED	5 μL	5 μL

a: The recipe listed here is for preparation of two gels.

3.3.5.4. Running, staining and imaging of gels

The loaded gel was subjected to a voltage of 180 V (native and glycine SDS-PAGE) or 100 V (tricine SDS-PAGE) until the dye front approached the bottom of the gel. All gels were stained using 0.3% Coomassie brilliant blue R 250 for 1 h at 20 °C. The de-staining solution contained 10% v/v acetic acid and 10% v/v 2-propanol, and the gels were left in the de-staining solution 24-48 h at 20 °C, with shaking. Gels were scanned using a molecular imager Gel Doc XR system (Bio-Rad Laboratories, CA) and images were analyzed using either QuantityOne or ImageLab software.

3.3.5.5. 2-Dimensional nonreducing-reducing (2D NR-R) SDS-PAGE

For 2D NR-R PAGE analysis, the methodology described previously by Havea et al. (1998) was followed to investigate disulfide bonding in the fibrils. The first dimension was under non-reducing conditions and the second dimension used reducing conditions. The surface-washed pellets suspended in the non-reducing PAGE buffer were resolved on gels (49.5% T and 3% C, 20% resolving gel) using tricine buffer system and the lanes with protein bands were excised using a clean scalpel. The excised lanes were then reduced in 200 mM DTT solution at 56 °C for 15 minutes followed by washing with excess water for 10 minutes. The washed gel strips were placed horizontally between the gel casting plates in the stacking gel area on top of the resolving gel. The resolving gel was poured from the sides to a height that left a gap of 10 mm between the lower part of the gel strip and the surface of resolving gel. Stacking gel was poured around and over the reduced gel strip to cement it in place and remove air from around it. The reduced sample was loaded into a single well on the side as a control. The resolving gel concentration was 20% (49.5% T, 3% C) in both dimensions.

3.3.5.6. Densitometry

The residual intensities of the β -Lg band at different times (I) were measured and corrected against the background intensities using a global background subtraction. The corrected intensities were then normalized against the intensity of the unheated sample in the same gel (I_0). The data from a minimum of two independent experiments were averaged and used for curve fitting. The intensities were fitted using a first order rate equation of Equation (3.8) in which t is time in h, while k_h is the rate constant.

$$I = I_0 e^{-k_d t} \quad \dots\dots\dots (3.8)$$

The molecular weights of peptide bands were estimated as described by Weber et al. (1969). The samples were analyzed along with the known molecular weight standards on the same gel. A standard curve of log (Molecular weight) vs R_f was plotted, where

$$R_f = \frac{L_{band}}{L_{dye\ front}} \quad \dots\dots\dots (3.9)$$

In the above equation R_f is the relative migration distance, L_{band} and $L_{dye\ front}$ are the distances of the protein/peptide band and the dye front from the top of the resolving gel respectively. The weight of the β -Lg band calculated using the standard curve was normalized by the known mass of the β -Lg (18,363 Da) and a correction factor was calculated. The weights of peptide bands calculated from the standard curve were corrected relative to that of β -Lg using the correction factor.

3.3.6. CD spectroscopy

3.3.6.1. Introduction

The phenomenon of circular dichroism arises due to the ability of certain molecules to absorb circularly polarized light (Kelly et al., 2005; Kelly et al., 1997). Circularly polarized light consists of two non-superimposable components of equal intensities. When viewed at the light source, these components can be considered as one moving in a clockwise direction (R) and the other in anticlockwise (L). In the absence of any absorption, the magnitude of rotation for both components is the same (Figure 3.3, A) and there is no CD signal (Kelly et al., 2005; Kelly et al., 1997). When passed through a sample consisting of chiral constituents, the L and R components are

absorbed at different magnitudes resulting in an elliptical polarization of the incident light (Figure 3.3, B) (Johnson Jr., 1996; Kelly et al., 2005; Kelly et al., 1997). The absorption of the polarized light by the chiral compounds follows Beer-Lambert's law indicating the absorption is proportional to concentration and path length of the cuvette/cell used. The details of different types of spectropolarimeters and their advantages have been discussed in reviews elsewhere (Kelly et al., 2005; Woody, 1995).

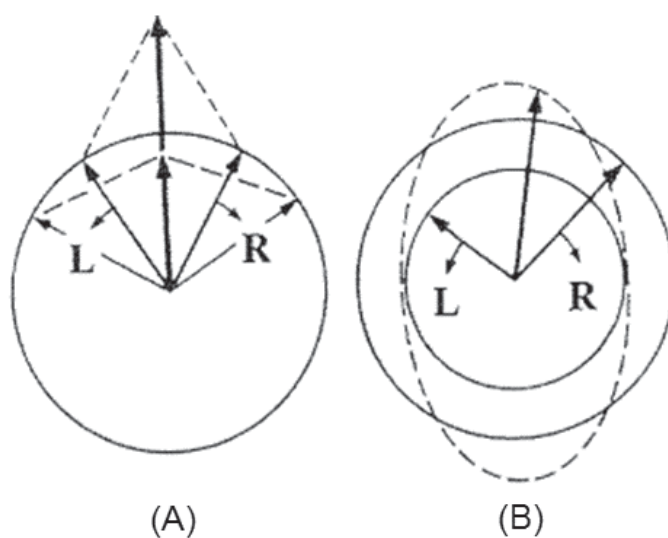


Figure 3.3 Components of circularly polarized light (A) without absorption and (B) after absorption by chiral component. Adapted from Kelly et al. (2005).

In proteins, the CD signals largely arise due to the absorption by the peptide bonds (below 240 nm), side chains of aromatic amino acids, chiral di-sulfide bonds, bound co-factors and ligands (Woody, 1978). The peptide bonds of the polypeptide backbone absorb polarized light around 220 nm and 190 nm due to the $n-\pi^*$ and $\pi-\pi^*$ transitions respectively (Kelly et al., 2005; Woody, 1978). The spectra collected in the region 178 to 260 nm also known as the far UV (FUV) region represents the secondary structure of proteins (Kelly et al., 2005; Woody, 1978). The proportion of

different conformational elements of the secondary structure can be calculated from algorithms using the CD and crystallographic data of the protein (Kelly et al., 2005). However for accurate and reliable estimations, complete CD data in the FUV range especially below <190 nm is desirable (Kelly et al., 2005; Provencher et al., 1981; Sreerama et al., 2004; Yang et al., 1986).

The absorption by specific amino-acid residues such as at around 290 nm by Trp, between 275 and 282 nm by Tyr and around 260 nm by Phe results in distinct absorption patterns (Kelly et al., 2005). The spectra covering this range 260 to 320 nm is referred to as the near UV spectra and represents the tertiary structure of proteins. Since the number of aromatic amino-acid residues and their spatial arrangement in the folded protein molecule may vary, different proteins may have their own characteristic spectra of the native protein (Kelly et al., 2005).

The choice of buffer system used for the sample preparation has an important bearing on the quality of spectra. Chloride ions strongly absorb polarized light below 200 nm (see Annexure 11.2) and hence the use of phosphate in low pH buffer systems is recommended (Kelly et al., 2005). The details about considerations for the choice of different buffer systems and their absorption are discussed in detail by Kelly et al. (2005)

3.3.6.2. Sample preparation

β -Lg spectra were measured on a Chirascan, CD spectrometer using a cuvette of path length 10 mm. The concentration of β -Lg for scans in the near UV (NUV) region was 1 mg/mL and 0.01 mg/mL for the far UV (FUV) region. In all the CD experiments in this work, HCl was used to adjust pH to avoid ion-specific effects of phosphate ions and to maintain consistency in the sample preparation method with

Chapter 3. Materials and Methods

that used for investigating self-assembly. A stock solution of β -Lg was made in HPLC grade water at pH 2 (adjusted using 6 M HCl) and the sample was allowed to hydrate overnight at 4 °C. The samples were then diluted to the desired concentration, filtered using a syringe filter of pore size 0.2 μ m and pH re-adjusted to pH 2.00 \pm 0.02. Protein concentrations were determined as described above.

3.3.6.3. Recording scans

Scans of native β -Lg were obtained at 20 °C. The temperature of the sample was raised from 20 to 80 °C in the instrument at a rate of 12 °C/min. As soon as the temperature reached 80 °C, continuous scans were taken for one hour at a scan rate of 1 nm/s. For NUV region, scans were taken between wavelengths 260 and 320 nm in a total scan time (including the interval between two successive scans) of 40 seconds. Data from three scans were averaged over 2-minute time intervals. Each FUV scan in the range 180-250 nm took 1 minute and data from two successive scans were averaged. The baseline scans for both NUV and FUV regions were recorded and averaged as above using water at pH 2 instead of β -Lg. Averaged scans of baselines were subtracted from β -Lg scans and molar ellipticity was calculated according to the following equation (Woody, 1995).

$$[\theta]_M^\lambda = \frac{100 \times \theta_\lambda}{L \times C} \dots \dots \dots (3.10)$$

Where, θ_λ is the measured ellipticity (deg) at wavelength λ , L is path length of the cuvette used (cm) and C is the protein concentration (dmol/L).

The subtracted scans were smoothed using SigmaPlot 12.0 software. The smoothing algorithm fitted a quadratic function with negative exponential (Gaussian) weighting to successive windows of five points. To compare the kinetics of structural changes

in β -Lg upon heating, the relative change in ellipticity at 293 nm or 208 nm was calculated using the following equations:

$$\left(\frac{\Delta[\theta]_t}{\Delta[\theta]_0}\right)_{293} = \frac{[\theta]_t - [\theta]_{60}}{[\theta]_0 - [\theta]_{60}} \dots\dots\dots (3.11)$$

$$\left(\frac{\Delta[\theta]_t}{\Delta[\theta]_{60}}\right)_{208} = \frac{[\theta]_t - [\theta]_0}{[\theta]_{60} - [\theta]_0} \dots\dots\dots (3.12)$$

Where subscripts t , 0 and 60 indicate ellipticities at times t , 0 min and 60 min. The differences between these two equations reflect the fact that heating caused ellipticity at 293 nm to become less negative during heating, whereas ellipticity at 208 nm became more negative over time during heating.

In this method of calculating relative changes in secondary and tertiary structure, the losses of intensities were calculated relative to the initial intensities. This methodology did not account for conditions when the native structure of β -Lg was stabilized. To account for these situations, the Equations 3.11 and 3.12 were modified slightly as below:

$$\left(\frac{\Delta[\theta]_t}{\Delta[\theta]_0}\right)_{293} = \frac{[\theta]_t - [\theta_c]_{60}}{[\theta]_0 - [\theta_c]_{60}} \dots\dots\dots (3.13)$$

$$\left(\frac{\Delta[\theta]_t}{\Delta[\theta]_{60}}\right)_{208} = \frac{[\theta]_t - [\theta_c]_0}{[\theta]_{60} - [\theta_c]_0} \dots\dots\dots (3.14)$$

In above equations, $[\theta_c]_{60}$ represents the molar ellipticity in the control sample β -Lg, which was fully unfolded after 60 minutes at 80 °C. Equations 3.13 and 3.14 have been used to monitor heat-induced changes in the native structure of β -Lg in the presence of polyols in Chapter 7.

3.3.7. Mass Spectrometry

In this section, the basic principles of protein analysis by mass spectrometry with reference to experimental analysis used in the subsequent chapters are discussed.

3.3.7.1. Introduction

Two different MS methods: electro-spray ionization mass spectrometry (ESI MS) and matrix assisted laser desorption ionisation time of flight (MALDI-TOF) were used to characterize polypeptides in the samples. These methods primarily differ in the way the sample is ionized and have their own advantages. The ESI MS is preferred due to its mild analysis conditions. In contrast, MALDI-TOF offers higher sensitivity for low molecular weight peptides, but the conditions of ionization can have a detrimental effect on the sample (Kinter et al., 2000). The principle of analysis and the components of these two methods is explained below, which has been reviewed in detail by Kinter et al. (2000).

The block diagram showing the components of a mass spectrometer is shown in Figure 3.4. The major components of a mass spectrometer include an ion source, a mass analyzer and a detector. In ESI MS, the sample is usually passed through an HPLC system, or is acidified before injection resulting in the protonation of charged residues such as lysine and arginine. The sample is then passed through a needle, with a small diameter maintained at a high positive voltage. The positive voltage of the needle repels the positively charged sample into the spectrometer which is accompanied by vaporization of the sample. The purity of the sample is of utmost importance while using ESI MS and requires efficient removal of contaminants such as urea, or guanidine hydrochloride, which are commonly used in protein sample preparation intended for the MS analysis. In comparison, in MALDI TOF analysis,

the acidified sample is embedded into a UV absorbing matrix. During analysis, the matrix containing the sample is gradually vaporized by application of discrete pulses of UV laser light. The MALDI mass spectrometers usually use the time-of-flight mass analyzers. The MALDI-TOF MS is comparatively more tolerant to contaminants, and hence does not require combination with HPLC at the inlet.

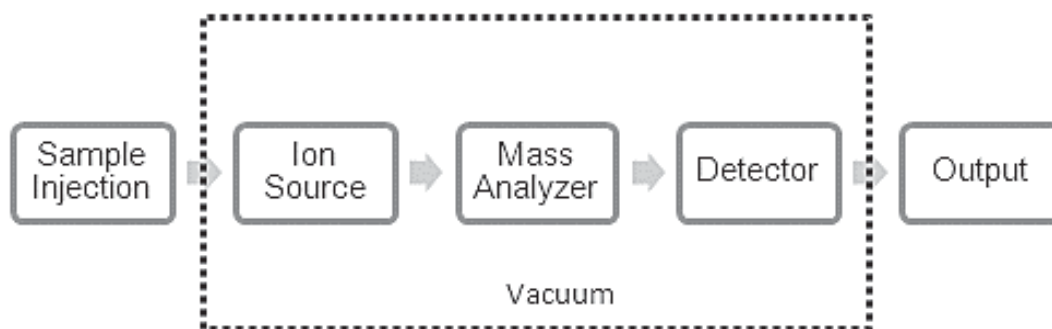


Figure 3.4 Schematic representation of mass spectrometer.

Both spectrometers used in this work had TOF mass analyzers. The sample ions in the TOF analyzers are imparted a fixed amount of kinetic energy by an electric field, following which they enter a region without any electric field. The velocity of the ions in this region is inversely related to their mass/charge ratio (m/z). Thus, ions with a larger m/z will travel slowly while those with low m/z travel much faster to the detector. The TOF mass analyzers require the sample ions to be introduced in discrete pulses and hence they are ideally suited for instruments which use a laser to produce ions (MALDI).

The electro-spray ionizers produce a continuous stream of ions and require modulation of ions entering the analyzer. In the ESI mass spectrometer, this is achieved by using a quadrupole-TOF mass analyzer. A quadrupole is a set of electrodes which form opposite poles for radio frequency (RF) and direct current (DC)

Chapter 3. Materials and Methods

voltages. The movement of sample ions through the analyzer can be modulated by controlling the voltage on these electrodes. In addition, the quadrupole also allows selection of specific charged ions for further analysis serving as an ion filter (Mann et al., 2001).

The data from the masses of the ions from the mass analyzers is expressed as m/z in the plot of abundance vs m/z and can be deconvoluted to obtain actual mass of the polypeptide. In the subsequent experimental chapters, this approach has been used to identify, β -Lg variants A, B and C (Chapter 5) and glycosylated β -Lg in Chapter 6. For a mixture of peptides, the MS data can be searched against measured peptide masses in specific databases to predict sequences in the peptides. This approach is known as peptide mass mapping (Jensen et al., 1997). A more accurate characterization of sequences in polypeptides can be achieved by using tandem MS.

In tandem MS, the ions are first separated based on m/z and used for further fragmentation into smaller fragment ions (Biemann et al., 1987). Upon fragmentation, each precursor or parent ion results in two fragment ions which are classified based on the retention of charge on the ion and are denoted as a, b or c ions, or as x, y or z ions (Mann et al., 2001). The details of the nomenclature and the origin of respective ions are discussed in detail on Mascot search database (Perkins et al., 1999) help-page ("Matrix science help: Peptide Fragmentation,") and by Kinter et al. (2000). The information from the two set of ions can be integrated separately to deduce sequences from the opposite ends of the protein (Eng et al., 1994). This approach for characterizing peptide sequences has been used to identify sequences present in fibrils in Chapter 4.

3.3.7.2. Determination of molecular weights

β -Lg powder was dissolved in water (pH 2) and filtered using a 0.2 μ m syringe filter and then subjected to RP-HPLC at a flow rate of 1 mL/min. The composition of the buffers were 10% (v/v) acetonitrile (MeCN) in water containing 0.1% trifluoro acetic acid (TFA) for buffer A and 90% (v/v) MeCN and 10% (v/v) water with 0.08% TFA for buffer B. The sample was eluted using the following program: 2 minute wash with buffer A followed by a linear gradient of buffer B from 0 to 65% in 13 minutes and then to 100% B in 1 minute. This was followed by isocratic elution of buffer B for 5 minutes and then a gradient to 0% B in 1 minute after which a wash with buffer A for 2 minutes followed. A single large peak was eluted when the MeCN concentration was 38%, and this peak was collected and concentrated to approximately 100 μ L by evaporation under vacuum. The samples were stored at -86 $^{\circ}$ C until further analysis. At the time of analysis, the sample was thawed and centrifuged at 10,000 g and analysed by ESI-MS.

HPLC purified samples (2 μ L) were auto-injected into an Agilent 1200 LC system (Agilent Technologies, USA) on bypass mode. The isocratic mobile phase comprised of 0.1% (v/v) formic acid/ 50% (v/v) MeCN/ 50% (v/v) water at a flow rate of 100 μ L/min. The LC eluent was directed to the electrospray ionization (ESI) source at a capillary voltage of 3.4 kV of the mass spectrometer. Sample analysis was performed in positive ion mode and the data were stored in profile mode. MS scans (100-1,700 m/z) were obtained with fragmentor and skimmer voltages at 175 and 65V, respectively. Other source parameters were: drying gas temperature 325 $^{\circ}$ C; gas flow-rate 6 L/min; and nebulizer gas pressure 30 psig. Total ion chromatograms (TIC) obtained were examined and spectra deconvoluted using Agilent MassHunter Workstation Qualitative Analysis software (version B.03.01)

with BioConfirm plugin (Agilent Technologies, Santa Clara, CA, USA). The intensity of the peaks was normalized by assigning the most intense peak in the spectrum to 100%.

3.3.7.3. Sequence characterization by MALDI-TOF MS/MS

For MALDI-TOF MS, the complete-washed pellets from β -Lg (1% w/v) (see Section 3.3.4) that had been heated for 12 h were suspended in 5 mL buffer (8 M guanidinium chloride, 0.15 M Tris and 0.1 M DTT, pH of 8) and then held at room temperature until they were dissolved. After 14 days, the sample appeared transparent and did not show the presence of any insoluble material. A 1 mL aliquot of this solution was diluted to a final guanidinium chloride concentration of 5 M then centrifuged at 14,100 g for 10 minutes and filtered (0.2 μ m filter).

A 100 μ L aliquot of the filtered sample was subjected to RP-HPLC using a C₁₈ column at a flow rate of 1 mL/min. After loading, the sample was washed with buffer A (10% acetonitrile (MeCN), 90 % water and 0.01% trifluoro acetic acid (TFA)) for 1 min, and then eluted using the following program: 0 to 20% buffer B (90% MeCN 10% water and 0.08% TFA) over 10 minutes; 20% to 100% B over 1 minute 100% B for 5 minutes; 100 to 0% B in 1 min; 0% B for 5 minutes. The elution was monitored by absorbance at 214 nm and 280 nm and peaks due to buffer sample components were identified by running each of the buffer components separately. Peaks eluting at acetonitrile concentrations of 25% and 90% collected from five runs were pooled and stored at 4 °C until further analysis. The samples from 2 runs were collected, pooled and concentrated by centrifugation under vacuum prior to analysis.

The analysis of samples was carried out at the Centre for Protein Research, University of Otago, Dunedin, New Zealand. A 1 μ L sample was pre-mixed with 1

μL of matrix (10 mg/mL, cyano-4-hydroxycinnamic acid, dissolved in 65% (v/v) acetonitrile containing 0.1% (v/v) TFA). A sample (0.8 μL) was spotted onto a MALDI sample plate (opti-TOF 384-well plate, Applied Biosystems, MA) and air-dried. Samples were analyzed on a 4800 MALDI TOF analyzer (MALDI TOF/TOF, Applied Biosystems, MA). Calibration was done for the mass range 1,000 to 25,000 m/z on a 5 peptide/protein calibration mix, and the mass range between 20,000 and 10,000 m/z on the BSA 1+ and 2+ ions (66,000 and 33,000 m/z). All MS spectra were acquired in linear, positive-ion mode with 1200 laser pulses per sample spot. The 15 to 20 strongest precursor ions of each sample spot were selected for MS/MS collision-induced dissociation (CID) analysis. CID spectra were acquired with 2,000-4,000 laser pulses per selected precursor using the 2 kV mode and air as the collision gas at a pressure of 1×10^{-6} torr.

For protein identification, MS/MS data was searched against the SWISS-PROT sequence database using the Mascot search engine (Perkins et al., 1999). The search was set up for no enzyme cleavage specificity and with deamidation of asparagine (N) and glutamine (Q) and oxidation of methionine (M) included as variable modifications. The precursor mass tolerance threshold was 15 ppm and the maximum fragment mass error 0.4 Da. A probability cut-off of $P < 0.05$ was used, which gave a threshold cut-off ion score of 55. The sample contained only a single protein (β -Lg), so the traditional decoy approach for database searching was not applicable.

3.3.7.4. Characterization of sequences in fibrils by ESI-MS/MS

Characterization of peptides present in fibrils was also carried out by in-gel digestion followed by ESI MS-MS using a methodology described previously (Soskic et al., 2001). For in-gel digestion ESI-MS, the final surface-washed pellet was suspended

Chapter 3. Materials and Methods

(Section 3.3.4) in 10% SDS and allowed to stir for 3 days. After three days, the samples appeared clear and 250 μL of this solution was diluted 1:1 in reducing PAGE loading buffer (4% w/v, SDS) then analyzed by tricine SDS-PAGE as described above. A control sample suspended in PAGE loading buffer (4%, w/v SDS) was run on the same gel. The concentration of the resolving gel was 20% and the stacking gel 4%. The gels were stained using colloidal Coomassie blue to identify peptide bands (Candiano et al., 2004). Five major bands identified in the pellet were cut from the gels and de-stained using warm water. For the control sample, the single band corresponding to the β -Lg monomer band was excised. Samples were reduced using 50 mM tris(2-carboxyethyl) phosphine hydrochloride and alkylated with 360 mM acrylamide to prevent re-formation of disulfide bridges during subsequent steps. The gel pieces were digested using trypsin Gold (final concentration 400 μM) at 37 $^{\circ}\text{C}$ for 20 h. Peptides obtained after digestion were extracted from the gel pieces by washing with acetonitrile containing 1% (v/v) formic acid and concentrated to a minimum volume of 25 μL in a vacuum concentrator. The samples were stored at -80 $^{\circ}\text{C}$ until analysis by ESI-mass spectrometry.

Aliquots (5 μL) of samples were injected into an HPLC-Chip Cube Interface (G4240A) with ProtID-Chip-43 (II) chip on an Agilent 1260 infinity LC system and analyzed using a Q-TOF mass spectrometer (6520, Agilent Technologies Ltd.). The capillary voltage was 1850 V, the drying gas temperature was 300 $^{\circ}\text{C}$ at a flow-rate of 4 $\mu\text{L}/\text{min}$, the fragmenter voltage was 175 V and the skimmer voltage was 65 V. Precursor ions were scanned from 100 to 1,700 m/z at 6 spectra/s. For MS-MS analysis, ions were scanned from 50-1,700 m/z at 4 scans/s. The data were analyzed using the Mascot search engine allowing the variable modifications described above

with trypsin cleavage, a precursor mass tolerance threshold 15 ppm and the maximum fragment mass error of 0.4 Da. For the control β -Lg band, since the sample was not heated, deamidation of asparagine and glutamine (N or Q) and oxidation of methionine (M) were not included as variable modifications. The probably cut-off $P < 0.05$ was used for all searches for the peptide bands which gave a threshold ion score cut-off of 46, while the threshold cut off for the control β -Lg band was 42.

3.3.8. Transmission electron microscopy

For TEM analysis, a methodology described by Loveday et al. (2010) was used. Fibrils were first separated using the ultrafiltration method of Bolder et al. (2007c). Previous method development work at our lab (Wang, 2009) showed that imaging of fibrils after their separation from the heated solution using centrifugal filters provided superior results than when the heated sample was used for imaging.

The centrifugal filter with molecular weight cut off (MWCO) 100 kDa was first wetted with 2 mL filtered water (pH 2) and centrifuged at 3,000 g for 5 minutes. Two hundred μ L of the heated solution was then added to the filters and mixed with 2 mL of water (pH 2) followed by centrifugation for 15 minutes. Water (2 mL, pH 2) was added for washing the retentate and the filters were re-centrifuged at 3,000 g for 15 min at 20 °C. The washing step was repeated three times in total. After the final washing step, 1 mL water (pH 2) was added to the retentate and mixed by inverting several times. This resulted in dilution of total protein concentration by approximately 10-fold (Loveday et al., 2010). For TEM analysis, 200 μ L of the filtered sample was mixed with 200 μ L of water (pH 2) and 20 μ L of bovine serum

Chapter 3. Materials and Methods

albumin (BSA) (0.5%, w/v), in an Eppendorf tube. The TEM images of BSA solution without any fibrils did not show any aggregates (Annexure 11.3).

At the time of analysis, a 200 mesh copper grid coated with carbon Formvar was gently placed on a drop of the sample and allowed to be in contact with the sample for 5 minutes. The grid was then removed from the sample and the excess sample removed by touching the sides of a filter paper. The filter paper was touched to the grid at different locations on the grid circumference to allow an even spread of the sample on the grid. The sample side of the grid was then put in contact with on a drop of 2% (w/v) uranyl acetate solution for 5 minutes. The excess of the stain was removed using a filter paper as described above and the sample was allowed to air dry. The imaging of the grids was done on a Phillips CM10 transmission electron microscope (Eindhoven, Netherlands) operating at 80 kV. Ten grid squares were randomly selected from different locations on the grid for imaging. Images were captured at different magnifications 25,000 to 64,000 x and recorded in the .tiff format.

3.4. Software packages

All image processing work was done using Adobe Photoshop Elements 7.0. The processing of the images was limited to converting them to gray scale and adjusting the contrast. Unless, stated otherwise, all calculations were done in MS excel, while SigmaPlot 12.0 was used for preparation of graphs, non-linear regression curve fittings and deriving statistical parameters.

Chapter 4

4. Characterization of β -Lactoglobulin self-assembly: Structural changes in early stages and disulfide bonding in fibrils

The contents of this chapter have been published in a peer-reviewed journal article and adapted with permission from:

Dave, A. C., Loveday, S. M., Anema, S. G., Loo, T. S., Norris, G. E., Jameson, G. B., & Singh, H. (2013). β -Lactoglobulin self-assembly: structural changes in early stages and disulfide bonding in fibrils. *Journal of Agricultural and Food Chemistry*, 61(32), 7817-7828. Copyright (2013) American Chemical Society.

4.1. Abstract

Bovine β -lactoglobulin (β -Lg) self-assembles into long amyloid-like fibrils when heated at 80 °C, pH 2 and low ionic strength (<0.015 mM). Heating β -Lg under fibril-forming conditions shows a lag phase before fibrils start forming. This study investigated the structural characteristics of β -Lg during the lag phase and the composition of β -Lg fibrils after their separation using ultracentrifugation. During the lag phase, the CD spectra of heated β -Lg showed rapid unfolding, and SDS-PAGE of samples showed increasing hydrolysis of β -Lg. The SDS-PAGE profiles of fibrils separated by ultracentrifugation showed that after six hours, the fibrils consisted of a few preferentially accumulated peptides. 2D SDS-PAGE under reducing and non-reducing conditions suggests the presence of disulfide-bonded fragments in the fibrils. The sequences in these peptide bands were characterized by

Chapter 4. Characterization of β -Lg Self-Assembly

in-gel digestion ESI-MS/MS. The composition of solubilized fibrils was also characterized by MALDI TOF MS/MS. Both MS analyses showed that peptides in fibrils were primarily from the N-terminal region, although there was some evidence of peptides from the C-terminal part of the molecule present in the higher molecular weight gel bands. It is suggested that although the N-terminal region of β -Lg is almost certainly involved in the formation of the fibrils, other peptide fragments linked through disulfide bonds may be present in the fibrils.

4.2. Introduction

Bovine β -lactoglobulin (β -Lg) is a water-soluble globular protein present in milk at concentrations of approximately 0.18 to 0.50% (w/v) (Sawyer, 2003) and accounts for approximately 50% of the total whey proteins. It has a molecular weight of approximately 18.4 kDa and mainly exists in polymorphic forms A and B that differ, respectively by the substitutions Asp for Gly at position 64 (on an exposed loop) and Val for Ala at position 118 (at a partly internal site) (Sawyer, 2003). In its native state, β -Lg has two disulfide bonds between residues Cys66-Cys160, linking the CD loop with the C-terminal region and Cys106-Cys119 linking loops G and H and a free thiol group at Cys121 (Brownlow et al., 1997). At pH 2 and low ionic strength β -Lg exists as a monomer (Uhrinova et al., 2000) and shows high heat stability (Kella et al., 1988). It has a well-defined secondary structure consisting of 50% β -sheet, 10% α -helix and 35% random coil (Qi et al., 1997), the latter mostly found on the structure-stabilizing flexible loops connecting the different β -strands in the structure (Jameson et al., 2002). β -Lg self-assembles into amyloid-like fibrils upon incubation with solvents (Gosal et al., 2002), heating in the presence of urea (Hamada et al., 2002) and heating at low ionic strength and low pH (Arnaudov et al., 2006; Bolder et al., 2007c; Gosal et al., 2002; Ikeda et al., 2002). Protein-based fibrils have received intense attention due their potential applications in biotechnology (Raynes et al., 2011) and as food ingredients to improve functionality (Loveday et al., 2012b).

Heating at low pH and low ionic strength has been the most common method used for investigating β -Lg fibril formation, due to relatively rapid kinetics of self-assembly under these conditions. β -Lg self-assembly shows typical characteristics of amyloid fibril formation (Bromley et al., 2005; Lara et al., 2011; Loveday et al.,

Chapter 4. Characterization of β -Lg Self-Assembly

2010) with fibrils showing β -sheets running perpendicular to the fibril axis (Bromley et al., 2005). Fibrils formed during heating at pH 2 appear long and semi-flexible, and they have a diameter of ~ 4 nm and lengths of up to 10 μm (Ikeda et al., 2002). The factors affecting the kinetics of self-assembly at low pH include the temperature of heating (Kroes-Nijboer et al., 2011; Loveday et al., 2012c), mode of heating (Hettiarachchi et al., 2012), pH (Loveday et al., 2010), seeding (Bolder et al., 2007a; Loveday et al., 2012b) and shear conditions during self-assembly (Bolder et al., 2007a; Dunstan et al., 2009). In unstirred solutions, β -Lg fibril formation shows an initial lag phase, followed by a rapid increase in the rate of self-assembly, i.e. a growth phase, and finally a stationary phase, during which the rate of self-assembly declines (Bromley et al., 2005; Loveday et al., 2010). It has been reported that during the lag phase the monomers undergo activation that leads to the formation of nuclei that then promote self-assembly (Arnaudov et al., 2003; Bromley et al., 2005). Most studies characterizing β -Lg self-assembly (Akkermans et al., 2008b; Bolder et al., 2007a; Kroes-Nijboer et al., 2011; Lara et al., 2011) use shear during heating. Shear force during self-assembly affects the kinetics of fibril formation by inducing changes in protein structure (Morinaga et al., 2010) and by enhancing nucleation (Dunstan et al., 2009) in the lag phase. Enhanced nucleation can come about through shear-induced fragmentation of protofibrils, whose fragments act as nuclei and promote self-assembly (Bolder et al., 2007a; Hill et al., 2006). Thus, information about the behavior of β -Lg before formation of nuclei in the lag phase and the nature of the nuclei still remains elusive.

A recent study has suggested a relationship between an increase in the rate of self-assembly and the rate of hydrolysis of β -Lg at high temperatures (Kroes-Nijboer et al., 2011). Akkermans et al. (2008b) reported that peptides generated during heating

at low pH are the building blocks of fibrils, but this analysis was carried out on fibrils formed after heating β -Lg for 20 h at 85 °C under constant shear conditions. Separately, fibrils from hen egg-white lysozyme have been reported to contain intact monomers as well as peptides generated upon hydrolysis (Mishra et al., 2007). Thus, it is not yet known whether hydrolysis is a prerequisite for β -Lg self-assembly. In addition the composition of fibrils or protofibrils formed from β -Lg at short heating times in the growth phase is not known with certainty.

This chapter explores the structural changes in the β -Lg monomer during the lag phase and investigates the role of hydrolysis in the formation of β -Lg fibrils, to gain insight into the structural transitions and chemical changes in β -Lg preceding self-assembly. Accordingly, the composition of fibrils formed after different heating times during self-assembly was studied by SDS-PAGE after their separation using ultracentrifugation. 1D and 2D non-reducing and reducing SDS-PAGE were used to determine disulfide bonding in fibrils, while mass spectrometry was used to characterize the makeup of β -Lg fibrils in the growth phase.

4.3. Materials and Methods

All materials and chemicals used in this study have been described in Chapter 3. All samples and reagents were made in Milli Q water. Fibrils from β -Lg were prepared using method described in Section 3.3.2. The Thioflavin T (ThT) assay (Section 3.3.3) was used to detect fibrils in the heated samples. Fibrils from samples were separated by ultracentrifugation (Section 3.3.4). For SDS-PAGE protocols described in Sections 3.3.5.2 to 3.3.5.4 were used. 2D non-reducing-reducing (NR-R) SDS-PAGE as performed as per Section 3.3.5.5. Circular dichroism (CD) spectroscopy

was performed as per the protocol described in Section 3.3.6. For MS, the samples were prepared as per protocol described in 3.3.7.2 to 3.3.7.4

4.4. Results

4.4.1. Characterization of β -Lg isolated from WPI

The proximate composition of β -Lg isolated by salt precipitation method described in Section 3.3.1 is shown in Table 4.1. The isolated β -Lg was analyzed by native-PAGE and SDS-PAGE. The native-PAGE showed the presence of two distinct major bands corresponding to β -Lg variants A and B (Figure 4.1). In addition, there were faint additional bands with mobility lower than that of β -Lg A and B. The SDS-PAGE showed a single major band (band 2, Figure 4.2), most likely corresponding to monomeric β -Lg, under both reducing and non-reducing conditions. Reducing SDS-PAGE of β -Lg showed an additional band (band 1, Figure 4.2) with molecular weight approximately equal to that of β -Lg dimer. This band appeared less distinct in the absence of the reducing agent. In addition, there were two additional faint bands (band 3 and 4, Figure 4.2) with molecular weights less than that of β -Lg. These bands were also present in the WPI analyzed under reducing conditions. The band 4, most likely corresponded to the α -lactalbumin while the identity of band 3 was not known.

Table 4.1 Proximate composition of extracted β -Lg

Composition	Amount (%w/w) ^a
Protein %	97.1
Moisture %	3.2
Salt %	0.17

a: For reference method see Annexure 11.4.

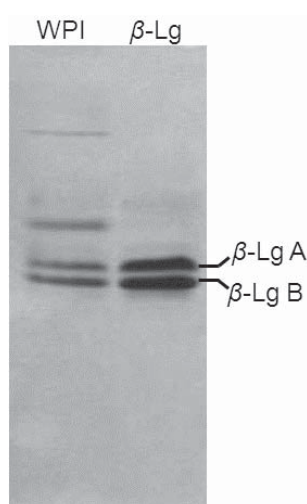


Figure 4.1 Native PAGE pattern of β -Lg isolated from WPI by salt precipitation.

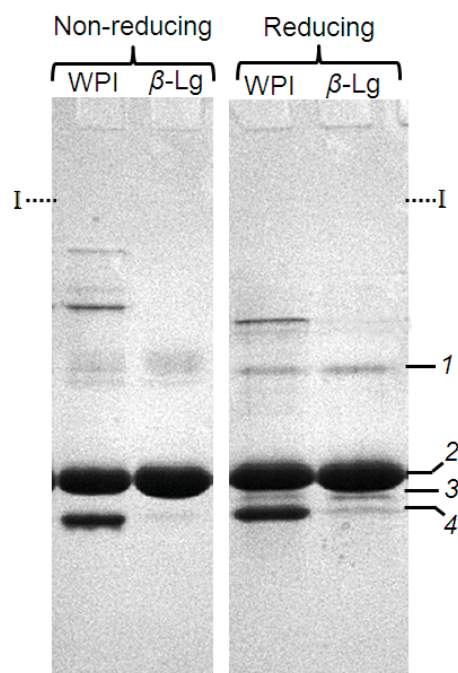


Figure 4.2 SDS-PAGE (with or without reducing agent) patterns of β -Lg isolated from WPI by salt precipitation method. I represents interface of stacking and resolving gel. For description of bands 1 to 4, see text.

It is interesting to note that band 1 (Figure 4.2) appeared less distinct under non-reducing conditions but appeared as a distinct band when analyzed in the presence of the reducing agent. This indicates that band 1 consisted of both disulfide- and non-disulfide-linked covalent dimers. The non-disulfide covalent dimerization of β -Lg can occur during heating of β -Lg at neutral pH (Mudgal et al., 2011), resulting from the isopeptide linkages involving amine group of lysine and carboxylic group of aspartate or glutamate (Stryer, 1995). The proportion of additional contaminant bands including the β -Lg dimeric band was much lower in comparison to major β -Lg band and hence the extracted β -Lg was used without any further purification.

The β -Lg was also characterized by mass spectrometry and the deconvoluted spectrum of β -Lg is shown in Figure 4.3. The MS spectra of the β -Lg showed two major peaks corresponding to the masses of β -Lg A and B. The proportion of β -Lg A

in the sample was higher than that of β -Lg B. There was no evidence of any other β -Lg species. The native structure of β -Lg was also analyzed by CD spectroscopy and the results from this study are discussed later in this section.

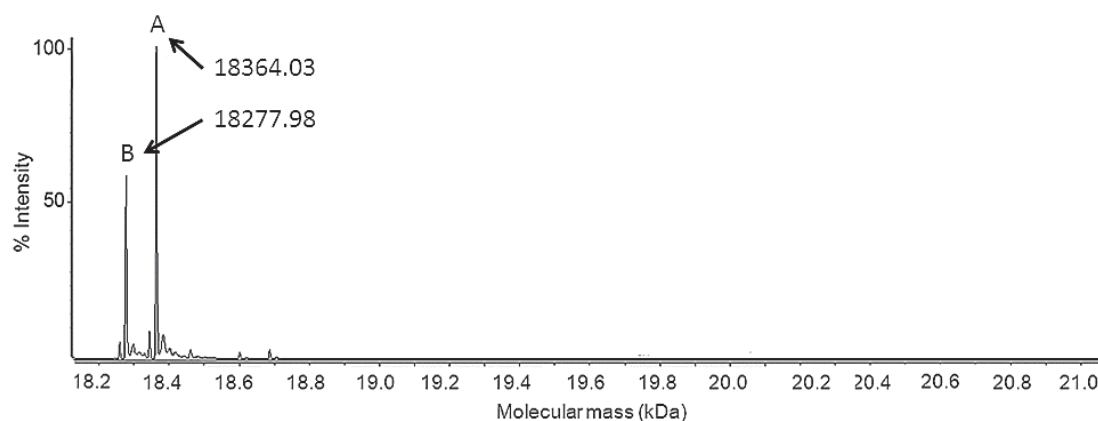


Figure 4.3 Deconvoluted MS spectrum of the isolated β -Lg.

4.4.2. Self-assembly of β -Lg

Self-assembly of β -Lg was studied using the ThT assay (Figure 4.4). ThT only binds to the β -sheets present in the β -Lg fibrils (Krebs et al., 2005). A net increase in fluorescence can therefore be used to indicate an increase in the concentration of fibrils. The samples showed low fluorescence intensity for approximately 4 h suggesting a distinct lag phase. It is widely believed that during the lag phase β -Lg forms nuclei capable of forming mature fibrils upon prolonged incubation. All samples with heating times of more than 4 h showed an increase in fluorescence intensity indicating the presence of fibrils in the heated samples.

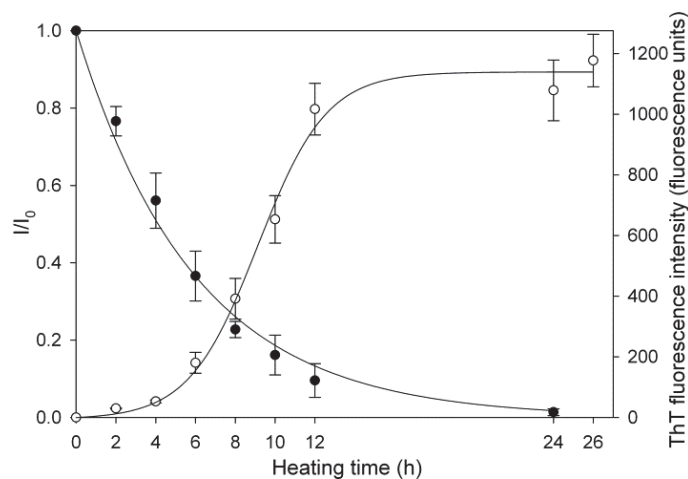


Figure 4.4 Thioflavin T (ThT) fluorescence intensity (empty circles) at 486 nm for 1% β -Lg at pH 2 heated at 80 °C. Error bars show standard deviations for triplicate measurements for three separate samples and the solid line show fit of Equation 3.1. Filled circles represent normalized intensity of the SDS-PAGE band corresponding to intact monomer. Error bars show standard deviations from three separate samples while the solid line shows fit of Equation 3.8.

The fluorescence showed a rapid increase in intensity between 6 h and 12 h, indicating the occurrence of a growth phase. The fluorescence intensity data were fitted to the model represented by Equation 3.1 ($R^2 = 0.99$). The value for t_{lag} was 5.7 h, which agreed with the experimental data that showed an increase in fluorescence after only 6 h. The value of $t_{1/2 \text{ max}}$ was calculated to be 9.1 h.

4.4.3. Hydrolysis of β -Lg in heated samples

β -Lg samples after heating for the times shown in Figure 4.4 were analyzed by tricine SDS-PAGE under reducing conditions (Figure 4.5). The unheated sample did not show evidence of hydrolysis. In contrast, all the heated samples showed differing degrees of hydrolysis of the β -Lg monomer into peptides with molecular masses ranging from 15 kDa to less than 3.5 kDa. As the time of heating increased, the

intensity of the band corresponding to the β -Lg monomer (β -Lg band) decreased with a corresponding increase in the intensities of the peptide bands.

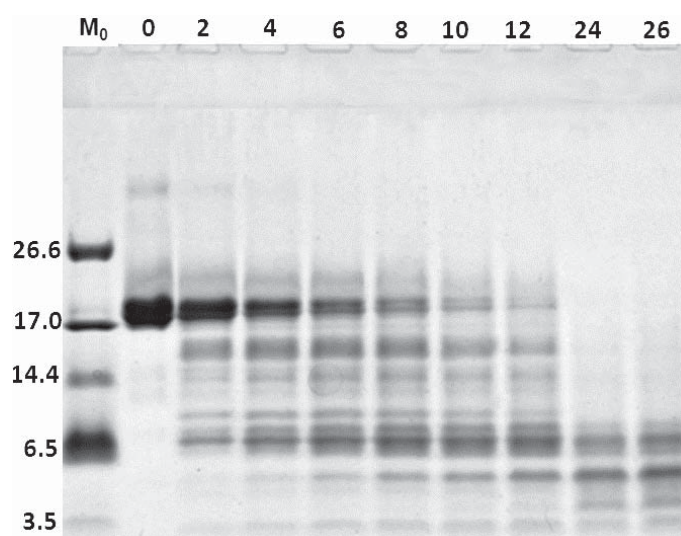


Figure 4.5 Reduced SDS-PAGE of β -Lg heated at 80 °C and pH 2 for different times. M_0 , Molecular mass marker in kDa; 0, unheated sample, numbers above the lanes indicate the heating times in hours.

The β -Lg band was quantified using a densitometer and normalized relative to the intensity of unheated β -Lg and plotted against heating time (Figure 4.4). The rate of hydrolysis was fitted using a first-order model (Equation 3.8), giving a value for the rate constant, (k_h) of $2.8 \times 10^{-3} \text{ min}^{-1}$ ($R^2 = 0.99$, estimated standard deviation 0.5×10^{-3}). This value was lower than that reported by Kroes-Nijboer et al. (2011) for β -Lg hydrolysis at 80 °C during self-assembly ($3.9 \times 10^{-3} \text{ min}^{-1}$) ($R^2 = 0.88$). This latter study involved heating with continuous shearing, whereas in this study the heating was carried out without shearing in order to minimize secondary nucleation, which would have interfered with close analysis of events in the lag phase. The % difference in the k_h values is typical of inter-laboratory variation in statistically derived parameters, so the effect of shear on k_h was probably negligible during

Chapter 4. Characterization of β -Lg Self-Assembly

heating at 80 °C. Since the objective of this study was to explore the structural transitions of β -Lg preceding self-assembly, no shearing was used during heating.

The time required to hydrolyze 50% of the β -Lg was 4.1 h. The intensity of the β -Lg band at the beginning of the growth phase, after ~6 h incubation, was calculated to be approximately 36% of the initial intensity, indicating that a major proportion of the monomer had undergone hydrolysis before significant formation of any fibrils.

Hydrolysis of β -Lg continued in the growth phase, with increasing losses of higher molecular weight peptides at >8 h. No intact β -Lg remained after 24 h and the samples contained only peptides with molecular weights below 10 kDa suggesting that larger peptides formed first and then these underwent further hydrolysis as heating continued resulting in the formation of smaller peptides. The stacking gels in all samples did not show any evidence of high molecular weight aggregates. The SDS-PAGE buffer containing the sample that had been heated for 12 h did not show any intact fibrils when analyzed by transmission electron microscopy (results not shown), confirming complete dissociation of fibrils in the PAGE sample buffer.

4.4.4. Structural transitions in the lag phase

4.4.4.1. Hydrolysis of β -Lg

Changes to β -Lg during the lag phase were explored by analyzing samples heated at 80 °C for times less than 4 h (i.e. in the lag phase) using SDS-PAGE under reducing conditions. This showed that peptides with approximate molecular weights from 15 kDa to less than 3.5 kDa appeared within 30 minutes of heating at 80 °C (Figure 4.6). The molecular weights of the bands observed in these samples were similar to those observed in the growth phase (Figure 4.5) and their intensities steadily increased throughout the lag phase. This suggests that heating β -Lg monomer at pH

2 initiates hydrolysis almost immediately. Moreover, hydrolysis of the monomer proceeds more rapidly than the subsequent hydrolysis of the higher molecular weight peptides (8-15 kDa) during this period as revealed in Figures 4.4 and 4.5. Indeed, only after longer heating times (>8 h), when the concentration of β -Lg drops to below 20% of its initial concentration, does the concentration of the higher molecular weight fragments (8-15 kDa) start to fall.

At pH 2, the free cysteine residue in β -Lg remains protonated and hence the likelihood of aggregation by intermolecular thiol-disulfide exchange reactions is greatly reduced (Mudgal et al., 2011; Otte et al., 2000). Peptide bonds with either aspartic or glutamic acid on the C-terminal side have been shown to be preferentially cleaved during heating in acidic conditions (Harris et al., 1956).

There have been several previous reports of β -Lg hydrolysis during fibril formation at low pH, high temperature and protein concentrations $\leq 2\%$ (w/v) (Bateman et al., 2010; Bolder et al., 2007c; Kroes-Nijboer et al., 2011; Lara et al., 2011; Mudgal et al., 2011). However, the shortest heating times in most cases was ≥ 3 h (Bateman et al., 2010; Bolder et al., 2007c; Lara et al., 2011; Mudgal et al., 2011) and where shorter heating times were used the fibrils were not separated from the non-fibril material (Oboroceanu et al., 2010). An increase in the rate of fibril formation at temperatures above 80 °C was shown to be related to an increase in the rate of hydrolysis of the monomer at these temperatures (Kroes-Nijboer et al., 2011). In that study, samples were stirred during heating, in order to eliminate the lag phase by promoting secondary nucleation, thereby simplifying the kinetic modeling. Thus, previous studies have not presented a comprehensive view of the events during the lag phase, particularly the role of hydrolysis. The results of this study suggest that

hydrolysis may have an important role to play in the formation of nuclei in the lag phase.

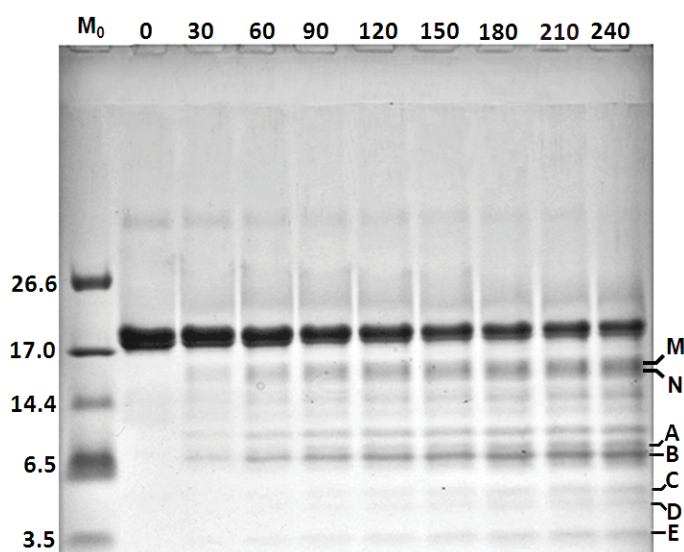


Figure 4.6 Reduced SDS-PAGE of β -Lg (1% w/v) heated at 80 °C and pH 2 during the lag phase. M_0 , Molecular mass marker (kDa); 0, unheated sample; Numbers above the lanes indicate the heating time in minutes. For description of bands A-E, M and N, see text.

4.4.4.2. Unfolding of β -Lg during heating

Structural changes in the β -Lg monomer in the early stages of the lag phase, before significant hydrolysis had occurred, were investigated using CD spectroscopy. Since the unfolding of the monomer is rapid, the samples were heated to 80 °C in a temperature-controlled cell holder in the instrument and scans were recorded continuously once the temperature reached 80 °C. The duration of heating was restricted to 1 h since the samples with heating times less than 1 h showed that the major proportion of β -Lg still remained intact (approximately 80%, from Figure 4.4). Continued heating of β -Lg beyond 1 h resulted in significant hydrolysis of the

protein monomer (Figure 4.6), so that the resulting spectra would be a mixture of those arising from β -Lg monomer and peptides.

The near UV (NUV) circular dichroism (CD) spectrum of native β -Lg provides information about the tertiary structure of the protein and is characterized by two sharp troughs at about 286 and 293 nm that are due to Trp at position 19 (Manderson et al., 1999). Small troughs observed in the region between 262 and 269 nm are attributed to Phe residues (Strickland, 1974). Heating of β -Lg from 20 °C to 80 °C resulted in a slight loss of intensities of these troughs, indicating a change in the environment around Trp19. A similar change in β -Lg tertiary structure has been reported to occur on heating from 37 °C and 75 °C (Molinari et al., 1996). Continued heating of β -Lg caused a rapid decrease in intensity of these troughs (Figure 4.7, A). Complete loss of CD signal for Trp was observed within the first 10 minutes of heating after which the spectrum remained unchanged for the rest of the heating time. These results suggest that heating of β -Lg leads to complete destruction of its native tertiary structure within the first 10 minutes after reaching 80 °C. The plot of $\left(\frac{\Delta[\theta]_t}{\Delta[\theta]_0}\right)_{293}$ against time calculated using Equation 3.11 is shown in Figure 4.8 (A).

The far UV (FUV) CD spectrum (180 to 230 nm) gives information on the secondary structure of a protein, as it measures the absorption of polarized light by peptide bonds of the polypeptide chain (Johnson Jr, 1990; Woody, 1995). Scans for unheated β -Lg showed a characteristic trough with a minimum at 217 nm suggesting the presence of β -sheets, consistent with the known structure (Molinari et al., 1996; Qi et al., 1997; Uhrinova et al., 2000). Averaged scans for samples recorded during continued heating showed that, almost immediately after commencement of heating the trough deepened with ellipticity between 220 and 230 nm becoming increasingly

Chapter 4. Characterization of β -Lg Self-Assembly

more negative. The CD spectrum then remained approximately constant with continued heating (Figure 4.7 (B)). Simultaneously, there was a shift in the trough at 217 nm, characteristic of β -sheets in the unheated protein, towards shorter wavelengths (< 210 nm). The bulk of this shift occurred during the first 10 minutes of heating, and continued heating caused only a further small deepening of the trough. A similar shift in the trough at 222 nm was seen in a diluted sample containing β -Lg fibrils (Hettiarachchi et al., 2012; Lara et al., 2011). However, within the time scales used in those studies, it is likely that a significant proportion of β -Lg monomer has undergone hydrolysis so that the CD signals represent a composite signal of residual un-hydrolyzed monomer, peptides and fibrils. In contrast, the time scale used for data collection in this study allows structural measurements to be made before significant hydrolysis occurred. The relative change in ellipticity at 208 nm represented by $\left(\frac{\Delta[\theta]_t}{\Delta[\theta]_{60}}\right)_{208}$ was calculated using Equation 3.12 and plotted against heating time (Figure 4.8, B).

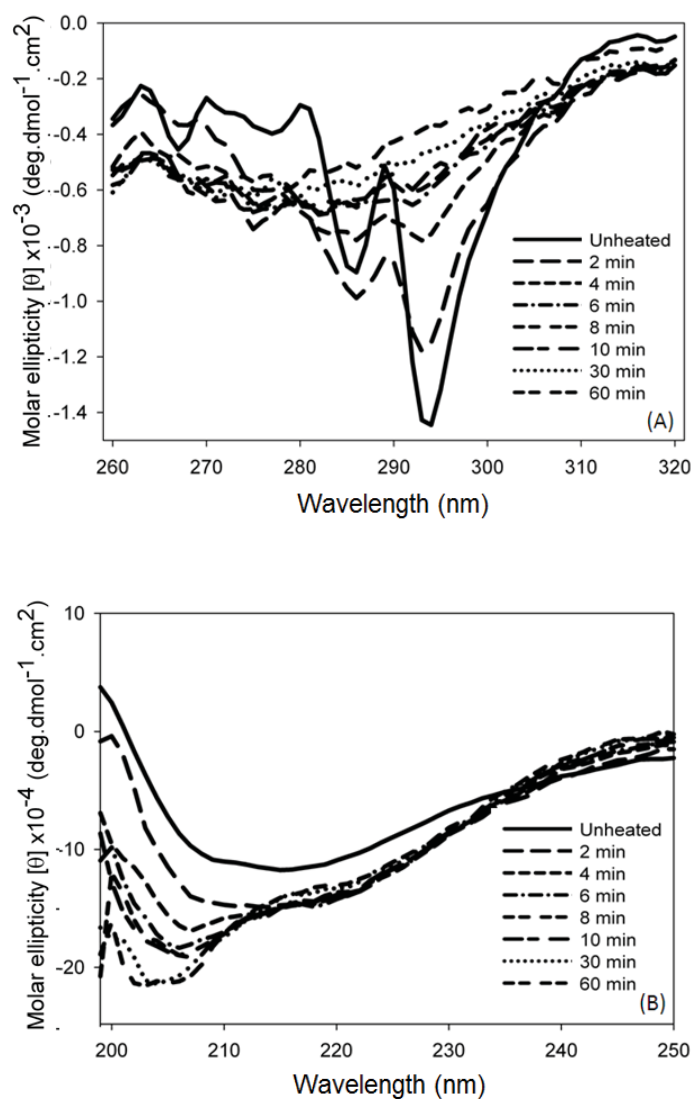


Figure 4.7 CD spectra of β -Lg at pH 2 and 80 °C. (A) Near-UV scans, (10 mg/mL). (B) Far-UV spectra (0.01 mg/mL). Conditions for data collection were: path length 10 mm, temperature 80 °C and scans were averaged at 2-minute intervals each.

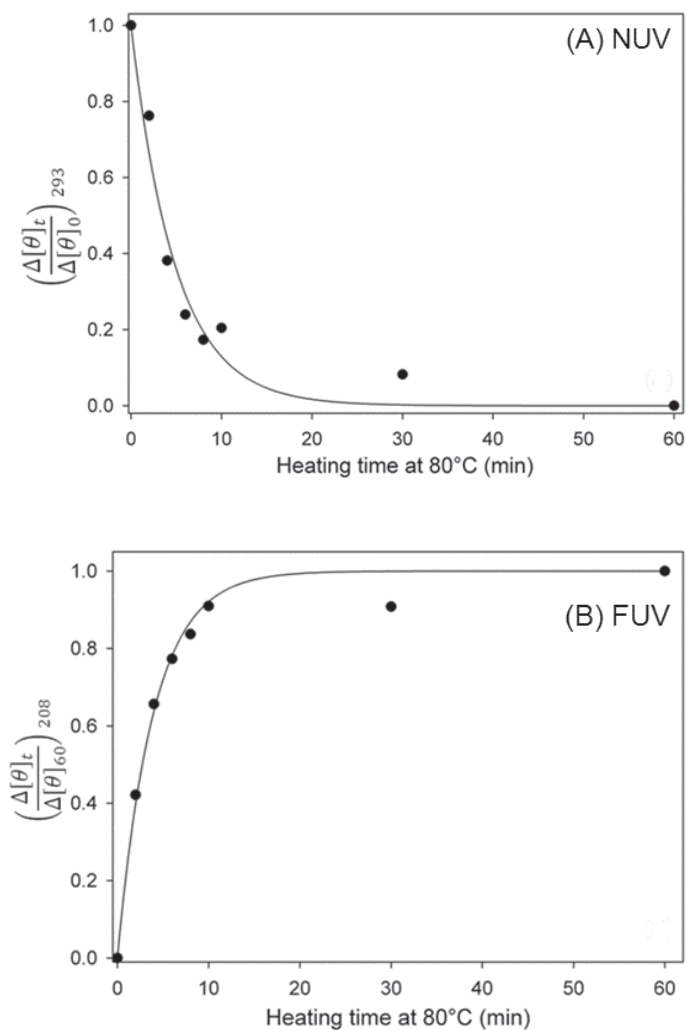


Figure 4.8 Relative change in ellipticity at (A) 293 nm representing the loss of tertiary structure, and (B) 208 nm representing change in secondary structure, calculated from data shown in Figure 4.7. Solid lines are for visual reference.

The data below 200 nm were characterized by a high detector high-tension (HT) value ($>1,000$ V) (Figure 4.9), which represents high absorbance by the sample making the spectra difficult to interpret. Chloride ions strongly absorb polarized light below 200 nm (Kelly et al., 2005). Since HCl was used for adjusting the sample pH, chloride ions contributed to the high absorbance at wavelengths in this region.

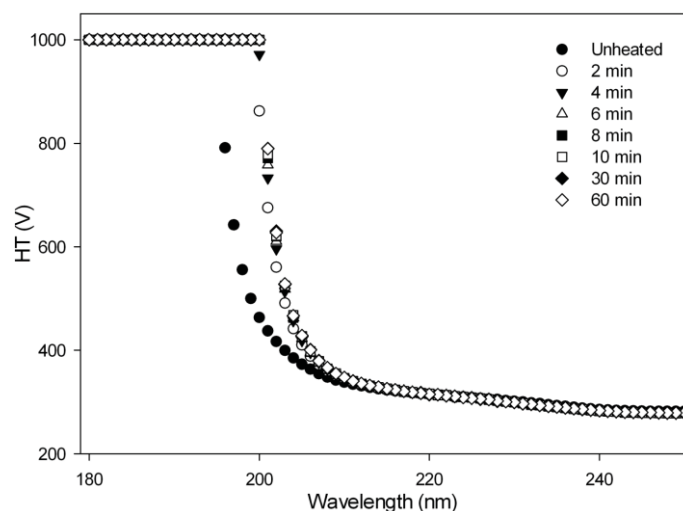


Figure 4.9 High-tension (HT) curves of circular dichroism scans shown in Figure 4.7 (B) showing high absorption by the sample between 180 and 200 nm.

4.4.5. Characterization of fibril composition

4.4.5.1. Composition of fibrils after different heating times.

Akkermans et al. (2008b) reported that peptides are the building blocks of fibrils formed at pH 2, 85 °C, and 3% protein, after 20 h under constant shear. The make-up of fibrils at earlier stages of self-assembly when a fraction of β -Lg remains unhydrolyzed is not yet known. Samples heated for different times were ultracentrifuged at 2.4×10^5 g for 60 minutes. The supernatants analyzed by ThT assay showed low fluorescence, indicating complete sedimentation of fibrils from the heated solutions (Figure 4.10). All samples heated for more than 4 h gave a

Chapter 4. Characterization of β -Lg Self-Assembly

transparent pellet upon ultracentrifugation, whereas those heated for 2 or 4 h produced no pellet.

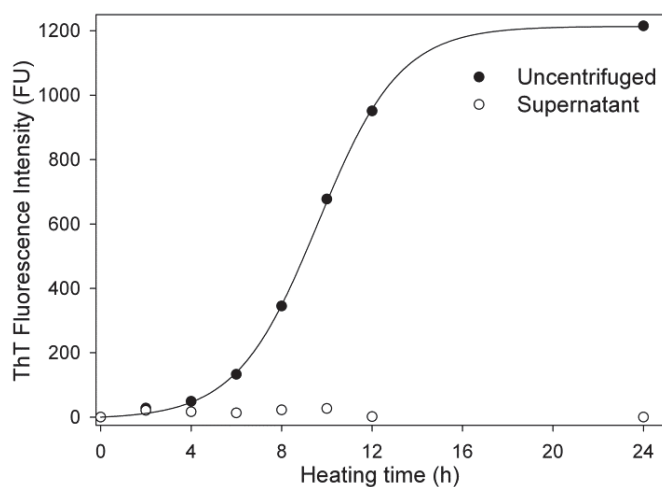


Figure 4.10 Thioflavin T fluorescence intensities at 486 nm in heated β -Lg (1%) samples (filled circles) and supernatants in (empty circles) obtained after centrifugation at 2.4×10^5 g for 60 minutes. The pellets were used for SDS-PAGE analysis shown in Figure 4.12. Solid line shows the fit of Equation 3.1.

The heated solutions and their corresponding supernatants and pellets were examined by SDS-PAGE under reducing conditions (Figure 4.11). At all heating times, the peptide compositions of the supernatants were similar to those of the parent uncentrifuged solutions. Most of the β -Lg monomers in the heated samples at all heating times remained in the supernatant, while very little intact monomer was observed in the pellets. This suggests that the fibrils formed under these conditions (pH 2, 80 °C, 1% protein) consist primarily, and probably exclusively, of peptide fragments. It is interesting to note that not all peptides generated upon hydrolysis were observed in the fibrils (pellets). Five distinct peptides (Figure 4.11, bands A-E) preferentially accumulated in fibrils, with peptides labeled D and E with approximate masses 4.1 kDa and 3.2 kDa, being the most intense bands. The intensities of all

bands, except intact β -Lg, increased with heating time. Bands M and N with an approximate molecular weight of 14 kDa showed slightly reduced intensity after subsequent washing and re-centrifugation steps (Figure 4.12). It is likely that one or more peptides in these bands before washing represented contaminant un-assembled peptides from the supernatant that were entrapped within the fibril pellet, and were dislodged during washing.

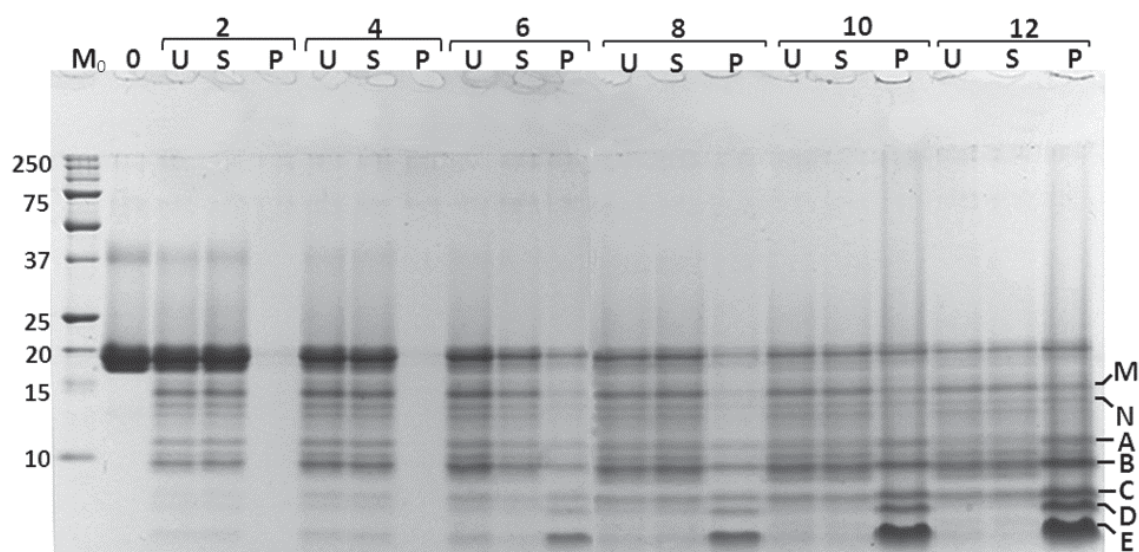


Figure 4.11 Comparison of reduced SDS-PAGE profiles of centrifuged samples at different heating times. M_0 , Molecular mass marker, weights in kDa; 0, unheated sample; U, heated and uncentrifuged; S, supernatant; P, pellet. Numbers above the lanes indicate heating times in hours. Uncentrifuged sample and supernatants were diluted 1:10 with the PAGE sample buffer. Surface-washed pellets were suspended in the loading buffer without dilution. For description of bands M, N and A to E see text.

The profiles of fibrils separated at 10 and 12 h showed a light smear in addition to the peptide bands (Figure 4.11), which may result from incomplete dispersion of the protein in the compact pellet obtained at these heating times. Ultracentrifugation of the sample heated for 24 h gave a very compact pellet that was difficult to disperse in PAGE buffer and hence rendered SDS-PAGE analysis difficult. Since continued

Chapter 4. Characterization of β -Lg Self-Assembly

heating of β -Lg for 24 h resulted in complete hydrolysis of the β -Lg monomer (Figure 4.5), it was expected that the fibrils after 24 h would be made up of only peptide fragments of β -Lg. To confirm this, the complete-washed pellet from a sample heated for 24 h was dispersed in reducing PAGE sample buffer with 4% SDS and allowed to dissolve for 7 days at 20 °C. The PAGE profiles of the sample were compared with those from pellets from samples that had been heated for both 6 and 12 h (suspended in sample buffer containing 4% SDS) under reducing conditions (Figure 4.12). Comparing the PAGE profiles of these fibrils with those of heated samples from the lag phase (Figures 4.6 and 4.11), it is clear that peptides A-E from the fibrils were first observed after just 30 minutes of heating. At heating times of less than 30 minutes, these peptides were not visible by SDS-PAGE, although it is possible that they could be present in solution at very low concentrations. While the intensity of these bands increased throughout the lag phase, there was no accompanying increase in ThT fluorescence (Figure 4.4), suggesting that self-assembly of these peptides into fibrils proceeds only once a certain minimum or critical concentration of peptides is reached.

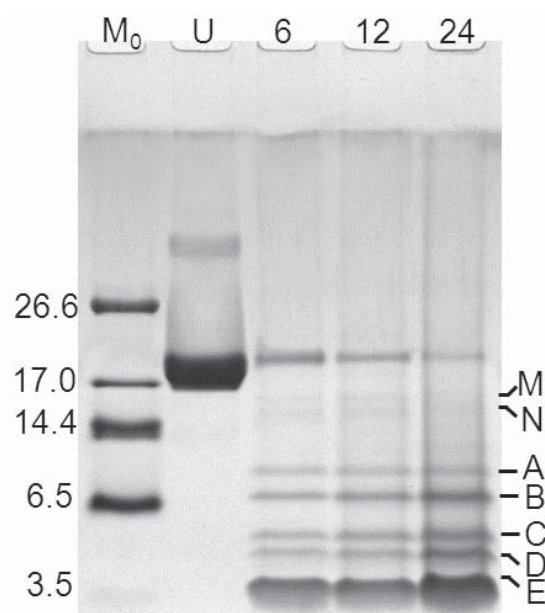


Figure 4.12 SDS-PAGE profiles of pellets obtained after centrifugation of heated samples (1% β -Lg) at different stages of self-assembly. Pellets were obtained by ultracentrifugation and were complete-washed (see Chapter 3 for details). The washed pellets were suspended in PAGE loading buffer with 4% SDS and 100 mM DTT and allowed to dissolve for 7 days 20 °C. Samples were run on tricine SDS-PAGE gels prepared in house. M₀: Molecular weight marker (weights in kDa); U: unheated; numbers above the lanes indicate heating times in h. For description of bands A to E, M and N see text.

4.4.5.2. Disulfide bonding in fibrils

To determine the presence of disulfide bonds in fibrils, a sample heated for 12 h was divided into two and ultracentrifuged. Complete-washed pellets (obtained after vortexing and re-centrifugation) from one of the samples were suspended in non-reducing PAGE loading buffer while the other was suspended in loading buffer containing reducing agent (DTT). Figure 4.13 shows the comparison of fibril peptides under reducing and non-reducing conditions. Both the reducing (lane 4, Figure 4.13) and non-reducing (lane 5, Figure 4.13) showed the same three distinct peptides corresponding to bands C-E in Figure 4.11, suggesting that these three peptides do not contain disulfide bonds. Additionally, the sample showed several faint bands with molecular weights higher than that of the monomer. Bands corresponding to peptides A and B appeared faint under non-reducing conditions, but became considerably more intense under reducing conditions, as this was especially evident in the SDS-PAGE shown in Figure 4.13. This indicates that some peptide bands eluting with bands A and B might be disulfide-linked under non-reducing conditions.

The disulfide linkage in fibrils was further investigated by subjecting complete-washed pellets obtained after 12 h heating to 2D NR-R PAGE (Havea et al., 1998). Using this technique, peptides without disulfide bonds will lie on the diagonal, while those with disulfide bonds will separate into two bands off the diagonal, due to different electrophoretic mobilities, after reduction. As expected, bands C-E eluted as distinct spots (Figure 4.14) along with spots A and B indicating that the bands A-E did not contain any disulfide linkages. Two additional spots marked P and Q appeared on the electrophoretic paths of spots M and N indicating that peptides labeled M and N were involved in disulfide linkages with peptides labeled P and Q

respectively. The relative mobilities of the peptides represented by spots P and Q were similar to those of peptides in A and B respectively, indicating they could be the same peptides when analyzed in the by 1D PAGE. In 2D NR-R PAGE, several additional peptide spots appeared adjacent to P and Q indicating that they are most likely to be disulfide-linked to P and Q. Further characterization work is necessary to determine the identity the peptides represented by these additional spots. Nonetheless, these results, together with the 1D SDS-PAGE results, indicate that the fibrils do contain disulfide-linked peptides.

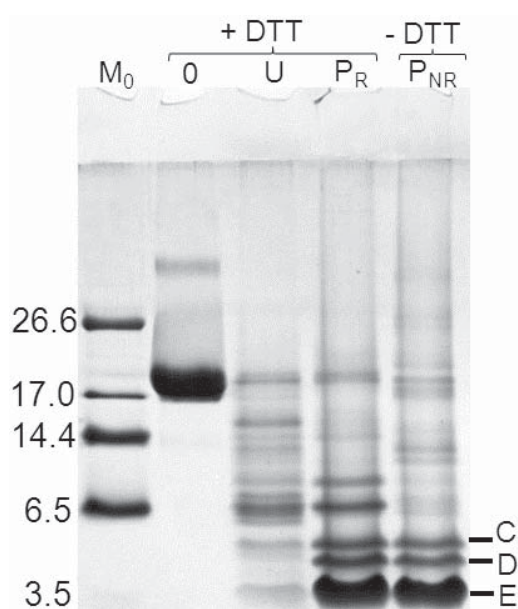


Figure 4.13 SDS-PAGE comparison of peptide bands in fibrils under reducing and non-reducing conditions. Complete-washed pellets obtained after ultracentrifugation for 12 h. M_0 , Molecular mass marker (weights in kDa); 0, unheated sample; U, heated and uncentrifuged sample; P_R , complete-washed pellet suspended in reducing PAGE buffer; P_{NR} , complete-washed pellet suspended in non-reducing PAGE buffer. For description of bands C, D and E, see text.

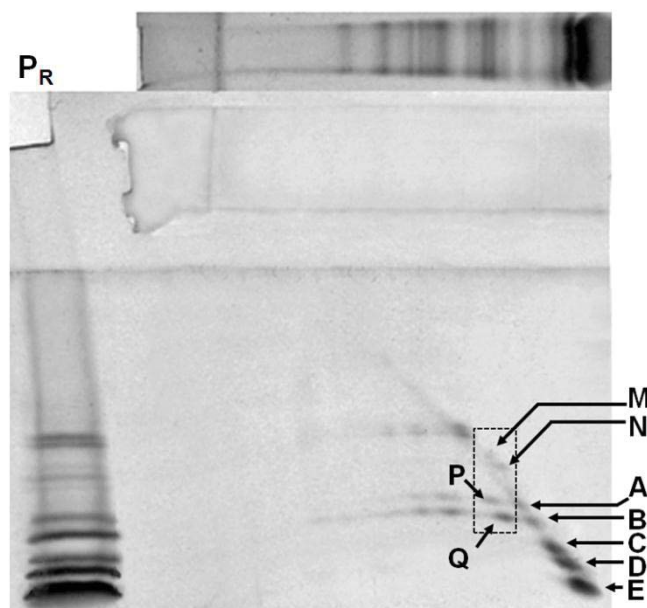


Figure 4.14 2D SDS-PAGE of the pellet obtained from a sample heated for 12 h. Complete-washed pellet suspended in buffer containing 4% SDS and run under non-reducing conditions in 1D. The target gel lane was excised, reduced and run in the 2nd dimension. P_R : reduced sample obtained from the same sample.

4.4.5.3. Characterization of sequences of fibril peptides

Peptides present in the pellet (fibrils) were identified using MALDI-TOF MS/MS. Table 4.2 shows the peptides observed in the fibrils with molecular weights of 1.2 to 3.4 kDa are derived from regions 1-53 and probably 153-162. All peptides showed cleavage at peptide bonds involving aspartic acid (D) residues. A similar composition of peptides in β -Lg fibrils has been reported previously (Akkermans et al., 2008b; Hettiarachchi et al., 2012). The fact that fewer peptides were observed in this study can be explained on the basis of the difference in method of fibril separation and sample preparation. Whereas the previous studies employed ultra-filtration to separate the fibrils, ultracentrifugation was used in the current study, and fibrils were washed by multiple cycles of vortexing and re-centrifugation to ensure that there was minimal contamination from the non-fibril material.

Chapter 4. Characterization of β -Lg self-assembly

Table 4.2 Peptides from β -Lg hydrolysis present in fibrils analyzed by MALDI-TOF MS/MS.

Amino acid sequence of peptides in fibrils ^a	Seq.	Observed molar mass (Da)	Delta mass (ppm) ^d	Expect values ^e	Ion score ^f
LIVTQTMKGLDIQKVAGTWYSLAMAASDISLL(D) ^b	1-32	3437.7673	-21.8	7.0×10^{-9}	130
(D)IQKVAGTWYSLAMAAS(D)	12-27	1695.8839	10.9	1.2×10^{-2}	63
(D)IQKVAGTWYSLAMAASD(I)	12-28	1810.9064	7.7	1.3×10^{-6}	104
(D)ISLLDAQSAPLRVYVEELKPTPEG(D)	29-52	2624.4136	2.87	5.3×10^{-4}	78
(D)IQKVAGTWYSLAMAASDISLLD(A)	12-33	2352.2144	4.64	1.9×10^{-3}	73
(D)ISLLDAQSAPLRVYVEELKPTPEGD(L)	29-53	2739.4434	3.79	2.0×10^{-3}	73
(N)PTQLEEQCHI(-) ^c	153-162	1197.5506	0.89	1.5×10^{-2}	61

a: Letters in the parentheses indicate the amino acids adjacent to the peptides. *b:* Peptide from N- terminal region. *c:* Peptide from the C- terminal region. *d:* Delta mass indicates the difference (error) between experimental and calculated mass. *e:* Expect value (expectation value) represents the number of times, the peptide score is equal or higher, purely by chance. The smaller the expectation value, the better is the significance of the match. *f:* The ions score represents the probability of the match being a random event .

Chapter 4. Characterization of β -Lg self-assembly

To determine the exact sequences of fibril peptides marked A-E in Figure 4.11, in-gel digestion of these bands using trypsin was carried out. The digested peptides were extracted from the gel matrix using acetonitrile and analyzed by nano LC-ESI-MS/MS. As the bands are digested using trypsin, the digest will contain small peptides cleaved at peptide bonds involving lysine or arginine residues and the sequences obtained from MS/MS represent a part of the original peptide sequence, not the whole sequence. Table 4.3 summarizes the sequences present in fibril peptides. The integrity of the results was verified based on the quality of the data. A typical MS/MS spectrum for a peptide above the cut-off ion threshold is shown in Figure 4.15. The spectrum showed all major ion peaks assigned with masses. Table 4.4 shows the masses of most of the ions shown in Figure 4.15.

All bands contained a few peptides with cleavage of peptide bonds at hydrophobic amino acids in addition to those involving lysine and arginine. An explanation for this is that the trypsin used in the study must have contained chymotrypsin despite being treated with N-tosyl-L-phenylalanine chloromethyl ketone (TCPK) which inhibits chymotrypsin. Chymotrypsin is known to cleave peptide bonds involving hydrophobic amino acids tyrosine (Y), methionine (M) or leucine (L) and alanine (A) upon prolonged incubation. ESI MS/MS of fragments from the tryptic digest of unheated β -Lg also showed cleavage at hydrophobic residues, supporting the notion that chymotrypsin was present (Table 4.5). The repeat in-gel digestion MS/MS analysis of peptide bands excised from fibrils made separately showed similar sequences (see Annexure 11.5).

Chapter 4. Characterization of β -Lg Self-Assembly

Table 4.3 Peptide sequences of peptide bands A to E (Figure 4.12) in the pellet (12 h) analyzed by ESI-MS/MS after extraction following *in-gel* digestion with trypsin.

Band	Amino acid sequence of peptides in bands ^a	Seq.	Observed molar mass (Da)	Delta Mass (ppm) ^e	Expect value ^f	Ion score ^g
A	(K)VAGTWYSLAMAASDISLLDAQSA PLR(V) ^{b,c,d}	15-40	2706.3690	0.12	1.1x10 ⁻⁸	100
	(Y)SLAMAASDISLLDAQSAPLR(V) ^{b,c,d}	21-40	2029.0547	1.63	3.1x10 ⁻⁸	115
	(M)AASDISLLDAQSAPLR(V) ^{c,d}	25-40	1626.8595	1.11	1.4x10 ⁻⁷	89
	(R)VYVEELKPTPEG(D)	41-52	1359.6932	0.76	1.2x10 ⁻³	57
	(R)VYVEELKPTPEGD(L)	41-53	1474.7236	3.04	2.7x10 ⁻⁴	59
	(R)VYVEELKPTPEGDLEILLQK(W)	41-60	2312.2600	3.69	8.0x10 ⁻⁵	57
	(K)VLVLDTDYK(K)	92-100	1064.5803	4.62	4.0x10 ⁻⁵	71

Chapter 4. Characterization of β -Lg Self-Assembly

	(R)TPEVDDEALEK(F)	125-135	1244.5794	1.79	1.5×10^{-3}	53
	(R)LSFNPTQLEEQCHI ^q	149-162	1728.8148	0.4	6.1×10^{-4}	47
B	LIVTQTMK(G) ^{c,d,p}	1-8	932.5406	4.44	8.0×10^{-4}	60
	(K)VAGTWYSLAMAASDISLLDAQSA PLR(V) ^{b,c,d}	15-40	2706.3766	2.93	8.0×10^{-7}	81
	(Y)SLAMAASDISLLDAQSAPLR(V) ^{b,c,d}	21-40	2029.0612	4.88	5.0×10^{-7}	88
	(L)AMAASDISLLDAQSAPLR (V)	23-40	1828.9366	0.75	6.0×10^{-6}	78
	(M)AASDISLLDAQSAPLR(V) ^{c,d}	25-40	1626.8592	0.96	7.0×10^{-9}	107
	(R)VYVEELKPTPEGD(L)	41-53	1474.7280	6.02	4.0×10^{-3}	54
	(R)VYVEELKPTPEGDLEILLQK(W)	41-60	2312.2615	4.33	6.0×10^{-6}	65
	(K)VLVLDTDYK(K)	92-100	1064.5747	-0.65	8.0×10^{-5}	57
	(K)VLVLDTDYKK(Y)	92-101	1192.6718	1.27	1.0×10^{-4}	52
C	(K)VAGTWYSLAMAASDISLLDAQSA	15-40	2706.3777	3.34	1.4×10^{-6}	77

Chapter 4. Characterization of β -Lg Self-Assembly

	PLR(V) ^b								
	(Y)SLAMAAASDISLLDAQSAPLR(V) ^{b,c,d}	21-40	2029.0525	0.55	6.3x10 ⁻⁷	100			
	(L)AMAAASDISLLDAQSAPLR (V)	23-40	1828.9375	1.21	4.1x10 ⁻⁴	59			
	(M)AASDISLLDAQSAPLR(V) ^{c,d}	25-40	1626.8582	0.36	2.6x10 ⁻⁸	101			
	(R)VYVEELKPTPEGD(L)	41-53	1474.7225	2.29	6.2x10 ⁻⁵	76			
	(R)VYVEELKPTPEGDLEILLQK(W)	41-60	2312.2609	4.09	2.2x10 ⁻⁵	58			
D	LIVTQTMK(G) ^p	1-8	932.5411	4.90	4.3x10 ⁻³	53			
	(K)VAGTWYSLAMAAASDISLLDAQSA PLR(V) ^{b,c,d}	15-40	2706.3814	4.69	1.7x10 ⁻⁶	72			
	(Y)SLAMAAASDISLLDAQSAPLR(V) ^b	21-40	2029.0600	4.25	1.1x10 ⁻⁴	62			
	(Y)SLAMAAASDISLLDAQSAPLR(V) ^{b,c,d}	22-40	2029.0519	0.25	8.5x10 ⁻¹⁰	115			
	(L)AMAAASDISLLDAQSAPLR (V)	23-40	1828.9310	-2.33	9.5x10 ⁻⁸	102			
	(A)MAASDISLLDAQSAPLR(V)	24-40	1757.8996	0.84	3.7x10 ⁻⁸	99			

Chapter 4. Characterization of β -Lg Self-Assembly

	(M)AASDISLLDAQSAPLR(V) ^{c,d}	25-40	1626.8573	-0.24	2.0×10^{-6}	86
	(R)VYVEELKPTPE(G)	41-51	1302.6732	1.90	1.1×10^{-3}	56
	(R)VYVEELKPTPEG(D)	41-52	1359.6947	1.83	6.0×10^{-3}	54
	(R)VYVEELKPTPEGD(L)	41-53	1474.7336	9.82	2.3×10^{-5}	76
	(R)VYVEELKPTPEGDEILLQK(W)	41-60	2312.2591	3.30	5.4×10^{-5}	56
E	(A)LIVTQTMK(G) ^{b,c,p}	1-8	933.5230	2.73	3.9×10^{-3}	54
	(R)VYVEELKPTPEG(D)	41-52	1359.6957	2.55	9.0×10^{-4}	56
	(R)VYVEELKPTPEGD(L)	41-53	1474.7352	10.90	5.9×10^{-2}	51
	(M)AASDISLLDAQSAPLR(V)	25-40	1626.8591	0.89	1.9×10^{-5}	70

a: Letters in the parentheses indicate the amino acids adjacent to the peptides. *p*: Peptide from N- terminal region. *q*: Peptide from the C- terminal region. *b*: Deamidation of glutamine (Q). *c*: Deamidation of asparagines (N). *d*: Oxidation of methionine (M). *e*: Expect value (expectation value) represents the number of times, the peptide score is equal or higher, purely by chance. The smaller the expectation value, the better is the significance

Chapter 4. Characterization of β -Lg Self-Assembly

of the match. f : The ions score represents the probability of the match being a random event. The threshold probability cutoff $P < 0.05$ was used which gave an ion score threshold cutoff of 46.

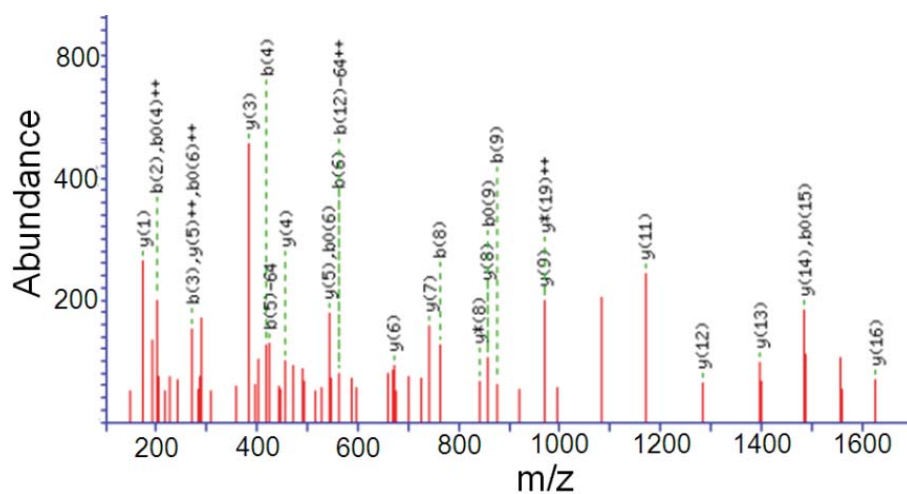


Figure 4.15 Typical MS/MS spectra of showing ions with assigned masses for peptide SLAMAASDISLLDAQSAPLR (with oxidation of methionine) from band C in Table 4.2 with a cut-off ion score of 100 (expect value 6.3×10^{-7}).

Chapter 4. Characterization of β -Lg Self-Assembly

Table 4.4 MS/MS data from Mascot search showing masses of the assigned ion peaks shown in Figure 4.16.

Residue No.	Peptide Sequence	b	b^0	b^{0++}	y
1	S	88.0393	70.0287	35.518	
2	L	<u>201.1234</u>	183.1128	92.06	1959.022
3	A	<u>272.1605</u>	254.1499	127.5786	1845.938
4	M	<u>419.1959</u>	401.1853	201.0963	1774.9
5	A	490.233	472.2224	236.6149	<u>1627.865</u>
6	A	<u>561.2701</u>	<u>543.2595</u>	272.1334	1556.828
7	S	648.3021	630.2916	315.6494	<u>1485.791</u>
8	D	<u>763.3291</u>	745.3185	373.1629	<u>1398.759</u>
9	I	<u>876.4131</u>	<u>858.4026</u>	429.7049	<u>1283.732</u>
10	S	963.4452	945.4346	473.2209	<u>1170.648</u>
11	L	1076.5292	1058.519	529.763	1083.616
12	L	1189.6133	1171.603	586.305	<u>970.5316</u>
13	D	1304.6402	1286.63	643.8185	<u>857.4476</u>
14	A	1375.6774	1357.667	679.337	<u>742.4206</u>
15	Q	1503.7359	<u>1485.725</u>	743.3663	<u>671.3835</u>
16	S	1590.768	1572.757	786.8823	<u>543.3249</u>
17	A	1661.8051	1643.795	822.4009	<u>456.2929</u>
18	P	1758.8578	1740.847	870.9273	<u>385.2558</u>
19	L	1871.9419	1853.931	927.4693	288.203

Numbers in the first column indicate position of the residues. Bold and underlined values indicate that the respective ions were present in the sample more than by chance. Values in bold and italics indicate that the matches for these ions could be by chance. For interpretation of table and notations in columns, see Mascot database search home page ("Matrix science help: Peptide Fragmentation,").

Chapter 4. Characterization of β -Lg Self-Assembly

Table 4.5 Peptides obtained by in-gel digestion of unheated β -Lg followed by ESI-MS/MS. β -Lg loaded on to SDS-PAGE gel (resolving gel concentration 20%). After running, the β -Lg band was excised and processed along with the peptide bands A-E which have been characterized in Table 4.3.

Amino acid sequence of peptides in bands	Seq.	Observed molar mass (Da)	Delta Mass (ppm) ^e	Expect value ^f	Ion score ^g
(K)ALKALPMHIR(L)	139-148	1148.69	7.19	6.4×10^{-4}	46
LIVTQTMK(G) ^g	1-8	932.54	3.59	8.9×10^{-3}	45
(V)LVLDTDYK(K)	92-100	965.51	-0.53	3.1×10^{-3}	48
(K)VLVLDTDYK(K)	91-100	1064.58	5.54	3.3×10^{-5}	73
(R)TPEVDDEALEKFDK(A)	125-138	1634.78	5.19	3.9×10^{-5}	74
(A)MAASDISLLDAQSAPLR(V)	24-40	1757.91	5.94	4.2×10^{-7}	84
(K)VLVLDTDYKK(Y)	92-101	1192.68	5.16	1.4×10^{-4}	68

Chapter 4. Characterization of β -Lg Self-Assembly

(L)AMAAISLLDAQSAPLR(V)	23-40	1828.95	6.78	1.6×10^{-6}	78
(R)TPEVDDEALEK(F)	125-135	1244.58	5.03	7.8×10^{-5}	67
(N)PTQLEEQCHI ^b	151-162	1267.59	0.65	2.4×10^{-5}	60
(D)ISLLDAQSAPLR(V)	29-40	1282.73	4.46	3.1×10^{-6}	77
(R)VYVEELKPTPE(G)	41-51	1302.67	1.81	3.5×10^{-4}	48
(Y)SLAMAAISLLDAQSAPLR(V)	21-40	2029.06	4.97	2.3×10^{-8}	95
(S)DISLLDAQSAPLR(V)	28-40	1397.76	3.16	2.7×10^{-4}	60
(P)EVDDEALEKFDK(A)	127-138	1436.67	2.89	9.5×10^{-3}	49
(K)PTPEGDLEILLQK(W)	48-60	1451.79	1.31	1.6×10^{-4}	56
(R)VYVEELKPTPEGD(L)	41-53	1474.73	3.61	4.3×10^{-4}	50
(A)SDISLLDAQSAPLR(V)	27-40	1484.79	3.35	3.4×10^{-7}	98
(S)FNPTQLEEQCHI ^b	153-162	1528.70	0.93	3.2×10^{-4}	43

Chapter 4. Characterization of β -Lg Self-Assembly

(R)VYVEELKPTPEGDLEILLQK(W)	41-60	2312.26	3.69	7.2×10^{-8}	89
(F)CMENSAEPEQSLACQCLVR(T)	106-124	2323.02	4.67	3.1×10^{-6}	69
(A)ASDISLLDAQSAPLR(V)	26-40	1555.82	1.87	1.6×10^{-9}	110
(M)AASDISLLDAQSAPLR(V)	25-40	1626.86	3.66	2.8×10^{-11}	137
(R)TPEVDDEALEKFDK(A)	125-138	1634.77	3.37	4.3×10^{-6}	87
(R)LSFNPTQLEEQQCHI ^b	149-162	1728.82	4.5	2.0×10^{-9}	102
(A)MAASDISLLDAQSAPLR(V)	24-40	1757.90	2.23	1.9×10^{-10}	112
(N)SAEPEQSLACQCLVR(T)	110-124	1774.83	-1.22	7.7×10^{-6}	59
(K)VAGTWYSLAMAASDISLLDAQSAPLR(V)	15-40	2706.38	4.9	1.1×10^{-10}	112
(L)AMAASDISLLDAQSAPLR(V)	23-40	1828.94	2.48	4.6×10^{-8}	102
(K)YLLFCMENSAEPEQSLACQCLVR(T)	102-124	2859.31	0.25	2.1×10^{-7}	73
(S)LAMAASDISLLDAQSAPLR(V)	22-40	1942.02	-1.35	6.6×10^{-10}	109

Chapter 4. Characterization of β -Lg Self-Assembly

(K)IDALNENKVLVLDTDYK(K)	84-100	1962.03	-2.47	1.4×10^{-5}	53
(Y)SLAMAAADISLLDAQSAPLR(V)	21-40	2029.05	0.37	4.7×10^{-13}	157
(Y)VEELKPTPEGDLEILLQK(W)	41-60	2050.12	0.34	1.7×10^{-3}	43
(K)GLDIQKVAGTWYSLAMAAADISLLD AQSAPLR(V)	9-40	3360.77	10	9.8×10^{-12}	122
(R)VYVEELKPTPEGDLEILLQK(W)	41-60	2312.26	1.3	7.1×10^{-5}	70
(F)CMENSAEPEQSLACQCLVR(T)	106-124	2323.01	-0.42	7.3×10^{-9}	93
(K)VAGTWYSLAMAAADISLLDAQSAPL R(V)	15-40	2706.37	1.65	1.9×10^{-13}	151
(K)YLLFCMENSAEPEQSLACQCLVR(T)	102-124	2859.29	-6.51	2.4×10^{-8}	87

Letters in the brackets indicate the amino acids adjacent to the peptides. *a*: Peptide from N-terminal region; *b*: Peptide from the C-terminal region. For descriptions of *e*, *f* and *g* see footnote of Table 4.3. Since β -Lg used for digestion was not heated, deamination of N and Q were not included during the search. Peptides with an ion score threshold cut-off of >42 ($P < 0.05$) are listed in the table.

Chapter 4. Characterization of β -Lg Self-Assembly

A schematic comparison of the sequences found in different peptide bands is shown in Figure 4.16. All the five bands (A to E, Figure 4.12) showed peptides from the region containing residues 25-53 suggesting this region is important in fibril formation as it is present in all peptides. In addition, although at reduced significance, band A showed sequences 92-101, 125-135 and 149-162, while band B showed 92-101. The sequences 92-100/101 and 125-135 have signs of tryptic hydrolysis (cleavage involving a Lys (K) or an Arg (R) residue) at both ends and do not have any sites of acid hydrolysis between them. In addition, cysteine residues at positions 106, 119 and 121 are in the vicinity of these peptide fragments. A possible explanation for this arises from the presence of a large peptide involving residues 92 to 135 and probably till 162 accounting for the sequence 149-162 in band A. It is likely that the chymotrypsin further cleaved the tryptic-digest peptides into smaller sequences which were not able to be detected by MS.

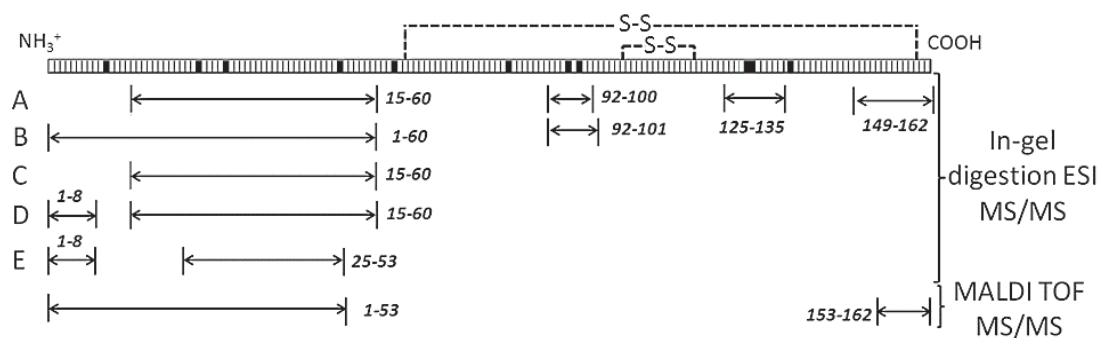


Figure 4.16 Schematic representation of regions found in peptides from in-gel digestion ESI-MS/MS and MALDI-TOF MS/MS. The dark blocks in the sequence show location of aspartic acid residues indicating potential sites of acid hydrolysis of β -Lg. Sequence of β -Lg variant A is shown. Variant B has glycine instead of aspartic acid at residue 64 and alanine instead of valine at residue 118.

4.5. Discussion

The objective of this study was to characterize the events occurring in the early stages of self-assembly. To this effect, the effect of heating on the native structure of β -Lg was studied using CD spectroscopy. At the beginning of heating at 80 °C, the tertiary structure of β -Lg unfolded rapidly and complete loss of structure was observed within the first 10 minutes of heating. At approximately similar times, there was a change in secondary structure characterized by an increase in ellipticity at 222 nm and the shift of the trough from 217 nm to <210 nm. This suggests that the heating of β -Lg led to a decrease in the β -sheet content with a concomitant increase in α -helix structure. Such a shift in the trough for the FUV region has previously been reported upon heating β -Lg at pH 2 (Molinari et al., 1996) and during β -Lg self-assembly under shear after 12 h at 80 °C (Dunstan et al., 2009) and this has been attributed to the formation of a non-natively folded α -helix (Aouzelleg et al., 2004). The increase in non-native α -helix upon protein unfolding is thought to be the same intermediate characterized during the refolding of β -Lg (Hamada et al., 1996; Kuwata et al., 2001). This intermediate is thought to involve residues 12-24, which form part of the β -A strand of β -Lg (Kuwata et al., 2001). The current study shows that this is one of the first structural changes to occur during the lag phase of β -Lg self-assembly and precedes hydrolysis.

The results from SDS-PAGE analysis of samples in the lag phase suggest that once unfolded, the monomers were hydrolyzed by the low pH and high heat conditions of self-assembly. Hydrolysis may have an important role in the formation of the nuclei that initiate β -Lg self-assembly. Once initiated, the hydrolysis of the β -Lg monomer and larger peptides continues during heating irrespective of fibril formation. A comparison of peptide bands of fibrils formed after different heating times and

separated by ultracentrifugation showed the presence of bands almost identical to those in material subjected to less intense heat treatment (Figures 4.6, 4.12 and 4.13). This suggests that fibrils are made up of similar peptides regardless of how long they are heated. In addition, once incorporated in the fibrils, the peptides do not undergo further hydrolysis.

A comparison of SDS-PAGE data for fibril peptides in 1D and 2D NR-R (Figure 4.14 and 4.15) showed that peptides in spots P and Q eluted in bands A and B under reducing conditions. The fragments from this region have also been found in fibrils formed by conventional (Akkermans et al., 2008b) and microwave heating (Hettiarachchi et al., 2012). Hamada et al. (2009) showed that sequences 102-109 (β -strand G) and 118-123 (β -strand H) and β -strand I (residues 146-152) in the C-terminal region were capable of forming fibrils, but did not promote self-assembly from full length β -Lg upon seeding in the presence of urea. This suggests that the peptides from these regions may primarily contribute to growth of nuclei during self-assembly at pH 2.

It is interesting to note that the in-gel digestion MS of band A showed the sequences 12-60 and 149-162, which are located at opposite ends of the β -Lg polypeptide chain. The peptides from these regions were also found in the MALDI-TOF MS analyses from this study (Table 4.2) and consistently appear in previous reports of β -Lg fibril composition (Akkermans et al., 2008b; Hettiarachchi et al., 2012). In the absence of conditions promoting unrestrained disulfide exchange reactions at pH 2, it is possible that the disulfide bond between Cys160 and Cys66 is conserved in fibrils and may be responsible for disulfide-bonded peptides found in 2D NR-R SDS-PAGE (spots M and P or N and Q, Figure 4.15). This disulfide linkage is one of the two disulfide bonds present in the native β -Lg molecule (Brownlow et al., 1997).

Chapter 4. Characterization of β -Lg Self-Assembly

Since the sequence between cysteine residues 106 and 119 does not have any aspartate residues, it is likely that these residues were present on the same peptide after reduction in 2D SDS-PAGE. Although the region with Cys66 was not found in the in-gel digestion of band A, this could be explained due to a number of closely located lysine residues (at residues 60, 69, 70 and 75) which act as sites of tryptic cleavage. Since small peptides are often not detected by MS analysis, it is not surprising that peptides from this region were not detected after in-gel digestion. The in-gel digestion of unheated β -Lg followed by ESI MS/MS analysis also failed to detect any peptides covering 60-83 which contains the residue Cys66 (Table 4.5). Since all previous studies to characterize composition of fibrils involved dissolving fibrils under reducing conditions, the presence of disulfide bonds was not considered, even though the relevant cysteine residues were shown to be present in fibrils from both A and B variants of β -Lg (Akkermans et al., 2008b; Hettiarachchi et al., 2012). This suggests that fibrils could contain peptides from disparate regions if they are linked by a disulfide bridge. This hypothesis is illustrated in Figure 4.17.

The in-gel digestion ESI-MS found that the peptide bands A-E contained peptides from the region 15-53, which includes most of the β -A strand (residues 16-21). This region is involved in a non-native α -helix formation during re-folding (Damodaran, 1996; Hamada et al., 1996) and is highly amyloidogenic in concentrated urea (Hamada et al., 2009). It is the predominant region in heat-induced fibrils, and it appears that once the tertiary structure is disrupted (which is very rapid), this region is prevented from assembling by adjacent non-amyloidogenic regions, which hinder the mutual alignment of assembling regions into a stable β -sheet structure of fibrils. That constraint can be overcome by removing the non-assembling regions with acid hydrolysis, as shown in this study, enzymatic hydrolysis of β -Lg (Akkermans et al.,

2008a), or by microwave excitation of the protein (Hettiarachchi et al., 2012). Non-thermal effects of microwaves apparently speed up the alignment of assembling regions into correct positions, and/or speed up the movement of non-core regions into sterically-favourable positions (Hettiarachchi et al., 2012).

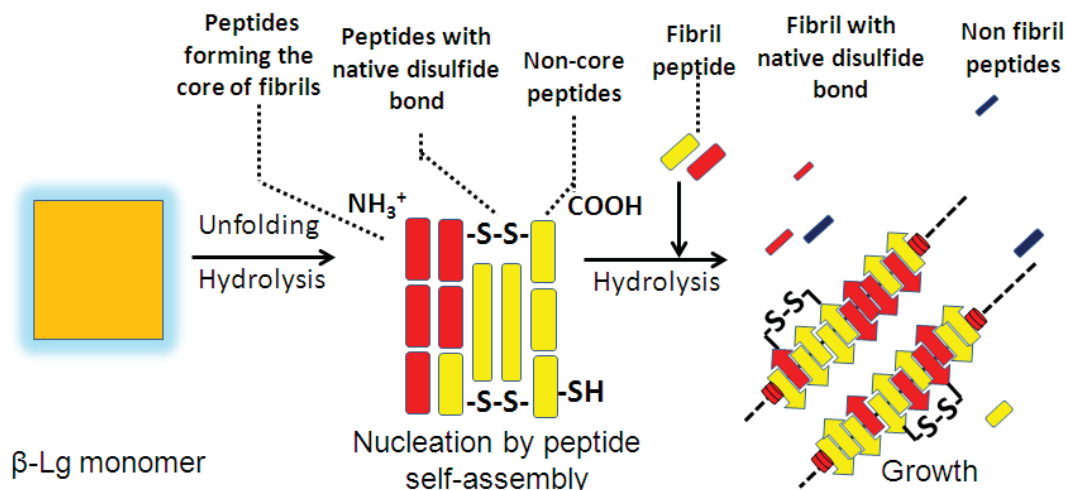


Figure 4.17 Schematic illustration of how disulfide-bonded peptides come to be present in fibrils. Red colored regions indicate the N-terminal region (1-53) of the β -Lg sequence.

From the SDS-PAGE under reducing conditions and the results of the mass-spectrometric analyses, likely compositions of peptides comprising bands A-E can be predicted. The molecular weights of reduced SDS-PAGE bands of Figure 4.11 were calculated using Equation 3.9 and corrected to the known mass of bovine β -Lg, giving values about 5% less than those derived from molecular weight markers (Table 4.6).

Band A (estimated mass 8.2 kDa and containing tryptic fragments spanning residues 12-162) may be identified with peptides comprising residues 12-85 (calculated mass 8.2 kDa and pI 4.9) and with lower probability residues 86-162 and/or 96-162

Chapter 4. Characterization of β -Lg Self-Assembly

(calculated masses 8.8 kDa and pI 4.7 and 7.8 kDa, pI 4.8). The latter bands are most likely to be associated with band P in the 2D NR-R SDS-PAGE.

Band B (estimated mass 6.7 kDa and containing tryptic fragments spanning residues 1-101) may be associated with peptides 1-62 (hydrolysis at exposed Glu62 on loop CD, calculated mass 6.8 kDa) and 54-114 (hydrolysis at exposed Glu114, calculated mass 7.1 kDa). Band C (estimated mass 4.7 kDa and containing tryptic fragments spanning residues 12-60) may be associated with peptides 1-53 (calculated mass 4.6 kDa) and 28-64 (calculated mass 4.1 kDa). Similarly, band D (estimated mass 4.1 kDa and containing tryptic fragments spanning residues 1-60) may be associated with peptides 34-64 (calculated mass 3.7 kDa) and 12-51 (hydrolysis at exposed Glu51 on loop BC, calculated mass 4.4 kDa).

Band E (estimated mass 3.2 kDa and containing tryptic fragments spanning residues 1-53) may be associated with peptides 1-28 (calculated mass 3.0 kDa), 1-34 (calculated mass 3.4 kDa) and 34-62 (hydrolysis at exposed Glu62 on loop CD, calculated mass 3.3 kDa). Generally, the tryptic/chymotryptic digests with fragments beyond Asp53 have lower ion scores and expect values. This may be due to intrinsically lower abundance due to hydrolysis at an exposed glutamate residue (especially the exposed Glu62 on loop CD), instead of the more hydrolytically susceptible aspartate residues.

The prevailing mechanistic models for β -Lg nanofibril self-assembly assume nucleation-dependent polymerization, with activation of β -Lg monomers and nucleation followed by growth of nuclei into mature fibrils (Arnaudov et al., 2003; Bolder et al., 2007a; Bromley et al., 2005). For self-assembly to proceed, the nuclei must grow to a critical size, below which their self-assembly is reversible (Aymard

et al., 1999). Light-scattering studies have shown that nucleation/aggregation during the early stages of self-assembly is reversible upon cooling (Arnaudov et al., 2003; Aymard et al., 1999). The fibril-forming peptides, predominantly from the N-terminal region, probably self-assembled into weakly-associated nuclei, which disintegrated upon cooling. The end of the lag phase therefore represents the point at which the concentration of fibrillogenic peptides is sufficiently large and the rate of assembly and growth of nuclei exceeds the rate of disassembly. The peptides from other regions of β -Lg molecule then self-assembled onto the nuclei resulting in their growth to macroscopic sized fibrils. Assembly is rapid beyond this critical point, as indicated by the sharp increase in ThT fluorescence.

Under the conditions used here, hydrolysis occurs at a constant rate and constant temperature, irrespective of fibril formation. The rate of fibril formation in the growth phase will depend on environmental conditions (e.g. temperature, pH, salts, shear) as well as the supply of fibril-forming peptides, which are formed by monomer hydrolysis and potentially destroyed by over-hydrolysis. Self-assembly is ultimately curtailed by the depletion of these peptides as the stationary phase is reached. Hydrolysis and self-assembly occurred concurrently towards the end of the lag phase, but these two reactions have quite different underlying mechanisms. Hydrolysis is effectively a uni-molecular reaction at pH 2 in aqueous solution, whereas self-assembly is multi-molecular reaction which may be limited by the diffusion of peptides towards each other.

Chapter 4. Characterization of β -Lg Self-Assembly

Table 4.6 Possible sequences of peptides present in SDS-PAGE bands of fibrils.

Band	location	Sequence ^a	Molar mass (kDa) ^d	Calc. SDS-PAGE ^b (kDa)
A	12-85	IQKVAGTWYSLAMAASDISLLDAQAPLRVYVEELKPTPEGDLEILLQKWENDECAQ	8.2	8.2
		KKIIAEKTKIPAVFKID(A)		
	86-162	(D)ALNENKVLVLDTDYKYYLLFCMENSAPESLVCQCLVRTPEVDDEALEKFDKA LKALPMHIRLSFNPTQLEEQCHI	8.8	
B	96-162	(D)YKKYLLFCMENSAPESLVCQCLVRTPEVDDEALEKFDKALKALPMHIRLSFN PTQLEEQCHI	7.8	
		LIVTQTMKGLDIQKVAGTWYSLAMAASDISLLDAQAPLRVYVEELKPTPEGDLEILL QKWE(N)		
	1-62	(D)LEILLQKWENDECAQKKIIAEKTKIPAVFKIDALNENKVLVLDTDYKYYLLFCME NSAEPE(Q)	6.8	6.7
	54-114		7.1	

Chapter 4. Characterization of β -Lg Self-Assembly

C	1-53	LIVTQTMKGLDIQK VAGTWYSLAMAASDISLLDAQSAPLRVYV(E)	4.6	4.7
	28-64	(S)DISLLDAQSAPLRVYVEELKPTPEGDLEILLQKWEND(E)	4.1	
D	34-64	(L)DAQSAPLRVYVEELKPTPEGDLEILLQKWEND(E)	3.7	4.1
	12-51	(D)IQK VAGTWYSLAMAASDISLLDAQSAPLRVYVEELKPTPEG(D)	4.4	
E	1-28	LIVTQTMKGLDIQK VAGTWYSLAMAASD(I)	3.0	3.2
	34-62	(D)AQ S A P L R V Y V E E L K P T P E G D L E I L L Q K W E (N)	3.3	
	1-33	LIVTQTMKGLDIQK VAGTWYSLAMAASDISLL(D)	3.4	

a: sequences computed from ExPASy compute pI/Mw tool . Sequences have been predicted using peptide sequences found in bands A-E characterized by MS/MS (Table 4.5). Peptide bonds involving aspartic acid (D) or glutamic acid (E) were considered as sites of acid cleavage. Sequence of β -Lg A was used for prediction. *b:* Values calculated from the Equation $y = -0.782x + 3.7086$.

Chapter 5

5. Self-assembly from β -Lg A, B and C

The contents of this chapter have been accepted for publication in a peer-reviewed journal article and adapted from:

International Dairy Journal (2015), *In press*, Dave, A. C., Loveday, S. M., Anema, S. G., Jameson, G. B., & Singh, H. Formation of nano-fibrils from A, B and C variants of bovine β -lactoglobulin. Copyright (2015) with permission from Elsevier.

5.1. Abstract

Bovine β -lactoglobulin (β -Lg) self-assembles into amyloid-like fibrils when heated at 80 °C, pH 2 and low ionic strength. In this chapter the self-assembly of purified genetic variants of β -Lg, A, B and C was examined. β -Lg solutions (1% w/v) were heated for different heating times and analyzed by the thioflavin T (ThT) assay for the detecting fibrils. Reducing sodium dodecyl sulfate polyacrylamide gel electrophoresis (SDS-PAGE) was used to follow heat-induced acid hydrolysis of β -Lg monomers. Fibrils were characterized by SDS-PAGE and transmission electron microscopy (TEM) after their separation from the heated solutions. The results suggest that the substitution of amino acid residues in β -Lg variants A, B and C did not significantly affect the kinetics of acid hydrolysis, self-assembly of these variants, or the morphology of the fibrils. The fibrils from β -Lg A, B and C were, however, slightly different in peptide compositions. The

Chapter 5. Self-Assembly from β -Lg A, B and C

latter may be explained on the basis of sites of genetic substitution, in particular the Asp64 of β -Lg A that is Gly in variants B and C.

5.2. Introduction

β -Lg commonly exists in three polymorphic forms (A, B and C), that are different from each other due to minor modifications/substitutions in their amino acid sequences (Sawyer, 2003). β -Lg A has Asp at position 64 and Val at 118 instead of Gly and Ala, respectively, in β -Lg B and C. β -Lg C differs from, β -Lg B by the substitution of His for Gln at position 59 (Sawyer, 2003), and from β -Lg A by substitution Ala for Val at position 118. Although the native structure of the three β -Lg variants is largely similar (Bewley et al., 1997; Monaco et al., 1987), the minor amino acid substitutions greatly influence the heat stability, aggregation propensity and properties of aggregates formed upon heating at neutral pH (Manderson et al., 1999; Nielsen et al., 1996; Qin et al., 1999). On the other hand, at pH 2, Le Bon et al. (2002) noted no difference in the rate of heat-induced aggregation of β -Lg A and B between 55 to 73 °C; however, the scope of this study did not include investigating fibril formation.

The sites of substitutions at residue 64 (β -Lg A with respect to β -Lg B and C) and 59 (β -Lg C with respect to β -Lg A and B) have been found on the peptide sequences present in the fibrils (Akkermans et al., 2008b; Hettiarachchi et al., 2012). Under highly acidic conditions of self-assembly, the substitution of Asp64 in β -Lg A would provide an additional site for acid-hydrolysis. Similarly, the substitution of His59 in β -Lg C would increase the net positive charge on the monomer at pH 2, which in turn may affect the electrostatic interactions between peptides, resulting in altered kinetics of self-assembly or morphology of fibrils. To this end, the self-assembly of purified β -Lg variants A, B and C has been investigated using the same methods as used in the previous chapter.

5.3. Materials and Methods

All materials, instruments and protocols used in the experimental work of this chapter have been described in Sections 3.1, 3.2 and 3.3 of Chapter 3. The genetic variants of β -Lg A, B and C were characterized by non-denaturing native PAGE (Section 3.3.5.1) and ESI-MS (Sections 3.3.7.2 of Chapter 3). The samples for CD spectroscopy were prepared using the protocol described in Section 3.3.6.2. Native structures of β -Lg A, B and C and their unfolding were monitored by CD spectroscopy (Section 3.3.6.3). β -Lg samples for self-assembly were prepared and heated using a protocol described in the Section 3.3.2. The heated solutions were analyzed using the ThT assay (Section 3.3.3). The fluorescence intensities were fitted with a sigmoidal function of Equation 3.1 and the kinetic parameters of self-assembly from the Equations 3.2 to 3.4. Heated samples were centrifuged and the compositions of separated components (Section 3.3.4) were characterized by reducing SDS-PAGE (Section 3.3.5.3). TEM was used to examine the morphology of fibrils (Section 3.3.8).

5.4. Results

5.4.1. Characterization of β -Lg variants

The native alkaline PAGE analysis of β -Lg variants A, B and C showed two major bands (Figure 5.1) corresponding to both monomeric and dimeric forms of β -Lg. The electrophoresis patterns of Figure 5.1 are in agreement with those found by Manderson et al. (1998). The identity of β -Lg variants was confirmed by ESI-MS analysis. The deconvoluted ESI-MS spectra of samples are shown in Figure 5.2. All spectra showed a single major peak corresponding to masses 18364 Da for β -Lg A, 18278 Da for β -Lg B and 18287 Da for β -Lg C. The spectra of β -Lg A and C also showed one additional peak each with an incremental mass of 324.0 Da (Figure 5.2, (A) and (C)) suggesting that a fraction of monomers in these variants were lactosylated.

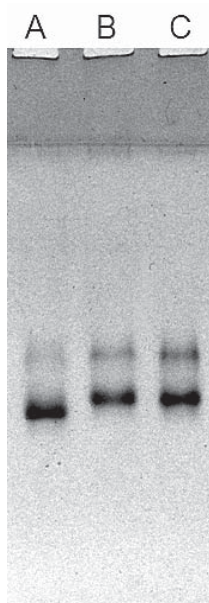


Figure 5.1 Native non-denaturing PAGE of β -Lg A, B and C.

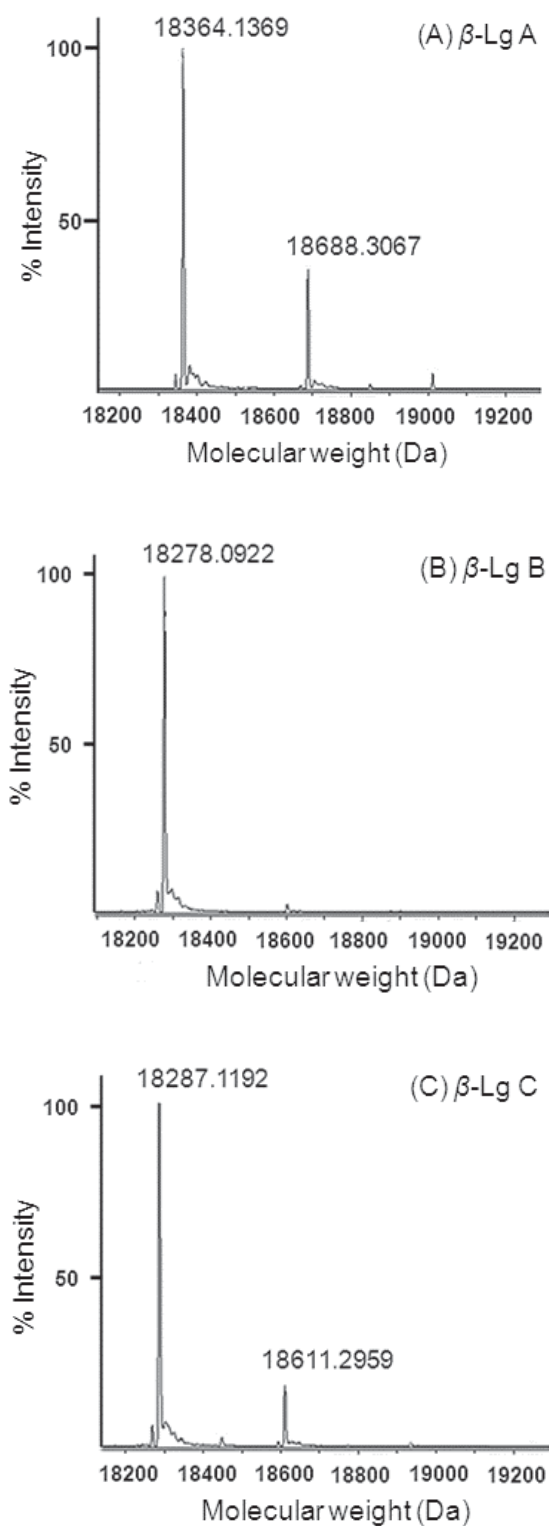


Figure 5.2 De-convoluted MS spectra of β -Lg variants. (A) β -Lg A, (B) β -Lg B and (C) β -Lg C.

5.4.2. Unfolding of β -Lg

The unfolding behavior of β -Lg A, B and C in the early lag phase was investigated using CD spectroscopy. The scans of native β -Lg were recorded at 20 °C after which the temperature of the sample was raised to 80 °C. As soon as the temperature reached 80 °C the scans were recorded continuously for 1 h. The scans were averaged at 2 minute intervals each and the relative losses of ellipticities were calculated from Equations 3.11 and 3.12.

The NUV scans arising from the tertiary structure of β -Lg at 20 °C showed two sharp, characteristic troughs at 293 nm and 286 nm and a shallow trough at approximately 265 nm Figure 5.3 (A) in agreement with the results shown in Chapter 4. The absorption between 260 to 280 nm in the spectra of β -Lg C was higher than that of β -Lg A and B. Manderson et al. (1999) have reported a similar shape of spectra for β -Lg C at pH 6.7.

The spectra of all three β -Lg showed rapid loss of signals at these wavelengths upon heating at 80 °C (Figure 5.4, A, C and E). The relative loss of ellipticity at 293 nm were calculated using Equation 3.11 for comparison and the values of $\left(\frac{\Delta\theta_t}{\Delta\theta_0}\right)_{293}$ were plotted against heating time at 80 °C (Figure 5.5, A). The unfolding of β -Lg A, B and C followed similar patterns with complete loss of signals observed within the first few minutes of heating.

The FUV scans of native β -Lg representing the secondary structure of β -Lg are shown in Figure 5.3 (B). All the three variants showed a broad trough at 217 nm and a positive trough with a maximum at approximately <200 nm. Accurate estimations of secondary structure were not possible due to high absorption by the sample at <197 nm (See

Chapter 5. Self-Assembly from β -Lg A, B and C

Annexure 11.1). The scans of β -Lg A, B and C in Figure 5.3 (B) are in agreement with a number of previous studies at neutral pH (Griffin et al., 1993; Manderson et al., 1999; Qi et al., 1997) indicating that all the three variants have high proportion of β -sheets in their secondary structure.

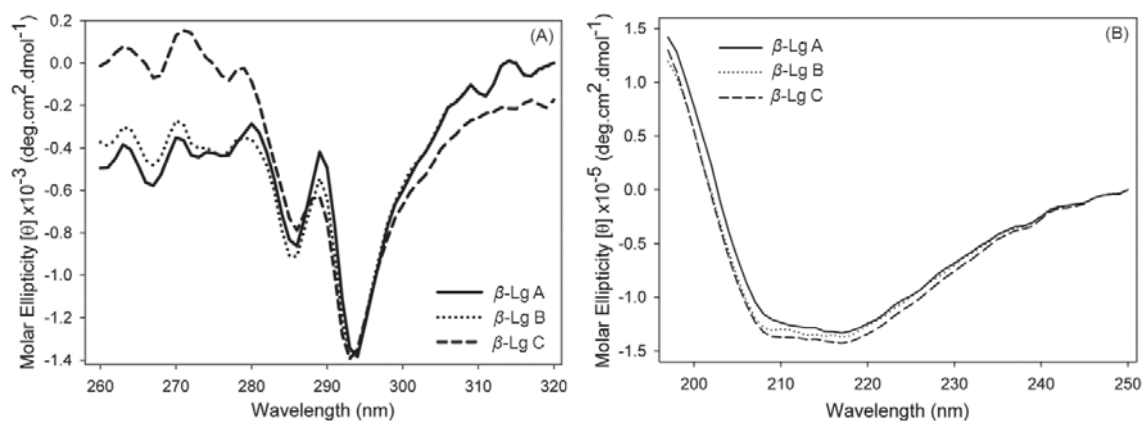


Figure 5.3 Spectra of native β -Lg A, B and C at pH 2. (A) NUV spectra (1 mg/mL) and (B) FUV spectra (0.01 mg/mL).

The FUV scans of β -Lg A, B and C are shown in Figure 5.4 (B, D and F). Heating resulted in a rapid shift of the trough towards lower wavelengths along with the deepening of the trough at <210 nm. The pattern of changes in the secondary structure of β -Lg A, B and C was similar to those observed in Chapter 4 at pH 2 and those at neutral pH observed by others (see above references). The plots of relative loss of ellipticities in the FUV region $\left(\frac{\Delta\theta_t}{\Delta\theta_{60}}\right)_{208}$ were calculated using Equations 3.12. From Figures 5.4 (F) and Figure 5.5 (B), the unfolding of β -Lg C appeared to be slightly faster than β -Lg A and C.

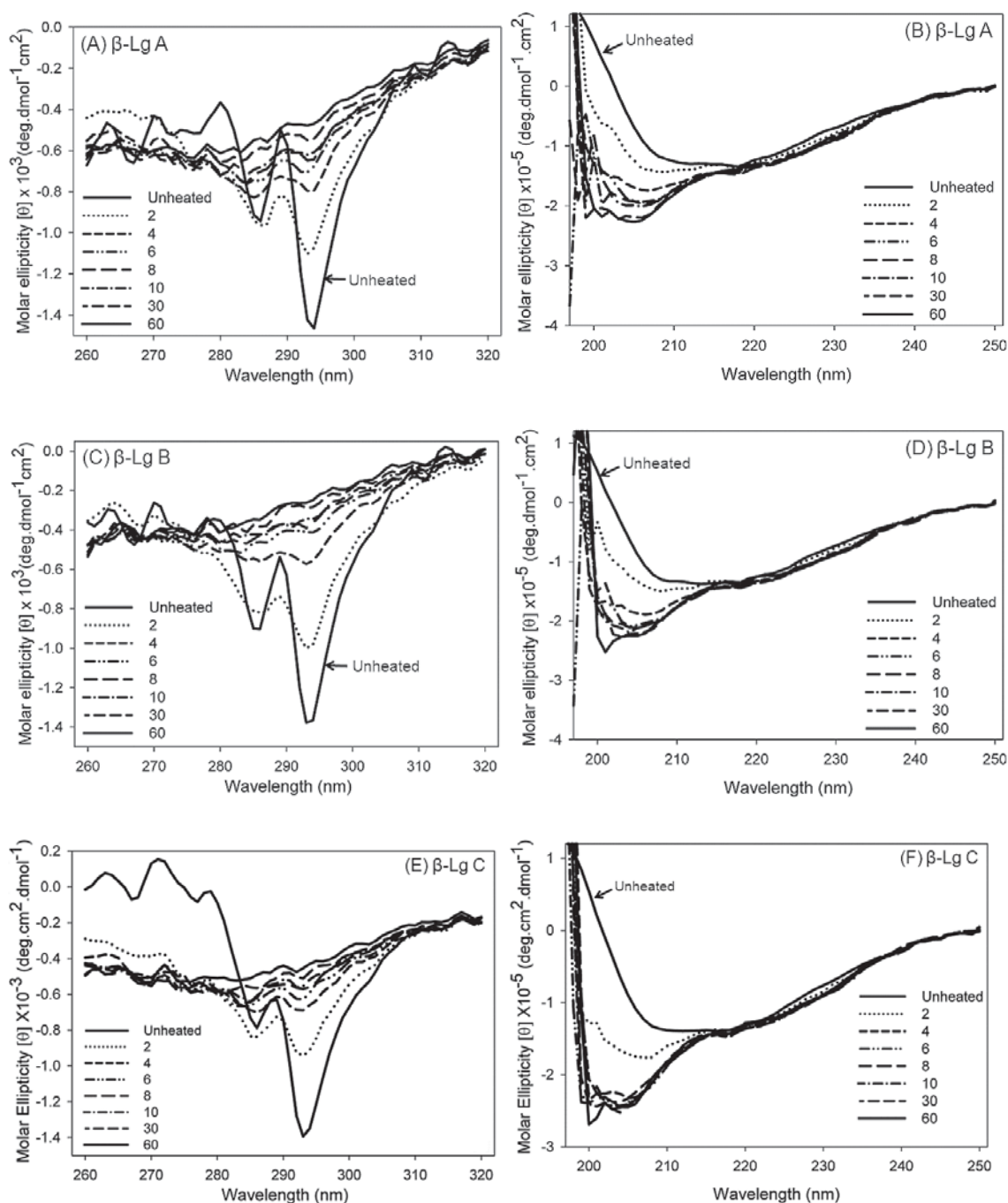


Figure 5.4 Unfolding of the β -Lg A, B and C upon heating at 80 °C. The NUV scans in (A), (C) and (D) show effect of heating on the tertiary structure, while FUV scans in (B), (D) and (E) show the effect of heating on the secondary structure of β -Lg A, B and C respectively. The concentration of β -Lg was 1 mg/mL for the NUV scans, and 0.01 mg/mL for the FUV scans.

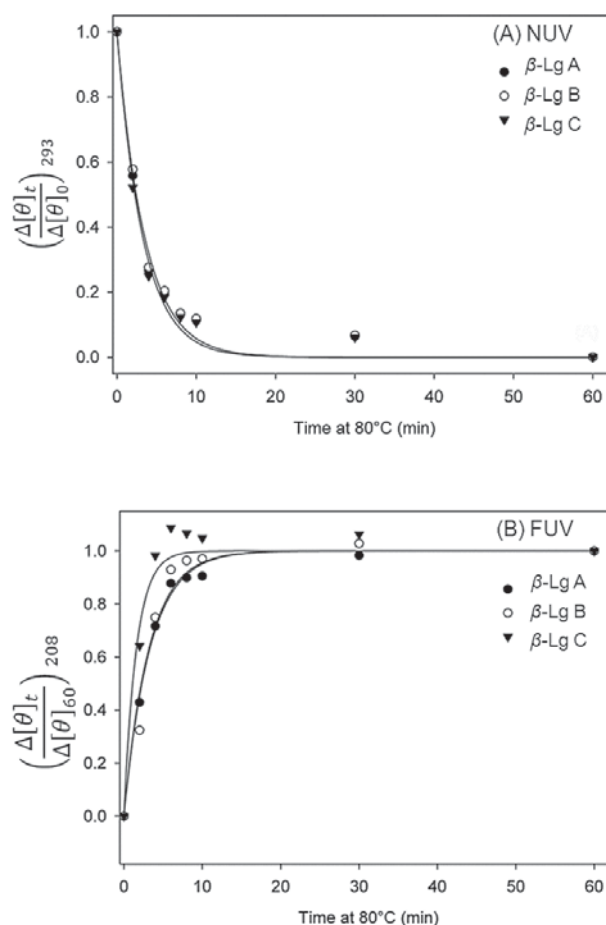


Figure 5.5 Relative losses of ellipticities at (A) 293 nm and (B) 208 nm calculated from Equations 3.11 and 3.12. Solid lines are for visual reference.

5.4.3. SDS-PAGE of heated samples

The heat-induced acid hydrolysis of the β -Lg monomers was investigated by reducing SDS-PAGE. The SDS-PAGE profiles of these samples showed several peptide bands with molecular weights less than that of the β -Lg monomer (Figure 5.6). The rate of hydrolysis for all the three variants followed first-order kinetics (Figure 5.7) and the rate constants are given in Table 5.1. The rates of hydrolysis of β -Lg A, B and C were similar ($P < 0.47$, likelihood ratio test). The band marked Q is likely to be a non-disulfide linked β -Lg dimer. Such non-disulfide linked dimeric aggregates of β -Lg result from the

Chapter 5. Self-Assembly from β -Lg A, B and C

heat treatment of β -Lg at neutral pH (Mudgal et al., 2011). Non-disulfide linked protein aggregates in proteins are formed by the isopeptide linkage between amine groups of lysine and carboxyl groups of aspartic or glutamic acids (Mudgal et al., 2011; Stryer, 1995). The heat treatment of milk or whey, during or prior to extractions of β -Lg A, B or C used in this study may have resulted in such aggregates in the samples. Nevertheless, their relative proportion for all three proteins was relatively small.

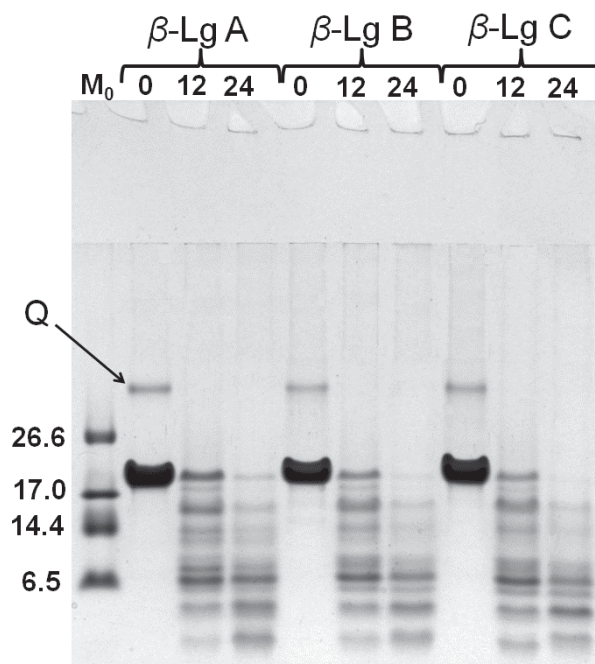


Figure 5.6 Reducing tricine SDS-PAGE profiles of control and heated samples after heating for 12 and 24 h at 80 °C. M_0 Molecular weight marker; molecular weights are in kDa. For description of band Q, see text.

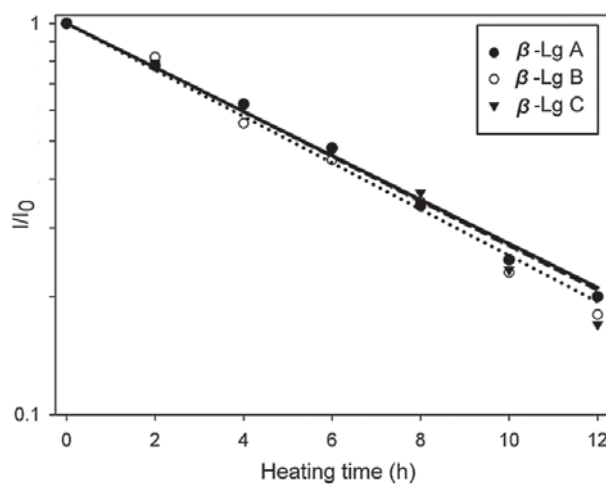


Figure 5.7 Residual intensities of β -Lg band at different heating times. Each value represents an average of two separate experiments. Solid lines indicate fit of Equation 3.8. Thick solid lines represent β -Lg A; dots, β -Lg B; and dashes, β -Lg C.

Table 5.1 Rate constants of monomer hydrolysis calculated from Equation 3.8.

Sample	k_h	Adj.	$S_{y x}^a$
details	$\times 10^{-3} \text{ (min}^{-1}\text{)}$	R^2	$\times 10^{-3}$
β -Lg A	2.18 (0.05)	0.9952	0.34
β -Lg B	2.30 (0.09)	0.9892	0.54
β -Lg C	2.21 (0.08)	0.9901	0.50

Numbers in parenthesis indicate standard deviations, a : standard error of regression.

5.4.4. Self-assembly of β -Lg A, B and C

The self-assembly of β -Lg A, B and C was studied using the ThT assay (Figure 5.8). The rates of self-assembly of all three β -Lg variants followed a sigmoidal curve with a distinct lag phase of around 4 h. Continued heating beyond 4 h resulted in a rapid increase in the corresponding fluorescence intensities. The differences in the self-assembly of β -Lg A, B and C were not significant ($P=0.52$) in the likelihood ratio test. The kinetic parameters of self-assembly, calculated using Equations 3.2 to 3.4, were similar for all the three β -Lg variants (Table 5.2).

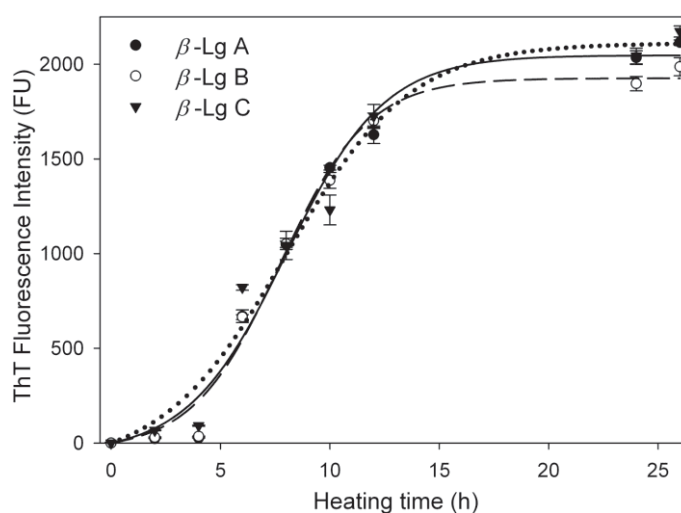


Figure 5.8 ThT fluorescence intensities at 486 nm in heated samples of β -Lg A, B and C (1% w/v) at 80 °C and pH 2. Error bars represents standard error of measurements from two experiments with two replicates in each. Solid lines indicate fit to Equation 3.1. Thick solid lines represent β -Lg A; dots, β -Lg B; and dashes, β -Lg C.

Chapter 5. Self-Assembly from β -Lg A, B and C

Table 5.2 Kinetic parameters of self-assembly calculated from Equations 3.2 to 3.4.

Sample details	t_{lag} (h)		$\left(\frac{df}{dt}\right)_{max}$	$t_{\frac{1}{2}max}$	f_{max}
	Observed	Calculated	$\times 10^2$ (FU/h)	(h)	$\times 10^3$ (FU)
β -Lg A	4	3.8 (0.7)	2.2 (0.3)	8.5 (0.4)	2.0 (0.08)
β -Lg B	4	3.5 (0.5)	2.8 (0.3)	6.9 (0.3)	1.9 (0.07)
β -Lg C	4	2.8 (0.3)	2.4 (0.4)	7.4 (0.4)	2.1 (0.10)

Numbers in parenthesis indicate standard deviations, a : Standard error of regression.

5.4.5. Morphology of fibrils

Fibrils from β -Lg A, B and C appeared long, unbranched and semi-flexible. Further, the fibrils from all three proteins were found to be uniform in diameter and were up to 1 μ m in length (Figure 5.9). These fibrillar features were analogous to those of the fibrils formed at low ionic strength under similar conditions (Hettiarachchi et al., 2012; Loveday et al., 2010).

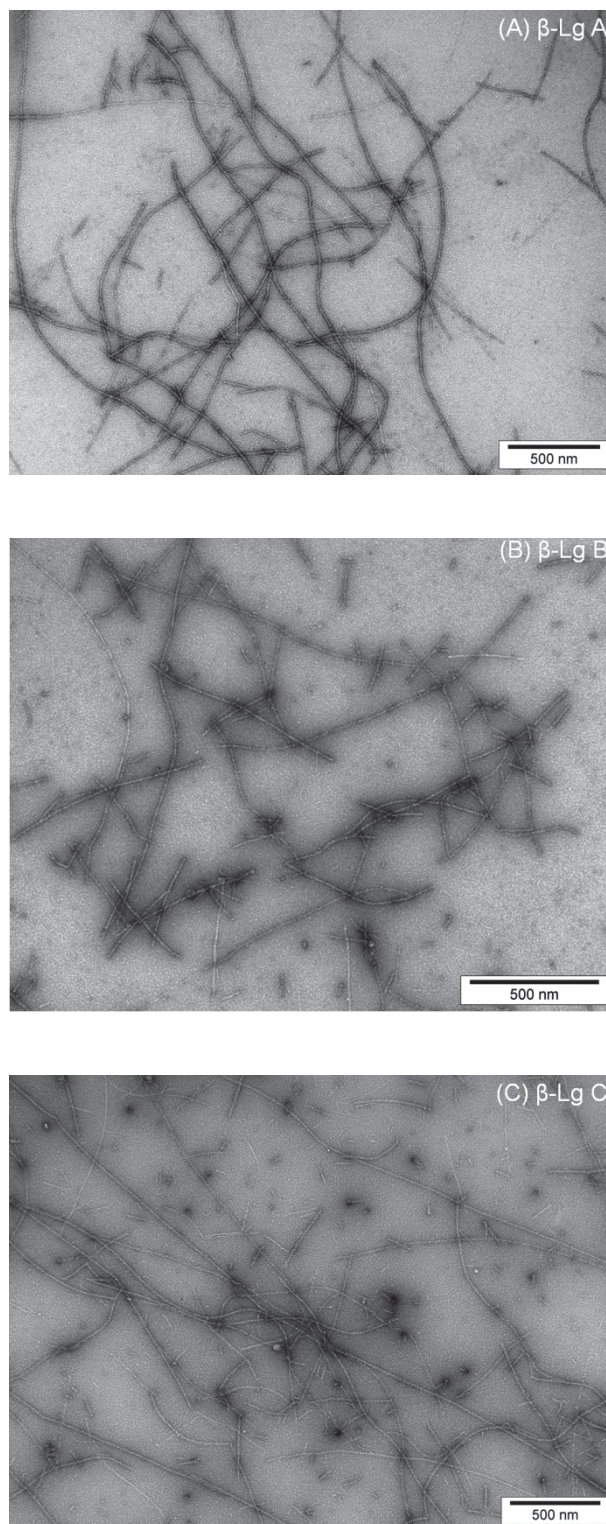


Figure 5.9 TEM images of fibrils from β -Lg A, B and C after 24 h at 80 °C.

5.4.6. Composition of fibrils

SDS-PAGE profiles of fibrils, separated by ultracentrifugation from the heated solutions after 12 h at 80 °C, showed that fibrils from all three variants consisted of few preferentially accumulated peptides (Figure 5.10). A comparison of peptide bands in fibrils indicated minor differences in the number and intensity of these bands. Fibrils from β -Lg A had an additional band R as compared to those in β -Lg B and C. Similarly, the intensity of peptide band in β -Lg A sample, marked 'C' in region was considerably higher than that in β -Lg B and C. In addition, β -Lg B had two weak additional bands (region i) in the pellet (fibrils) compared to β -Lg A and β -Lg C. In addition, β -Lg B had two weak additional bands (region i) in the pellet (fibrils) compared to β -Lg A and β -Lg C.

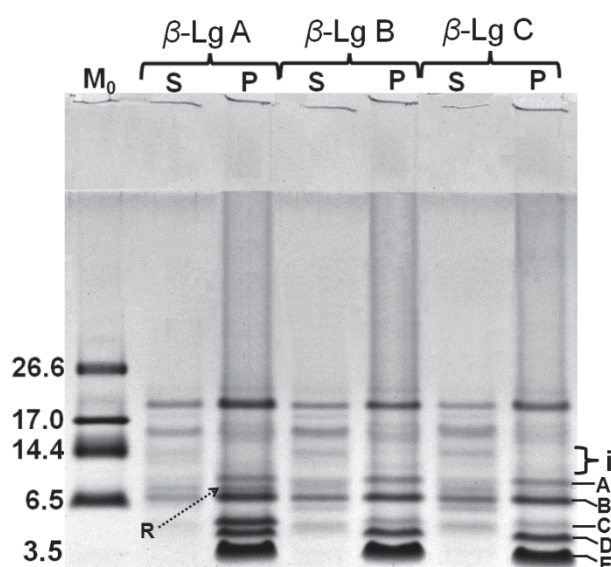


Figure 5.10 Reducing tricine SDS-PAGE of fibrils formed after heating at 80 °C for 12 h and separated by ultracentrifugation. M₀, Molecular weight marker; S, supernatant; P pellet containing fibrils. Molecular weights in kDa; for descriptions of (i), bands A to E and R, see text.

5.5. Discussion

β -Lg A, B and C show marginal differences in their heat stabilities, which may be related to the amino acid substitutions in these proteins (Manderson et al., 1999; Qin et al., 1999). This study showed that the unfolding of the tertiary structure during heating at pH 2 occurred rapidly, and there were no real differences between β -Lg A, B and C. Transitions in the native structure were very rapid and further experiments using techniques with greater sensitivity are necessary to characterize the details of the unfolding kinetics.

Continued heating results in heat-induced acid hydrolysis of the unfolded β -Lg monomers resulting from the preferential cleavage of peptide bonds involving Asp residues (Akkermans et al., 2008b; Hettiarachchi et al., 2012). The rate of heat-induced acid hydrolysis of β -Lg A, B and C were similar (Table 5.1) indicating that the additional site of acid-hydrolysis (Asp64, β -Lg A) did not affect the overall rate of hydrolysis of the β -Lg A monomer. Thus, the heated samples of β -Lg A, B and C had approximately similar concentrations of peptides necessary for self-assembly.

The ThT data from Figure 5.8 and Table 5.2 indicate that the kinetic parameters of self-assembly were similar for β -Lg A, B and C. All samples had similar t_{lag} which may be attributed to the similar overall rates of monomer hydrolysis and the homology of primary sequences of these proteins in the N-terminal region (1-58). This region (1-53) has been suggested to form the core of fibrils and play an important role in nucleation during self-assembly (Chapter 4). The df/dt max and f_{max} for heated β -Lg A, B and C followed a similar trend, suggesting that the peptide-peptide interactions leading to the

Chapter 5. Self-Assembly from β -Lg A, B and C

growth of the nuclei may be similar for these samples. This indicates that the additional charge on β -Lg C at pH 2 was not sufficient to significantly impact the peptide-peptide interactions during self-assembly. The morphology of fibrils of β -Lg A, B and C were similar (Figure 5.2).

The SDS-PAGE analysis of ultracentrifuged samples revealed some interesting details about the peptide composition of the fibrils formed from β -Lg A, B and C. Fibrils of β -Lg A showed two intense bands (band R and C, Figure 5.10) which were either absent or lighter in intensity in the fibrils of β -Lg B and C. This may be explained on the basis of the amino acid substitutions in these variants. Based on the in-gel digestion ESI-MS/MS data for the peptide bands in fibrils of Chapter 4, the possible sequences present in Bands A to E and R were constructed (Table 5.3). In β -Lg A, the preferential cleavage of the peptide bond involving Asp64 would be expected to result in two distinct additional peptides (Band R: seq. 65-136, and band C: seq. 12-64) in comparison to those in β -Lg B.

Thus, from this study it can be concluded that the genetic substitution of amino acids in β -Lg had no significant effect on the mechanism of their self-assembly into fibrils. Fibrils of β -Lg A, B and C were similar in morphology; however, there were minor differences in the peptide composition of the fibrils which may be attributed to the amino acid substitutions in these variants.

Chapter 5. Self-Assembly from β -Lg A, B and C

Table 5.3 Possible sequences present in the peptide bands of fibrils of β -Lg A, B and C, shown in Figure 5.10.

β -Lg Variant	Band	Location ^a	Possible Sequence ^{a, b}	Predicted	SDS-
				Mass (kDa) ^c	PAGE Mass (kDa) ^d
β -Lg A	A	12-96	(D)IQKVAGTWYSLAMAASDISLLDAQSAPLRVYVEELKPTPEGDLEI	9.3	8.9
			LLQKWENDECAQKKIIAEKTKIPAVFKIDALNENKVLVLD(T)		
	54-130	(D)LEILLQKWENDECAQKKIIAEKTKIPAVFKIDALNENKVLVLDTD YKKYLLFCMENS AEPEQSLVCQCLVRTPEVDD(E)	8.9		
β -Lg A	R	65-136	(D)ECAQKKIIAEKTKIPAVFKIDALNENKVLVLDTDYKKYLLFCMEN SAEPEQSLVCQCLVRTPEVDDEALEKF(D)	8.2	8.0
β -Lg B	B	1-64	(-)LIVTQTMKGLDIQKVAGTWYSLAMAASDISLLDAQSAPLRVYVE ELKPTPEGDLEILLQKWEND(E)	7.1	7.2
		34-98	(D)AQSAPLRVYVEELKPTPEGDLEILLQKWENDECAQKKIIAEKTKIP	7.1	

Chapter 5. Self-Assembly from β -Lg A, B and C

		AVFKIDALNENKVLVLD(Y)	
C	12-64	(D)IQKVAGTWYSLAMAASDISLLDAQSAPLRVYVEELKPTPEGDLEILL QKWEND(E)	5.9 5.7
D	1-52	(-)LIVTQTMKGLDIQKVAGTWYSLAMAASDISLLDAQSAPLRVYVEEL KPTPEG(D)	5.6 5.2
	53-96	(G)DLEILLQKWENDECAQKKIIAEKTKIPA VFKIDALNENKVLVLD(T)	5.1
E	12-52	(D)IQKVAGTWYSLAMAASDISLLDAQSAPLRVYVEELKPTPEG(D)	4.4 4.4
	1-33	(-)LIVTQTMKGLDIQKVAGTWYSLAMAASDISLLD(A)	3.6
<hr/>			
A	12-95	(D)IQKVAGTWYSLAMAASDISLLDAQSAPLRVYVEELKPTPEGDLEILLQK WENGEC AQKKIIAEKTKIPA VFKIDALNENKVLVLD(D)	9.3 9.0
	85-162	(I)DALNENKVLVLDTDYKKYLLFCMENSAEPEQSLACQCLVRTPEVDDEAL EKFDKALKALPMHIRLSFNPTQLEE QCHI(-)	8.9
β -Lg B			
B	34-98	(D)AQSAPLRVYVEELKPTPEGDLEILLQKWENGEC AQKKIIAEKTKIPA VFKI DALNENKVLVLDTD(Y)	7.3 7.5

Chapter 5. Self-Assembly from β -Lg A, B and C

C	1-53	(-) PEGD(L)	LIVTQTMKGLDIQKVAGTWYSLAMAASDISLLDAQSAPLRVYVEELKPT	5.7	5.7
	34-84	(D) (D)	AQSAPLRVYVEELKPTPEGDLEILLQKWENGECAQKKIIAEKTKIPAVFKI	5.7	
D	53-96	(G)	DLEILLQKWENGECAQKKIIAEKTKIPAVFKIDALNENKVLVLD(T)	5.1	5.3
	1-52	(-) PEG(D)	LIVTQTMKGLDIQKVAGTWYSLAMAASDISLLDAQSAPLRVYVEELKPT	5.6	
E	12-52	(D)	IQKVAGTWYSLAMAASDISLLDAQSAPLRVYVEELKPTPEG(D)	4.4	4.4
	1-33	(-)	LIVTQTMKGLDIQKVAGTWYSLAMAASDISLLD(A)	3.6	
A	12-95	(D)	IQKVAGTWYSLAMAASDISLLDAQSAPLRVYVEELKPTPEGDLEILLHK	9.3	9.3
			WENGECAQKKIIAEKTKIPAVFKIDALNENKVLVLD(D)		
β -Lg C	85-162	(I)	DALNENKVLVLDTDYKKYLLFCMENSAPAEQSLACQCLVRTPEVDDEAL EKFDKALKALPMHIRLSFNPTQLEEQCHI(-)	8.9	

Chapter 5. Self-Assembly from β -Lg A, B and C

B	34-98	(D)AQSAPLRVYVEELKPTPEGDLEILLHKWENGECAQKKIIAEKTKIPAVFKI DALNENKVLVLDTD(Y)	7.3	7.4
C	1-53	(-)LIVTQTMKGLDIQKVAGTWYSLAMAASDISLLDAQSAPLRVYVEELKPT PEGD(L)	5.7	5.7
D	34-84	(D)AQSAPLRVYVEELKPTPEGDLEILLHKWENGECAQKKIIAEKTKIPAVFKI (D)	5.7	
D	53-96	(G)DLEILLHKWENGECAQKKIIAEKTKIPAVFKIDALNENKVLVLD(L)	5.1	5.3
E	12-52	(D)IQKVAGTWYSLAMAASDISLLDAQSAPLRVYVEELKPTPEG(D)	4.4	4.4
E	1-33	(-)LIVTQTMKGLDIQKVAGTWYSLAMAASDISLLD(A)	3.6	

Letters in the parentheses indicate the amino acid residue adjacent to the peptide while (–) indicates either, N- terminal or C- terminal end of the β -Lg. *a*: Locations and possible sequences in peptide bands predicted based on the sequences found experimentally by in-gel digestion MS/MS, in peptide bands of fibrils (Chapter 4). *b*: only peptide bonds involving aspartic acid residues (D) were

Chapter 5. Self-Assembly from β -Lg A, B and C

considered as sites of acid hydrolysis; *c*: predicted molecular weights calculated from ExPASy compute pI/MW resource tool ; *d*: calculated from the Equation: $\text{Log (molecular weight)} = -1.69 (R_f) + 5.16$ ($R^2 = 0.97$) computed from the of log (molecular weight) vs R_f curve of molecular weight markers of Figure 5.10

Chapter 6

6. Glycation as a tool to probe the mechanism of β -lactoglobulin self-assembly

The contents of this chapter have been published in a peer-reviewed journal article and adapted with permission from:

Dave, A. C., Loveday, S. M., Anema, S. G., Jameson, G. B., & Singh, H. (2014). Glycation as a tool to probe the mechanism of β -lactoglobulin self-assembly. *Journal of Agricultural and Food Chemistry*. 62(14), 3269-3278. Copyright (2014) American Chemical Society.

6.1. Abstract

This study investigates the effects of different levels of glucosylation and lactosylation on β -lactoglobulin (β -Lg) self-assembly into nanofibrils at 80 °C and pH 2. Fibrils in heated samples were detected with the Thioflavin T (ThT) assay and transmission electron microscopy (TEM), while SDS-PAGE was used to investigate the composition of the heated solutions and fibrils. Glycation had different effects on nucleation and growth phases. The effect of glycation on the nucleation phase depended on the degree of glycation but not sugar type, whereas both the type of sugar and degree of glycation affected the rate of fibril growth. Glycation by either sugar strongly inhibited the self-assembly in the growth phase, and lactosylation produced a much stronger effect than glucosylation. The results from this study suggest that the varying glycation susceptibility of lysine residues can explain these

Chapter 6. Effect of Glycation on Self-Assembly

observations. The large, polar sugar residues on the fibrillogenic peptides may inhibit fibril assembly by imposing steric conformational restrictions and disrupting hydrophobic interactions.

6.2. Introduction

The mechanism of β -Lg self-assembly has been extensively investigated by altering the conditions of self-assembly. Another approach, which has largely been unexplored, is to investigate the self-assembly of chemically-modified β -Lg. Chemical modification of β -Lg involves the interactions of reactive functional groups of amino acid side chains, e.g. amine groups of lysine and arginine, and this reaction has been used as a tool to modify the functional properties of β -Lg (Chevalier et al., 2001b; Medrano et al., 2009; Nacka et al., 1998). It is not known what effect chemical modifications of different amino acid side-chain functional groups of β -Lg, e.g. glycation of lysine residues, may have on its self-assembly.

Glycation of β -Lg by the Maillard reaction or non-enzymatic browning involves the interaction of the reactive side-chain amine groups with the free carbonyl groups of the reducing sugars. The details of the various steps involved in Maillard reaction of milk proteins have been reviewed and described previously (O'Brien, 1995). β -Lg has 19 free amine groups that are available for Maillard reaction: 15 from lysine and 3 from arginine residues and the N-terminal amine group. Studies using lactosylation have shown that lysine residues at positions 47 (Fenaille et al., 2004; Fogliano et al., 1998; Morgan et al., 1998), 91 (Fenaille et al., 2004; Morgan et al., 1998; Morgan et al., 1999b) and 100 (Fogliano et al., 1998) are particularly susceptible to glycation. Glycation of β -Lg can be achieved by incubating the protein-sugar mixture at pH 7 under controlled conditions in the dry state or aqueous state. Glycation in the dry state, also referred to as solid-state glycation, is much faster than aqueous glycation (French et al., 2002; Morgan et al., 1998; Morgan et al., 1999a; Morgan et al., 1999b).

Chapter 6. Effect of Glycation on Self-Assembly

Solid-state glycation of β -Lg conserves its native-like structure (Morgan et al., 1999a; Morgan et al., 1999b; van Teeffelen et al., 2005) and its association tendency (Morgan et al., 1999b), and yields a heterogeneous mixture of glycoforms that differ in the degree and sites of glycation (Morgan et al., 1997). In contrast, aqueous glycation induces significant changes in the native β -Lg structure (Chevalier et al., 2002; Morgan et al., 1999b) and leads to sugar-induced protein cross-linking (Da Silva Pinto et al., 2012; Morgan et al., 1998; Morgan et al., 1999b). The effects of β -Lg glycation include improved heat stability (Broersen et al., 2004; Liu et al., 2013b; Medrano et al., 2009; Mulsow et al., 2009), lowered isoelectric point (Broersen et al., 2007; Chevalier et al., 2001a), decreased surface hydrophobicity due to polar sugar groups (Medrano et al., 2009; Mulsow et al., 2009), and inhibition of aggregation due to the steric effect of sugar residues (Liu et al., 2013b; Mulsow et al., 2009).

Modification of the amine groups of amyloidogenic proteins α -synuclein (Lee et al., 2009) and insulin (Oliveira et al., 2011) by dicarbonyl compounds slowed their self-assembly into fibrils *in vitro*. On the other hand, glycation promoted self-assembly in bovine serum albumin (Bouma et al., 2003). Glycation is likely to affect β -Lg self-assembly since almost all of the potential glycation sites are located on the regions involved in fibril-formation (Akkermans et al., 2008b; Hettiarachchi et al., 2012).

Liu et al. (2013a) recently prepared nanofibrils from β -Lg after solid-state incubation with lactose. However, the incubation produced changes in secondary structure, and Maillard reactions progressed well beyond the addition of integer numbers of sugars, due to the extreme incubation conditions (80 °C for 2 h at 70% relative humidity). Lactose-reacted β -Lg fibrils had modified functional properties, but little mechanistic information could be obtained due to the heterogeneity of the starting material.

The objective of this chapter is to investigate how glycation affects the structural and chemical events involved in fibril formation. Glycated β -Lg was prepared under mild conditions in order to prevent advanced Maillard reactions and produce a well-defined starting material without marked changes to the secondary or tertiary structure of the protein.

6.3. Materials and methods

The chemicals used in the experimental work in this chapter have been listed in Chapter 3 and MilliQ water was used for preparing reagents. β -Lg was extracted in-house using the protocol in Section 3.3.1 of Chapter 3. Glycated β -Lg was prepared as described below, while the degree of glycation in samples was investigated using mass spectrometry using protocols in Sections 3.3.7.2.1 and 3.3.7.3.1. The sample preparation protocol for self-assembly studies is described in Section 3.3.2; fibrils in the samples were detected using the ThT assay, as described in Section 3.3.3. Fibrils from samples were separated by ultracentrifugation (Section 3.3.4). The SDS-PAGE of samples was followed as per Sections 3.3.5.3, 3.3.5.4 and 3.3.5.6. The unfolding of glycated β -Lg was investigated using circular dichroism (CD) spectroscopy (Sections 3.3.6.2 and 3.3.6.3). Fibrils of glycated β -Lg were examined using TEM (Section 3.3.9).

6.3.1. Preparation of glycated β -Lg

A stock solution of β -Lg (pH 7) was allowed to hydrate at 4 °C overnight. The solution was then centrifuged at 44,000 g for 30 minutes at 20 °C and the supernatant was filtered using a syringe filter (pore size 0.2 μ m, Minisart[®] CE, Sartorius Stedim Biotech GmbH, Goettingen, Germany). Glucose and lactose powders were mixed with the filtered β -Lg solution (molar ratio β -Lg:sugar = 1:100) and the pH of the solutions were re-adjusted to 7.00 \pm 0.02. The samples were then frozen at -18 °C overnight and freeze-dried. For glycation, the freeze-dried powders were placed in a glass petri dish and transferred to separate desiccators with a saturated potassium bromide (KBr) solution. The desiccators were sealed and a vacuum of 125 mbar was applied. The desiccators were then transferred to an oven maintained at 40.0 \pm 0.5 °C. The saturated KBr solution gave a relative humidity of 80% inside the desiccators. For glucosylation, samples were removed from the desiccators after 8, 16 or 24 h, while for lactosylation the durations were 3, 5, and 7 days. Longer incubation times were not investigated, since samples incubated for times showed extensive brown discoloration, indicating the presence of advanced Maillard reaction products. After completion of the glycation reaction, the samples were dissolved in Milli Q water (pH 7) and dialyzed (molecular weight cut-off of 6 to 8 kDa, Spectra/Por[®], Spectrum Laboratories Inc., USA) against water for 48 h at 4 °C to remove the excess un-reacted sugar. The dialyzed protein solution was then freeze-dried and stored at -18 °C until further analysis. For self-assembly studies, fresh samples were made using selected glycation times by the above described method.

6.4. Results

6.4.1. Preliminary experiments

The β -Lg prior to glycation showed only two peaks corresponding to variants A and B (Figure 4.3, Chapter 4). The extent of glycation of β -Lg with glucose and lactose after different glycation times is shown in the deconvoluted MS spectra in Figures 6.1 and 6.2 respectively. The degree of glycation after 8 h glucosylation and 3 days lactosylation were similar, and hence these glycation times were selected for further investigation. For subsequent studies in this chapter, the samples made using these conditions are referred to as low glucose (LowGlu) and low lactose (LowLac) β -Lg respectively. Similarly, for the high degree of glycation, the durations selected were 36 h for glucosylation and 7 days for lactosylation. The samples made using these time-points will be referred to as high glucose (HighGlu) and high lactose (HighLac) β -Lg respectively. Fresh glycated samples were made using the selected glycation time-points and analyzed by MS. For each of the glycation treatments, a β -Lg sample without sugar was used as control.

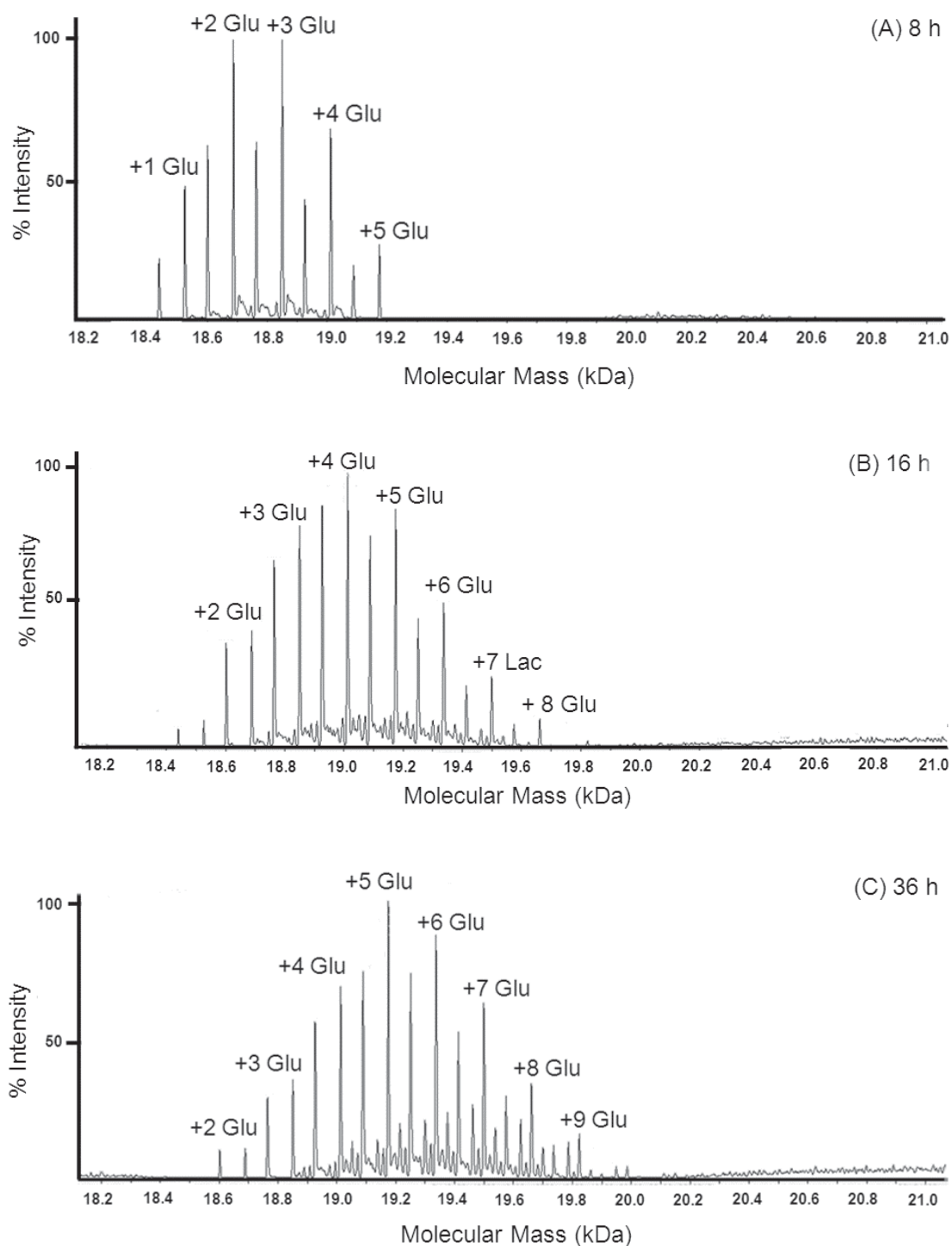


Figure 6.1 De-convoluted MS spectra of glycosylated β -Lg (A) 8 h, (B) 16 h and (C) 36 h. Numbers in the figure represent the number of glucose residues attached on the β -Lg variant A.

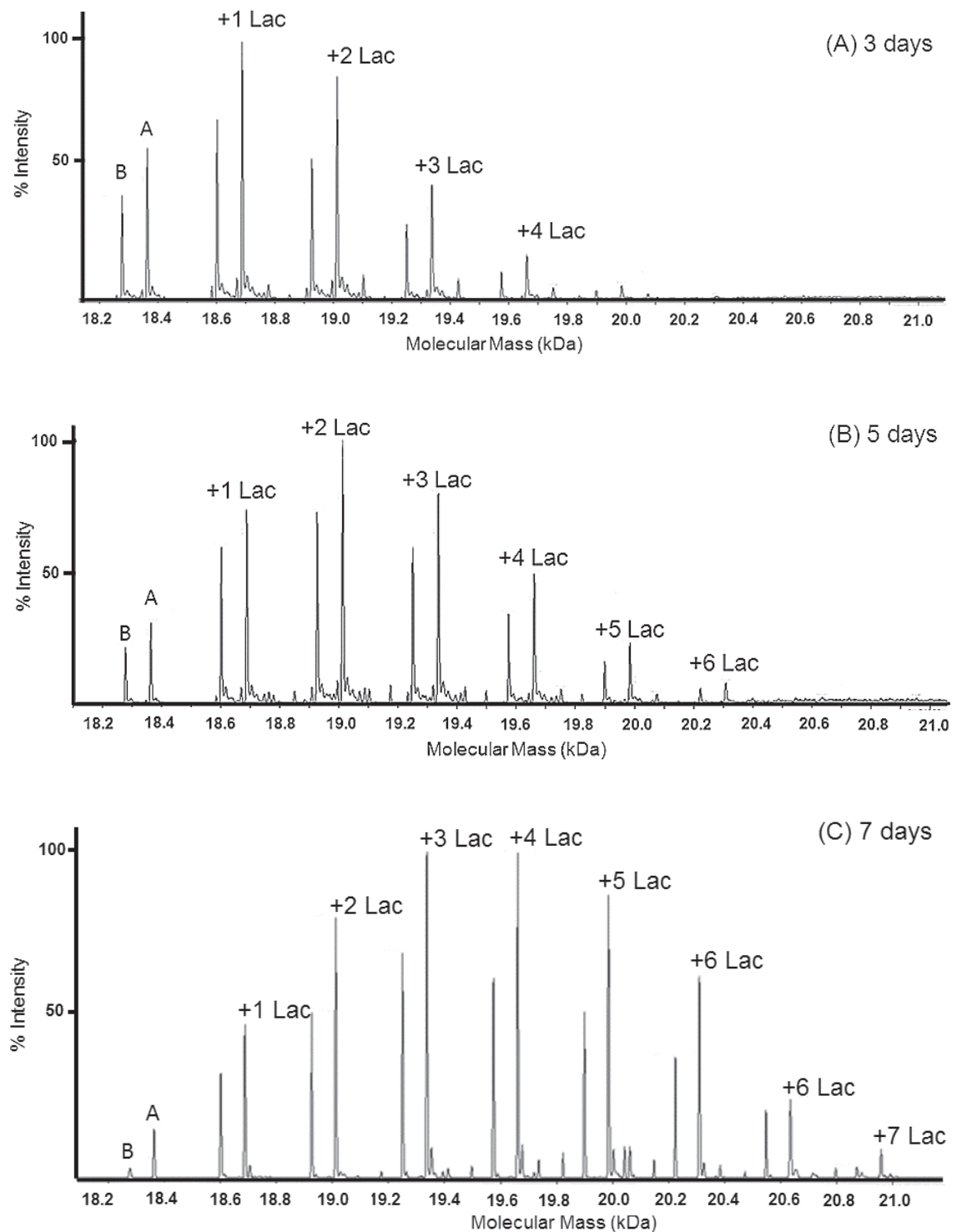


Figure 6.2 De-convoluted MS spectra of lactosylated β -Lg (A) 3 days, (B) 5 days and (C) 7 days. Numbers in the figure represent the number of lactose residues attached on the β -Lg variant A.

6.4.2. Characterization of glycated β -Lg for self-assembly studies

The de-convoluted MS spectra of glucosylated and lactosylated β -Lg are shown in Figures 6.3 and 6.4. All glycated samples showed a series of peak pairs with mass increments of either 162 Da (Figure 6.3 (A) and (B), glucosylation) or 324 Da (Figure 6.4 (A) and (B) lactosylation) indicating that both the variants B (18277 Da) and A (18364 Da) participated in glycation. Peaks corresponding to un-glycated β -Lg appeared only in the scans of LowLac β -Lg, and at low levels in that case. Variants A and B showed a similar propensity for glycation, and the glucosylation of both variants was faster than lactosylation. The presence of multiple peaks in the spectrum indicated heterogeneity of glycoforms of β -Lg with respect to number of sugar residues attached to β -Lg molecule. These results are in agreement with previous studies that showed similar reactivities of β -Lg A and B (Meltretter et al., 2013), faster rates of glucosylation than those of lactosylation of β -Lg (Medrano et al., 2009), and a presence of heterogeneous mixture of glycoforms in samples with respect to the number of attached sugar residues (Broersen et al., 2007; Broersen et al., 2004; Morgan et al., 1998; Morgan et al., 1997, 1999a).

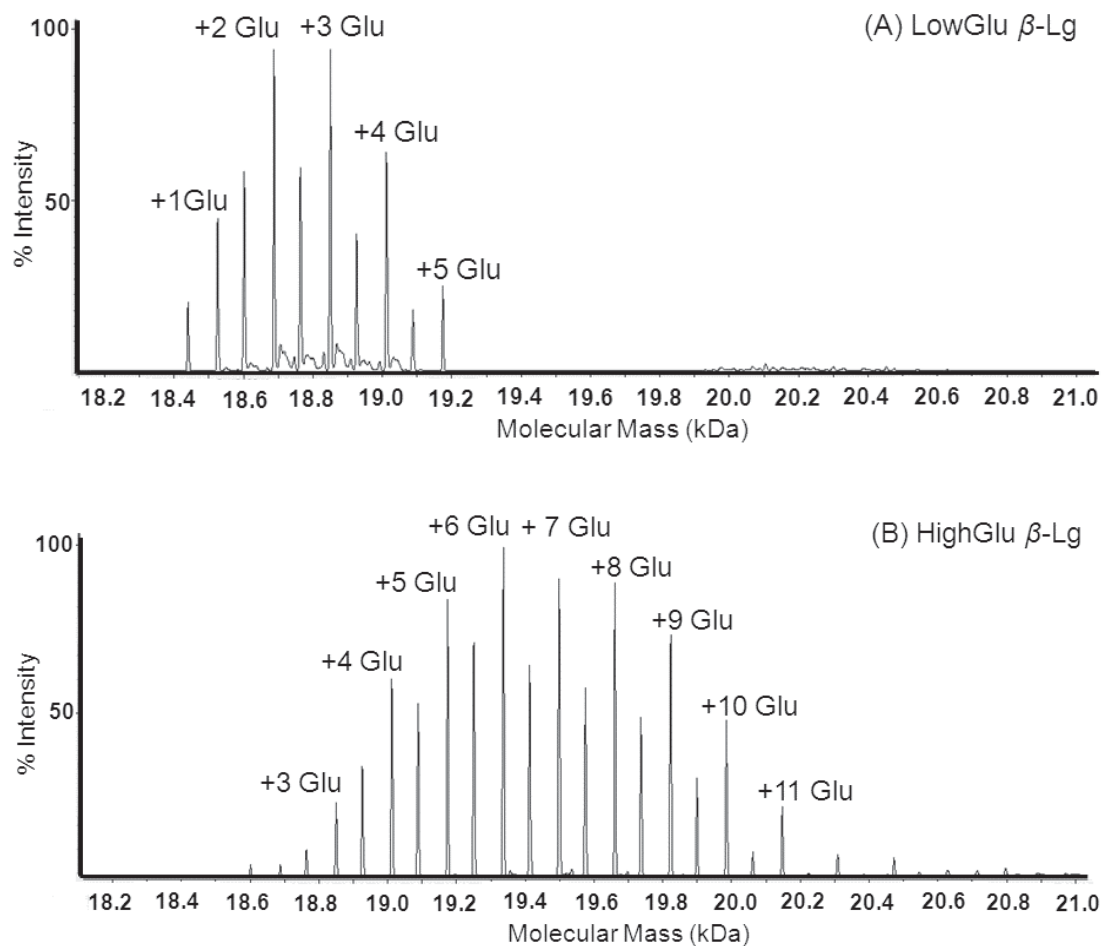


Figure 6.3 De-convoluted MS spectra of glucosylated (A) LowGlu β -Lg and (B) HighGlu β -Lg. Peak labels show the number of attached glucose residues.

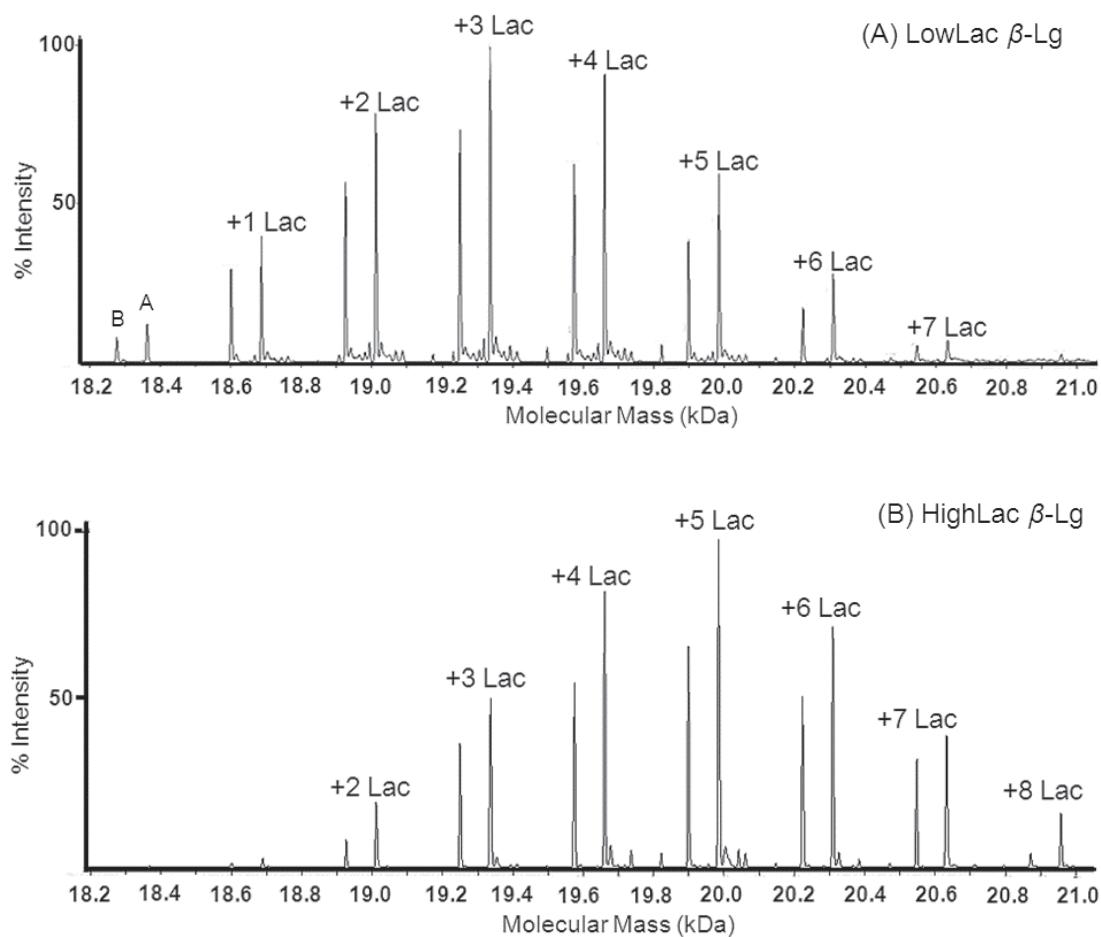


Figure 6.4 De-convoluted MS spectra of lactosylated (A) LowLac β -Lg and (B) HighLac β -Lg. Peak labels show the number of attached lactose residues.

6.4.3. Unfolding behavior of glycated β -Lg

The effect of glycation on β -Lg native structure and thermal unfolding was investigated using CD spectroscopy with *in situ* heating at 80 °C, as described previously (Chapter 4). In the NUV region, all unheated samples showed characteristic troughs at 293 and 286 nm (Figure 6.5, A) arising due to the tryptophan residue at position 19 (Manderson et al., 1999) indicating that the environment around Trp19 was unaffected by glycation. In addition, the scans showed a small trough at 265 nm contributed by the phenylalanine residues in the native β -Lg structure. These troughs in the NUV region rapidly decreased in intensity upon heating β -Lg under fibril-forming conditions (Chapter 4). Heating of glycated samples resulted in the rapid loss of the characteristic troughs at 293, 286 and 265 nm. A typical scan recorded for LowGlu β -Lg during heating is shown in Figure 6.6 (A) while Figure 6.7 (A) shows the comparison of relative loss of ellipticity at 293 nm upon heating.

In the FUV region, glycated samples showed a broad trough with a minimum at 217 nm (Figure 6.5, B), indicating that β -sheets were the dominant secondary structural conformation (Manderson et al., 1999). Heating β -Lg at 80 °C and pH 2 results in the shift of the trough towards lower wavelengths (Chapter 4), representing transitions in secondary structure. All glycated samples showed a rapid shift in the trough during heating. Figure 6.6 (B) illustrates the shift of the trough in the FUV region for LowGlu β -Lg during heating. The plot of $([\Delta\theta_i]/[\Delta\theta_{60}])_{208}$ against time comparing the change in the ellipticity at 208 nm upon heating is shown in Figure 6.7 (B).

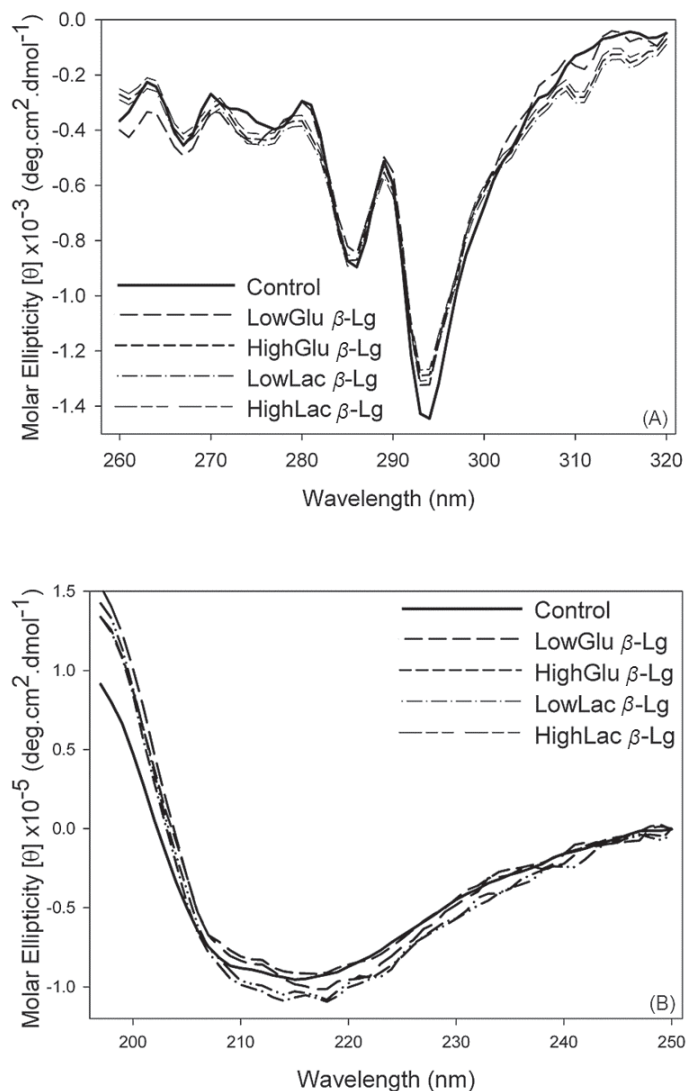


Figure 6.5 Comparison of CD spectra of β -Lg glycated with glucose and lactose (A) NUV (10 mg/mL β -Lg) and (B) FUV (0.01 mg/mL β -Lg) region.

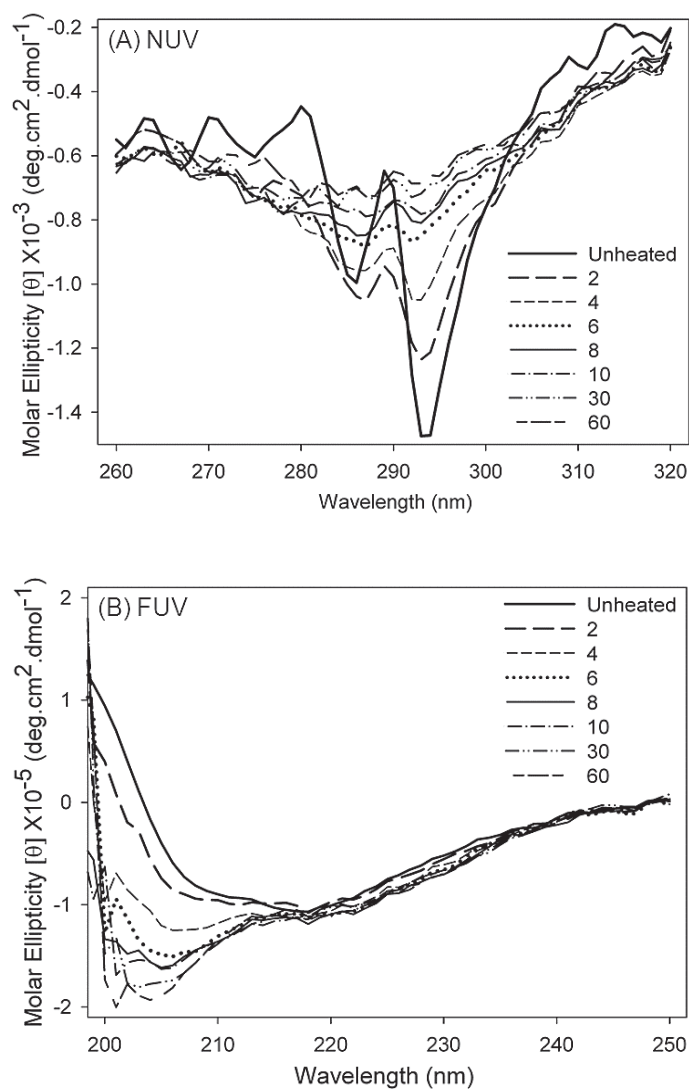


Figure 6.6 CD spectra of LowGlu β -Lg in the (A) NUV region (10 mg/mL β -Lg) and (B) in the FUV region (0.01 mg/mL β -Lg). The numbers in the figures indicate heating time in minutes.

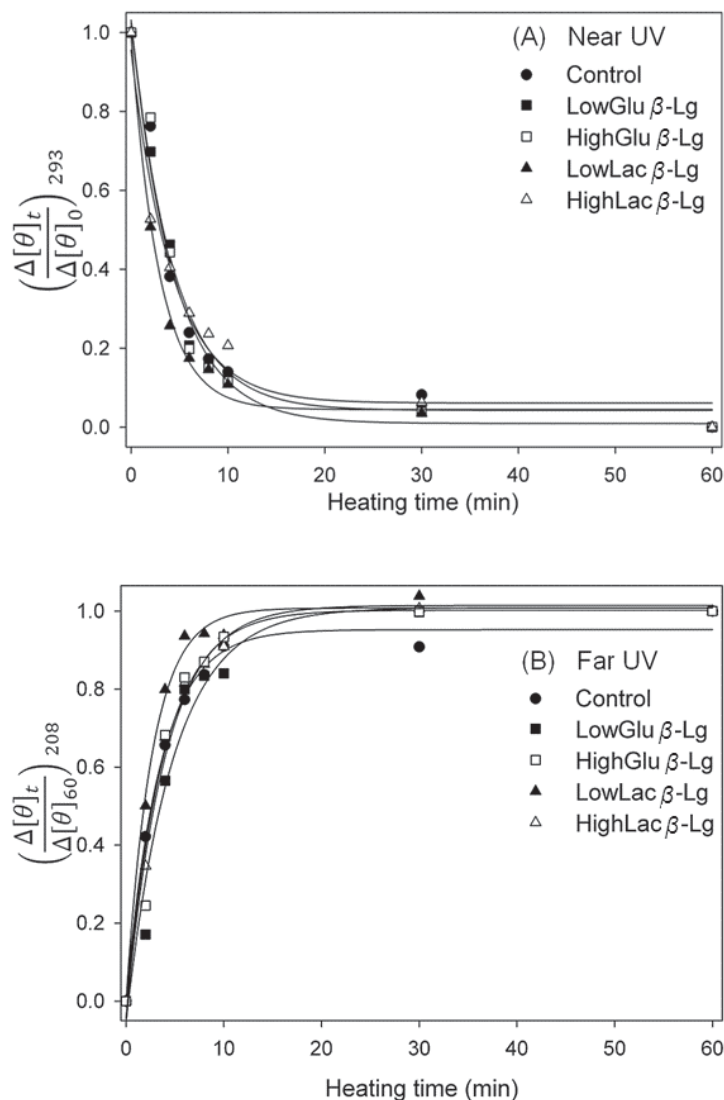


Figure 6.7 Relative change in ellipticity at (A) 293 nm in the NUV region and (B) 208 nm in the FUV region. Solid lines are for visual reference. For details of x and y-axes see Section 3.3.6.3, Chapter 3.

6.4.4. Heat-induced acid hydrolysis

To investigate the effect of glycation on the hydrolysis of β -Lg, the samples heated for different times were analyzed using tricine SDS-PAGE under reducing conditions. All samples showed hydrolysis of the β -Lg monomer with heating. A comparison of PAGE profiles of samples after heating for 12 h at 80 °C is shown in Figure 6.8. The peptide bands in glycated samples appeared less distinct than in control β -Lg. This may be attributed to the presence of a heterogeneous mixture of peptides with different degrees of glycation. In addition, modification of amine groups on the peptides may have altered the affinity of these peptides to bind to the staining dye (Tal et al., 1985). Amongst the glycated samples, the peptide bands in the lactosylated samples were the least well-defined.

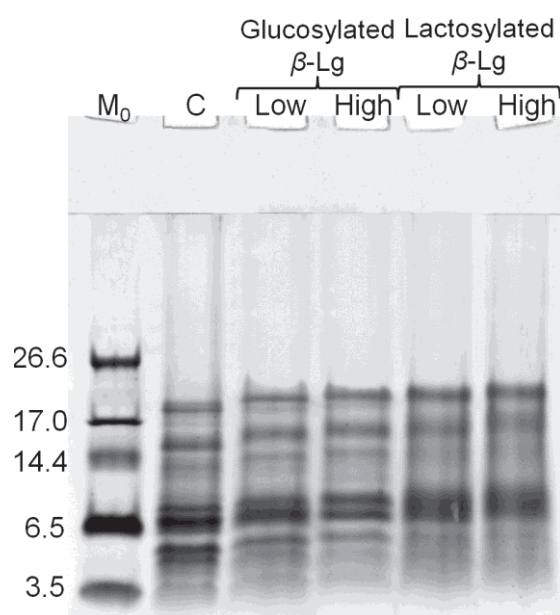


Figure 6.8 Tricine SDS-PAGE profiles of control and glycated samples after heating for 12 h at 80 °C, at pH 2. M_0 , Molecular weight markers in kDa; C, heated control.

Chapter 6. Effect of Glycation on Self-Assembly

The intensity of the band corresponding to the un-hydrolyzed β -Lg in the PAGE gels at different times was quantified and plotted against the heating times. Hydrolysis of the monomer in all samples followed first-order exponential decay kinetics (Figure 6.9); the rate constants (k_h), calculated using Equation 3.8 (Chapter 3), are listed in Table 6.1. Glycation reduced k_h by $\sim 15\%$, and this effect was independent of the type of sugar or the degree of glycation. However, the glycation effect was not significant ($P=0.2862$) in the likelihood ratio test. The PAGE analysis of β -Lg glycation controls showed that the hydrolysis rates were unaffected ($P=0.2515$, likelihood ratio test) by sample treatments in the absence of sugars (Figure 6.10 and Table 6.2).

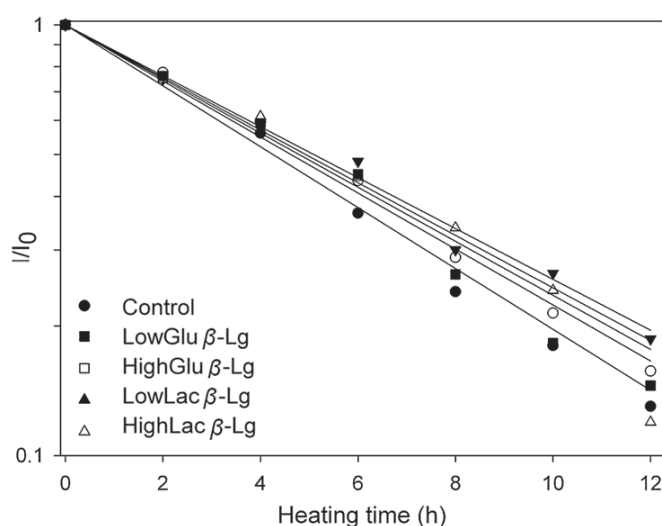


Figure 6.9 The normalized band intensities of the un-hydrolyzed β -Lg band at different times in glycated samples. Each value is an average of quantifications from two sets of independent experiments. The solid lines represent fits to the first-order exponential decay model of Equation 3.8.

Table 6.1 Rate constants of acid hydrolysis of glycated β -Lg calculated from data in Figure 6.9 and Equation 3.8.

Sample details	k_h ($\text{min}^{-1} \times 10^{-3}$)	Adj. R^2	$S_{y x}^b$ ($\times 10^{-3}$)
Control	2.8 (0.10)	0.9921	0.50
LowGlu β -Lg ^a	2.4 (0.08)	0.9925	0.41
HighGlu- β -Lg	2.3 (0.07)	0.9752	0.40
LowLac β -Lg ^a	2.3 (0.10)	0.9609	0.55
HighLac β -Lg	2.5 (0.11)	0.9746	0.60

Numbers in parenthesis indicate standard deviations. *a*: The degree of glycation in LowGlu and LowLac β -Lg was similar; *b*: standard error of regression.

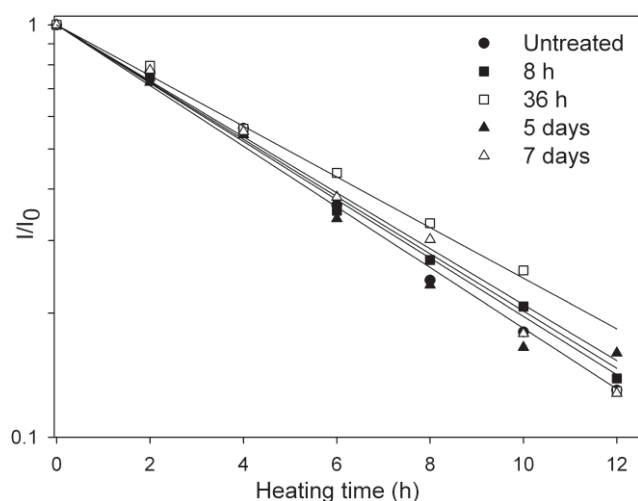


Figure 6.10 The normalized band intensities of the un-hydrolyzed β -Lg band at different times in the controls with no sugar added. Each value is an average of quantifications from two sets of independent experiments. The solid lines represent fits the first-order exponential decay model in Equation 3.8.

Table 6.2 Rate constants of acid hydrolysis of β -Lg used as glycation control calculated from the data in Figure 6.10 and Equation 3.8.

Sample details	k_h ($\times 10^{-3} \text{ min}^{-1}$)	Adj. R^2	$S_{y x}^a$ ($\times 10^{-3}$)
Untreated	2.78 (0.10)	0.9921	0.48
8 h	2.66 (0.06)	0.9961	0.33
36 h	2.36 (0.08)	0.9913	0.48
3 days	2.82 (0.09)	0.9941	0.40
7 days	2.60 (0.08)	0.9932	0.44

Numbers in parentheses indicate standard deviations; a : standard error of regression

6.4.5. Self-assembly from glycated β -Lg

Self-assembly from glycated samples followed a three-phase sigmoidal growth pattern (Figure 6.11, A), which is typical of β -Lg self-assembly under unstirred conditions. The ThT were data fitted well by Equation 3.1, and results from the likelihood ratio test confirmed that the effect of glycation treatments on various parameters was statistically highly significant ($P < 0.0001$). The kinetic parameters of self-assembly calculated from Equations 3.2-3.4 are listed in Table 6.3. A comparison of kinetic parameters of self-assembly is shown in Figure 6.11 (B). LowGlu β -Lg and LowLac β -Lg showed only a small increase in t_{lag} (6 h and 7 h respectively against 5.6 h for the control), whereas in HighGlu β -Lg and HighLac β -Lg the t_{lag} values were nearly twice that of the control (11.3 h and 11 h respectively).

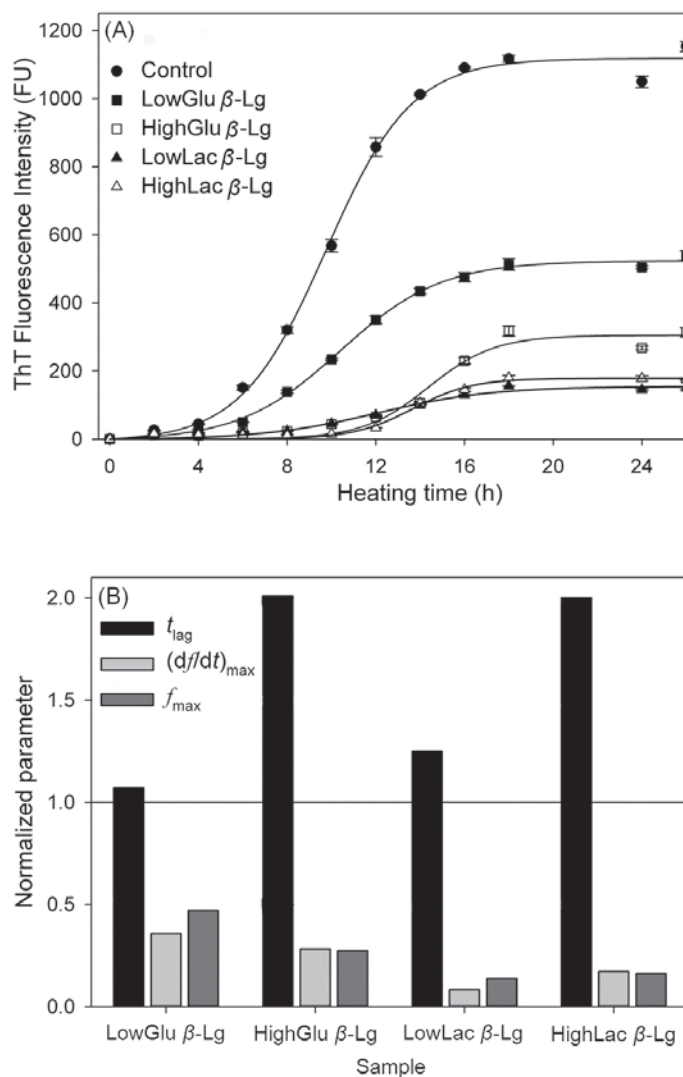


Figure 6.11 (A) ThT fluorescence intensity of control and glycated β -Lg (1% w/v) during heating at pH 2 and 80 °C. Each data point is an average of triplicates from two independent experiments, and error bars are standard deviations. Solid lines indicate the fit to Equation 3.1. (B) Normalized parameters of self-assembly calculated from Equations 3.2 and 3.4. The kinetic parameters of individual samples were normalized by those of control sample.

In the growth phase, glycation greatly decreased the rate of self-assembly denoted by $(df/dt)_{max}$. For glucosylated samples, this effect was more pronounced at high degrees of glycation. In contrast, lactosylation had a strong effect, irrespective of the degree of glycation. The effect of glycation on the stationary phase fluorescence (f_{max}) followed a similar trend. Control β -Lg samples were freeze-dried, incubated and dialyzed as with the glycated samples but without sugars, and these controls self-assembled normally (Figure 6.12 and Table 6.4). Thus, glucosylation and lactosylation had different effects on the different stages of self-assembly and the effect of lactosylation was more pronounced than that of glucosylation.

Table 6.3 Kinetic parameters describing β -Lg self-assembly calculated using Equations 3.2 to 3.4.

Sample	t_{lag}	$(\frac{df}{dt})_{max}$	$t_{\frac{1}{2}max}$	f_{max}	Adj. R^2	S_{yx}^a
Details	(h)	(FU/h)	(h)	(FU)		
Control	5.6 (0.2)	158.0 (8.4)	9.1 (0.1)	1117 (16.0)	0.9964	29
LowGlu β -Lg ^b	6.0 (0.2)	56.0 (2.9)	10.7 (0.2)	523 (6.7)	0.9974	10.9
HighGlu- β -Lg	11.3 (0.7)	51.0 (10.4)	14.3 (0.4)	305 (17.0)	0.9623	24.6
LowLac β -Lg ^b	7.0 (0.8)	15.5 (2.0)	12.0 (0.5)	155 (7.0)	0.9741	9.6
HighLac β -Lg	11.0 (0.4)	32.7 (4.8)	13.8 (0.3)	178 (6.0)	0.9842	9

Numbers in parentheses indicate standard deviations. *a*: standard error of regression.

b: The degree of glycation in LowGlu and LowLac β -Lg was similar.

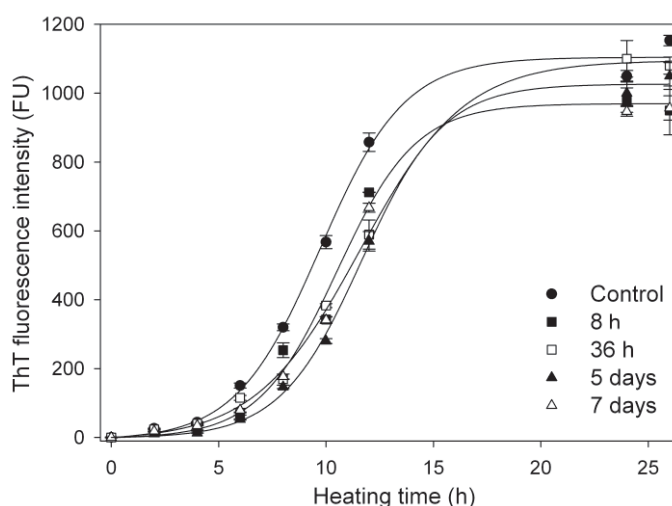


Figure 6.12 Self-assembly from β -Lg (1% w/v) without sugars used as control during glycation and treated similarly to the glycated samples. Error bars represent standard error of triplicate measurements in samples. Each value represents an average of triplicate values. Solid lines indicate fits to Equation 3.1.

Table 6.4 Kinetic parameters describing self-assembly calculated from Equations 3.1-3.4 for β -Lg samples used as controls during glycation experiments. The ThT fluorescence intensities are shown in Figure 6.12 above.

Glycation time ^a	t_{lag} (h)	$\left(\frac{df}{dt}\right)_{max}$ (FU/h)	$t_{\frac{1}{2}max}$ (h)	f_{max} (FU)	Adj. R^2	$S_{y x}$ ^b
Un-treated	5.6 (0.3)	154.0 (11)	9.1 (0.1)	1104.0 (23)	0.9947	34.0
8 h	6.6 (0.5)	142.0 (18)	6.6 (0.3)	970.0 (31)	0.9886	43.0
36 h	6.5 (0.2)	122.0 (7)	11.0 (0.2)	1094.0 (13)	0.9984	18.0
3 days	8.1 (0.2)	132.0 (9)	12.0 (0.1)	1027.0 (13)	0.9980	19.0
7 days	6.6 (0.3)	142.0 (10)	6.6 (0.1)	970.0 (16)	0.9886	43.0

Numbers in parentheses indicate standard deviations. *a*: Glycation times shown here are the times used for glucosylation and lactosylation *b*: Standard error of regression.

Fibrils in the samples heated for 24 h were separated using ultracentrifugation and analyzed using SDS-PAGE under reducing conditions. HighGlu β -Lg and HighLac β -Lg showed long t_{lag} and lower $(df/dt)_{max}$, so a heating time of 24 h was selected for studying the composition of fibrils. Figure 6.13 shows the peptide bands in centrifugally-separated fibrils from glycosylated β -Lg. The residual ThT intensities in the supernatant samples remained low indicating complete separation of fibrils upon ultracentrifugation (Figure 6.14).

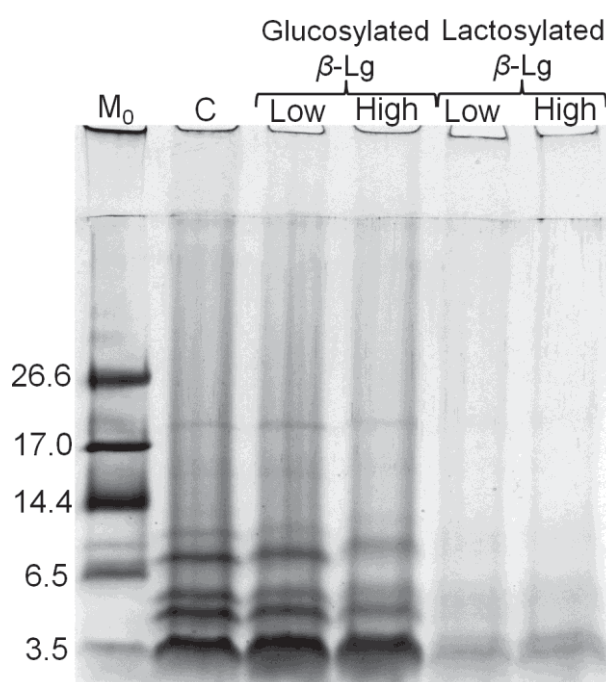


Figure 6.13 Tricine SDS-PAGE profiles of centrifugally separated fibrils made by heating glycosylated β -Lg at 80 °C for 24 h. M_0 , Molecular weight markers in kDa; C , control fibrils made from the same heat treatment.

All pellet samples contained only peptides, indicating that the building blocks of fibrils were predominantly peptides under the conditions used here (1% w/v protein, pH 2, heating at 80 °C). The same bands appeared in all glycosylated samples, but they were less distinct in glycosylated samples, and showed slightly reduced mobility indicating that these peptides may be glycosylated. The lighter overall intensity in

LowLac β -Lg and HighLac β -Lg lanes may result from lower fibril yields (Figure 6.11, A).

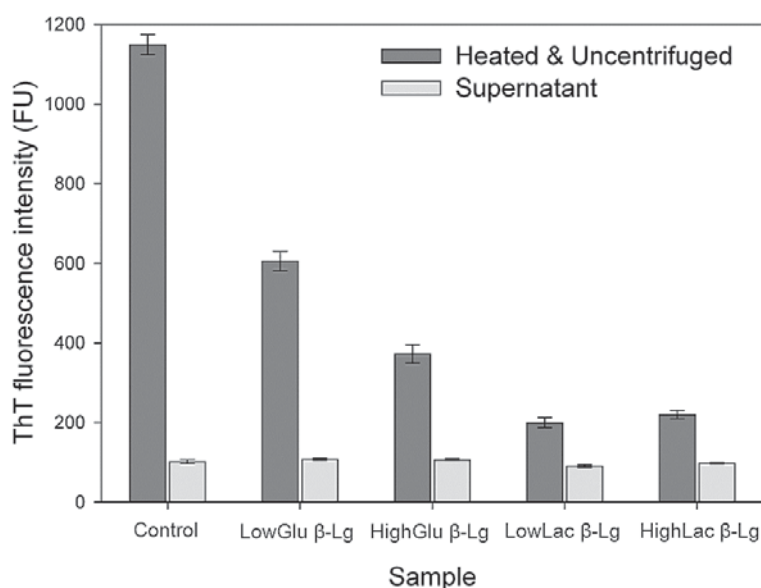


Figure 6.14 Residual ThT intensities in supernatants obtained for upon ultra centrifugation. Heated β -Lg solutions obtained after heating at 80°C for 24 h were ultracentrifuged. The pellets obtained after ultracentrifugation were used for SDS-PAGE (Figure 6.13).

6.4.6. Morphology of fibrils

The morphology of fibrils from glycosylated β -Lg was examined by TEM (Figures 6.15 and 6.16). The morphology of fibrils was unaffected by glycation. Fibrils appeared long, straight and un-branched similar to those in unmodified β -Lg, irrespective of glucosylation or lactosylation. Further, all samples showed both long and short fibrils.

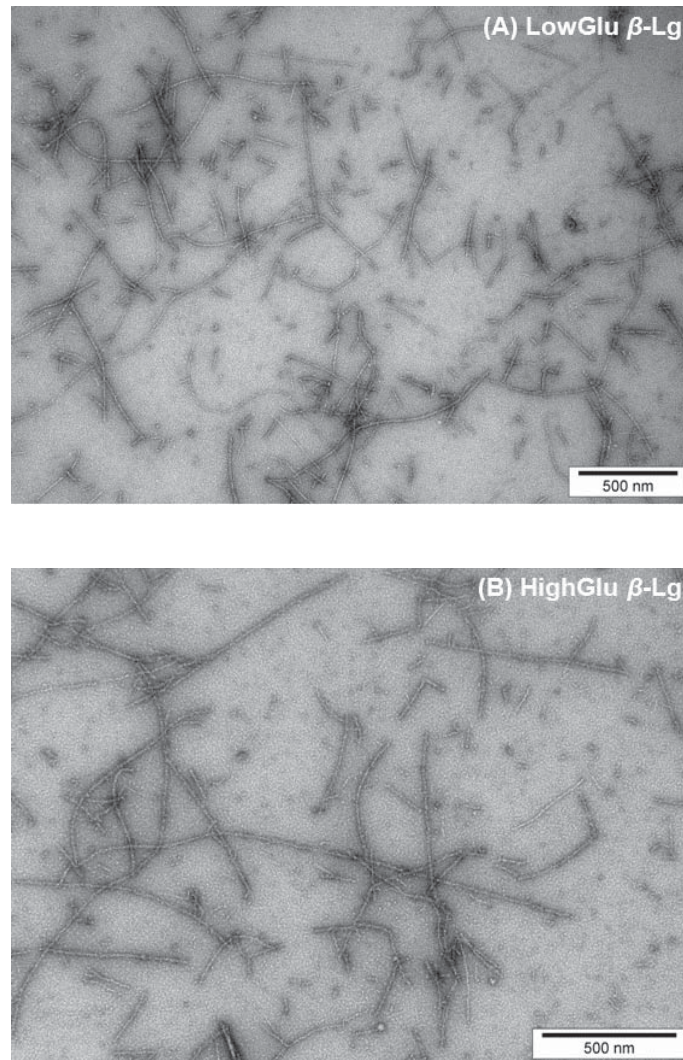


Figure 6.15 TEM images of fibrils from glycated β -Lg after heating for 24 h at 80 °C. (A) LowGlu β -Lg; (B) HighGlu β -Lg.

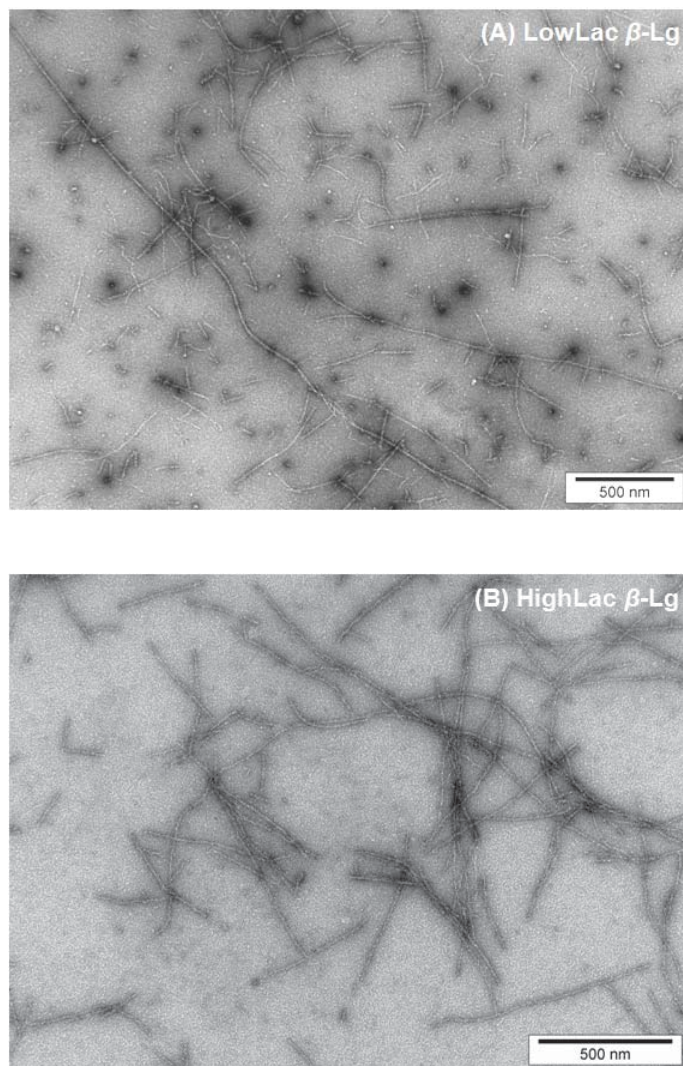


Figure 6.16 TEM images of fibrils from glycated β -Lg after heating for 24 h at 80 °C. (A) LowLac β -Lg; (B) HighLac β -Lg.

6.5. Discussion

The CD studies showed that glycosylation and lactosylation had only very minor effects on the native structure of β -Lg. The structural changes in β -Lg upon heating were very fast, and the CD results did not show differences between control and/or glycated treatments. However, the CD method used in this study took 40 to 60 sec to collect a spectrum, which meant that the temporal resolution was not high enough to detect subtle changes in the kinetics of unfolding. More targeted scanning of only selected wavelengths would be faster, and could potentially quantify the rate of unfolding with higher precision. An innate limitation of this method is that structural changes take place during the heating of the sample to 80 °C, thus making it impossible to define an accurate $t = 0$.

Glycation produced a consistent ~15% decrease in k_h . However, the proportion of unhydrolyzed β -Lg monomer at any one time (I/I_0 in Figure 6.9) never spanned more than 10 percentage points across all treatments. Thus, glycation had a minor impact on the amount of hydrolyzed material present, and the effects of glycation on fibril formation were primarily on peptide self-assembly.

Glycation of the lysine residues on β -Lg would reduce the net charge at pH 2 by +1 per lysine, and this charge reduction alone would be expected to increase the rate of self-assembly by reducing the electrostatic repulsion between peptides. However, glycation always reduced the rate of peptide self-assembly, indicating that the charge reduction effect was counter-balanced by a more dominant assembly-inhibiting factor.

Using succinylated ovalbumin, Ribeiro et al. (2006), showed that the net charge on the protein influences the morphology of its aggregates. However, glycation of β -Lg

Chapter 6. Effect of Glycation on Self-Assembly

did not appear to modify fibril morphology (Figures 6.14 and 6.15), even though MS spectra and SDS-PAGE patterns indicated that fibrils were most likely composed of glycosylated peptides.

The kinetic parameters shown in Table 6.3 and Figure 6.11 reveal some important details about the effects of glycation on self-assembly. The rate of nucleation (related to t_{lag}) was largely unaffected in LowGlu and LowLac β -Lg, which had a similar number of lysine residues modified (Figures 6.3 A, and 6.4 A). The longer t_{lag} for HighGlu β -Lg and HighLac β -Lg suggest that the amount of glycation had to reach a threshold before nucleation was adversely affected, but the size of the adduct had no effect. In contrast, fibril growth (related to $(df/dt)_{max}$) was affected by even low levels of glycosylation or lactosylation, and this effect was stronger for lactosylation than glycosylation. In the stationary phase, increasing glycosylation progressively decreased fibril yield (i.e. f_{max}), whereas even a small amount of lactosylation dramatically reduced yield. Lactose is approximately twice the size of glucose, and the stronger impact of lactose on growth kinetics and yield indicate that the effects of glycation on self-assembly are related to the size of the sugar residue.

Steric hindrance from bound sugar residues is thought to inhibit whey protein aggregation at pH 7 (Liu et al., 2013b; Mulsow et al., 2009) and it is likely that glycation inhibited self-assembly of peptides at pH 2 by a similar mechanism. The spacing between adjacent β -strands in an amyloid fibril is in the order of 4.87 Å (Nelson et al., 2005). The hydrodynamic diameters of glucose and lactose molecules in solution are 7 Å and 9 Å respectively (Rao et al., 2012), so these adducts would certainly disrupt β -strand packing, and thereby inhibit fibril assembly. In addition, the hydrophilic –OH side groups of sugar residues may interfere with hydrophobic

interactions between fibril-forming peptides, which contain many hydrophobic residues (Akkermans et al., 2008b; Hettiarachchi et al., 2012). Thus, glycation appears to reduce or abolish the ability of peptides to self-assemble, and glycated peptides may undergo further hydrolysis and/or may self-assemble into non-fibril aggregates, reducing the potential yield of fibrils. The schematic showing this hypothesis is shown in Figure 6.17.

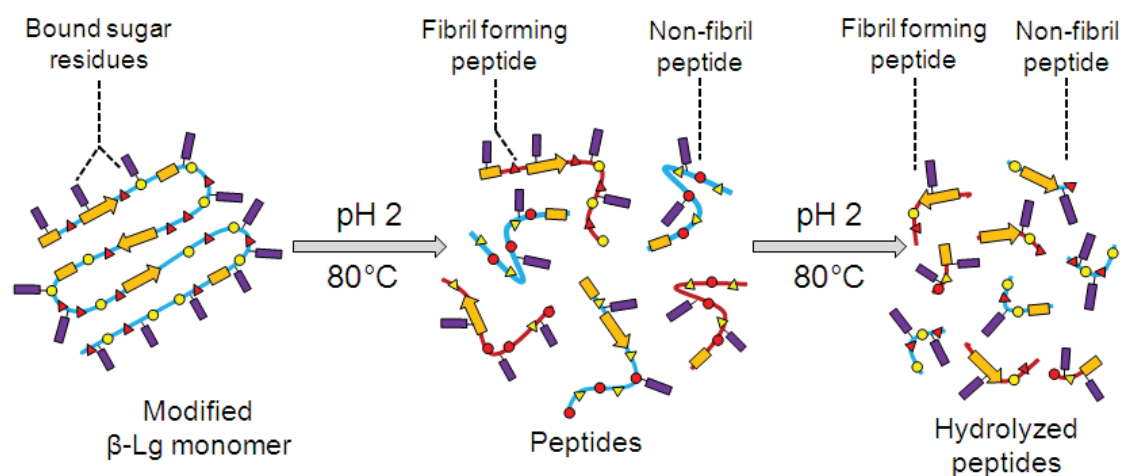


Figure 6.17 Proposed mechanism of inhibition of self-assembly of glycated β -Lg by the steric effect of the sugar adduct.

It may be questioned why fibril growth was sensitive to low levels of glycation, whereas nucleation was affected only with high levels of glycation. The answer lies in considering that the susceptibility of lysine residues to glycation varies from site to site. At shorter glycation times, lysines 47, 91 and 100 are preferentially glycated (Fogliano et al., 1998; Morgan et al., 1998; Morgan et al., 1999b). With an average of three bound sugar residues in LowGlu β -Lg and LowLac β -Lg (Figures 6.3 (A) and 6.4 (C)) it is likely that these lysine residues were glycated. More extensive glycation in HighGlu and HighLac would also affect amine groups in the N-terminal region (Lys8 and Lys14, and the N-terminal amine). It may be hypothesized that the N-terminal region, containing these late-glycating lysines, is the main region

Chapter 6. Effect of Glycation on Self-Assembly

involved in nucleation, whereas regions containing lysines that are preferentially glycosylated first are involved mainly in fibril growth.

This work has shown that even heavily glucosylated or lactosylated β -Lg retains the secondary and tertiary structures of native unglycosylated β -Lg. However, the steric constraints introduced by glycation substantially inhibit the self-assembly of glycosylated β -Lg fragments into fibrils, the effect being greater for the larger lactose moiety, even though the extent of lactosylation was lower than that of glucosylation. The inhibitory effect of glycation may be influenced by the location of glycosylated residues, which is related to the varying glycation susceptibility of different lysine residues in natively-folded protein.

Chapter 7

7. Modulating β -Lg self-assembly using polyols glycerol and sorbitol

The contents of this chapter have been published in a peer-reviewed journal article and adapted with permission from:

Dave, A. C., Loveday, S. M., Anema, S. G., Jameson, G. B., & Singh, H. (2014). Modulating β -lactoglobulin self-assembly into nanofibrils at pH 2 using polyols. *Biomacromolecules*, 15(1), 95-103. Copyright (2014) American Chemical Society.

7.1. Abstract

β -Lactoglobulin (β -Lg) forms fibrils when heated at 80 °C, pH 2 and low ionic strength (<0.015 mM). When formed at protein concentrations <3%, these fibrils are made up of peptides produced from the acid hydrolysis of the β -Lg monomer. The present study investigated the effects of the polyhydroxy alcohols (polyols) glycerol and sorbitol (0-50 % w/v) on β -Lg self-assembly at pH 2. Glycerol and sorbitol stabilize native protein structure and modulate protein functionality by preferential exclusion. In this study, both polyols decreased the rate of β -Lg self-assembly, but had no effect on the morphology of fibrils. The mechanism of these effects was studied using circular dichroism spectroscopy and SDS-PAGE. Sorbitol inhibited self-assembly by stabilizing β -Lg against unfolding and hydrolysis, resulting in fewer fibrillogenic species, whereas glycerol inhibited nucleation without inhibiting hydrolysis. Both polyols increased the viscosity of the solutions, but viscosity

Chapter 7. Effect of Polyols on β -Lg Self-Assembly

appeared to have little effect on fibril assembly, and the results from this study indicate that self-assembly was not diffusion-limited under these conditions. This is in agreement with previous reports for other proteins assembling under different conditions. The phenomenon of peptide self-assembly can be decoupled from protein hydrolysis using glycerol.

7.2. Introduction

This chapter explores the possibility of decoupling hydrolysis from fibril self-assembly by manipulating the composition of the aqueous solution using polyols. Polyhydroxy alcohols (polyols) have traditionally been used to stabilize native protein structures against chemical (Gerlsma, 1968; Tiwari et al., 2006) and thermal unfolding (Baier et al., 2003; Gekko et al., 1981b; Xie et al., 1997a). By stabilizing the protein structure, polyols can preserve enzyme activity (Tiwari et al., 2006) and modulate protein functionality (Chanasattru et al., 2007a; Dierckx et al., 2002). They can increase the strength of protein-protein interactions (McClements, 2002; Timasheff, 1993, 1998) and thereby increase the strength of heat-induced gels (Baier et al., 2004; Baier et al., 2003; Chanasattru et al., 2007a). The stabilizing effect of polyols increases with an increase in the number of hydroxyl groups (Gerlsma, 1968; Politi et al., 2010; Romero et al., 2007; Tiwari et al., 2006), and with a decrease in pH (Singh et al., 2011) and temperature (Xie et al., 1997b).

Protein stabilization by polyols can be explained by preferential exclusion of polyols from the surface of the protein, leading to an excess of water molecules in the immediate vicinity of the surface. This preferential exclusion has two main elements: a non-specific steric exclusion that results from polyol molecules being larger than water molecules, and a second effect related to the strong affinity of polyols for hydrogen-bonded water molecule networks, a moderate affinity for protein polar groups and a strong phobia towards protein nonpolar groups (McClements, 2002; Timasheff, 1998). The net result of the second effect is the enhancement of hydrophobic interactions (Kamiyama et al., 1999; Timasheff, 1998). Other effects contributing to preferential exclusion are related to how polyols influence the surface

Chapter 7. Effects of Polyols on Self-Assembly

tension at the protein-solvent interface, but these are very complex and somewhat controversial (Chanasattru et al., 2007b; Kaushik et al., 1998; Kita et al., 1994).

Denaturation of a globular protein leads to an increase in solvent-exposed surface area, and especially the exposure of non-polar groups that are buried in the interior of the native structure (Damodaran, 1996). Interaction of water molecules with non-polar residues is entropically unfavorable, so unfolding carries a free-energy cost. This cost of unfolding is raised by polyols because of their preferential exclusion from the protein surface; hence denaturation is inhibited (Timasheff, 1998). At higher concentrations, polyols can exert an influence on diffusion-limited reactions, such as protein aggregation *via* an increase in viscosity (Kulmyrzaev et al., 2000b).

In this study, glycerol ($\text{CH}_2\text{OHCHOHCH}_2\text{OH}$) and sorbitol ($\text{CH}_2\text{OH}(\text{CHOH})_4\text{CH}_2\text{OH}$) were chosen as compounds to perturb the self-assembly process. Both are preferentially excluded from the β -Lg surface (Gekko et al., 1981a; Timasheff, 1998), but to a different extent. At neutral pH, sorbitol increases the thermal denaturation temperature of β -Lg more than glycerol does, which is attributed to sorbitol being larger than glycerol (Chanasattru et al., 2008; Tiwari et al., 2006), and to the weaker differential interaction effects for glycerol (Baier et al., 2004; Chanasattru et al., 2008). Glycerol may be able to partly penetrate into the solvation layer surrounding the proteins, especially at higher concentrations because of its relatively small size and slightly amphiphilic character (Chanasattru et al., 2008; Gekko et al., 1981a, 1981b; Timasheff, 1998; Vagenende et al., 2009).

Several studies have probed the effects of glycerol and/or sorbitol on fibril self-assembly with proteins other than β -Lg. The effect of polyols varies with the type of protein and the stage of self-assembly. Glycerol stabilized the native structure of

insulin, and thereby delayed nucleation for this protein (Grudzielanek et al., 2005). Both glycerol and sorbitol had similar effects on a synthetic β -hairpin peptide MET16, but they also increased the final yield of fibrils (Sukenik et al., 2012; Sukenik et al., 2011). For amyloid- β peptide, glycerol accelerates the transition from random coil to β -sheet-rich structure, thereby stimulating fibril formation (Yang et al., 1999).

The present study is the first to investigate β -Lg self-assembly in presence of glycerol and sorbitol. During self-assembly, the polyols may stabilize the native β -Lg against unfolding and inhibit self-assembly, once β -Lg monomers unfold, they may promote their self-assembly by volume exclusion effects or stabilize unfolded monomers. In addition, the high solution viscosities of the solutions containing polyols may have a profound effect on kinetics of self-assembly by limiting the rates of diffusion. The aim of this study is to investigate how self-assembly is perturbed by sorbitol and glycerol, and thereby, to understand the interactions involved in nucleation during self-assembly. The effects of polyols on the fibril morphology have also been investigated.

7.3. Materials and Methods

All chemicals used in this study have been described in Chapter 3. Unless otherwise stated, all reagents were prepared in Milli Q water. β -Lg used in the study was extracted using the protocol described in Section 3.3.1 of Chapter 3. For self-assembly studies, the samples were prepared as per protocol described below in Section 7.3.1. The method for Thioflavin T (ThT) assay, SDS-PAGE, circular dichroism (CD) spectroscopy, and TEM have been described in Section 3.3 of Chapter 3.

7.3.1. Preparation of fibrils

β -Lg solutions were prepared using a method described previously (Section 3.3.2, Chapter 3). A fixed volume of a β -Lg stock solution (pH 2), was mixed with water and/or different amounts of glycerol and sorbitol to obtain the desired protein and polyol concentrations (10-50% w/v). The final β -Lg concentration in all samples was 1% (w/v). The protein concentration of the control was determined by spectrophotometry using an extinction coefficient of 0.94 cm²/mg (Swaisgood, 1982a). After adjusting the pH of samples to 2.00 \pm 0.02 using 6 M HCl, the samples were stirred at room temperature for 1 h. 1 mL of sample was transferred into 1.5 mL polypropylene tubes and heated in a temperature-controlled water bath maintained at 80.0 \pm 0.2 °C. Samples were drawn at different times and quenched by rapid cooling in an ice bath and were analyzed by ThT assay. The samples intended for imaging by TEM were stored at 4 °C and analyzed within 7 days, while those intended for SDS-PAGE were frozen at -18 °C.

7.3.2. Effect of polyols on ThT assay

To determine the effect of glycerol and sorbitol on the detection of fibrils by the ThT assay a 1% (w/v) β -Lg sample without glycerol or sorbitol was heated at 80 °C for 12 h. The heated sample was diluted 1:1 (w/w, assuming the density of heated β -Lg solution as 1) with either water or different levels of polyols. The final polyol concentration in the samples was same as those used for self-assembly studies. A total of two samples were prepared for each of the polyols concentration. All samples were then analyzed by the ThT assay.

7.4. Results

7.4.1. Effect of polyols on the rate of β -Lg self-assembly

The ThT assay showed that self-assembly followed a sigmoidal pattern, even with increasing amounts of glycerol and sorbitol (Figure 7.1). The results were fitted well by Equation 3.1, and polyol effects were confirmed by a highly significant result ($P < 0.0005$) in the likelihood ratio test. Kinetic parameters from Equations 3.1 to 3.3 are shown in Table 7.1. The presence of polyols did not affect the binding of the ThT dye to fibrils at all concentration used (Figure 7.2).

Both polyols progressively increased t_{lag} and decreased $(df/dt)_{\text{max}}$ and f_{max} , especially above 10% w/v. However in the range 10-30% w/v, sorbitol affected t_{lag} more strongly, whereas the effects on $(df/dt)_{\text{max}}$ and $t_{1/2 \text{ max}}$ were stronger for glycerol. The polyol solutions without β -Lg, heated at 80 °C for 24 h, did not show any fluorescence when analyzed by the ThT assay (results not shown).

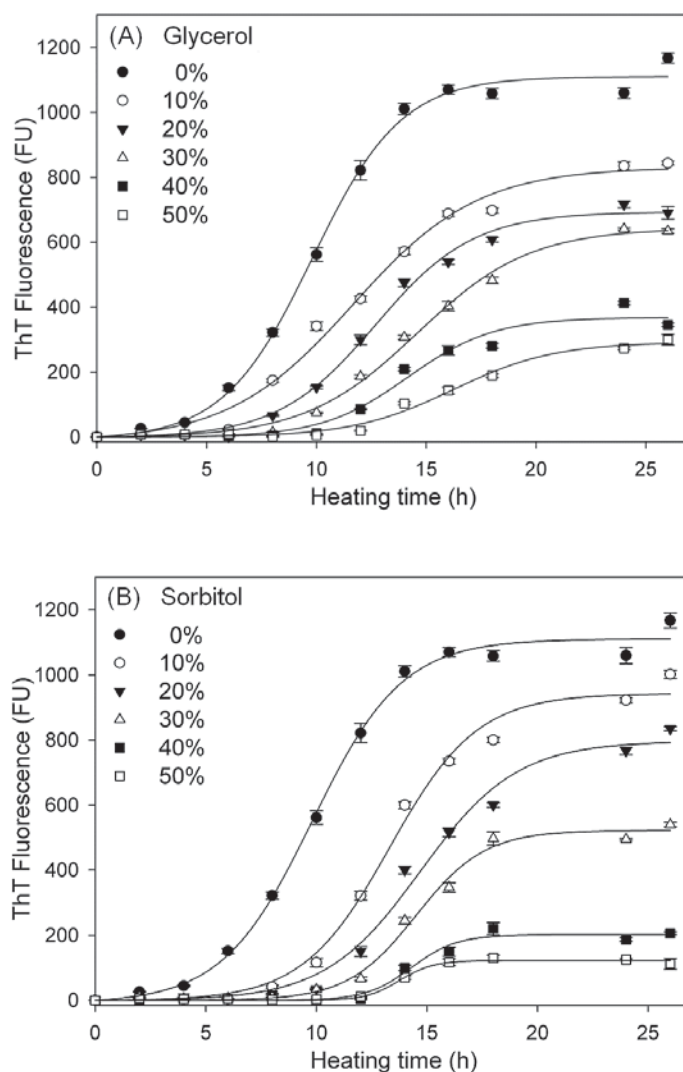


Figure 7.1 Thioflavin T (ThT) fluorescence intensity at 486 nm for β -Lg (1%, w/v) heated at 80 °C and pH 2 in presence of different levels (% w/v) of (A) glycerol and (B) sorbitol. Solid lines indicate the fit using Equation 3.1. Error bars represent the standard errors of measurements from two separate experiments with three replicates in each.

Chapter 7. Effects of Polyols on Self-Assembly

Table 7.1 Kinetic parameters from Equation (3.2-3.4) showing effect of glycerol and sorbitol on β -Lg self-assembly.

Polyol concentration (% w/v)	t_{lag} (h)	$(df/dt)_{max}$ (FU/h)	$t_{1/2 max}$ (h)	f_{max} (FU)	Adjusted R^2 (-)	$S_{y x}^a$ (-)
0	6.2 (0.3)	125.4 ± 9.0	10.6 (0.2)	1110.1 (17.2)	0.9959	30.3
Glycerol						
10	6.3 (0.6)	72.0 (7.0)	12.1 (0.4)	831.0 (28.0)	0.9888	35.7
20	8.7 (0.4)	76.0 (5.3)	13.5 (0.2)	693.0 (15.0)	0.9947	21.2
30	9.6 (0.4)	62.0 (4.4)	15.0 (0.3)	643.0 (16.0)	0.9944	18.9
40	10.0 (0.6)	48.0 (8.1)	14.0 (0.5)	368.0 (19.0)	0.9706	26.8
50	11.4 (0.5)	32.1 (4.0)	16.0 (0.3)	292.0 (12.0)	0.9851	13.7

Chapter 7. Effect of polyols on β -lg self-assembly

Sorbitol						
10	9.9 (0.4)	111.3 (11)	14.1 (0.3)	942.5 (25.0)	0.9918	36.4
20	10.2 (0.6)	95.2 (10)	14.3 (0.3)	796.0 (28.0)	0.9868	37.4
30	11.7 (0.2)	81.8 (9.0)	14.8 (0.3)	522.0 (14.0)	0.9913	20.7
40	12.2 (0.5)	49.0 (10.0)	14.3 (0.2)	202.0 (8.3)	0.9790	13.4
50	12.2 (0.3)	39.8 (7.0)	13.8 (0.2)	123.0 (3.0)	0.9918	5.1

Numbers in parenthesis indicate standard deviations. *a*: Standard error of the regression, numbers in parenthesis indicate standard deviations.

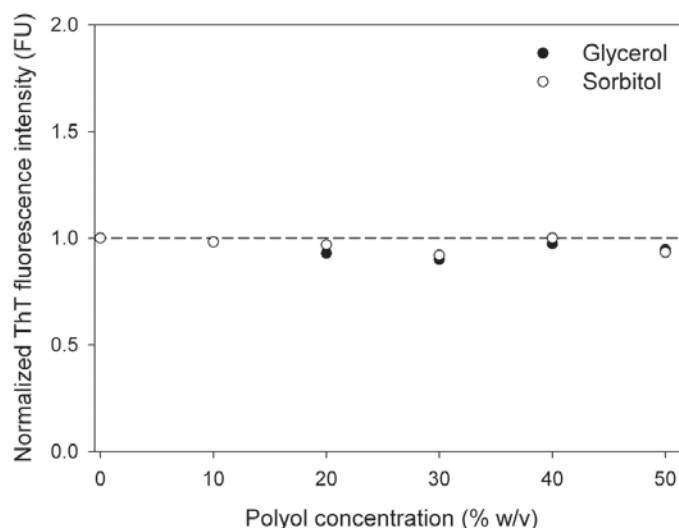


Figure 7.2 Normalized ThT fluorescence intensities β -Lg sample containing fibrils diluted using different levels of polyols (0-50% w/v, used for self-assembly studies). The ThT fluorescence intensity in the undiluted sample was 920 fluorescence units. The intensity of the sample diluted using water (pH 2) was used for normalization. A value close to 1 indicates that the fluorescence intensity in samples diluted with water or polyols were similar.

7.4.2. Effects of polyols on pre- self-assembly processes

7.4.2.1. Heat-induced acid hydrolysis

The effects of glycerol and sorbitol on β -Lg hydrolysis were investigated by analyzing the heated samples using reduced SDS-PAGE (Figure 7.3). All heated samples showed a monomer band at about 18 kDa and several additional lower molecular weight bands with masses between 17 kDa and 3.5 kDa. The pattern of these peptide bands in samples with polyols was similar to the pattern observed in the control sample, but the amount of each peptide varied with polyol concentration and heating time. The PAGE gels did not show any stained material in the stacking gel, indicating that high molecular weight aggregates were not present, and pointing to complete disruption of fibrils in the PAGE sample buffer. Glycerol had a small but

Chapter 7. Effects of Polyols on Self-Assembly

statistically significant ($P < 0.001$, likelihood ratio test) effect on hydrolysis while sorbitol slowed hydrolysis at all concentrations. At 50% sorbitol, virtually all the β -Lg monomer was still intact after 12 h.

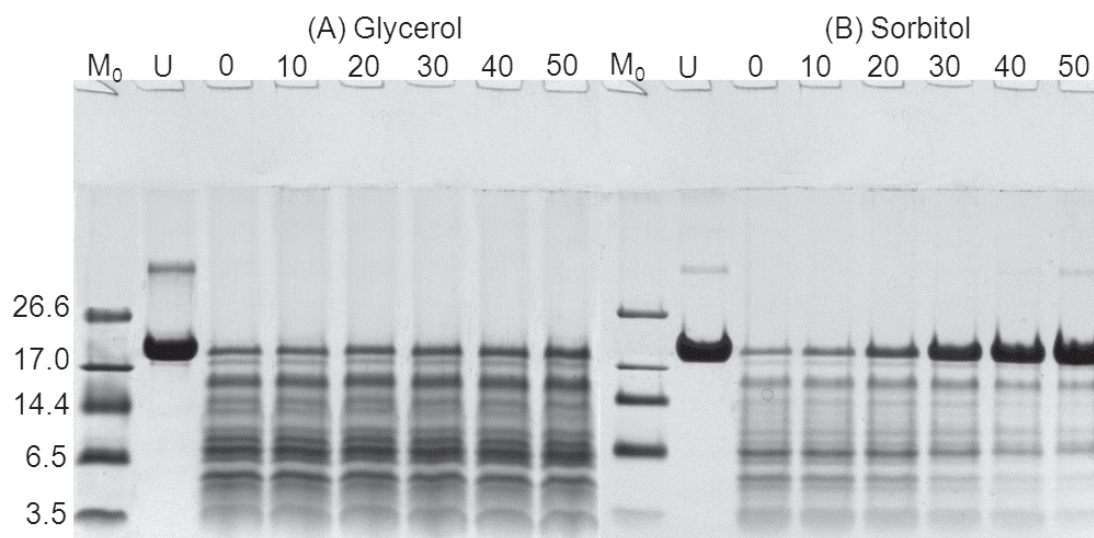


Figure 7.3 Reduced SDS-PAGE of samples heated at 80 °C for 12 h in the presence of different concentrations of (A) glycerol or (B) sorbitol. (M_0) Molecular weight marker in kDa; (U) unheated sample. Numbers above the lanes indicate polyol concentrations (% w/v).

The β -Lg monomer band intensities were quantified by densitometry and normalized (Figure 7.4) to the values for the control experiments (no glycerol or sorbitol). The data were fitted using Equation 3.8, and fit parameters are given in Table 7.2. Both glycerol and sorbitol reduced the rate of β -Lg monomer hydrolysis, but the effect was much larger with sorbitol. An increase in glycerol concentration from 10 to 30% (w/v) resulted in a small decrease in the rate of hydrolysis, but the effect was more pronounced at 40 and 50% (w/v) glycerol. Sorbitol, however, strongly stabilized β -Lg against hydrolysis at concentrations of 20% or more. The kinetic parameters of hydrolysis (SDS-PAGE) and fibril growth (ThT assay) are combined in Figure 7.5.

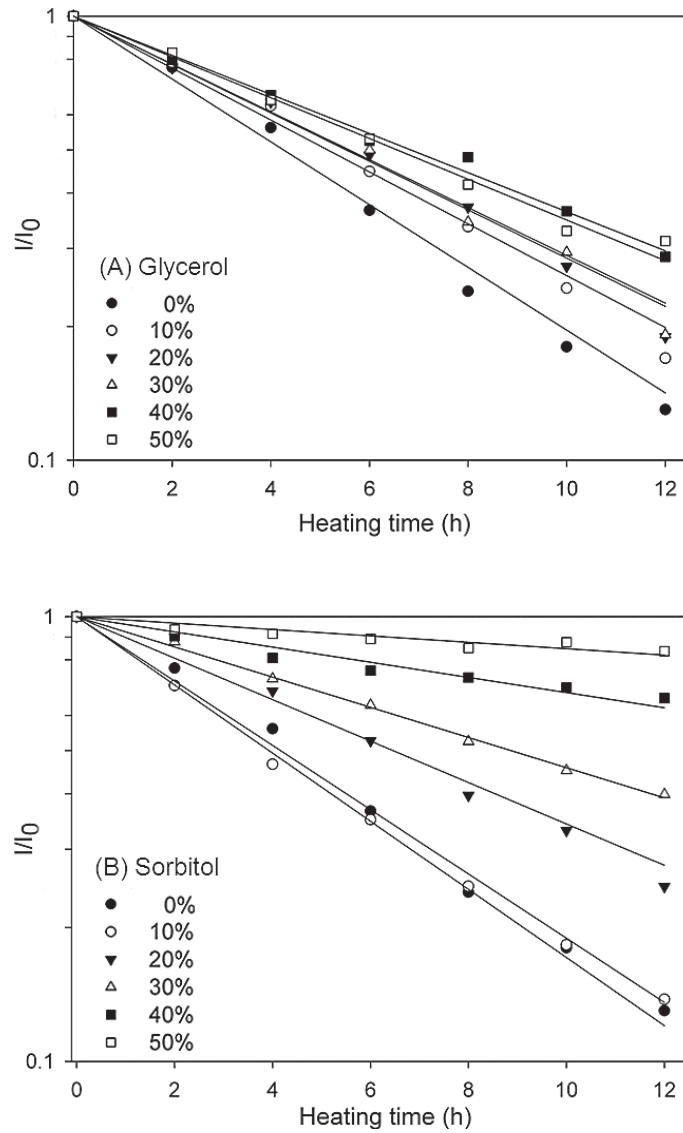


Figure 7.4 Normalized β -Lg band intensities from SDS-PAGE gels of samples containing different concentrations of (A) glycerol and (B) sorbitol. Values are the average of two independent experiments. Solid lines indicate fit to Equation 3.8.

Table 7.2 Fit parameters from Equation 3.8 describing the kinetics of acid hydrolysis of β -Lg during heating under fibril forming conditions.

Polyol concentration (% w/v)	k_h ($\text{min}^{-1} \times 10^{-3}$)	Adjusted R^2	$S_{y x}^a$ ($\times 10^{-3}$)
0	2.71 (0.10)	0.9921	0.50
Glycerol			
10	2.25 (0.07)	0.9939	0.39
20	2.10 (0.06)	0.9943	0.36
30	2.10 (0.07)	0.9923	0.42
40	1.70 (0.04)	0.9942	0.31
50	1.76 (0.04)	0.9955	0.30
Sorbitol			
10	2.95 (0.05)	0.9979	0.25
20	1.78 (0.08)	0.9779	0.71
30	1.30 (0.01)	0.9972	0.20
40	0.65 (0.03)	0.9437	0.50
50	0.28 (0.01)	0.8205	0.40

Numbers in parenthesis indicate standard deviations. a : Standard error of the regression

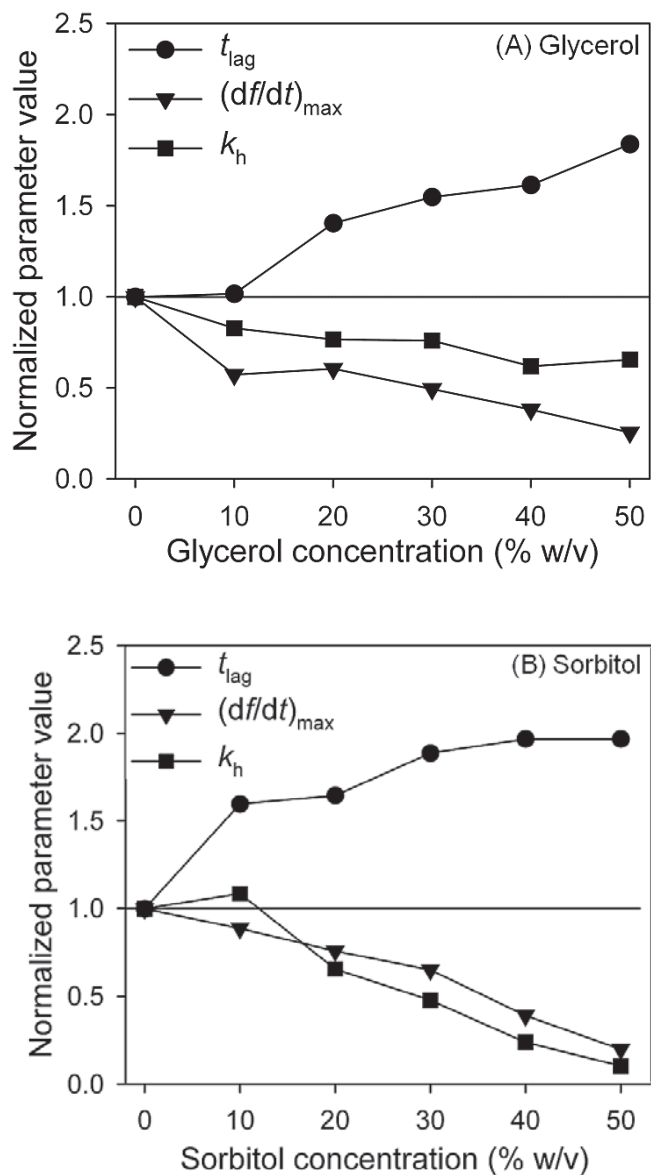


Figure 7.5 Effect of glycerol (A) and sorbitol (B) on the normalized kinetic parameters of hydrolysis and self-assembly.

7.4.2.2. Unfolding behavior of β -Lg in presence of polyols

Effects of glycerol and sorbitol on the structure of native β -Lg and its unfolding behavior were studied using CD spectroscopy. Solutions of β -Lg with or without polyols were heated to 80 °C *in situ* in the sample holder. It took 5 minutes to raise the temperature from 20 °C to 80 °C, and the time at which the temperature reached 80 °C was designated '0 min'. From then on, spectra were recorded continuously.

Spectra of unheated β -Lg indicated that polyols had no effect on the native tertiary structure at pH 2 (Figure 7.6, A and B). All samples containing glycerol showed a rapid loss of ellipticity at 293 and 286 nm once they reached 80 °C, indicating loss of tertiary structure within the first few minutes of heating. Samples with 10% sorbitol showed a similar but slower loss of ellipticity. However, sorbitol concentrations of $\geq 20\%$ strongly retarded the loss of ellipticity and, hence, of the tertiary structure. Figures 7.7 (A) and (B) show examples of spectra collected sequentially during heating at 80°C with 30% glycerol or sorbitol. To compare the effects of glycerol and sorbitol on unfolding of β -Lg tertiary structure, the relative loss of ellipticities, represented by $(\Delta[\theta]_t/\Delta[\theta]_0)_{293}$, was calculated using Equation 3.13 and plotted against time (Figure 7.8). A comparison of ellipticities at 293 nm after 10 minutes at 80°C in the samples is shown in Figure 7.9.

Glycerol slightly accelerated unfolding at 80°C, and its effect was independent of the concentration: within 10 min, less than 20% of the original ellipticity remained. In contrast, 20-50% w/v sorbitol markedly retarded the loss of ellipticity in a concentration-dependent manner. In this concentration range, ellipticity attained steady state within 30 min at a level that ranged from 40% to 90% of the original ellipticity, depending on sorbitol concentration. The attainment of steady state is a strong indication that the stabilizing effects of sorbitol are likely to persist on a time

scale of hours, and therefore to impinge on hydrolysis and assembly processes. However, polyol effects at > 60 min are difficult to confirm with *in situ* spectrometry at 80°C, which becomes problematic with longer heating times due to unknown signal contributions from peptides, and potentially significant moisture losses from the cuvette.

In the far-UV region, the secondary structure of native β -Lg at 20 °C produced a wide trough with a minimum at 217 nm (Figure 7.6) Heating β -Lg with glycerol at 80 °C and pH 2 deepened the trough at 222 nm and shifted the minimum towards lower wavelengths. These changes in the secondary structure were similar to those for β -Lg heated without polyols (Chapter 4). Figure 7.7 (C) and (D) show examples of FUV spectra of β -Lg heated with 30% glycerol or sorbitol respectively. Glycerol had little effect on the heat-induced changes in the FUV spectrum. Sorbitol inhibited the structural changes seen in the FUV region, and the effect was dependent on the concentration. The spectra below 205 nm were difficult to interpret due to the high absorbance and hence quantification of changes in secondary structure was not possible. The high tension curves for the FUV scans of β -Lg shown in Figure 7.7 (C) and (D) are shown in Figure 7.10.

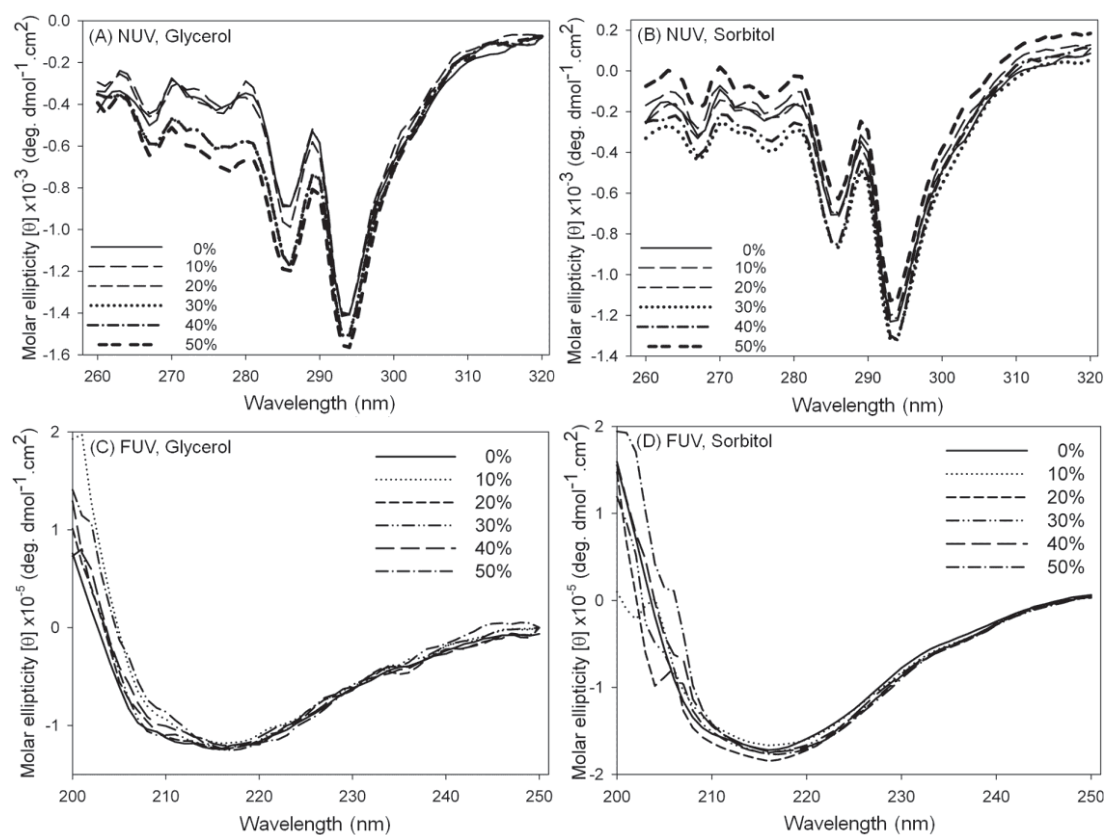


Figure 7.6 CD spectra of β -Lg at 20 °C in presence of different levels of (A) and (C) glycerol and (B) and (D) sorbitol. For the NUV scans (A) and (B), the concentration of β -Lg was 1 mg/mL, while that for FUV spectra (C) and (D) was 0.01mg/mL. The sample scans were corrected by subtracting the baseline scans and smoothed.

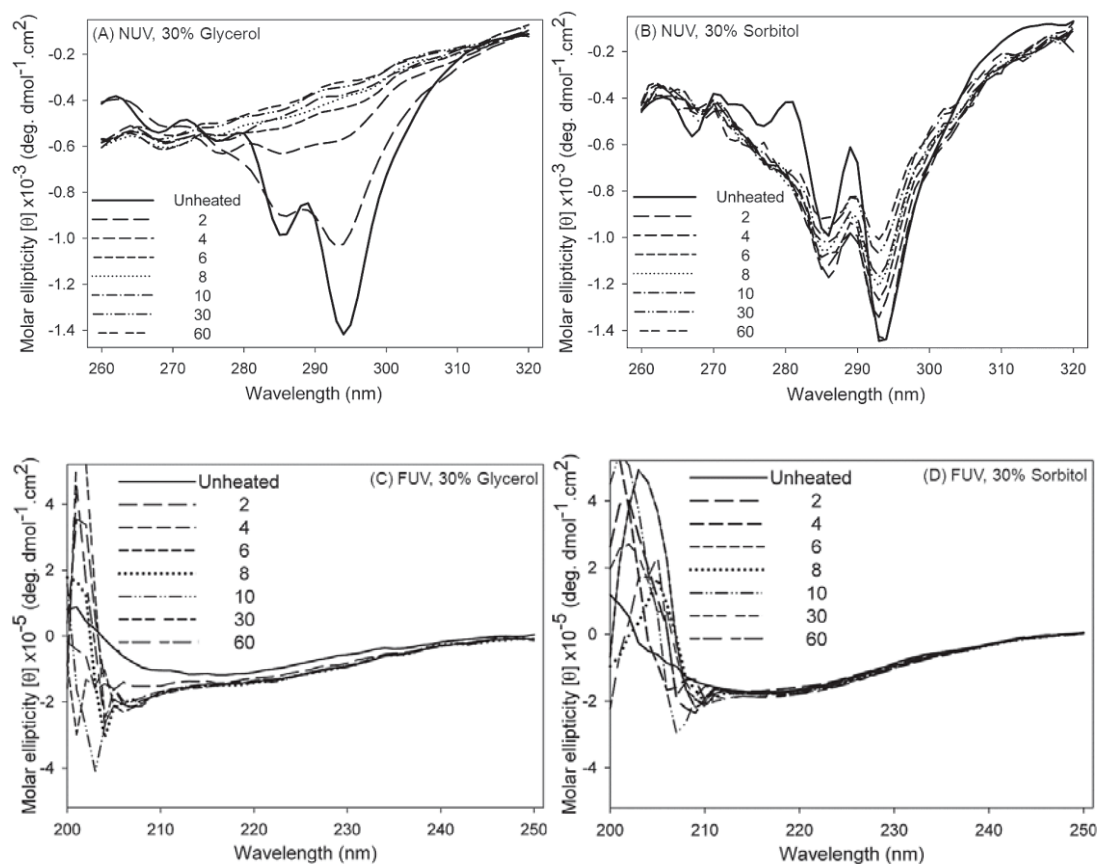


Figure 7.7 NUV (A, B) or FUV (C,D) circular dichroism spectra of β -Lg during heating at 80 °C and pH 2 with 30% glycerol (A,C) or 30% sorbitol (B,D). Numbers indicate the heating time in minutes.

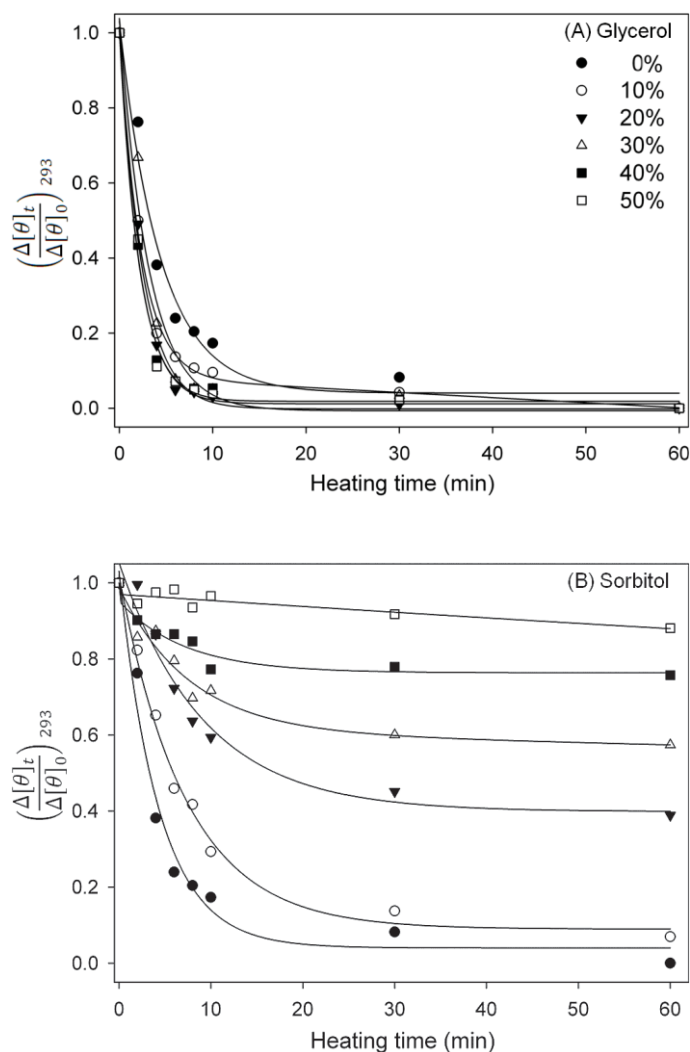


Figure 7.8 Relative loss of ellipticity at 293 nm in β -Lg solutions during heating at 80 °C with 0-50% glycerol (A) or sorbitol (B) calculated from Equations 3.13 and 3.14. For details of the notations of Y axis see Section 3.3.6.3 in Chapter 3. The same symbols representing glycerol concentrations in (A) apply for sorbitol concentrations in (B). Solid lines are a visual guide only.

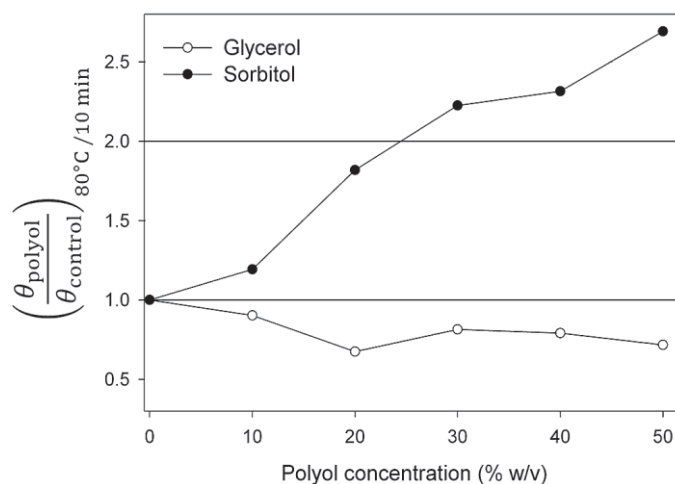


Figure 7.9 Normalized ellipticities in the samples at 293 nm at the end of 10 minutes at 80 °C. Absolute ellipticities in the samples with different levels of polyols (θ_{polyol}) were normalized by the ellipticity of the control sample without any polyols ($\theta_{control}$). Values >1 indicates a higher residual signal in the sample and hence the stabilized state of β -Lg. Solid lines are a visual guide.

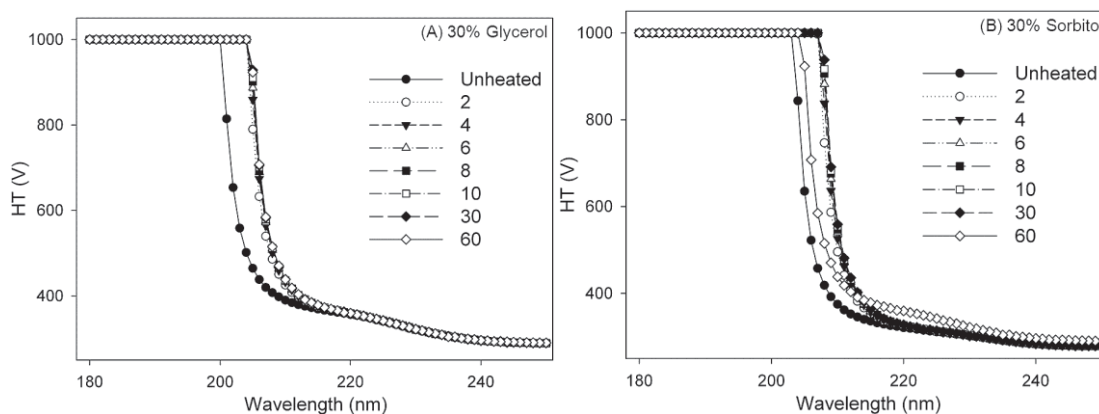


Figure 7.10 High tension curves for FUV scans of β -Lg in presence of 30% w/v of (A) glycerol and (B) sorbitol during heating at 80 °C. The data in A and B represent the high tension (HT) values for the same scans shown in Figure 7.7 C and D. Solid lines are a guide and are not fitted with any mathematical model.

7.4.3. Morphology of fibrils in presence of glycerol and sorbitol

The effect of glycerol and sorbitol on the morphology of β -Lg fibrils was investigated by TEM (Figure 7.11). Fibrils formed in the presence of glycerol and sorbitol appeared straight and un-branched with uniform width. They varied in length, but were generally slightly shorter than fibrils from the control β -Lg. A similar effect of sorbitol has been reported for MET16 peptide fibrils (Sukenik et al., 2011). The TEM images of fibrils formed in the presence of 50% (w/v) glycerol and sorbitol is shown in Figure 7.12. The images of these samples showed fewer fibrils than those of samples with lower polyol concentrations. In some cases, small round structures were present in the TEM images, as seen previously (Hettiarachchi et al., 2012; Loveday et al., 2012c; Oboroceanu et al., 2010). Oboroceanu et al. (2010) suggested that these aggregates consist of disordered non-fibril peptides. The proportion of these aggregates decreased markedly in the sample containing 50% sorbitol (Figure 7.12).

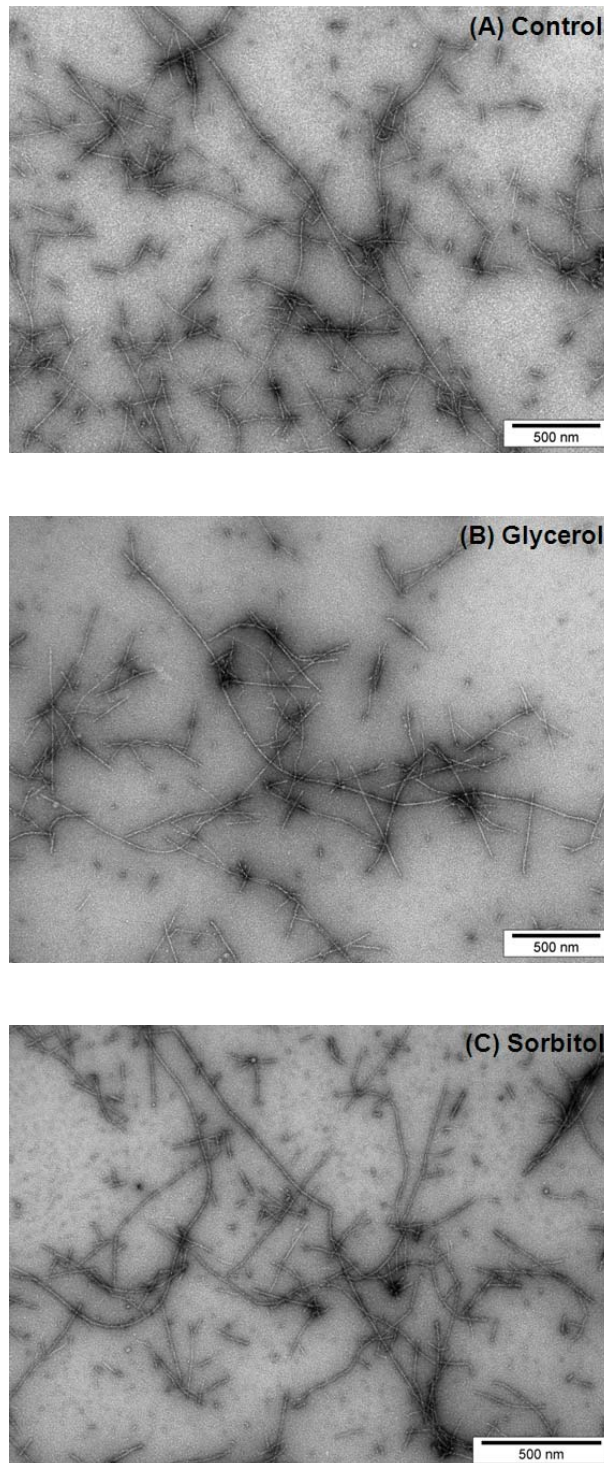


Figure 7.11 Transmission electron microscopy images of β -Lg fibrils separated from heated solutions. (A) Without any polyol; (B) With 20% glycerol; and (C) With 20% sorbitol. Samples heated at 80 °C, pH 2 and 24 h.

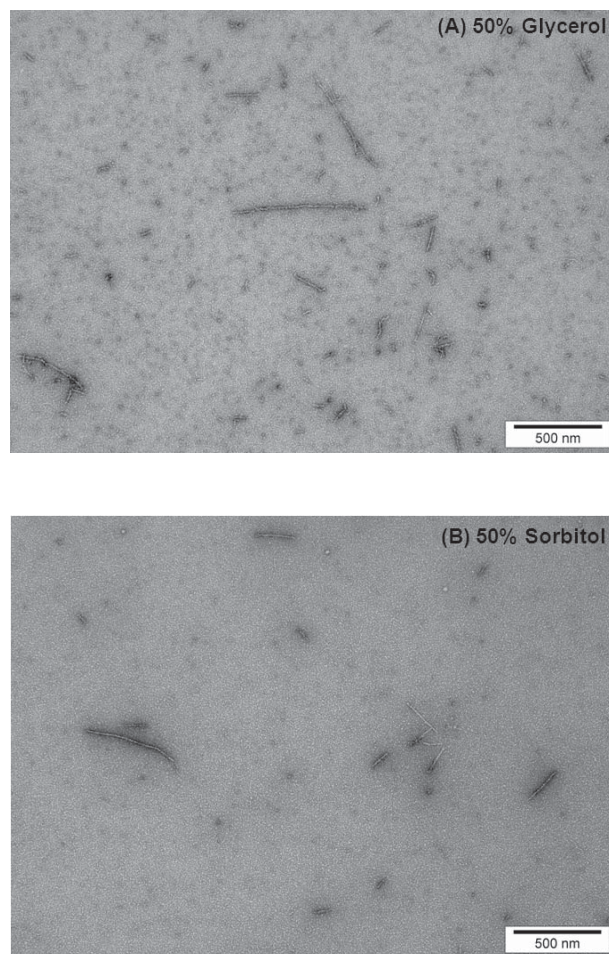


Figure 7.12 Transmission electron microscopy images of β -Lg fibrils separated from β -Lg samples heated at 80 °C, pH 2 and 24 h in the presence of (A) 50% (w/v) glycerol and (B) 50% (w/v) sorbitol at 80 °C, pH 2 and 24 h.

7.5. Discussion

During β -Lg self-assembly, nucleation can be divided into three different stages: 1) monomer unfolding, 2) monomer hydrolysis, and 3) nuclei formation by peptide self-assembly. Secondary or ‘heterogeneous’ nucleation occurs when fibrils rupture, producing two new growth sites with each breakage. The lag phase can be completely abolished with rapid stirring, which has been tentatively attributed to the promotion of secondary nucleation (Dunstan et al., 2009; Hill et al., 2006). In order to investigate the interactions occurring in the lag phase, and to minimize secondary nucleation, the samples were not stirred during heating. Another reason for not stirring was to improve comparability with other studies, since magnetic stir bars induce highly non-uniform shear fields that depend on rotation rate and stirring vessel dimensions, and the nature of the shear field affects fibril assembly and growth pathways (Dunstan et al., 2009).

The data from CD studies at pH 2 (Figures 7.6 to 7.9) indicate that glycerol slightly increased the rate of thermal unfolding, whereas sorbitol strongly stabilized β -Lg against unfolding. This observation is in agreement with previous studies at neutral pH (Baier et al., 2004; Baier et al., 2003; Chanasattru et al., 2007a). The lack of a stabilizing effect with glycerol is attributed to its smaller size and slightly amphiphilic character, resulting in a weaker preferential exclusion of glycerol from the β -Lg surface, than that of sorbitol (Chanasattru et al., 2008).

The effect of polyols on hydrolysis followed a similar trend. Within the timescales used in this study, sorbitol inhibited hydrolysis more effectively than glycerol (Figures 7.3 and 7.4, and Table 7.2), which may be related to different effects of these polyols on unfolding. Unfolding of monomers would promote hydrolysis by

Chapter 7. Effects of Polyols on Self-Assembly

exposing sites of cleavage to the solvent and increasing the likelihood of cleavage. Thus, stabilization of the native structure by sorbitol would reduce the rate of monomer hydrolysis, resulting in fewer fibril-forming peptides and thereby slowing down self-assembly. In contrast, glycerol slightly accelerated monomer unfolding during the first hour of heating, but this did not translate into accelerated hydrolysis. The amount of peptides capable of forming nuclei was therefore unchanged, as confirmed with SDS-PAGE. However, glycerol still delayed the onset of self-assembly, i.e. it extended the lag phase. The contrasting effects of glycerol and sorbitol on fibril formation process are illustrated schematically in Figure 7.13.

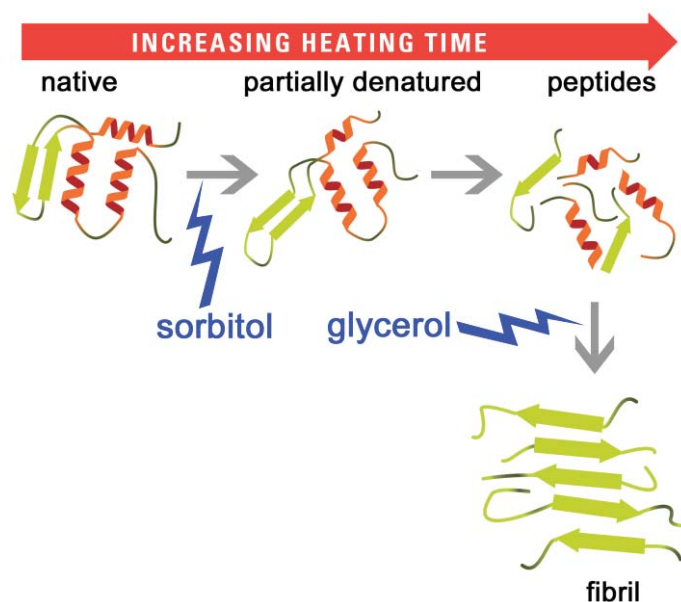


Figure 7.13 Schematic illustration of how β -Lg fibril assembly is affected by sorbitol (slowing unfolding) and glycerol (slowing assembly of peptides).

It is tempting to conclude that glycerol inhibited nucleation by slowing the diffusion and/or alignment of fibril building blocks due to a combination of viscosity enhancement and preferential interactions. Such phenomena would be expected to also inhibit fibril growth, which occurs by a similar process. However the concentration-dependence of glycerol effects on t_{lag} was different from the pattern

with $(df/dt)_{\max}$: for t_{lag} there was no change when 10% glycerol was added and then a steady increase occurred at higher concentrations, whereas $(df/dt)_{\max}$ dropped sharply with 10% glycerol and plateaued at 10-30% then decreased with 40 and 50% glycerol. The effect of glycerol on fibril growth was clearly different from that on nucleation.

The viscosity of solutions increased more rapidly on adding sorbitol than that with same amount of glycerol addition on a % w/v basis, and 50% w/v sorbitol produced a 5-fold increase in viscosity at 80 °C (Figure 7.14). Figure 7.15 shows the kinetic parameters of self-assembly in Figure 7.5 plotted as a function of viscosity at different polyol concentrations. Sorbitol strongly decreased $(df/dt)_{\max}$ (Table 7.1), but the effect is at least partly attributable to a slowing of hydrolysis (Figure 7.4 and Table 7.2). In fact, for sorbitol-containing samples $(df/dt)_{\max}$ was highly correlated with k_h ($R = 0.967$, $P = 0.002$), suggesting that the influence of sorbitol was solely due to its effect on hydrolysis, and the effect of increased viscosity was negligible. A similar analysis with glycerol results was not statistically reliable because the span of $(df/dt)_{\max}$ and k_h values was too small.

These findings are consistent with recent work by Sukenik et al. (Sukenik et al., 2012; Sukenik et al., 2011) who investigated the effect of polyols on the self-assembly of a 16-residue synthetic β -hairpin peptide MET16, at pH 7 and 25 °C. They reported that t_{lag} was strongly dependent on glycerol/sorbitol concentration, whereas the elongation time (roughly equivalent to the inverse of $(df/dt)_{\max}$) had no consistent concentration-dependence for either polyol. The fact that glycerol and sorbitol had minor effects on $(df/dt)_{\max}$ for β -Lg self-assembly (once the k_h effects are accounted for) despite substantially increasing the viscosity has an important

Chapter 7. Effects of Polyols on Self-Assembly

implication: β -Lg fibril growth is not diffusion-limited under these conditions. This is consistent with previous literature, which underlines the important role of protein conformational re-arrangement in generating amyloid fibril nuclei (Dobson, 1999, 2003b; Uversky et al., 2004). Further experiments using a series of iso-viscous solutions of glycerol and sorbitol containing similar proportion of building blocks may further ascertain the mechanistic differences responsible for the effects of polyols on self-assembly.

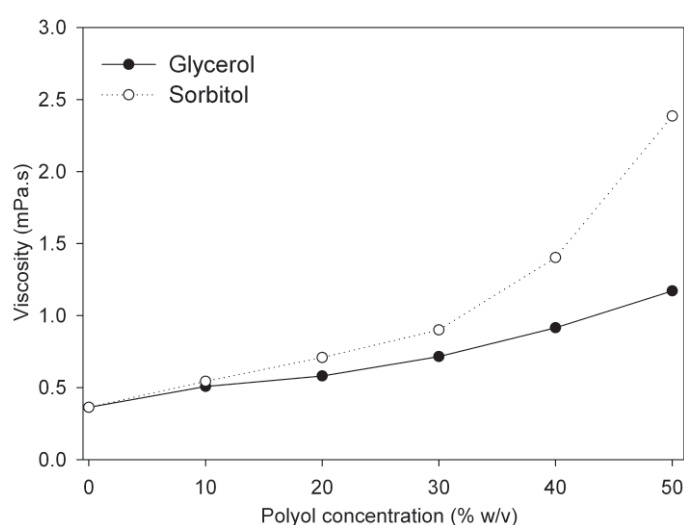


Figure 7.14 Viscosity of polyol solutions at 80 °C at a shear rate of 1 s^{-1} . Polyol solutions were made in Milli Q water without pH adjustment. Measurements were carried out on an AR-G2 rheometer (TA Instruments, New Castle, DE) using a double gap measuring system equilibrated at 80 °C for two minutes prior to measurements.

Sukenik et al. (2011) reached a similar conclusion for MET16 assembly, and subsequently showed with kinetic modeling that the rate of monomer detachment from a growing fibril was the most likely rate-limiting step, in accordance with other experimental and theoretical studies (Sukenik et al., 2012). If we conclude that self-assembly is not diffusion-limited under these conditions, then it follows that the self-

assembly promoting effects of shearing or stirring (Bolder et al., 2007a; Dunstan et al., 2009) do not stem from improved mixing or delivery of building blocks to growing sites. The most likely alternative explanation is that shearing promotes secondary (heterogenous) nucleation by fracturing growing fibrils into ‘seeds’ (Hill et al., 2006). Sufficiently high shear may facilitate the rearrangement of β -Lg oligomers into nuclei (Dunstan et al., 2009), and under some conditions shear can produce alterations to protein tertiary structure (Bekard et al., 2011). However, it is unclear whether shear-induced unfolding is a factor in studies where β -Lg was stirred at pH 2 and 80 °C, particularly since controlled shear (e.g. in a couette geometry) and variable shear (e.g. with a stir bar, which is used in most cases) give different results (Dunstan et al., 2009).

Sukenik et al. (2011) observed that sorbitol, and to a lesser extent glycerol, produced a concentration-dependent increase in the yield of fibrils, and conceived a scenario in which “osmolytes may destabilize the aggregating nucleus in favor of the monomeric state, while concurrently acting to stabilize the fibril once it is formed” (Sukenik et al., 2011). In this study, an opposite effect on fibril yield (f_{\max} in Table 7.1 and Figure 7.1) was observed for both glycerol and sorbitol. A possible explanation for this observation lies in the fact that peptides and unfolded proteins can follow alternative non-fibril reaction pathways. When nucleation is inhibited, by either sorbitol (blocking unfolding and hydrolysis) or glycerol (blocking self-assembly), the unassembled fibril building blocks could be ‘consumed’ in non-fibril oligomers and aggregates as has been suggested previously (Munishkina et al., 2008). It is likely that the fibril building blocks had alternate pathways (Loveday et al., 2012c) for aggregation in presence of polyols and the inhibitory effect of glycerol or sorbitol promoted pathways that compete with fibril assembly.

Chapter 7. Effects of Polyols on Self-Assembly

Thus, in this study, glycerol and sorbitol slowed down the early stages of β -Lg fibril self-assembly, which complements previous work on speeding up self-assembly by manipulating the ionic environment and temperature (Loveday et al., 2011b), or by microwave radiation (Hettiarachchi et al., 2012). Slowing down self-assembly with polyols indicates that self-assembly is not diffusion-limited under these conditions. This study, for the first time, demonstrated how hydrolysis can be decoupled from self-assembly using glycerol. It may be possible to isolate assembly-competent peptides using this technique and use them to explore the driving forces for fibril assembly in more detail.

Chapter 8

8. Interactions of β -Lactoglobulin and β -casein during self-assembly

8.1. Abstract

In this study, the effect of β -casein on β -lactoglobulin (β -Lg) self-assembly at 80 °C, pH 2 and low ionic strength, has been investigated. β -Casein shows chaperone-like properties and inhibits the heat-induced aggregation of β -Lg at neutral pH, but its effect on β -Lg self-assembly at low pH is not known. The SDS-PAGE analysis of samples showed that heating resulted in hydrolysis of both β -Lg and β -casein into peptides and the kinetics of heat-induced hydrolysis were similar for both proteins. The ThT assay showed that β -casein had a small but consistent effect in inhibiting β -Lg self-assembly in heated β -Lg- β -casein mixtures (molar ratios 1:0.0625 to 1:1). The TEM images of solutions showed irregular, coiled and ribbon-like structures co-existing with fibrils. The peptide-peptide interactions of β -casein and β -Lg peptides may inhibit fibril formation from β -Lg resulting in non-fibrillar aggregates and indicating an alternate pathway for β -Lg assembly-competent peptides during self-assembly.

8.2. Introduction

In the previous chapter (Chapter 7), it was found that glycerol and sorbitol inhibited self-assembly, but by different mechanisms. The data in Chapters 6 and 7 clearly demonstrate that there are multiple competing pathways for assembly-competent peptides during their aggregation or hydrolysis. Another approach to investigate self-assembly utilizing this mechanism, which has not yet been explored, is the use of molecular chaperones. An investigation of β -Lg-chaperone interactions during β -Lg fibril formation would provide further insights into the mechanism of β -Lg fibril formation.

Molecular chaperones are defined as a "class of cellular proteins whose function is to ensure that the folding of certain other polypeptide chains and their assembly into oligomeric structures occur correctly" (Ellis, 1988). In order to be classified as a molecular chaperone, the chaperone protein must be necessary for the correct folding or assembly of the target protein but must not be a component of the assembled protein structure (Ellis, 1993). Caseins, which form the major fraction of milk proteins, have been reported to possess molecular chaperone-like properties at neutral pH (Morgan et al., 2005; O'Kennedy et al., 2006). A number of properties of caseins show resemblance to small heat-shock proteins (Morgan et al., 2005; Yong et al., 2010); these include similar molecular weights, ability to form oligomers and the ability to preferentially bind to the unfolded protein by non-covalent interactions, including hydrophobic and electrostatic interactions (Kehoe et al., 2011; O'Kennedy et al., 2006). The casein fractions possessing chaperone-like activity include α_{s1} -, β - and κ -casein (Bhattacharyya et al., 1999; Morgan et al., 2005).

Chapter 8: Effect of β -Casein on β -Lg Self-Assembly

In this study, bovine β -casein was used to investigate its effect on β -Lg self-assembly since it retains its chaperone-like activity at high temperatures (>75 °C) (Kehoe et al., 2011; Yong et al., 2008). β -Casein is one of the major casein fraction in milk and has a molecular weight of 24.0 kDa with 209 residues (Swaisgood, 1993). It has a high proportion of proline and glutamine residues in its primary sequence and is devoid of any cysteine residues (Ribadeau Dumas et al., 1972). β -Casein does not have a defined tertiary structure (Bhattacharyya et al., 1999) and has only a small proportion of secondary structure (Qi et al., 2004). β -Casein is unlikely to form amyloid-like fibrils, because its high proline content inhibits formation of ordered β -sheets but it exhibits micellization behavior that depends on temperature (Buchheim et al., 1979; de Kruif et al., 2002; Mikheeva et al., 2003; Moitzi et al., 2008; O'Connell et al., 2003; Takase et al., 1980) and concentration (Mikheeva et al., 2003) as a result of its amphiphilic character (Horne, 2002).

β -Casein does not affect the unfolding of the target protein (Gerrard et al., 2012; Kehoe et al., 2011), but its subsequent interaction with the unfolded protein inhibits interactions leading to the aggregation of the unfolded protein (Ghahghaei et al., 2011; O'Kennedy et al., 2006; Yong et al., 2008; Zhang et al., 2005). During its chaperone-like activity, the highly hydrophobic C-terminal region of β -casein preferentially interacts with the hydrophobic patches on the unfolded protein (Ghahghaei et al., 2011). The negatively charged phosphoserine residues of β -casein in the N-terminal region then stabilize the complex by a combination of steric hindrance and electrostatic repulsion (Koudelka et al., 2009; Yousefi et al., 2009). The chaperone-like activity of β -casein decreases with the increase in ionic strength or when pH is lowered from 6.5 to 5.8 (Kehoe et al., 2011). Its activity at pH below its isoelectric point (5.3 to 5.5) has not yet been investigated.

At neutral pH, β -casein inhibits heat- and chemically-induced aggregation of a number of proteins including alcohol dehydrogenase (Hassanisadi et al., 2008; Zhang et al., 2005), ovotransferrin (Matsudomi et al., 2004), α -chymotrypsin (Rezaei-Ghaleh et al., 2008), lysozyme (Zhang et al., 2005), whey protein isolate (O'Kennedy et al., 2006), bovine serum albumin (Kehoe et al., 2011), α -lactalbumin (Kehoe et al., 2011), and bovine β -lactoglobulin (Kehoe et al., 2011; Yong et al., 2008). It inhibits fibril formation from κ -casein (Thorn et al., 2005) and it is not known whether it has a similar effect on β -Lg fibril formation upon heating under acidic conditions.

8.3. Materials and Methods

The materials, chemicals and instruments used in the study have been listed in Section 3.1. The methodology for preparation of β -Lg- β -casein mixtures for self-assembly is described below in Sections 8.3.1 and 8.3.2. The protocols for the ThT assay, ultracentrifugation, SDS-PAGE, and TEM have been described in Chapter 3.

8.3.1. Preparation of β -casein

β -Casein was purchased from Sigma-Aldrich (St. Louis, MO, USA). β -Casein was dissolved in Milli Q water and the pH of the solution was adjusted to 7.0 ± 0.02 . The sample was dialyzed for 48 h at 4 °C using reverse osmosis-treated (RO) water to reduce the effect of ionic strength on its solubility at low pH (Cayot, 1991). After dialysis, the sample was freeze dried to get β -casein powder.

To prepare a stock solution, freeze-dried β -casein was dissolved in Milli Q water and hydrated overnight at 4 °C. After hydration, the temperature of the solution was lowered to 1 °C using an ice-bath, and the pH of the solution was adjusted to 2.1 ± 0.02 using 6 M HCl. The sample was then stirred for a minimum of 2 h in an ice-

Chapter 8: Effect of β -Casein on β -Lg Self-Assembly

bath and then centrifuged at 44,000 g for 30 minutes at 20 °C. The supernatant was filtered through 0.2 μm filter. The concentration of β -casein in the stock solution was determined by spectrophotometry using an extinction coefficient of 0.46 cm^2/g (Thompson et al., 1964).

8.3.2. Preparation of samples for self-assembly

A stock solution of β -Lg was prepared as described in Section 3.3.2 and the concentration of β -Lg was measured by spectrophotometry using an extinction coefficient 0.94 cm^2/mg (Swaisgood, 1982b). For self-assembly studies, stock solutions of β -Lg and β -caseins were mixed in different molar ratios. The final concentration of β -Lg in all samples was 1% w/v and the concentrations of β -casein in β -Lg- β -casein mixtures are shown in Table 8.1. The control sample of β -Lg was prepared from the stock solution by diluting the stock solution with Milli Q water (pH 2). For each of the molar ratios, β -casein controls were prepared as above except the samples did not contain any β -Lg. The final pH of the solution was adjusted to 2.0 ± 0.02 before heating.

Table 8.1 Composition of β -Lg- β -casein mixtures.

Molar Ratio β -Lg: β -casein	Final concentrations			
	β -Lg		β -casein	
	mM ^a	% (w/v)	mM ^a	% (w/v)
1:0 ^b	0.54	1	NA	NA
1:0.0625	0.54	1	0.03	0.08
1:0.125	0.54	1	0.07	0.16
1:0.250	0.54	1	0.13	0.37
1:0.50	0.54	1	0.30	0.65
1:1	0.54	1	0.54	1.3

a: For molarity calculations, the molecular weights used were 18,400 Da for β -Lg and 24,000 Da for β -casein. *b*: Control β -Lg sample did not contain any β -casein.

8.4. Results

8.4.1. Self-assembly from β -Lg in the presence of β -casein

The ThT intensities of heated β -Lg- β -casein mixtures at different times are shown in Figure 8.1 and the kinetic parameters of self-assembly are listed in Table 8.2. The self-assembly from β -Lg in presence of β -casein showed sigmoidal curves with distinct lag, growth and stationary phases.

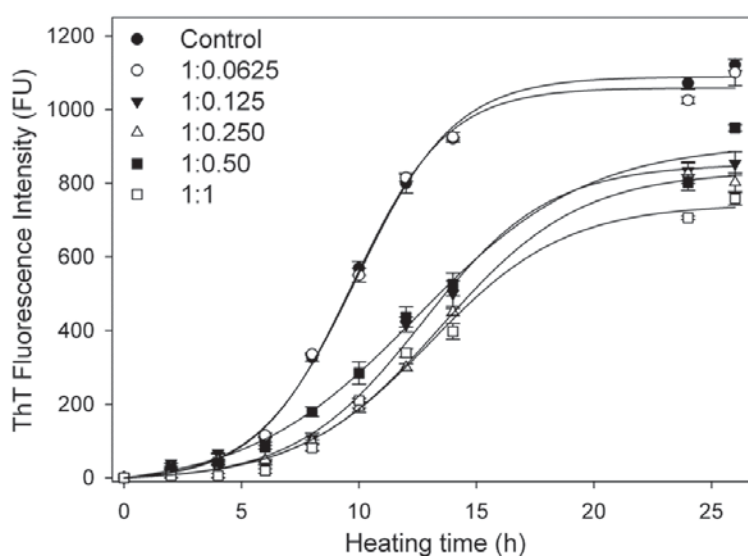


Figure 8.1 ThT fluorescence intensities at 486 nm in samples of heated β -Lg- β -casein mixtures. The control sample contained β -Lg alone. Error bars show the standard errors of measurements from two separate experiments with two replicates for each data point. Solid lines indicate fit of Equation 3.1.

At a low β -casein concentration (molar ratio β -Lg- β -casein 1:0.0625), fibril formation was largely unaffected, while at all other molar ratios studied, β -casein inhibited self-assembly. At molar ratios corresponding to β -casein $> 0.08\%$ (w/v), the t_{lag} increased by up to 30%, $(df/dt)_{\text{max}}$ decreased by up to 40% and f_{max} by up to 25%. At these concentrations ($>0.08\%$, w/v), this effect was independent of β -casein. The β -casein control samples heated without β -Lg did not show any increase

in the ThT fluorescence (Annexure 11.6), indicating that no β -sheets-rich aggregates were produced.

Table 8.2 Kinetic parameters of self-assembly calculated from Equations 3.2-3.4.

β -Lg: β - casein ratio	t_{lag} (h)	df/dt (FU/h)	$t_{1/2\ max}$ (h)	f_{max}	Adj. R^2	$S_{y x}$ ^a
Control	6.0 (0.3)	121.0 (7.5)	10.5 (0.2)	1088.0 (17)	0.9969	25.3
1:0.0625	5.5 (0.3)	142.0 (7.9)	9.2 (0.1)	1058.0 (18)	0.9964	26.6
1:0.125	7.8 (0.6)	74.0 (9.1)	13.5 (0.4)	851.0 (24)	0.9907	32.0
1:0.250	7.8 (0.3)	70.6 (4.6)	13.7 (0.2)	831.7 (13)	0.9975	15.7
1:0.5	5.7 (0.8)	65.6 (8.4)	13.4 (0.5)	907.2 (38)	0.9870	38.5
1:1	7.0 (0.8)	70.3 (8.0)	12.3 (0.3)	763.0 (24)	0.9900	29.1

Numbers in parenthesis indicate standard deviations. *a*: Standard error regression.

8.4.2. Heat-induced acid hydrolysis of β -Lg and β -casein

The samples heated at different times, as shown in Figure 8.1, were analyzed by SDS-PAGE. Heating at 80 °C resulted in the hydrolysis of β -Lg and β -casein monomers into several peptides. A comparison of peptide bands in the samples with different β -Lg- β -casein molar ratios, heated for 12 h at 80 °C, is shown in Figure 8.2 (A). Continued heating resulted in further hydrolysis of the β -Lg monomers and of the large peptides into smaller ones (Figure 8.2, B). The hydrolysis of β -casein followed a similar trend with the β -casein monomers and larger peptides showing progressive hydrolysis with continued heating (Figures 8.3, A and B).

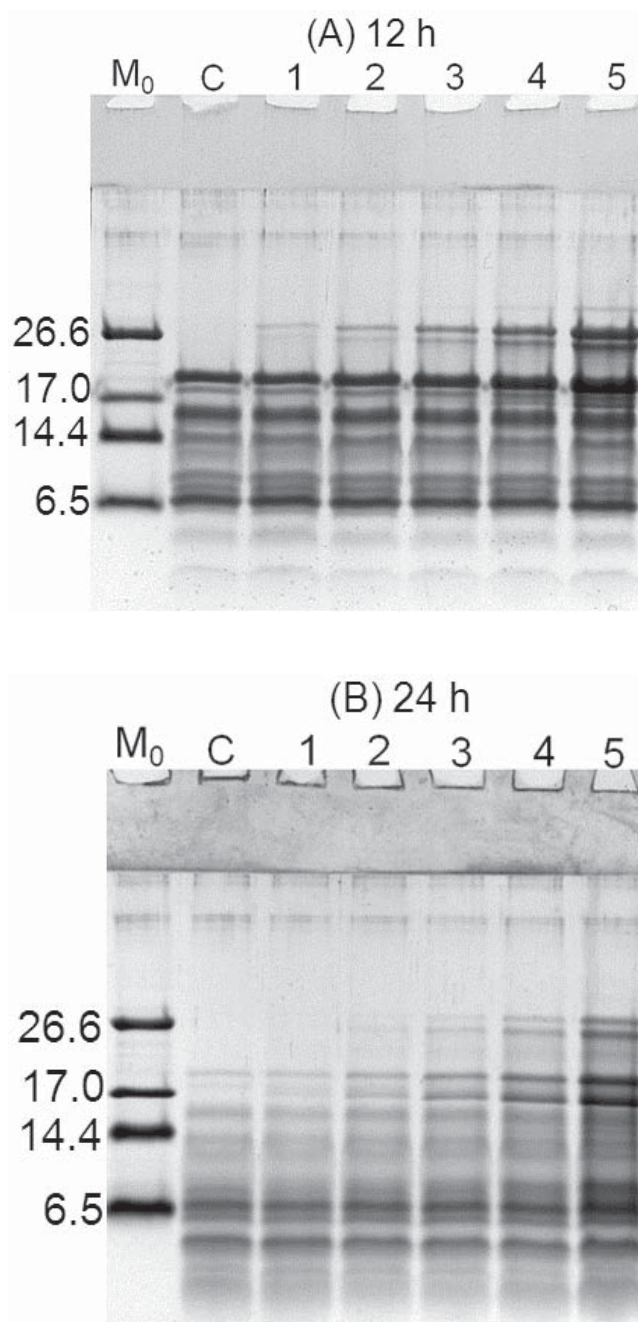


Figure 8.2 Reduced SDS-PAGE of β -Lg and β -casein mixtures heated at 80 °C for (A) 12 h and (B) 24 h. M₀ molecular weight marker (kDa); C, control. Lanes marked 1 to 5 represent β -Lg and β -casein mixtures at different molar ratios. Lane marked 1 represents a molar ratio 1:0.0625; 2, 1:0.125; 3, 1:0.250; 4, 1:0.50; 5, 1:1.

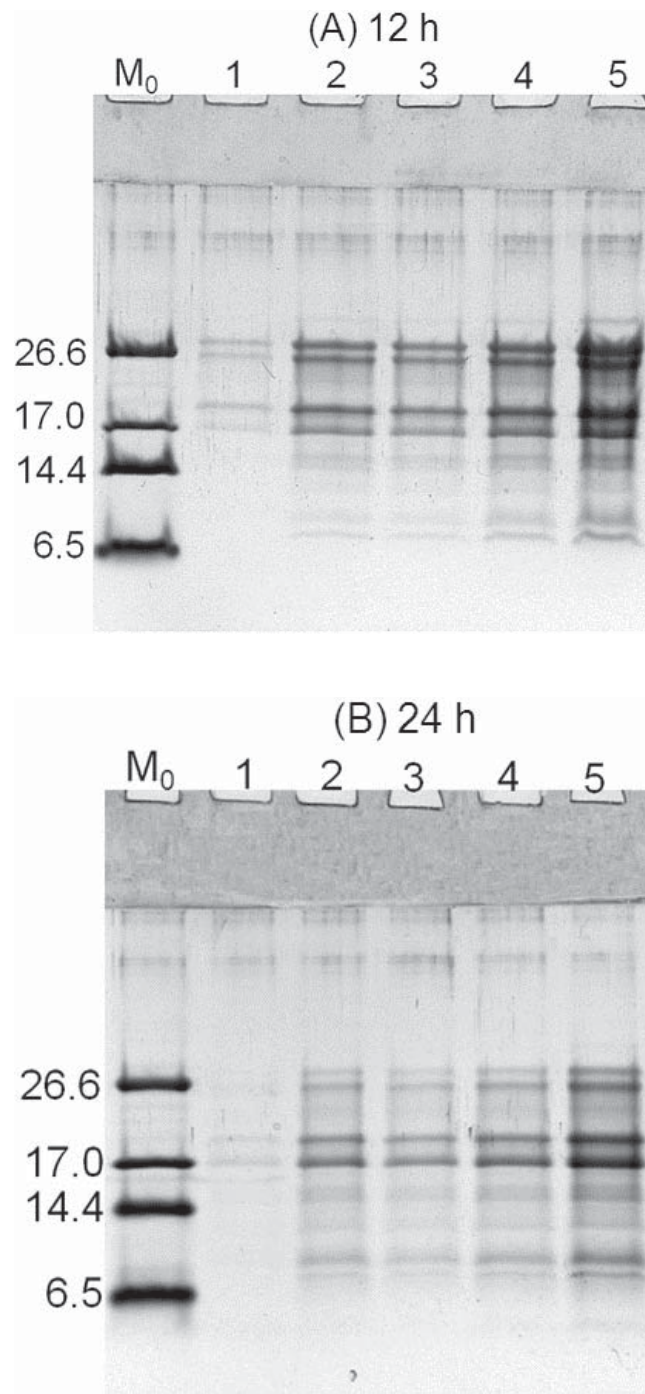


Figure 8.3 Reduced SDS-PAGE of β -casein controls heated at 80 °C for (A) 12 h and (B) 24 h. M_0 molecular weight marker (kDa); Lanes marked 1 to 5 represent the same β -casein concentrations as used in β -Lg- β -casein mixtures of Figure 8.4.

Chapter 8: Effect of β -Casein on β -Lg Self-Assembly

The peptide band comparison of heated mixtures with those of control β -Lg or β -casein revealed some important details about β -casein hydrolysis. Figure 8.4 shows a comparison of peptide bands in heated controls and the mixture containing both proteins (molar ratio 1:1). The acid hydrolysis of β -Lg resulted in more peptides as compared to those from β -casein. The cleavage of β -casein monomer resulted in a peptide (band H) with molecular weight approximately similar to that of intact β -Lg, which meant that the two bands could not be resolved when both proteins were present.

The molecular weight of bands marked G to H were estimated from Figure 8.4 using the protocol described in Section 3.3.5.6 by computing the relationship between R_f and Log (Molecular weight) of the standard molecular weight markers. The calculated weight of band F (monomeric β -casein), was normalized by the known molecular weight of β -casein (24,000 Da) and the resulting factor was used for correcting the molecular weights of the peptide bands which are listed in Table 8.2.

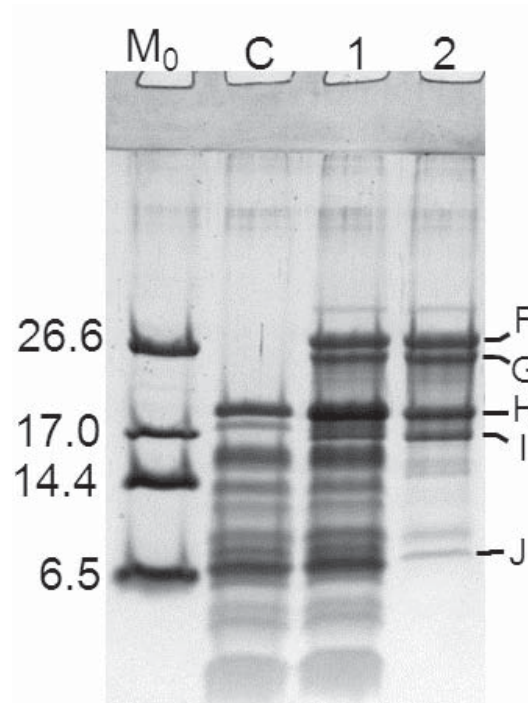


Figure 8.4 Peptide compositions of heated solutions after 12 h at 80 °C. M_0 molecular weight marker (kDa); C, control β -Lg (without β -casein); 1, β -Lg and β -casein mixture (molar ratio 1:1) and 2, control β -casein (without β -Lg) at same concentration as in 1. For description of band F to J, see text. All samples analyzed under reducing conditions.

Chapter 8: Effect of β -Casein on β -Lg Self-Assembly

Table 8.3 Predicted sequences of β -casein peptides shown in Figure 8.6.

Band	Location	Possible Sequence ^{a, b}	Calculated mass ^b	SDS-PAGE mass ^c
G	1-184 ^d	(~)RELEELNVGIVEVLSSEESITRINKKIEKFQSEEQQTEDELQDKIHFAQTQSL	20805	21838
		VYFPFGPIPNSLPQNIPPLTQTPVVVPPFLQPEVMGVSKVKEAMAPKHKEMPPPKYYPV		
		EPFTESQSLTLTDVENLHPLPLLLQSWMHQHPQLPPTVMFPPQSVLSLSQSKVLPVPV QKAVPYPQRD(M)		
H	47-183	(D)KIHFAQTQSLVYFPFGPIPNSLPQNIPPLTQTPVVVPPFLQPEVMGVSKVKEAMA PKHKEMPPPKYYPVEFTESQSLTLTDVENLHPLPLLLQSWMHQHPQLPPTVMFPPQ SVLSLSQSKVLPVPQKAVPYPQR(D)	15215	15385
		(E)DELQDKIHFAQTQSLVYFPFGPIPNSLPQNIPPLTQTPVVVPPFLQPEVMGVSKVVK EAMAPKHKEMPPPKYYPVEFTESQSLTLTDVENLHPLPLLLQSWMHQHPQLPPTV MFPPQSVLSLSQSKVLPVPQKAVPYPQR(M)		
		(~)RELEELNVGIVEVLSSEESITRINKKIEKFQSEEQQTEDELQDKIHFAQTQSL VYFPFGPIPNSLPQNIPPLTQTPVVVPPFLQPEVMGVSKVKEAMAPKHKEMPPPKYYPV EPFTESQSLTLTD(V)		
I	1-129 ^d	(~)RELEELNVGIVEVLSSEESITRINKKIEKFQSEEQQTEDELQDKIHFAQTQSL VYFPFGPIPNSLPQNIPPLTQTPVVVPPFLQPEVMGVSKVKEAMAPKHKEMPPPKYYPV EPFTESQSLTLTD(V)	14446	13628
		(T)DVENLHPLPLLLQSWMHQHPQLPPTVMFPPQSVLSLSQSKVLPVPQKAVPYPQR		
J	129-184	(T)DVENLHPLPLLLQSWMHQHPQLPPTVMFPPQSVLSLSQSKVLPVPQKAVPYPQR	6357	6496

Chapter 8: Effect of β -casein on β -Lg self-assembly

D(M)

1-47^d (~)RELEELNVPGEIVESLSSEESITRINKKIEKFQEEQQTEDELQDKIHD(K) 5986

Letters in the parentheses indicate the amino acid residue adjacent to the peptide while (~) indicates either, 'N' terminal or 'C' terminal end of the β -casein; *a*: Only the peptide bonds involving aspartic acid residues (D) were considered as sites of acid hydrolysis; *b*: Predicted molecular weights calculated from ExPASy compute pI/MW resource tool; *c*: estimated from the SDS-PAGE analysis (Figure 8.4), *d*: peptides with phosphoserine residues.

Chapter 8: Effect of β -Casein on β -Lg Self-Assembly

The rates of hydrolysis of β -Lg and β -casein were quantified by SDS-PAGE and densitometry. For quantification of β -Lg hydrolysis in the β -Lg- β -casein mixtures, mixed samples were analyzed together with β -casein controls on the same gel. An unheated control of the β -Lg- β -casein mixture was also included on the same gel. The residual intensities of the β -Lg band in the mixtures were measured and corrected against the β -casein peptide intensities measured from the β -casein control sample. The subtracted intensities were then normalized against the intensity of the unheated β -Lg of the same gel. The normalized intensities of the β -Lg band were plotted against heating time and were fitted with Equation 3.8. The acid hydrolysis of the β -Lg monomers followed first-order exponential kinetics (Figure 8.5, A) and the rate constants of hydrolysis are listed in Table 8.4.

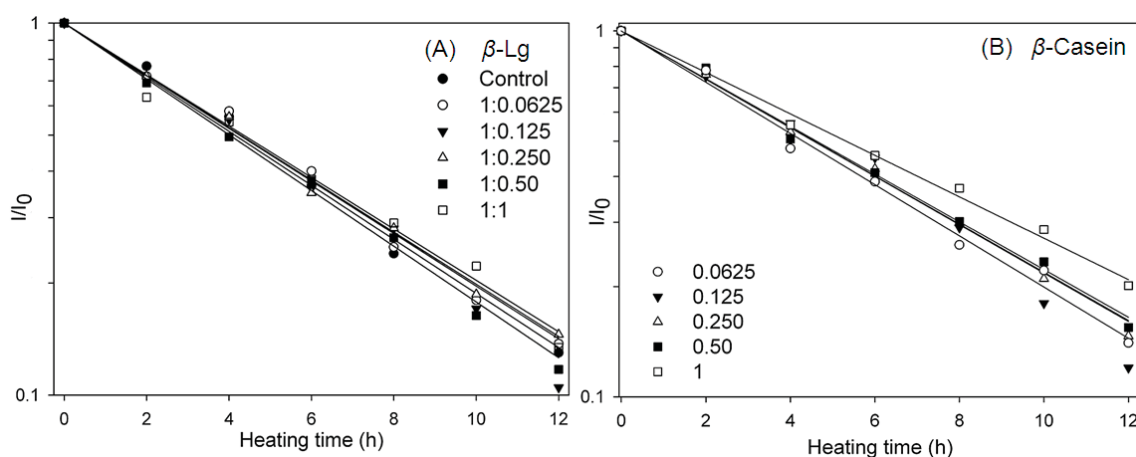


Figure 8.5 Residual SDS-PAGE monomeric band intensities of (A) β -Lg and (B) β -casein in heated β -Lg- β -casein mixtures. Symbols in (B) represent the same β -casein concentrations as used in (A). Values are an average of two separate estimations. Solid lines indicate fit of Equation 3.8.

The rate constants of β -Lg hydrolysis were similar at all molar ratios studied and the differences were not found to be significant ($P=0.47$) in the likelihood ratio test. The acid hydrolysis of β -casein monomers followed a similar trend (Figure 8.5, B) and there was no significant difference ($P=0.14$, likelihood ratio test) between kinetics of

Chapter 8: Effect of β -Casein on β -Lg Self-Assembly

β -casein hydrolysis in the β -Lg- β -casein mixtures. In addition, the rate constants of β -casein hydrolysis were comparable to those of β -Lg hydrolysis (Table 8.4).

Table 8.4 Rate constants of acid hydrolysis of β -Lg and β -casein in heated β -Lg- β -casein mixtures during heating at 80 °C.

Sample details	k_h ($\text{min}^{-1} \times 10^{-3}$)	Adjusted R^2	$S_{y x}^a$ ($\times 10^{-3}$)
<i>β-Lg</i>			
Control	2.71 (0.10)	0.9921	0.5
1:0.0625	2.65 (0.09)	0.9926	0.5
1:0.125	2.79 (0.08)	0.9948	0.4
1:0.250	2.70 (0.07)	0.9960	0.3
1:0.50	2.71 (0.10)	0.9921	0.5
1:1	2.71 (0.14)	0.9817	0.7
<i>β-casein^b</i>			
1:0.0625	2.70 (0.11)	0.9898	0.5
1:0.125	2.54 (0.10)	0.9902	0.5
1:0.250	2.53 (0.05)	0.9977	0.2
1:0.50	2.50 (0.09)	0.9919	0.5
1:1	2.30 (0.06)	0.9950	0.3

Numbers in parenthesis indicate standard deviations. *a*: Standard error of regression; *b*: estimated from residual β -casein band intensities in the β -Lg- β -casein mixtures.

8.4.3. Composition of aggregates in the heated solutions

The aggregates formed in the heated β -Lg- β -casein solution (molar ratio 1:0.5) after 12 h at 80 °C were separated by ultracentrifugation and analyzed by SDS-PAGE (Figure 8.6). The peptide bands in the pellet of control β -Lg (without β -casein) represent the peptides in fibrils, which is in agreement with previous results (Chapter 4, 5 and 6). These peptide bands could also be distinctly identified in the pellet of the heated β -Lg- β -casein mixture. In addition, this sample also showed a distinct β -casein band along with few additional faint peptide bands with molecular masses between those of β -casein and the β -Lg monomer. Although the pellets were washed extensively (for details of the methodology, see Section 3.3.4) the possibility of contamination from β -casein peptides entrapped in the pellet cannot be ruled out.

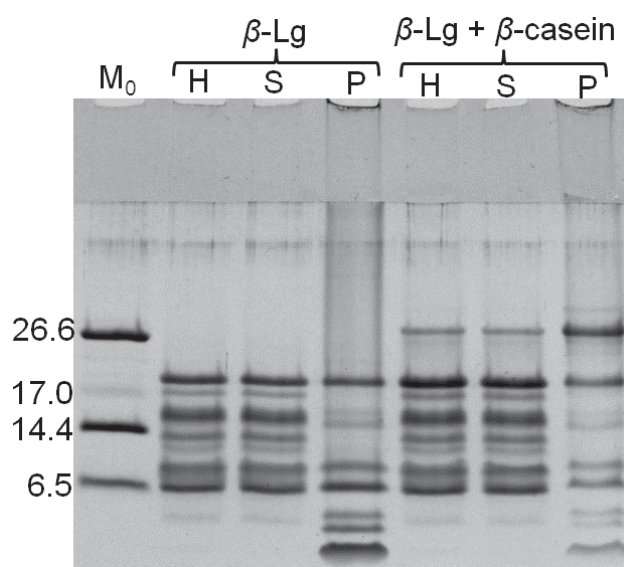


Figure 8.6 Composition of aggregates formed from the heated and ultracentrifuged samples containing β -Lg (1%, w/v) with (0.65% w/v, molar ratio 1:0.5) or without β -casein. Samples were heated at 80 °C for 12 h. M_0 represents molecular weight markers (kDa); H, heated solution; S, supernatant and P, Pellet. Supernatants were diluted 1:10 in reducing PAGE sample buffer, while the pellets were suspended in 1.2 ml PAGE sample buffer without further dilution.

8.4.4. Morphology of aggregates

The morphology of the aggregates formed in the heated β -Lg- β -casein mixtures (at molar ratios other than 1:0.0625) was examined by TEM (Figure 8.7). All samples showed long, semi-flexible fibrils similar to those in the β -Lg control. In addition, the fibrils in the β -Lg- β -casein mixtures (molar ratios 1:0.5 and 1:1) co-existed with long curved worm-like aggregates (white arrows, Figure 8.7, B to E). These aggregates were absent in control β -Lg sample, while the TEM images of β -casein heated without β -Lg had no evidence of fibrils or worm-like aggregates (Figure 8.8). β -Casein heated alone formed amorphous aggregates (Figure 8.8) upon heating. These aggregates are likely to result from the interaction of β -casein peptides, since the SDS-PAGE analysis of solutions heated for 24 h showed hydrolysis of β -casein monomers (Figures 8.2, 8.3 and 8.5).

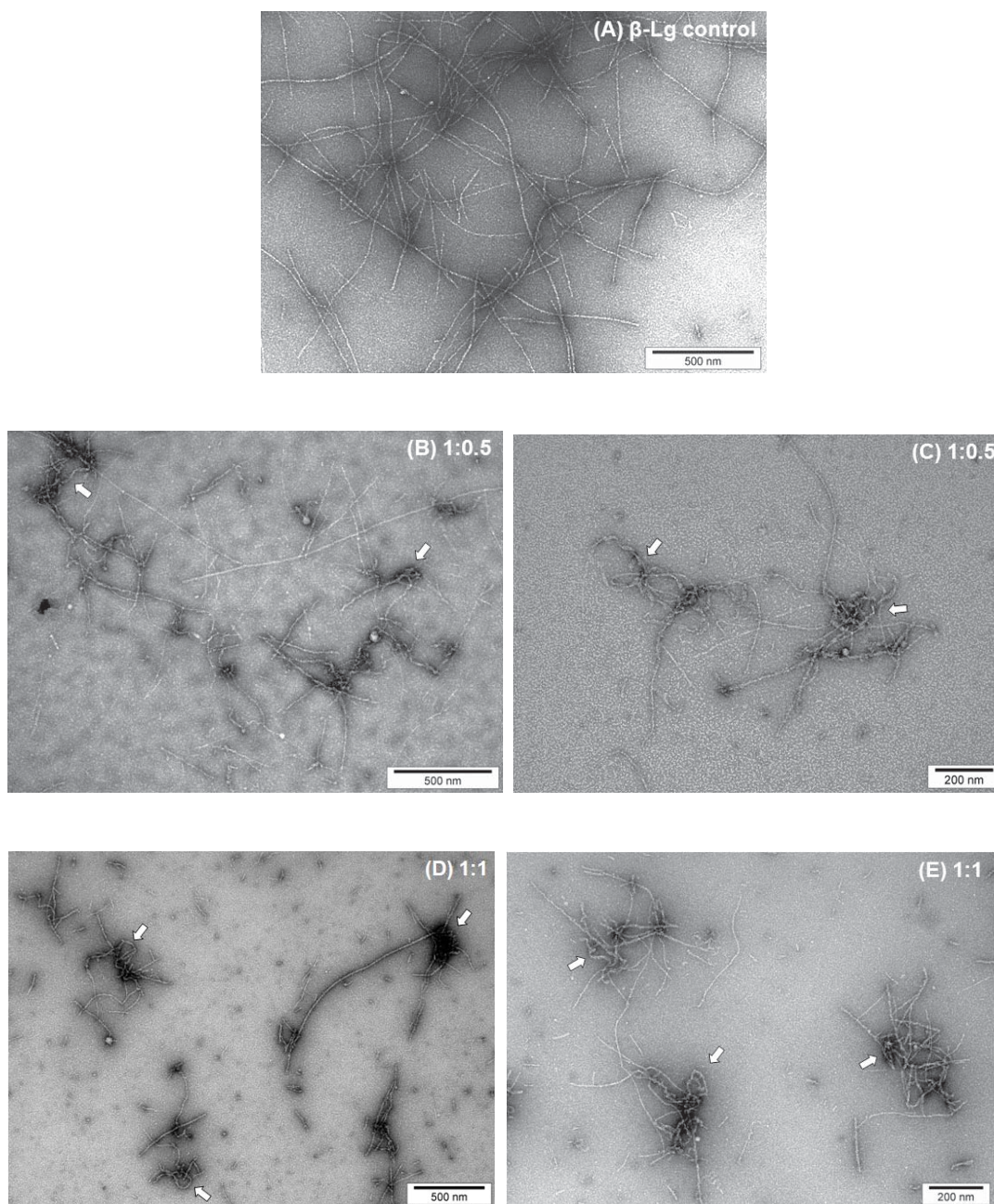


Figure 8.7 TEM images of β -Lg samples heated (A) without, and (B to D) with β -casein at molar ratios of 1:0.5 (B and C) or 1:1 (D and E). Samples heated at 80 °C for 24 h selected for TEM analysis. For description of white arrows see text.

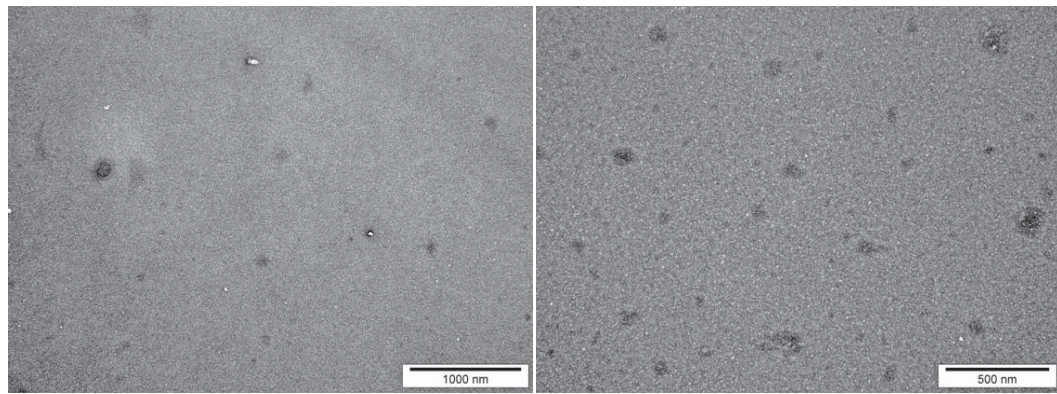


Figure 8.8 TEM images of β -casein samples heated at 80 °C for 24 h without β -Lg. The β -casein concentration was equivalent to that in mixed solutions at molar ratio of 1:0.5.

8.5. Discussion

β -Lg exists as a monomer at pH 2 (Uhrinova et al., 2000) and unfolds rapidly within the first few minutes of heating at 80 °C (Chapters 4 to 7). Heat-induced unfolding of β -Lg during heating at 80 °C exposes the hydrophobic groups and heat and acid labile peptide bonds buried in the native structure to the solvent (Chapter 7). In comparison, at pH 2, β -casein exists as stable micelles during heating up to 40 °C (Moitzi et al., 2008). The micelle characteristics at >40 °C are not known, but in the absence of conditions that disrupt the micelles (see Section 2.2.5.4) β -casein is likely to exist as micelles at 80°C.

The critical micelle concentration (CMC) required for β -casein micellization at low pH (2.6) is approximately 0.19% w/v at 25 °C. The concentration of β -casein used in the study (Table 8.1) at all molar ratios >1:0.125 was higher than this CMC suggesting that β -casein in β -Lg- β -casein mixtures is likely to exist as micelles.

During the chaperone-like action, β -casein monomers preferentially form complexes with the unfolded transitional states of the target protein (Yong et al., 2010) without

Chapter 8: Effect of β -Casein on β -Lg Self-Assembly

affecting its thermal unfolding (Kaushik et al., 1998; Kehoe et al., 2011). Under the fibril-forming conditions, the interaction of β -casein with the unfolded β -Lg monomers appeared unlikely, as subsequent processes such as acid hydrolysis of these proteins and β -Lg fibril formation remained unaffected. This may be explained by an enhanced electrostatic repulsion between these two proteins at low pH. At pH 2.0, the β -Lg and β -casein monomers have a net positive charge of +21 (Aymard et al., 1999) and +15.82 (pH 2.6) (Moitzi et al., 2008; Portnaya et al., 2008) respectively. The distribution of these charges along the polypeptide chains in both proteins is markedly different to that at neutral pH (Akkermans et al., 2008b; Moitzi et al., 2008). The comparison of charge distribution on β -casein polypeptide at near neutral and acidic pH is shown in Figure 8.9. This net positive charge distribution along its sequence may restrict the interaction of β -casein with the unfolded β -Lg monomers. Thus, in the absence of any strong interaction between these two proteins, both proteins appear to undergo acid hydrolysis independently.

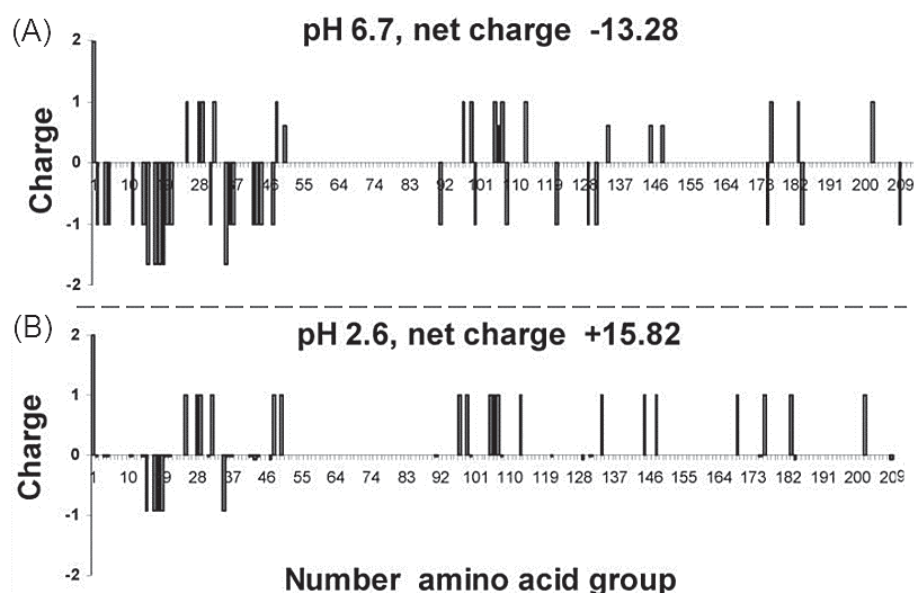


Figure 8.9 Charge distribution on β -casein polypeptide at pH (A) 6.7 and (B) 2.6. Adapted with permission from Moitzi et al. (2008), Copyright 2008 American Chemical Society.

Heating at low pH results in the hydrolysis of peptide bonds involving aspartic acid residues (Inglis, 1983). β -Lg has 10 Asp residues in its primary sequence and the heat-induced acid cleavage of Asp-X or X-Asp involving these residues during self-assembly has been well established (Akkermans et al., 2008b). By comparison β -casein has 4 Asp residues: 43, 47, 129 and 184 (Ribadeau Dumas et al., 1972) and it is likely that heating at low pH resulted in the hydrolysis of peptide bonds involving these residues. From the SDS-PAGE, it is reasonable to assume that the effect of β -casein on the β -Lg self-assembly may arise primarily from the interaction of β -casein peptides with assembly-capable peptides of β -Lg.

The ThT data showed that there exists a the threshold concentration of β -casein (0.08% w/v < threshold concentration < 0.16% w/v) necessary for its effect on β -Lg self-assembly. It appears that at concentrations below this threshold concentration, there were insufficient β -casein peptides available for interaction with the self-assembly-competent peptides of β -Lg, and β -Lg fibril-formation proceeded normally. Above this concentration, the presence of β -casein in samples increased the t_{lag} , and lowered $(df/dt)_{max}$ approximately to an equal extent. The longer t_{lag} , representing a delay in nucleation, indicates that a population of β -Lg fibril-forming species were unavailable for self-assembly. The fewer nuclei then resulted in lower $(df/dt)_{max}$ and the net effect of longer t_{lag} and lower $(df/dt)_{max}$ may translate into a lower yield of fibrils indicated by lower f_{max} . Although, the lower f_{max} may also result from the interaction of self-assembly-capable β -Lg peptides with β -casein peptides in the growth phase.

It is interesting to note that the effect of β -casein on β -Lg self-assembly was independent of its concentration above a threshold value. With increasing β -casein

Chapter 8: Effect of β -Casein on β -Lg Self-Assembly

concentrations and similar kinetics of acid hydrolysis, the concentration of β -casein peptides in samples released from its acid hydrolysis was expected to be higher. It appears that the effect of increasing concentration was off-set by a parallel phenomenon, perhaps a possible alternate association pathway for β -casein peptides.

The peptides released from the acid hydrolysis of β -casein (Bands G, H and I, Table 8.3) contained large patches of non-polar hydrophobic residues separated from clusters of charged residues. The schematic indicating the hydrophobicity of these peptides at neutral pH is shown in Figure 8.10. This may impart an amphiphilic character to the peptides, similar to that of the unhydrolyzed β -casein (Berry et al., 1975; Horne, 2002; Yousefi et al., 2009). This unique structural feature of the β -casein peptides may facilitate their aggregation into micelle-like aggregates similar to the micelles of the unhydrolyzed β -casein. Experimental studies elucidating the details of this micelle-like aggregation pathway of β -casein peptides, such as the mechanism of their formation, relationship between peptides and aggregated states at equilibrium and the reversibility of aggregation, provide an interesting area of future investigation.

If β -casein peptides aggregated into micelle-like aggregates, then the proportion of these aggregates would increase with increasing β -casein concentrations. This would result in concentration dependency at high β -casein concentrations but none was observed (Figure 8.1 and Table 8.2). The lack of concentration dependence (above a threshold concentration) suggests that the observed effect of β -casein on β -Lg self-assembly may primarily result from β -casein peptides and not their micelle-like aggregates, concurrent with the hypothesis for the chaperone-like activity of β -casein (O'Connell et al., 2003; Yousefi et al., 2009). The active species inhibiting the aggregation of the target protein during the chaperone-like activity of β -

casein monomers and not their micelles (Yousefi et al., 2009). Although, the assumption that β -casein micelles did not interact with β -Lg fibrillar species can only be ruled out by experimental evidence from future studies.

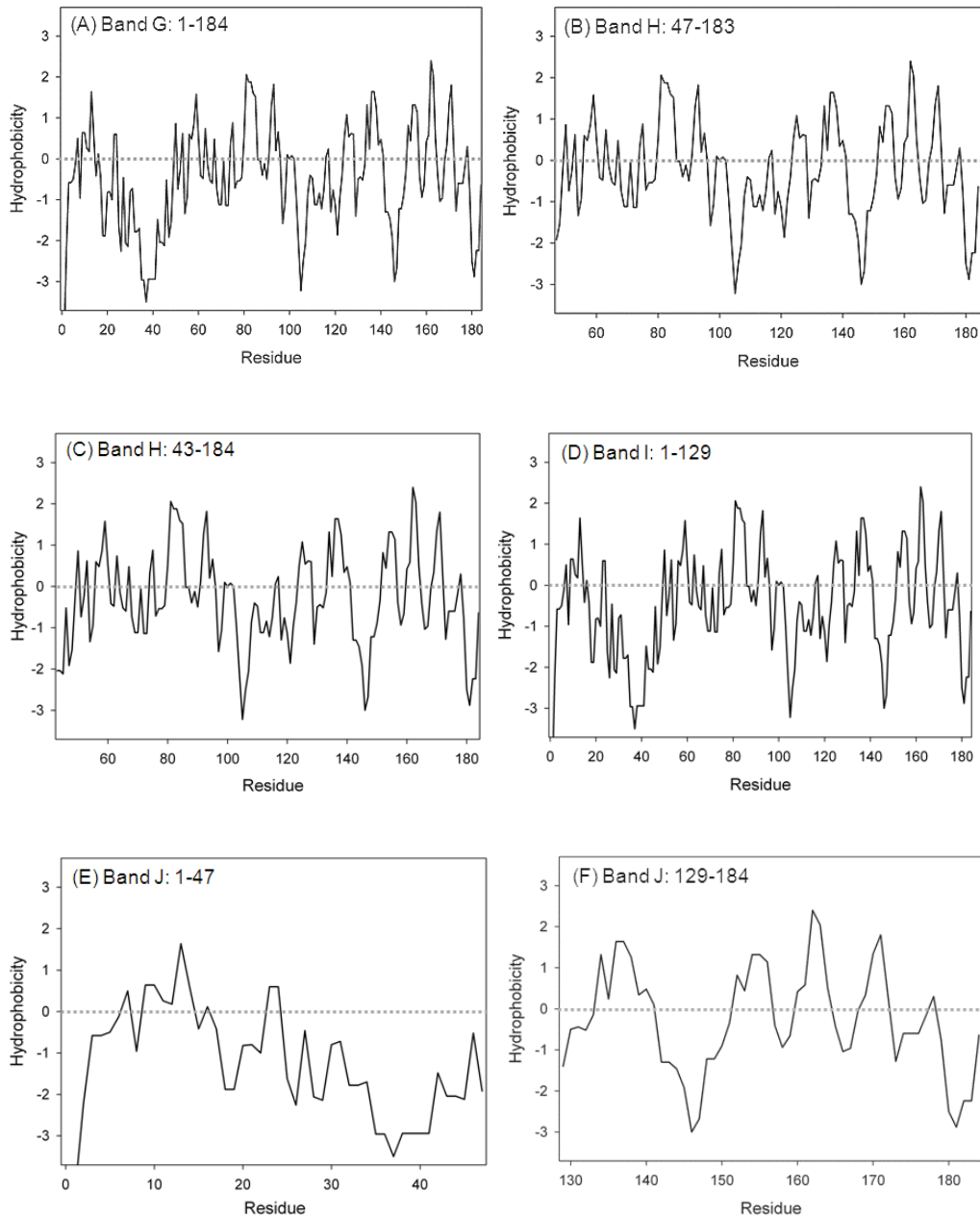


Figure 8.10 Overview of the hydrophobicity (pH 7) of β -casein peptides G to J of Figure 8.4 calculated using the method of Kyte et al. (1982). At pH 2, the hydrophobicity of the peptides is likely to be higher due to protonation of carboxylic groups of Asp and Glu (Kuhn et al., 1995). Bands G (A), I (D) and J (E) contain phosphate groups bound to serine residues.

From the results presented in this study, it is not known whether the β -casein peptides interacted with self-assembly-competent β -Lg peptides or their intermediates, or both. Nevertheless, taken together these results indicate that there are competing aggregation pathways for the peptides of both proteins (Figure 8.11). A fraction of reactive peptides from both proteins may preferentially interact with each other by pathway (i) (see Figure 8.11) resulting in the observed effect on β -Lg self-assembly. By comparison, a relatively larger proportion of these reactive species of either proteins self-assembled into homogenous aggregates i.e. micelle-like aggregates from β -casein (pathway ii, Figure 8.10) and fibrils from β -Lg (pathway i, Figure 8.11).

Chapter 8: Effect of β -Casein on β -Lg Self-Assembly

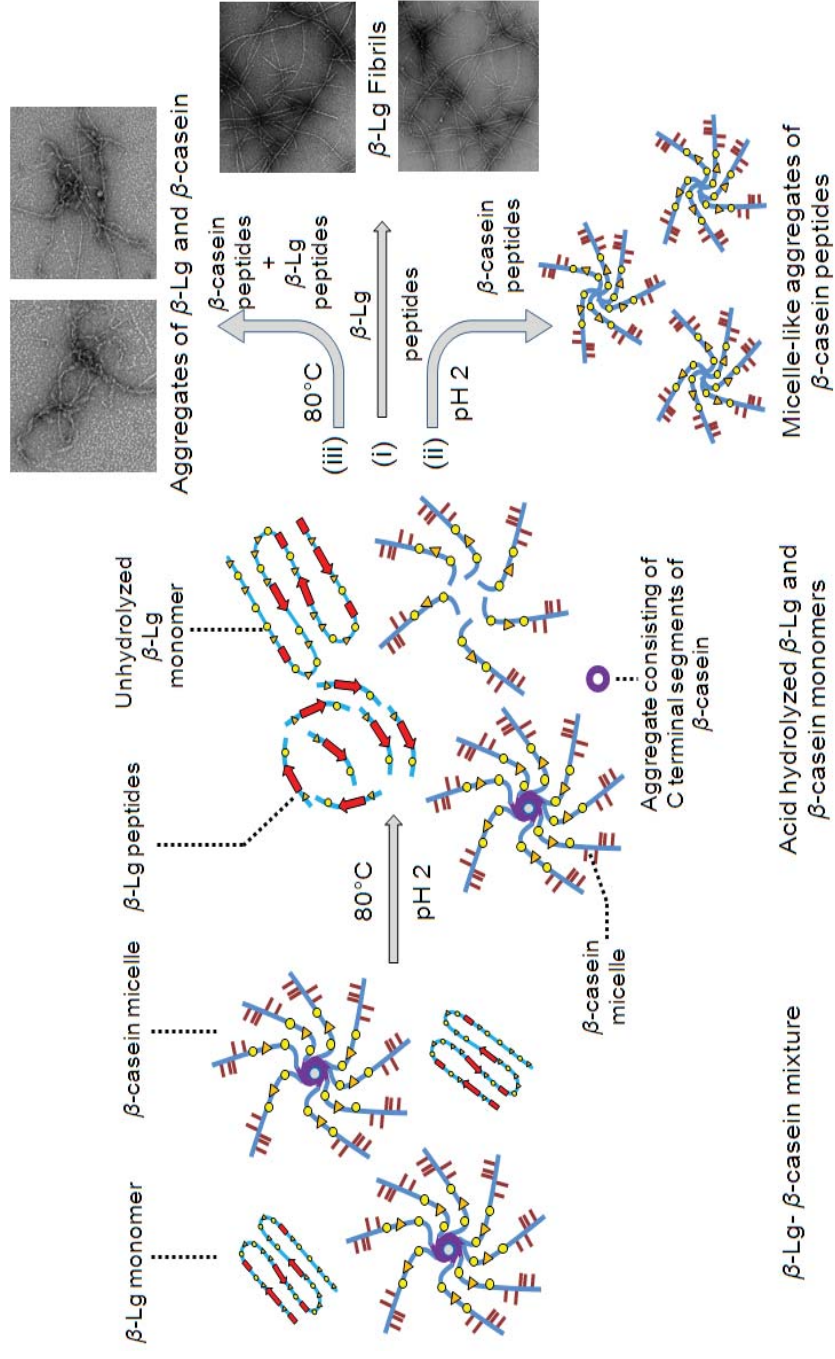


Figure 8.11 Proposed mechanism for the effect of β -casein on β -Lg self-assembly. (i), (ii) and (iii) represent aggregation pathways.

Chapter 8: Effect of β -Casein on β -Lg Self-Assembly

The primary sequence of β -casein is rich in proline residues (Ribadeau Dumas et al., 1972), which disrupt the formation of ordered β -sheets (MacArthur et al., 1991). Thus, the interaction of β -casein with the β -Lg fibril-forming species by pathway (iii) may result in aggregates which have a less ordered structure. The evidence of such an alternate pathway was provided by the TEM images of fibrils. The fibrils from β -Lg in β -Lg- β -casein mixtures were found to co-exist with irregular and twisted aggregates. Their absence in the heated control samples (β -Lg or β -casein) indicates that both β -Lg and β -casein peptides were necessary for their formation. Further characterization of the composition of these aggregates by mass spectrometry provides an interesting area for further investigation.

β -Casein controls heated at 80 °C for 24 h showed amorphous aggregates with a range of diameters (approximately 25 to 100 nm). These aggregates are unlikely to be micelles of residual unhydrolyzed β -casein monomers since their size was much larger than that of β -casein micelles (10 to 15 nm in diameter). It is not known why these aggregates were absent in β -Lg- β -casein mixtures; further investigation is necessary to determine the reason for the change in their aggregation behaviour in presence of β -Lg.

The composition of fibrils in the β -Lg- β -casein mixture (1:0.5) separated by ultracentrifugation after 12 h at 80 °C was very similar to that of control fibrils prepared without β -casein (Figure 8.8). Interestingly, distinct peptide bands (molecular weight < 18400 Da) attributable to β -casein could not be identified in this sample, but the sample showed a distinct band corresponding to the molecular weight of the intact β -casein monomer. β -Casein at low pH is known to form micelles (Moitzi et al., 2008) which may sediment along with the fibrils at the high ultracentrifugation speed employed in this study and may account for the monomeric

β -casein band in Figure 8.8. The absence of β -casein peptide bands in the pellet of the β -Lg- β -casein mixture may be explained by their small size at this heating time point. It is possible that the aggregates formed by the β -Lg- β -casein interaction were too small to be separated by the ultracentrifugation speed employed for separation. Continued heating of this sample may have resulted in the growth of these irregular aggregates seen in TEM images by addition of more peptides of either proteins as seen in the TEM. Thus in summary, β -casein inhibited self-assembly of β -Lg self-assembly slightly, but its effect was independent of its concentration above a threshold concentration. This study is in sharp contrast to its significant chaperone-like effect at neutral pH, where a molar ratio of 1:0.13 was sufficient to inhibit heat-induced non-fibrillar aggregation of β -Lg during heating at 90 °C for 20 minutes (Yong et al., 2008). The limited effect of β -casein at different concentrations probably resulted by the aggregation of β -casein peptides into micelle-like structures by an alternate pathway. Those peptides that escaped aggregation by the micellization pathway (pathway-ii, Figure 8.11) interacted with β -Lg fibril forming species resulted in irregular aggregates and the absence of any free reactive β -casein peptides, fibril-forming peptides of β -Lg self-assembled into mature fibrils.

Clearly, this study has opened up a number of avenues for future investigation. The characterization of reactive β -Lg species involved in the interaction with β -casein peptides, the effect of secondary structure of β -Lg peptides on β -Lg- β -casein peptide-peptide interactions, characterization of sequences present in the long, irregular, twisted aggregates formed during heating and a study exploring the properties and functionality of these aggregates provide an interesting area of future research.

Chapter 9

9. Overall discussion and avenues for future work

9.1. Summary

This study characterized the β -Lg self-assembly processes and composition of fibrils at different stages of self-assembly. β -Lg was heated at 80 °C, pH 2, low ionic strength and the conditions of self-assembly were perturbed using three different approaches in order to gain insight about the mechanism of self-assembly. In the first approach, the effect of change in the native structure of β -Lg was explored using either the genetic variants β -Lg A, B and C or using glucosylated and lactosylated β -Lg. In the second approach, the composition of the aqueous solution was used as a tool to perturb self-assembly and investigate its effect on the self-assembly processes. Glycerol and sorbitol were used to modify the solvent composition. Finally in the third approach, β -casein, known to possess chaperone-like activity, was used as a co-solute to understand the mechanism of self-assembly. The controlled conditions used in all these approaches ensured that the native structure of starting β -Lg, prior to fibril formation, was largely undisturbed in all the experimental studies. From the studies in Chapters 4 to 8, β -Lg self-assembly can be described by four main processes: 1) unfolding of β -Lg monomers, 2) heat-induced acid hydrolysis of the unfolded monomers 3) reversible self-assembly of peptides to form nuclei 4) irreversible self-assembly of peptides once a critical size of the nuclei is attained, resulting in formation of fibrils.

9.1.1. Unfolding of β -Lg

Unfolding of β -Lg was investigated by CD spectroscopy by continuously recording scans during *in situ* heating at 80 °C. This method allowed the monitoring of real-time transitions in the β -Lg native structure during heating. Heating resulted in rapid unfolding of the β -Lg tertiary structure, while transition in the secondary structure involved a possible non-native α -helix intermediate. The bulk of these structural transitions in the native structure were completed within the first few minutes of heating and after 1 hour at 80 °C, partially unfolded monomers, devoid of any tertiary structure but with a significant secondary structure, were formed.

The unfolding behavior of β -Lg A, B and C were similar (Chapter 5), while unfolding kinetics appeared to be unaffected by the type or extent of glycation (Chapter 6). The unfolding of β -Lg was also investigated in presence of structure-stabilizing cosolutes, glycerol and sorbitol. The unfolding kinetics appeared to be slightly hastened in the presence of glycerol while sorbitol strongly stabilized the native structure of β -Lg.

9.1.2. Heat-induced acid hydrolysis

Once the β -Lg monomers were unfolded, continued heating resulted in the preferential cleavage of peptide bonds involving Asp (D) residues (Chapter 4). Under the conditions used (1% w/v β -Lg, 80 °C, pH 2, low ionic strength and absence of any cosolutes), the kinetics of acid hydrolysis were much slower than that of unfolding (Chapters 4-7) and followed a first-order exponential model. Acid hydrolysis of β -Lg continued to occur throughout the heating process, irrespective of the stage of self-assembly. The transition from the nucleation to the growth phase coincided with approximately 60% hydrolysis of the monomers (Chapter 4) and the

hydrolysis of monomers occurred concurrently with the nuclei growth in the growth phase (Chapters 4-8). The kinetics of acid hydrolysis were unaffected by the genetic substitution of amino acids in β -Lg A, B and C, glucosylation or lactosylation. Similarly, the presence of glycerol or β -casein in solutions did not affect acid hydrolysis, but increasing concentrations of sorbitol progressively inhibited acid hydrolysis.

9.1.3. Self-assembly

The self-assembly from β -Lg followed nucleation-dependent growth showing distinct lag, growth and stationary phases. The fluorescence data were fitted with a sigmoidal model and the kinetic parameters of self-assembly were calculated. The time required for nucleation (t_{lag}), was similar for β -Lg A, B and C and was dependent only on the degree of glycation for glycated β -Lg. In comparison, presence of glycerol, sorbitol or β -casein in solutions increased t_{lag} .

In the growth phase, the rate of self-assembly increased exponentially (Chapters 4-8) but decreased upon glycation. The inhibitory effect of glycation followed the order: lactosylation > glucosylation (Chapter 6), notably the effect of glucosylation depended on the extent of glucosylation but the effect of lactosylation was independent of its extent (Chapter 6). The modification of the aqueous composition by polyols inhibited self-assembly progressively with increasing polyol concentrations (Chapter 7). In comparison, when β -casein was used to modify solvent composition, a small consistent reduction in the rate of self-assembly, that was independent of β -casein concentration above a certain threshold concentration, was observed. The mechanism of β -Lg self-assembly is depicted in Figure 9.1.

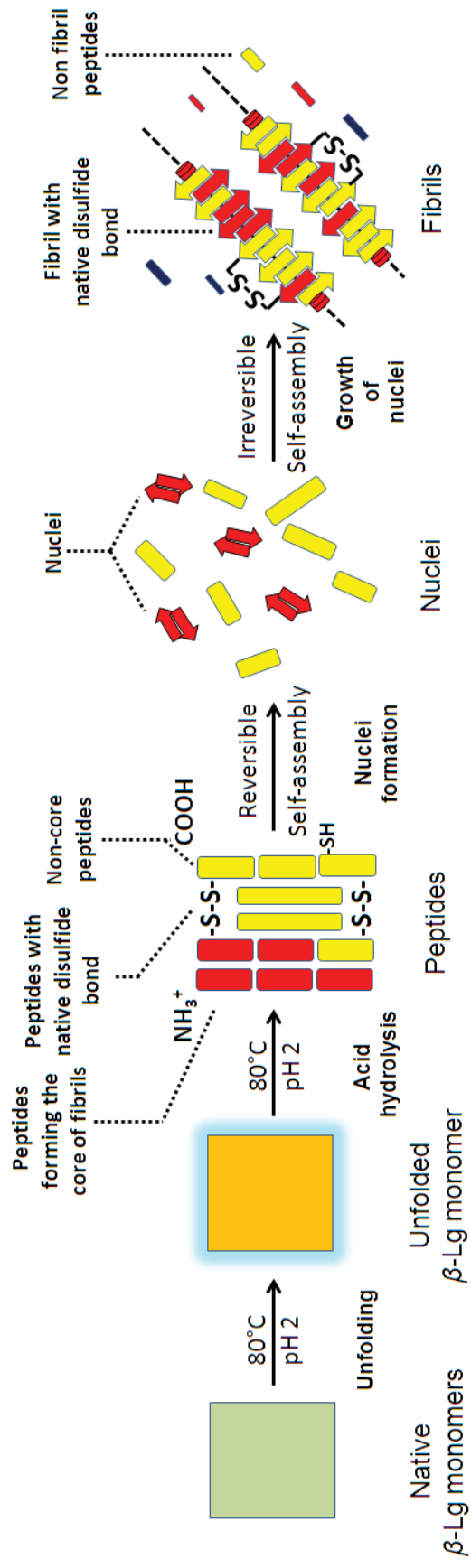


Figure 9.1 Mechanism of β -Lg self-assembly at 80°C , $\text{pH } 2$ at low concentrations ($<3\%$ w/v).

9.1.4. Fibril composition and amyloidogenic sequences

The composition of fibrils formed upon heating β -Lg at different times was compared by separating them from the unassembled material using ultracentrifugation. The SDS-PAGE of the separated fibrils showed that β -Lg fibrils always consisted of five major peptides (Chapters 4 to 6 and 8). These peptides in the fibrils were first observed at heating times corresponding to the lag phase and their concentration increased steadily with heating, indicating that the same peptides may be involved in nucleation and growth of fibrils (Chapter 4). Significantly, the peptide composition of fibrils did not change with heating time.

The sequences present in the peptides of fibrils were characterized using two different MS approaches. The peptide bands were digested by the in-gel digestion using trypsin and the extracted peptides were analyzed by ESI MS/MS. This analysis showed that the sequences from the region 1-53 frequently featured in all the five major peptide bands in fibrils. The composition of fibrils was also characterized by their dissociation using guanidinium hydrochloride followed by purification and MALDI-TOF MS/MS. The sequences found in fibrils from these analyses were in general agreement and both methods showed evidence of regions containing Cys66 and Cys160. This was explained based on the native disulfide bond between these residues being conserved in fibrils, which was also supported by the disulfide bonding in fibrils evidenced by the 2D NR-R SDS-PAGE analysis of fibrils (Chapter 4).

The likely differences in the composition of fibrils from β -Lg variants A, B and C were explored in Chapter 5. The SDS-PAGE peptide composition of fibrils of β -Lg A showed two additional peptide bands in comparison to those of β -Lg B or C. This difference in

Chapter 9. Summary, Conclusions and Avenues for Future Work

the peptide composition of fibrils from β -Lg A was attributed to the cleavage of peptide bonds Asp64-X or X-Asp64 in β -Lg A. The possible sequences in the peptides in the fibrils of β -Lg A, B and C were predicted using the SDS-PAGE data based on the in-gel digestion ESI-MS/MS (Chapter 4). The major peptide bands of fibrils characterized in Chapter 4 were also observed in fibrils of glycosylated β -Lg or of β -Lg- β -casein mixtures (Chapters 6 and 7). Interestingly, fibrils from β -Lg- β -casein mixtures analyzed by SDS-PAGE also contained additional peptide bands resulting from the hydrolysis of β -casein (Chapter 8).

9.1.5. Morphology of fibrils

β -Lg fibrils in all the studies appeared semiflexible, and the morphology of fibrils was largely unaffected by genetic variation or glycation (Chapters 5 and 6). Fibrils formed in the presence of polyols glycerol and sorbitol were semiflexible but were markedly shorter than in the absence of polyols (Chapter 7). In comparison, the presence of β -casein in the system resulted in long, twisted, irregular aggregates with non-uniform thickness which co-existed with the fibrils. The effects of treatments used to understand the mechanism of self-assembly in Chapters 4 to 7 are summarized in Table 9.1.

Chapter 9. Overall Discussion and Avenues for Future Work

Table 9.1 Summary of the results from Chapters 5-8.

Chapter	Treatment	Unfolding	Lag phase		Growth phase		Morphology of fibrils
			Acid hydrolysis	Self-assembly	Acid hydrolysis	Self-assembly	
5	Genetic Variation	=	=	=	=	=	=
		=	=	=	=	=	=
6	Low degree glucosylation	=	=	=	↓↓	↓↓	=
		=	=	=	↓↓↓	↓↓↓	=
		=	=	=	↓↓↓	↓↓↓	=
7	High degree glucosylation	=	=	↓↓	↓↓	↓↓	=
		=	=	↓↓	↓↓	↓↓	=
		=	=	↓↓	↓↓	↓↓	=
7	Glycerol Sorbitol	=	=	↓↓↓ ^a	↓↓↓ ^a	↓	↓ ^b
		↓↓↓ ^a	↓ ^b				

Chapter 9. Overall Discussion and Avenues for Future Work

8 β -casein ? = ↓ ↓ = ↓ =^c

Key: ↓mild, ↓↓ intermediate and ↓↓↓ strong inhibitory effect; ? not studied; = no effect, *a*: concentration dependent effect. *b*: fibrils appeared to be shorter than control fibrils. *c*: irregular, twisted and ribbon-like aggregates coexisted with fibrils.

9.2. Overall discussion

β -Lg self-assembly follows a classical nucleation-dependent growth model (Arnaudov et al., 2003; Aymard et al., 1999; Bolder et al., 2007a; Bromley et al., 2005). Most of the recent studies investigating self-assembly have used conditions that hasten the nucleation step, e.g. stirring during heating, and hence the processes in the lag phase have received little attention in comparison to those in the other stages of self-assembly. This study, for the first time, systematically explored the mechanism of β -Lg self-assembly starting from the interactions in the lag phase until the stationary phase and characterized the different processes involved in self-assembly and their inter-relationships.

β -Lg monomers undergo heat-induced denaturation upon heating at temperatures >80 °C (Clark et al., 2001; Langton et al., 1992). It is generally accepted that β -Lg self-assembly proceeds from denatured monomers (Bolder et al., 2007a) but the extent of denaturation necessary to facilitate fibril formation is not known. In this study, the CD technique was standardized to explore the heat-induced unfolding of secondary and tertiary structures of native β -Lg during heating. This protocol provides a new tool for monitoring the heat-induced unfolding kinetics of globular proteins.

The CD studies showed that heating resulted in molten-globule like partially unfolded monomers that had no native tertiary structure but retained a large proportion of the secondary structure (Chapters 4 to 7). This was in agreement with a number of previous studies (Belloque et al., 1998; Boye et al., 1996; Cairoli et al., 1994; Casal et al., 1988; Prabakaran et al., 1997) which reported a higher stability of β -Lg secondary structure

Chapter 9. Overall Discussion and Avenues for Future Work

towards thermal unfolding than its tertiary structure. Sorbitol stabilized the transitions in the native structure and inhibited self-assembly by inhibiting subsequent interactions (Figure 9.2). These results show that, under conventional heating conditions, the self-assembly of β -Lg occurs from the unfolded monomers in agreement with the model proposed for β -Lg self-assembly by Bolder et al. (2007a).

The role of protein unfolding in generating fibril precursors is well known (Chiti et al., 2006; Uversky et al., 2004). The sequences found in the β -Lg fibrils in this study (Chapter 4) and those by others (Akkermans et al., 2008b; Hettiarachchi et al., 2012) are buried in the native structure and unfolding of native structure may expose these sequences to the solvent and facilitate the interactions by hydrogen bonding, hydrophobic and electrostatic interactions (Uversky et al., 2004). In addition, from Chapters 4-7, the unfolding of β -Lg always preceded acid hydrolysis, while stabilization of the native structure also inhibited acid hydrolysis (Chapter 7). This suggests that acid hydrolysis of monomers may be related to their conformation state and unfolding facilitated the cleavage of labile peptide bonds by exposing them to the solvent. However, a faster unfolding did not translate into faster acid hydrolysis as apparent from the effect of glycerol on unfolding and acid hydrolysis of β -Lg (Chapter 7). This may be attributed to the fact that kinetics of hydrolysis (~ 12 h for 10 fold change in initial concentration, D) is much faster than protein unfolding ($D < 10$ minutes).

The acid hydrolysis of β -Lg during its self-assembly has been noted in previous studies (Akkermans et al., 2008b; Bateman et al., 2010; Bolder et al., 2007c; Hettiarachchi et al., 2012; Kroes-Nijboer et al., 2011; Lara et al., 2011; Oboroceanu et al., 2010) and occurs by preferential cleavage of peptide bonds involving aspartic acid residues (Inglis,

Chapter 9. Overall Discussion and Avenues for Future Work

1983; Partridge et al., 1950). From the results of this study (Chapters 4 to 8), the possible role of hydrolysis during self-assembly can be hypothesized. The fibril-forming regions capable of self-assembly may still be under significant structural constraints in the unfolded monomers and hydrolysis of monomers removed these constraints by separating these regions. The hydrolysis of monomers may create building blocks with enhanced flexibility that can readily self-assemble into fibrils.

It then follows that enzymatic hydrolysis can be expected to promote self-assembly, in agreement with the experimental studies (Akkermans et al., 2008a; Gao et al., 2013). This hypothesis is further supported by the findings of Mishra et al. (2007), who reported a decrease in the rate of self-assembly when intact monomers of hen egg white lysozyme were added to the solution. That acid hydrolysis promoted self-assembly under the conditions used here (80 °C, pH 2), is also evident from the faster kinetics of self-assembly (few hours) in this study, than those under other known conditions of β -Lg self-assembly such as incubation with urea (Hamada et al., 2002), thiocyanate (Rasmussen et al., 2007) or organic solvents (Gosal et al., 2002) where fibrils appear only after significantly long incubation times (≥ 3 days).

The genetic substitution of residues in β -Lg A, B and C did not affect their overall rate of hydrolysis (Chapter 5), while the rate of β -Lg hydrolysis was similar to that of β -casein despite having almost twice the number of Asp residues in its primary sequence (Chapter 8). Taken together, this indicates that the heat-induced acid hydrolysis of labile peptide bonds does not depend on the number of sites of acid hydrolysis but rather on their exposure to the solvent. Notably, characterization of peptides in the fibrils also showed that the peptides did not undergo further hydrolysis after their incorporation into

Chapter 9. Overall Discussion and Avenues for Future Work

the fibrils (Chapter 4). This may be attributed to the sites of preferential cleavage being concealed in the compact fibril structure, in agreement with the above hypothesis.

If we consider that the solvent exposure of the labile peptide bonds was necessary for their cleavage, then it can be concluded that conditions that promote peptide-peptide interactions are likely to result into peptides being incorporated into the fibrils without their further hydrolysis. This means that during self-assembly acid hydrolysis of assembly-competent peptides and their incorporation into fibrils are competing reactions. This is supported by the results of Hettiarachchi et al. (2012) which showed that peptides in the fibrils formed by microwave heating were much larger than the fibrils formed under conventional heating conditions. Thus, other conditions promoting self-assembly at pH 2, such as shearing during heating (Dunstan et al., 2009; Hill et al., 2006), seeding with preformed fibrils (Bolder et al., 2007a), high ionic strength (Loveday et al., 2010), Ca^{2+} (Loveday et al., 2011a; Loveday et al., 2010) Cu^{2+} (Zappone et al., 2013) are also likely to result in fibrils with slightly larger peptides.

During the nucleation step, the assembly-competent peptides align and form growth promoting nuclei (Aymard et al., 1999). The self-assembly during the lag phase is reversible until a critical size of nucleus is reached (Arnaudov et al., 2003; Aymard et al., 1999). The time required for nucleation is largely unaffected even when the assembly-opposing charges on the building blocks are screened with NaCl (Loveday et al., 2010). This reversibility of self-assembly in the lag phase could only be explained by fewer building blocks participating in nucleation resulting into weak nuclei. The SDS-PAGE data (Chapter 4) clearly identified the major fibril peptides in the samples heated for short times and their concentrations increased with heating time. Thus, it is

Chapter 9. Overall Discussion and Avenues for Future Work

possible that the critical size of nuclei may, in turn, depend on a certain minimum concentration of assembly-competent peptides necessary for strong intermolecular bonding.

The rate of acid hydrolysis of β -Lg (average $2.7 \pm 0.1 \times 10^{-3} \text{ min}^{-1}$) in this study (Chapters 4, 6 to 8) was closer to that reported during heating under shear ($3.9 \times 10^{-3} \text{ min}^{-1}$) (Kroes-Nijboer et al., 2011) indicating that shear did not affect acid hydrolysis and in these systems the rate of formation of assembly-competent peptides may be considered as constant. This means that the assembly-promoting effect of shear (Akkermans et al., 2006; Bolder et al., 2007a) is likely to arise from its effect on the self-assembly processes post-hydrolysis. This effect of shear is unlikely to result from enhanced diffusion (Chapter 7) and the most likely explanation for the effect of shear on the rate of self-assembly could involve shear-induced secondary nucleation by the fragmentation of growing nuclei or fibrillar intermediates (Hill et al., 2006). Based on the above discussion, it can be concluded that under the conventional heating conditions (without any cosolutes or protein modification) the rate-limiting step during nucleation and growth was the hydrolysis of β -Lg, in agreement with the findings of Kroes-Nijboer et al. (2011).

In comparison, the association behavior of peptides was modified significantly by the glycation or by the presence of glycerol in the aqueous solutions. It is notable that the rate of hydrolysis was largely unaffected in these conditions but the resulting peptides failed to self-assemble into fibrils. Clearly, the rate-limiting step in these systems was the self-assembly of peptides into β -sheets of the fibrils. Significantly, for the first time it was shown in these studies (Chapter 6 and 7) that acid hydrolysis can be decoupled

Chapter 9. Overall Discussion and Avenues for Future Work

from the self-assembly of peptides. A schematic showing the mechanism of decoupling fibril formation from acid hydrolysis is shown in Figure 9.2.

These findings are significant as they allow a more detailed investigation of peptides participating in fibril formation or design systems for optimizing fibril-functionality. For example, microwave heating which facilitates alignment of building blocks into fibrils (Hettiarachchi et al., 2012) could be explored to make fibrils with enhanced functional properties from the glycated β -Lg (Liu et al., 2013a).

The inhibition of fibril formation during the self-assembly from glycated β -Lg or in presence of cosolutes strongly indicates multiple aggregation pathways available for fibril-forming peptides during self-assembly. Fibril formation from proteins is a complex process and the main driving force during self-assembly is minimization of free energy. When the conditions of self-assembly were perturbed, it is possible that the conformations which minimize the free energy shifted to non-fibrillar aggregates. The direct evidence for one or more alternate pathways is provided by the TEM images of heated β -Lg and β -casein mixtures which showed the presence of long, twisted, irregular aggregates along with fibrils. In comparison, non-fibrillar aggregates formed, if any, from glycated β -Lg or in presence of glycerol were smaller than 100 kDa and absent in the TEM images of the heated samples. Further characterization of these aggregates may provide insights into their properties and opens up a new area of investigation of functionality of these aggregates.

Chapter 9. Overall Conclusions and Avenues For Future Work

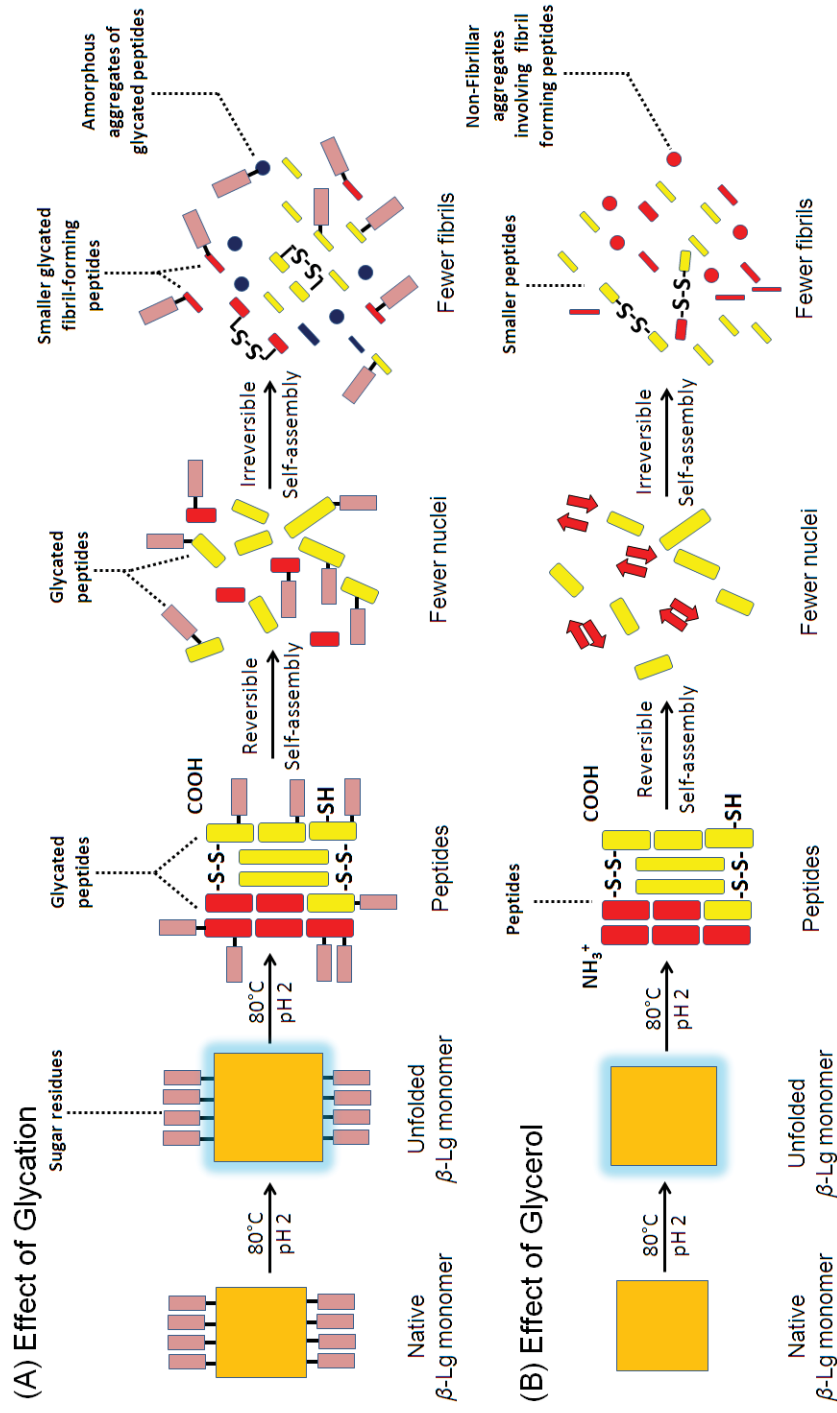


Figure 9.2 Strategies to decouple acid hydrolysis from self-assembly by modifying (A) glycation of β -Lg or (B) composition of aqueous solution by glycerol.

Chapter 9. Overall Discussion and Avenues for Future Work

To study the composition of fibrils, a new method for separation of the fibrils from the unassembled material using ultracentrifugation was developed. The composition of the fibrils and the unassembled fragments after different heating times was compared. This data confirmed previous reports that fibrils consist of only few peptides capable of self-assembly which belonged to the N-terminal region (1-53). Glycation of lysines in this region delayed nucleation indicating that this region may have an important role during nucleation and sequences from other regions of β -Lg may contribute only to the growth of fibrils. Overall, the sequences found in fibrils (Chapter 4) were in agreement with those observed by others (Akkermans et al., 2008b; Hettiarachchi et al., 2012). In general, it is not known why only a few sequences in the protein can form fibrils and numerous models have been proposed to predict the amyloidogenicity of protein (Bryan Jr et al., 2009; Frousios et al., 2009; Garbuzynskiy et al., 2010; Trovato et al., 2007). However, no single, universally accepted model is known and further research in this area is still ongoing.

The actual and predicted sequences of peptides in the fibrils covered all the major β -strands of β -Lg pointing to a possible relationship between the β -sheet rich regions and propensity to form fibrils. It is not known whether the β -strands had a role in promoting self-assembly. The MS and SDS-PAGE data in Chapter 4, for the first time provided strong evidence of disulfide bonding in the fibrils. Although the tertiary structure of β -Lg was completely destroyed within the first few minutes of heating, further disulfide-sulfahydril exchange reactions were inhibited due to the low pH resulting in protonation of free -SH groups. This indicates that the disulfide bonds in the native tertiary structure of β -Lg remain intact and that the disulfide bonding in the fibrils may be explained by the native Cys66-Cys160 linkage in the native structure. Bolder et al. (2007c) reported extensive disulfide bonding in heated

solutions containing fibrils when the solutions were stored at high pH (7 and 10). In that previous study fibrils were not separated from nonfibril material, but in this study the disulfide bonding in the fibrils was investigated after their separation by ultracentrifugation.

The substitution of amino acids in egg white lysozyme from different species has been shown to affect their amyloidogenicity. For example, the substitutions of Asp101 in chicken lysozyme (CL) by Gly in turkey lysozyme (TL) or Asp49 in CL with Gln in equine lysozyme (EL) altered the self-assembly kinetics (Krebs et al., 2004; Mishra et al., 2007). Similarly, the branched chain amino acid residues Ile, Val and Thr preferentially facilitate the formation of ordered β -sheets (Street et al., 1999). Thus, the substitutions in β -Lg A, B and C were expected to alter the kinetics of self-assembly especially for β -Lg A with substitutions at Asp64 and Val118. Similarly, the His59 substitution provided an additional positive charge to β -Lg C.

The kinetic parameters of self-assembly were similar for β -Lg A, B and C (Chapter 5) which indicates that these substitutions were not significant for self-assembly. This may be explained by careful consideration of the sequence homology of these proteins with similar sequence in the region 1-53 involved in the nucleation (Chapter 4). All the sites of substitutions in these proteins are outside this region and given the similar rates of acid hydrolysis, the pre-requisites for nuclei formation and their growth were unaffected in these proteins. It is interesting to note that the additional charge in β -Lg C due to the substitution His59 did not affect self-assembly. The likely explanation for this is that acid hydrolysis of β -Lg C monomer would separate the His59 on a single peptide, which may weaken the effect of the additional charge arising from this residue on the overall kinetics of self-assembly.

Chapter 9. Overall Discussion and Avenues for Future Work

β -Lg self-assembly attained a stationary phase after prolonged heating. Two possible mechanisms have been proposed for the termination step leading to a steady state in the rate of self-assembly. According to Bolder et al. (2007a), who assumed that fibrils are made up of unhydrolyzed β -Lg monomers, the termination of self-assembly upon prolonged heating can occur by the formation of intermolecular β -sheets, or by the hydrolysis of monomers or mature fibrils, which created fibril fragments unable to grow further. However, recent studies have shown that the fibrils are made up of peptides (Chapter 4) (Akkermans et al., 2008b; Hettiarachchi et al., 2012) and that acid hydrolysis promoted β -Lg self-assembly (Chapter 4) (Kroes-Nijboer et al., 2011). In addition, fibrils formed after prolonged heating (≥ 10 h at 80 °C) are capable of self-assembly, when used for seeding (Bolder et al., 2007a; Loveday et al., 2012b) and their fragmentation, if any, is only expected to speed up the rate of self-assembly in accordance with the effect of shear (Dunstan et al., 2009; Hill et al., 2006). In addition, as noted in Chapter 4 the peptides in fibrils did not change with heating. Thus, mechanistically the stationary phase may be attributed to the lack of building blocks available for self-assembly. This means that factors, such as shear, primarily affect the self-assembly of building blocks in the early stages and effectively reduce the time required to attain a given f_{\max} in the stationary phase. This is supported by the studies which note that shear treatment during the initial stages of self-assembly was sufficient to promote self-assembly but continuous shearing during heat-treatment did not have an additional self-assembly promoting effect (Akkermans et al., 2006; Bolder et al., 2007a).

Overall, this study has added a number of useful new insights about the mechanism of self-assembly. β -Lg self-assembly pathway essentially consists of multi-step transitions occurring in sequence until the highly stable fibrillar aggregated state

with minimum free energy is achieved. The understanding of the mechanism of self-assembly has shed light on the molecular basis for the effects of some previous studies e.g. effect of shear. Perturbing the conditions of self-assembly by either using chemically modified β -Lg, or by altering the composition of aqueous solution modified the association behavior of building blocks diverting the aggregation towards non-fibrillar pathways. The features of these alternate pathways and the properties of final aggregates resulting from these pathways open up a potential area of future work. By selecting, appropriate conditions of protein self-assembly, fibrils with desired functionality could be generated.

9.3. Applications

The findings of the study have a number of potential applications:

- The information about the mechanism of β -Lg self-assembly may provide useful insights about the self-assembly of other globular proteins, such as lysozyme, α -lactalbumin and bovine serum albumin which self-assemble under similar conditions.
- The knowledge of the self-assembly processes and the factors slowing down these processes (Chapters 4 to 8) could be used to design protocols for the control of β -Lg self-assembly and explore potential functionalities of the fibrils.
- Protein engineering approaches targeting improved functional properties of β -Lg fibrils could be adopted based on the results of Chapter 5. In such an approach, the point-mutations downstream to the sequence responsible for nucleation (1-53) could be adopted for obtaining desired functionality.

- The information derived from the self-assembly of glycosylated β -Lg (Chapter 6) would help in predicting the impact of β -Lg modification on its assembly properties. In addition, the results of this study will also help in adopting suitable protocols for preparing fibrils from chemically modified β -Lg. New approaches which enhance peptide-peptide interactions, such as microwave heating (Hettiarachchi et al., 2012), could be adopted to promote fibril formation from glycosylated β -Lg for which the rate-limiting step during self-assembly was peptide-peptide interactions.
- The properties of the different functional groups in the sequences in the fibrils, e.g. amine groups of lysine, and arginine, carbohydrate groups in glycosylated β -Lg or disulfide bonds, could be exploited to fine-tune applications. Some examples of these include cross-linking to improve stability, immobilizing enzymes, or delivery of bioactive components. Munialo et al. (2013) have used thiolation of Cys residues in β -Lg fibrils to modulate their gelation properties.
- The nano-sized aggregates formed during the co-self-assembly of β -Lg and β -casein could be used for applications similar to that of the fibrils.
- The fibrils can be explored as carriers for the delivery of bioactive peptides. Based on the sequence information for β -Lg, bioactive polypeptides of interest can be blended with hydrolysates of β -Lg and fibrils can be prepared by microwave treatments.

9.4. Avenues for Further Work

In light of the data obtained from this study, a number of potential areas are recommended for further work.

- Under the conditions used in the study (1% β -Lg, pH 2 and 80 °C) hydrolysis appeared to be necessary for self-assembly. However, it is not known whether hydrolysis would be necessary at higher protein concentrations. At these concentrations, the rates of self-assembly are likely to increase and could be a net effect of two mechanisms. A net higher proportion of peptides, released due to the simultaneous hydrolysis of a large population of β -Lg monomers, would promote self-assembly. In addition, the association properties of peptides would be expected to be modified due to an increased frequency of polypeptide contacts which may eliminate the requirement of extensive hydrolysis as that required at low concentrations. Thus, a detailed investigation, similar to that in Chapter 4, may elucidate the effect of protein concentration on β -Lg self-assembly.
- An investigation of the role of elements of secondary and tertiary structures during self-assembly can provide useful insights into the strategies to design systems for model self-assembly studies. Hamada et al. (2009) compared the fibril-forming propensities of different β -strands and thiol modified β -Lg. The results of this study showed sequences covering the β -strands of β -Lg fibrils formed at pH 2. A systematic study comparing the amyloidogenicity of different β -strands can clarify the role of sequence specificity and the secondary structure conformations during β -Lg self-assembly.

- It is not known whether hydrolysis of β -Lg monomers would promote its self-assembly at pH 7 in the presence of urea. A β -Lg hydrolysate prepared by enzymatic hydrolysis or acid hydrolysis using glycerol may be incubated at pH 7 in presence of urea to investigate whether hydrolysis of monomers is able to increase the rate of self-assembly.
- Ikeda et al. (2002) noted that the diameter of fibrils from WPI was almost twice as that of fibrils from pure β -Lg. Whey proteins α -lactalbumin (α -La) and bovine serum albumin (BSA), can form fibrils under conditions similar to those used in this study, although their self-assembly requires small to moderate amounts of NaCl (Goers et al., 2002; Veerman et al., 2003c). The co-self-assembly of whey protein mixtures by selecting appropriate conditions could be explored to increase the net yield of fibrils from whey protein isolate.
- The formation of novel non-fibrillar nanoaggregates formed upon heating in β -Lg- β -casein mixtures provides an interesting area of future research. The characterization of aggregation processes in these systems may be useful in exploring their novel functionalities. In addition, based on the findings of this study, β -Lg-sodium caseinate interactions could be explored in detail.
- Polyols are known to modulate the rheological properties of heat-set gels of globular proteins by influencing the protein-protein interactions in the gel structure (Baier et al., 2004; Baier et al., 2005; Chantrapornchai et al., 2002; Dierckx et al., 2002). The use of polyols to modulate the mechanical properties of the fibrils provides an interesting area for future investigation.

- Large macromolecular crowding agents, such as dextrans or polyethylene glycols, or other large molecular weight synthetic polymers greatly affect the kinetics of self-assembly of model peptides (Sukenik et al., 2012; Sukenik et al., 2011) and proteins (Munishkina et al., 2008) including β -Lg in the presence of urea (Ma et al., 2013). Understanding of the effect of macromolecular crowding on β -Lg self-assembly at pH 2 could provide further insights about the mechanism of fibril formation.
- The self-assembly of β -Lg in the presence of lipids has not yet been explored to date and could provide further information about protein-lipid interactions, β -Lg self-assembly and allow new functionalities and design strategies for emulsion studies.
- For designing successful commercial food applications of fibrils, their stability during common food processing unit operations such as heating, concentration and drying, needs to be determined. A composite design of experimental studies to investigate the effects of these operations may help to fine-tune the fibril properties for specific applications.
- The final frontier for successful adoption of fibrils for food applications is their safety. Very recent research suggests that mature fibrils of β -Lg are resistant to *in vitro* digestion by gastrointestinal proteases, but did not display any toxicity to Caco-2 cell lines (Lasse, 2013). In contrast, Bateman et al. (2010) showed that β -Lg fibrils could be easily hydrolyzed in simulated gastric fluids *in vitro*, however prolonged incubation promoted self-assembly generating fibrils with shorter peptides. Similar studies evaluating the safety of β -Lg fibrils with tailor-made functional

Chapter 9. Overall Discussion and Avenues for Future Work

properties, e.g. fibrils from glycated β -Lg (Liu et al., 2013a), may help to ensure food safety and their successful food applications.

- Future studies to evaluate dissociation/digestion of fibrils by gastrointestinal proteases will assist in the standardization of their applications, as carriers of functionally active biomolecules.

10. References

- Adamcik, J., Jung, J. M., Flakowski, J., de Los Rios, P., et al. (2010). Understanding amyloid aggregation by statistical analysis of atomic force microscopy. *Nature Nanotechnology*, 20(SUPPL.3), 180.
- Akkermans, C., van der Goot, A. J., Venema, P., Gruppen, H., et al. (2007). Micrometer-sized fibrillar protein aggregates from soy glycinin and soy protein isolate. *Journal of Agricultural and Food Chemistry*, 55(24), 9877-9882.
- Akkermans, C., Venema, P., Rogers, S. S., van der Goot, A. J., et al. (2006). Shear pulses nucleate fibril aggregation. *Food Biophysics*, 1(3), 144-150.
- Akkermans, C., Venema, P., van der Goot, A. J., Boom, R. M., et al. (2008a). Enzyme-induced formation of β -lactoglobulin fibrils by AspN endoproteinase. *Food Biophysics*, 3(4), 390-394.
- Akkermans, C., Venema, P., van der Goot, A. J., Gruppen, H., et al. (2008b). Peptides are building blocks of heat-induced fibrillar protein aggregates of β -lactoglobulin formed at pH 2. *Biomacromolecules*, 9, 1474-1479.
- Alting, A. C., de Jongh, H. H. J., Visschers, R. W., & Simons, J. (2002). Physical and chemical interactions in cold gelation of food proteins. *Journal of Agricultural and Food Chemistry*, 50(16), 4682-4689.
- Anuradha, S. N., & Prakash, V. (2008). Structural stabilization of bovine β -lactoglobulin in presence of polyhydric alcohols. *Indian Journal of Biotechnology*, 7(4), 437-447.
- Aouzelleg, A., Bull, L. A., Price, N. C., & Kelly, S. M. (2004). Molecular studies of pressure/temperature-induced structural changes in bovine β -lactoglobulin. *Journal of the Science of Food and Agriculture*, 84(5), 398-404.
- Arakawa, T., & Timasheff, S. N. (1982a). Preferential interactions of proteins with salts in concentrated solutions. *Biochemistry*, 21(25), 6545-6552.
- Arakawa, T., & Timasheff, S. N. (1982b). Stabilization of protein-structure by sugars. *Biochemistry*, 21(25), 6536-6544.
- Arakawa, T., & Timasheff, S. N. (1983). Preferential interactions of proteins with solvent components in aqueous amino acid solutions. *Archives of Biochemistry and Biophysics*, 224(1), 169-177.

References

- Arima, S., Niki, R., & Takase, K. (1979). Structure of β -casein. *Journal of Dairy Research*, 46(2), 281-282.
- Armstrong, A. H., Chen, J., McKoy, A. F., & Hecht, M. H. (2011). Mutations that replace aromatic side chains promote aggregation of the Alzheimers A β peptide. *Biochemistry*, 50(19), 4058-4067.
- Arnaudov, L. N., & de Vries, R. (2006). Strong impact of ionic strength on the kinetics of fibrillar aggregation of bovine β -lactoglobulin. *Biomacromolecules*, 7(12), 3490-3498.
- Arnaudov, L. N., de Vries, R., Ippel, H., & van Mierlo, C. P. M. (2003). Multiple steps during the formation of β -lactoglobulin fibrils. *Biomacromolecules*, 4(6), 1614-1622.
- Aymard, P., Durand, D., & Nicolai, T. (1996). The effect of temperature and ionic strength on the dimerisation of β -lactoglobulin. *International Journal of Biological Macromolecules*, 19(3), 213-221.
- Aymard, P., Nicolai, T., Durand, D., & Clark, A. (1999). Static and dynamic scattering of β -lactoglobulin aggregates formed after heat-induced denaturation at pH 2. *Macromolecules*, 32(8), 2542-2552.
- Azriel, R., & Gazit, E. (2001). Analysis of the minimal amyloid-forming fragment of the islet amyloid polypeptide. An experimental support for the key role of the phenylalanine residue in amyloid formation. *Journal of Biological Chemistry*, 276(36), 34156-34161.
- Back, J. F., Oakenfull, D., & Smith, M. B. (1979). Increased thermal stability of proteins in the presence of sugars and polyols. *Biochemistry*, 18(23), 5191-5196.
- Baier, S. K., Decker, E. A., & McClements, D. J. (2004). Impact of glycerol on thermostability and heat-induced gelation of bovine serum albumin. *Food Hydrocolloids*, 18(1), 91-100.
- Baier, S. K., & McClements, D. J. (2003). Impact of sorbitol on the thermostability and heat-induced gelation of bovine serum albumin. *Food Research International*, 36(9-10), 1081-1087.
- Baier, S. K., & McClements, D. J. (2005). Influence of cosolvent systems on the gelation mechanism of globular protein: Thermodynamic, kinetic, and structural aspects of globular protein gelation. *Comprehensive Reviews in Food Science and Food Safety*, 4(3), 43-54.

-
- Bateman, L., Ye, A. Q., & Singh, H. (2010). *In vitro* digestion of β -lactoglobulin fibrils formed by heat treatment at low pH. *Journal of Agricultural and Food Chemistry*, 58(17), 9800-9808.
- Bauer, R., Carrotta, R., Rischel, C., & Ogendal, L. (2000). Characterization and isolation of intermediates in β -lactoglobulin heat aggregation at high pH. *Biophysical Journal*, 79(2), 1030-1038.
- Baussay, K., Le Bon, C., Nicolai, T., Durand, D., et al. (2004). Influence of the ionic strength on the heat-induced aggregation of the globular protein β -lactoglobulin at pH 7. *International Journal of Biological Macromolecules*, 34(1-2), 21-28.
- Bekard, I. B., Asimakis, P., Bertolini, J., & Dunstan, D. E. (2011). The effects of shear flow on protein structure and function. *Biopolymers*, 95(11), 733-745.
- Bell, K., McKenzie, H. A., & Shaw, D. C. (1968). Amino acid composition and peptide maps of β -lactoglobulin variants. *Biochimica et Biophysica Acta-Protein Structure*, 154(2), 284-294.
- Belloque, J., & Smith, G. M. (1998). Thermal denaturation of β -lactoglobulin. A 1H NMR Study. *Journal of Agricultural and Food Chemistry*, 46(5), 1805-1813.
- Beringhelli, T., Eberini, I., Galliano, M., Pedoto, A., et al. (2002). pH and ionic strength dependence of protein (Un)folding and ligand binding to bovine β -lactoglobulins A and B. *Biochemistry*, 41(51), 15415-15422.
- Berry, G. P., & Creamer, L. K. (1975). The association of bovine β -casein. The importance of the C-terminal region. *Biochemistry*, 14(16), 3542-3545.
- Berson, J. F., Theos, A. C., Harper, D. C., Tenza, D., et al. (2003). Proprotein convertase cleavage liberates a fibrillogenic fragment of a resident glycoprotein to initiate melanosome biogenesis. *Journal of Cell Biology*, 161(3), 521-533.
- Bewley, M. C., Qin, B. Y., Jameson, G. B., Sawyer, L., et al. (1997). Bovine β -lactoglobulin and its variants: A three-dimensional structural perspective. *Proceedings of the IDF Seminar "Milk Protein Polymorphism II"* (pp. 100-109). Brussels, Belgium International Dairy Federation.
- Bhattacharyya, J., & Das, K. P. (1999). Molecular chaperone-like properties of an unfolded protein, α_s -casein. *Journal of Biological Chemistry*, 274(22), 15505-15509.

References

- Biancalana, M., & Koide, S. (2010). Molecular mechanism of Thioflavin-T binding to amyloid fibrils. *Biochimica et Biophysica Acta - Proteins and Proteomics*, 1804(7), 1405-1412.
- Biancalana, M., Makabe, K., Koide, A., & Koide, S. (2008). Aromatic cross-strand ladders control the structure and stability of β -rich peptide self-assembly mimics. *Journal of Molecular Biology*, 383(1), 205-213.
- Biemann, K., & Scoble, H. A. (1987). Characterization by tandem mass spectrometry of structural modifications in proteins. *Science*, 237(4818), 992-998.
- Bikker, J. F., Anema, S. G., Li, Y., & Hill, J. P. (2000). Thermal denaturation of β -lactoglobulin A, B and C in heated skim milk. *Milchwissenschaft*, 55(11), 609-613.
- Blackburn, S., & Lee, G. R. (1954). The liberation of aspartic acid during the acid hydrolysis of proteins. *Biochemical Journal*, 58(2), 227-231.
- Bolder, S. G., Hendrickx, H., Sagis, L. M. C., & van der Linden, E. (2006). Fibril assemblies in aqueous whey protein mixtures. *Journal of Agricultural and Food Chemistry*, 54(12), 4229-4234.
- Bolder, S. G., Sagis, L. M. C., Venema, P., & van der Linden, E. (2007a). Effect of stirring and seeding on whey protein fibril formation. *Journal of Agricultural and Food Chemistry*, 55(14), 5661-5669.
- Bolder, S. G., Sagis, L. M. C., Venema, P., & van der Linden, E. (2007b). Thioflavin T and birefringence assays to determine the conversion of proteins into fibrils. *Langmuir*, 23(8), 4144-4147.
- Bolder, S. G., Vasbinder, A. J., Sagis, L. M. C., & van der Linden, E. (2007c). Heat-induced whey protein isolate fibrils: conversion, hydrolysis, and disulphide bond formation. *International Dairy Journal*, 17(7), 846-853.
- Bolisetty, S., Adamcik, J., Heier, J., & Mezzenga, R. (2012). Amyloid directed synthesis of titanium dioxide nanowires and their applications in hybrid photovoltaic devices. *Advanced Functional Materials*, 22(16), 3424-3428.
- Bolisetty, S., Vallooran, J. J., Adamcik, J., & Mezzenga, R. (2013). Magnetic-responsive hybrids of Fe₃O₄ nanoparticles with β -lactoglobulin amyloid fibrils and nanoclusters. *ACS Nano*, 7(7), 6146-6155.

-
-
- Bouma, B., Kroon-Batenburg, L. M. J., Wu, Y. P., Brunjes, B., et al. (2003). Glycation induces formation of amyloid cross- β structure in albumin. *Journal of Biological Chemistry*, 278(43), 41810-41819.
- Bowerman, C. J., Ryan, D. M., Nissan, D. A., & Nilsson, B. L. (2009). The effect of increasing hydrophobicity on the self-assembly of amphipathic β -sheet peptides. *Molecular BioSystems*, 5(9), 1058-1069.
- Boye, J. I., Ismail, A. A., & Alli, I. (1996). Effects of physicochemical factors on the secondary structure of β -lactoglobulin. *Journal of Dairy Research*, 63(1), 97-109.
- Boye, J. I., Ma, C. Y., & Ismail, A. (2004). Thermal stability of β -lactoglobulins A and B: Effect of SDS, urea, cysteine and N-ethylmaleimide. *Journal of Dairy Research*, 71(2), 207-215.
- Boye, J. I., Ma, C. Y., Ismail, A., Harwalkar, V. R., et al. (1997). Molecular and microstructural studies of thermal denaturation and gelation of β -lactoglobulins A and B. *Journal of Agricultural and Food Chemistry*, 45(5), 1608-1618.
- Broersen, K., Elshof, M., de Groot, J., Voragen, A. G. J., et al. (2007). Aggregation of β -lactoglobulin regulated by glucosylation. *Journal of Agricultural and Food Chemistry*, 55(6), 2431-2437.
- Broersen, K., Voragen, A. G. J., Hamer, R. J., & de Jongh, H. H. J. (2004). Glycoforms of β -lactoglobulin with improved thermostability and preserved structural packing. *Biotechnology and Bioengineering*, 86(1), 78-87.
- Bromley, E. H. C., Krebs, M. R. H., & Donald, A. M. (2005). Aggregation across the length-scales in β -lactoglobulin. *Faraday Discussions*, 128, 13-27.
- Broome, B. M., & Hecht, M. H. (2000). Nature disfavors sequences of alternating polar and non-polar amino acids: Implications for amyloidogenesis. *Journal of Molecular Biology*, 296(4), 961-968.
- Brownlow, S., Morais Cabral, J. H., Cooper, R., Flower, D. R., et al. (1997). Bovine β -lactoglobulin at 1.8 Å resolution - Still an enigmatic lipocalin. *Structure*, 5(4), 481-495.
- Bryan Jr, A. W., Menke, M., Cowen, L. J., Lindquist, S. L., et al. (2009). Betascan: Probable β -amyloids identified by pairwise probabilistic analysis. *PLoS Computational Biology*, 5(3).
-

References

- Bryant, C. M., & McClements, D. J. (1998). Molecular basis of protein functionality with special consideration of cold-set gels derived from heat-denatured whey. *Trends in Food Science & Technology*, 9(4), 143-151.
- Buchheim, W., & Schmidt, D. G. (1979). On the size of monomers and polymers of β -casein. *Journal of Dairy Research*, 46(2), 277-280.
- Burova, T. V., Choiset, Y., Tran, V., & Haertle, T. (1998). Role of free Cys121 in stabilization of bovine β -lactoglobulin B. *Protein Engineering*, 11(11), 1065-1073.
- Byler, D. M., Farrell, H. M., & Susi, H. (1988). Raman-spectroscopic study of casein structure. *Journal of Dairy Science*, 71(10), 2622-2629.
- Cairolì, S., Iametti, S., & Bonomi, F. (1994). Reversible and irreversible modifications of β -lactoglobulin upon exposure to heat. *Journal of Protein Chemistry*, 13(3), 347-354.
- Candiano, G., Bruschi, M., Musante, L., Santucci, L., et al. (2004). Blue silver: A very sensitive colloidal Coomassie G-250 staining for proteome analysis. *Electrophoresis*, 25(9), 1327-1333.
- Carver, J. A., Rekas, A., Thorn, D. C., & Wilson, M. R. (2003). Small heat-shock proteins and clusterin: Intra- and extracellular molecular chaperones with a common mechanism of action and function? *IUBMB Life*, 55(12), 661-668.
- Casal, H. L., Kohler, U., & Mantsch, H. H. (1988). Structural and conformational changes of β -lactoglobulin B: An infrared spectroscopic study of the effect of pH and temperature. *Biochimica et Biophysica Acta - Protein Structure and Molecular Enzymology*, 957(1), 11-20.
- Cayot, P. (1991). Emulsifying properties of pure and mixed α_{s1} - and β -casein fractions: Effects of chemical glycosylation. *Journal of Agricultural and Food Chemistry*, 39(8), 1369-1373.
- Chanasattru, W., Decker, E. A., & McClements, D. J. (2007a). Modulation of thermal stability and heat-induced gelation of β -lactoglobulin by high glycerol and sorbitol levels. *Food Chemistry*, 103(2), 512-520.
- Chanasattru, W., Decker, E. A., & McClements, D. J. (2007b). Physicochemical basis for cosolvent modulation of β -lactoglobulin functionality: Interfacial tension study. *Food Research International*, 40(8), 1098-1105.

-
-
- Chanasattru, W., Decker, E. A., & McClements, D. J. (2008). Impact of cosolvents (polyols) on globular protein functionality: Ultrasonic velocity, density, surface tension and solubility study. *Food Hydrocolloids*, 22(8), 1475-1484.
- Chantrapornchai, W., & McClements, D. J. (2002). Influence of glycerol on optical properties and large-strain rheology of heat-induced whey protein isolate gels. *Food Hydrocolloids*, 16(5), 461-466.
- Chapman, M. R., Robinson, L. S., Pinkner, J. S., Roth, R., et al. (2002). Role of Escherichia coli curli operons in directing amyloid fiber formation. *Science*, 295(5556), 851-855.
- Cheison, S. C., Lai, M. Y., Leeb, E., & Kulozik, U. (2011). Hydrolysis of β -lactoglobulin by trypsin under acidic pH and analysis of the hydrolysates with MALDI-TOF-MS/MS. *Food Chemistry*, 125(4), 1241-1248.
- Chevalier, F., Chobert, J. M., Dalgalarondo, M., Choiset, Y., et al. (2002). Maillard glycation of β -lactoglobulin induces conformation changes. *Nahrung-Food*, 46(2), 58-63.
- Chevalier, F., Chobert, J. M., Dalgalarondo, M., & Haertle, T. (2001a). Characterization of the Maillard reaction products of β -lactoglobulin glucosylated in mild conditions *Journal of Food Biochemistry*, 25(1), 33-55.
- Chevalier, F., Chobert, J. M., Popineau, Y., Nicolas, M. G., et al. (2001b). Improvement of functional properties of β -lactoglobulin glycated through the Maillard reaction is related to the nature of the sugar. *International Dairy Journal*, 11(3), 145-152.
- Chiti, F., & Dobson, C. M. (2006). Protein misfolding, functional amyloid, and human disease. *Annual Review of Biochemistry*, 75, 333-366.
- Cioci, F. (1996). Effect of surface tension on the stability of heat-stressed proteins: A molecular thermodynamic interpretation. *Journal of Physical Chemistry*, 100(43), 17400-17405.
- Clark, A. H., Kavanagh, G. M., & Ross-Murphy, S. B. (2001). Globular Protein Gelation - Theory and Experiment. *Food Hydrocolloids*, 15(4-6), 383-400.
- Cohen, A. S. (1986). General introduction and a brief history of the amyloid fibril. In J. Marrink & M. H. van Rijswijk (Eds.), *Amyloidosis* (pp. 3-19). Nijhoff, Dordrecht.
- Cosentino, U., Varí, M. R., Saracino, A. A. G., Pitea, D., et al. (2005). Tetracycline and its analogues as inhibitors of amyloid fibrils: Searching for a geometrical
-

References

- pharmacophore by theoretical investigation of their conformational behavior in aqueous solution. *Journal of Molecular Modeling*, 11(1), 17-25.
- Creamer, L. K., & Harris, D. P. (1997). Relationship between milk protein polymorphism and physico-chemical properties *Proceedings of the IDF Seminar "Milk Protein Polymorphism II"* (pp. 110-123). Brussels, Belgium International Dairy Federation.
- Creighton, T. E. (1993). *Proteins: Second edition*. New York, USA: W. H. Freeman and Co.
- Cukalevski, R., Boland, B., Frohm, B., Thulin, E., et al. (2012). Role of aromatic side chains in amyloid β -protein aggregation. *ACS Chemical Neuroscience*, 3(12), 1008-1016.
- Da Silva Pinto, M., Bouhallab, S., de Carvalho, A. F., Henry, G., et al. (2012). Glucose Slows Down the Heat-Induced Aggregation of β -lactoglobulin at Neutral pH *Journal of Agricultural and Food Chemistry*, 60(1), 214-219.
- Dalgleish, D. G. (1990). The effect of denaturation of β -lactoglobulin on renneting - a quantitative study. *Milchwissenschaft*, 45(8), 491-&.
- Dalgleish, D. G. (1997). Structure-function relationships of caseins. In S. Damodaran (Ed.), *Food Proteins and Their Applications* (pp. 199-223). New York, USA: Marcel Dekker.
- Damodaran, S. (1996). Amino acids, peptides and proteins. In O. R. Fennema (Ed.), *Food Chemistry* (3rd ed.): Dekker, New York.
- Dannenbergh, F., & Kessler, H. G. (1988). Thermodynamic approach to kinetics of β -lactoglobulin denaturation in heated skim milk and sweet whey. *Milchwissenschaft*, 43(3), 139-142.
- de Kruif, C. G., & Grinberg, V. Y. (2002). Micellisation of β -casein. *Colloids and Surfaces A: Physicochemical and Engineering Aspects*, 210(2-3), 183-190.
- Dierckx, S., & Huyghebaert, A. (2002). Effects of sucrose and sorbitol on the gel formation of a whey protein isolate. *Food Hydrocolloids*, 16(5), 489-497.
- Diezel, W., Kopperschläger, G., & Hofmann, E. (1972). An improved procedure for protein staining in polyacrylamide gels with a new type of Coomassie Brilliant Blue. *Analytical Biochemistry*, 48(2), 617-620.
- Dobson, C. M. (1999). Protein misfolding, evolution and disease. *Trends in Biochemical Sciences*, 24(9), 329-332.

-
-
- Dobson, C. M. (2003a). Protein folding and disease: A view from the first Horizon Symposium. *Nature Reviews Drug Discovery*, 2(2), 154-160.
- Dobson, C. M. (2003b). Protein folding and misfolding. *Nature*, 426(6968), 884-890.
- Dobson, C. M., Swoboda, B. E. P., Joniau, M., & Weissman, C. (2001). The structural basis of protein folding and its links with human disease. *Philosophical Transactions of the Royal Society B: Biological Sciences*, 356(1406), 133-145.
- Dunn, M. J. (1993a). *Electrophoresis in presence of additives*. Oxford, UK: BIOS Scientific Publishers Limited.
- Dunn, M. J. (1993b). *Properties of polyacrylamide gels*. Oxford, UK: BIOS Scientific Publishers Limited.
- Dunstan, D. E., Hamilton-Brown, P., Asimakis, P., Ducker, W., et al. (2009). Shear-induced structure and mechanics of β -lactoglobulin amyloid fibrils. *Soft Matter*, 5(24), 5020-5028.
- Durand, D., Gimel, J. C., & Nicolai, T. (2002). Aggregation, gelation and phase separation of heat denatured globular proteins. *Physica A: Statistical Mechanics and its Applications*, 304(1-2), 253-265.
- Ellis, R. J. (1988). Proteins as molecular chaperones. *Nature*, 328(6129), 378-379.
- Ellis, R. J. (1993). The general concept of molecular chaperones. *Philosophical transactions of the Royal Society of London. Series B: Biological sciences*, 339(1289), 257-261.
- Ellis, R. J. (2001). Macromolecular crowding: Obvious but underappreciated. *Trends in Biochemical Sciences*, 26(10), 597-604.
- Elofsson, U. M., Dejmeek, P., & Paulsson, M. A. (1996). Heat-induced aggregation of β -lactoglobulin studied by dynamic light scattering. *International Dairy Journal*, 6(4), 343-357.
- Eng, J. K., McCormack, A. L., & Yates, J. R. (1994). An approach to correlate tandem mass spectral data of peptides with amino acid sequences in a protein database. *Journal of the American Society for Mass Spectrometry*, 5(11), 976-989.
- Euston, S. R., Ur-Rehman, S., & Costello, G. (2007). Denaturation and aggregation of β -lactoglobulin-A preliminary molecular dynamics study. *Food Hydrocolloids*, 21(7), 1081-1091.
-

References

- Fandrich, M. (2007). On the structural definition of amyloid fibrils and other polypeptide aggregates. *Cellular and Molecular Life Sciences*, *64*(16), 2066-2078.
- Farrell Jr, H. M., Wickham, E. D., Unruh, J. J., Qi, P. X., et al. (2001). Secondary structural studies of bovine caseins: Temperature dependence of β -casein structure as analyzed by circular dichroism and FTIR spectroscopy and correlation with micellization. *Food Hydrocolloids*, *15*(4-6), 341-354.
- Fenaille, F., Morgan, F., Parisod, V., Tabet, J. C., et al. (2004). Solid-state glycation of β -lactoglobulin by lactose and galactose: localization of the modified amino acids using mass spectrometric techniques. *Journal of Mass Spectrometry*, *39*(1), 16-28.
- Fogliano, V., Monti, S. M., Visconti, A., Randazzo, G., et al. (1998). Identification of a β -lactoglobulin lactosylation site. *Biochimica et Biophysica Acta, Protein Structure and Molecular Enzymology*, *1388*(2), 295-304.
- French, S. J., Harper, W. J., Kleinholz, N. M., Jones, R. B., et al. (2002). Maillard reaction induced lactose attachment to bovine β -lactoglobulin: Electrospray ionization and matrix-assisted laser desorption/ionization examination. *Journal of Agricultural and Food Chemistry*, *50*(4), 820-823.
- Frousios, K. K., Iconomidou, V. A., Karletidi, C. M., & Hamodrakas, S. J. (2009). Amyloidogenic determinants are usually not buried. *BMC Structural Biology*, *9*.
- Galani, D., & Owusu Apenten, R. K. (1999). Heat-induced denaturation and aggregation of β -lactoglobulin: Kinetics of formation of hydrophobic and disulphide-linked aggregates. *International Journal of Food Science and Technology*, *34*(5-6), 467-476.
- Gangnard, S., Zuev, Y., Gaudin, J. C., Fedotov, V., et al. (2007). Modifications of the charges at the N-terminus of bovine β -casein: Consequences on its structure and its micellisation. *Food Hydrocolloids*, *21*(2), 180-190.
- Gao, Y. Z., Xu, H. H., Ju, T. T., & Zhao, X. H. (2013). The effect of limited proteolysis by different proteases on the formation of whey protein fibrils. *Journal of Dairy Science*, *96*(12), 7383-7392.
- Garbuzynskiy, S. O., Lobanov, M. Y., & Galzitskaya, O. V. (2010). FoldAmyloid: A method of prediction of amyloidogenic regions from protein sequence. *Bioinformatics*, *26*(3), 326-332.

-
-
- Gazit, E. (2002). A possible role for π -stacking in the self-assembly of amyloid fibrils. *FASEB Journal*, 16(1), 77-83.
- Geddes, A. J., Parker, K. D., Atkins, E. D. T., & Beighton, E. (1968). "Cross- β " conformation in proteins. *Journal of Molecular Biology*, 32(2), 343-344,IN323,345-358.
- Gekko, K., & Timasheff, S. N. (1981a). Mechanism of protein stabilization by glycerol: Preferential hydration in glycerol-water mixtures. *Biochemistry*, 20(16), 4667-4676.
- Gekko, K., & Timasheff, S. N. (1981b). Thermodynamic and kinetic examination of protein stabilization by glycerol. *Biochemistry*, 20(16), 4677-4686.
- Gerlsma, S. Y. (1968). Reversible denaturation of ribonuclease in aqueous solutions as influenced by polyhydric alcohols and some other additives. *Journal of Biological Chemistry*, 243(5), 957-961.
- Gerlsma, S. Y. (1970). Effects of polyhydric and monohydric alcohols on heat induced reversible denaturation of chymotrypsinogen-A. *European Journal of Biochemistry*, 14(1), 150-&.
- Gerrard, J. A. (2002). Protein-protein crosslinking in food: Methods, consequences, applications. *Trends in Food Science and Technology*, 13(12), 389-397.
- Gerrard, J. A., Lasse, M., Cottam, J., Healy, J. P., et al. (2012). Aspects of physical and chemical alterations to proteins during food processing - Some implications for nutrition. *British Journal of Nutrition*, 108(SUPPL. 2), S288-S297.
- Gezimati, J., Creamer, L. K., & Singh, H. (1997). Heat-induced interactions and gelation of mixtures of β -lactoglobulin and α -lactalbumin. *Journal of Agricultural and Food Chemistry*, 45(4), 1130-1136.
- Ghahghaei, A., Bathaie, S., Shahraki, A., & Asgarabad, F. R. (2011). Comparison of the chaperoning action of glycerol and β -casein on aggregation of proteins in the presence of crowding Zahra agent. *International Journal of Peptide Research and Therapeutics*, 17(2), 101-111.
- Goers, J., Permyakov, S. E., Permyakov, E. A., Uversky, V. N., et al. (2002). Conformational prerequisites for α -lactalbumin fibrillation. *Biochemistry*, 41(41), 12546-12551.
- Gordon, A. H. (1975). Applicability of starch and acrylamide zone electrophoresis In T. S. Work & E. Work (Eds.), *Electrophoresis of Proteins in Polyacrylamide*
-

References

- and Starch Gels* (7 ed., pp. 7-33). Amsterdam: North Holland Publishing Company.
- Gosal, W. S., Clark, A. H., Pudney, P. D. A., & Ross-Murphy, S. B. (2002). Novel amyloid fibrillar networks derived from a globular protein: β -lactoglobulin. *Langmuir*, *18*(19), 7174-7181.
- Gough, P., & Jenness, R. (1962). Heat denaturation of β -lactoglobulins A and B. *Journal of Dairy Science*, *45*(9), 1033-1039.
- Gras, S. L., Tickler, A. K., Squires, A. M., Devlin, G. L., et al. (2008). Functionalised amyloid fibrils for roles in cell adhesion. *Biomaterials*, *29*(11), 1553-1562.
- Green, D. W., Aschaffenburg, R., Camerman, A., Coppola, J. C., et al. (1979). Structure of bovine β -lactoglobulin at 6 Å resolution. *Journal of Molecular Biology*, *131*(2), 375-397.
- Griffin, W. G., Griffin, M. C. A., Martin, S. R., & Price, J. (1993). Molecular basis of thermal aggregation of bovine β -lactoglobulin A. *Journal of the Chemical Society, Faraday Transactions*, *89*(18), 3395-3406.
- Groenning, M., Olsen, L., van de Weert, M., Flink, J. M., et al. (2007). Study on the binding of Thioflavin T to β -sheet-rich and non- β -sheet cavities. *Journal of Structural Biology*, *158*(3), 358-369.
- Groves, M. L., Hipp, N. J., & McMeekin, T. L. (1951). Effect of pH on the denaturation of β -lactoglobulin and its dodecyl sulfate derivative. *Journal of the American Chemical Society*, *73*(6), 2790-2793.
- Grudzielanek, S., Jansen, R., & Winter, R. (2005). Solvational tuning of the unfolding, aggregation and amyloidogenesis of insulin. *Journal of Molecular Biology*, *351*(4), 879-894.
- Hamada, D., & Dobson, C. M. (2002). A kinetic study of β -lactoglobulin amyloid fibril formation promoted by urea. *Protein Science*, *11*(10), 2417-2426.
- Hamada, D., Segawa, S., & Goto, Y. (1996). Non-native α -helical intermediate in the refolding of β -lactoglobulin, a predominantly β -sheet protein. *Nature Structural Biology*, *3*(10), 868-873.
- Hamada, D., Tanaka, T., Tartaglia, G. G., Pawar, A., et al. (2009). Competition between folding, native-state dimerisation and amyloid aggregation in β -lactoglobulin. *Journal of Molecular Biology*, *386*(3), 878-890.

-
-
- Harris, J. I., Cole, R. D., & Pon, N. G. (1956). The kinetics of acid hydrolysis of dipeptides. *Biochemical Journal*, 62(1), 154-159.
- Hartl, F. U., & Hayer-Hartl, M. (2002). Protein folding. Molecular chaperones in the cytosol: From nascent chain to folded protein. *Science*, 295(5561), 1852-1858.
- Hartl, F. U., & Hayer-Hartl, M. (2009). Converging concepts of protein folding *in vitro* and *in vivo*. *Nature Structural and Molecular Biology*, 16(6), 574-581.
- Harwalkar, V. R. (1980). Kinetics of thermal-denaturation of β -lactoglobulin at pH 2.5. *Journal of Dairy Science*, 63(7), 1052-1057.
- Harwalkar, V. R., & Ma, C. Y. (1992). Evaluation of interactions of β -lactoglobulin by DSC. *Protein Interactions*.
- Hassanisadi, M., Barzegar, A., Yousefi, R., Dalgalarrrondo, M., et al. (2008). Chemometric study of the aggregation of alcohol dehydrogenase and its suppression by β -caseins: A mechanistic perspective. *Analytica Chimica Acta*, 613(1), 40-47.
- Haug, I. J., Skar, H. M., Vegarud, G. E., Langsrud, T., et al. (2009). Electrostatic effects on β -lactoglobulin transitions during heat denaturation as studied by differential scanning calorimetry. *Food Hydrocolloids*, 23(8), 2287-2293.
- Havea, P., Singh, H., Creamer, L. K., & Campanella, O. H. (1998). Electrophoretic characterization of the protein products formed during heat treatment of whey protein concentrate solutions. *Journal of Dairy Research*, 65(1), 79-91.
- Hettiarachchi, C. A., Melton, L. D., Gerrard, J. A., & Loveday, S. M. (2012). Formation of β -lactoglobulin nanofibrils by microwave heating gives a peptide composition different from conventional heating. *Biomacromolecules*, 13(9), 2868-2880.
- Hill, E. K., Krebs, B., Goodall, D. G., Howlett, G. J., et al. (2006). Shear flow induces amyloid fibril formation. *Biomacromolecules*, 7(1), 10-13.
- Hoffman, M. A. M., & van Mil, P. J. J. M. (1999). Heat-induced aggregation of β -lactoglobulin as a function of pH. *Journal of Agricultural and Food Chemistry*, 47(5), 1898-1905.
- Hoffmann, M. A. M., & van Mil, P. J. J. M. (1997). Heat-induced aggregation of β -lactoglobulin: Role of the free thiol group and disulfide bonds. *Journal of Agricultural and Food Chemistry*, 45(8), 2942-2948.
-

References

- Holt, C., & Sawyer, L. (1993). Caseins as rheomorphic proteins: Interpretation of primary and secondary structures of the α_{s1} -, β - and κ -caseins. *Journal of the Chemical Society, Faraday Transactions*, 89(15), 2683-2692.
- Horne, D. S. (2002). Casein structure, self-assembly and gelation. *Current Opinion in Colloid and Interface Science*, 7(5-6), 456-461.
- Huang, X. L., Catignani, G. L., Allen Foegeding, E., & Swaisgood, H. E. (1994a). Comparison of the gelation properties of β -lactoglobulin genetic variants A and B. *Journal of Agricultural and Food Chemistry*, 42(5), 1064-1067.
- Huang, X. L., Catignani, G. L., & Swaisgood, H. E. (1994b). Relative structural stabilities of β -lactoglobulins A and B as determined by proteolytic susceptibility and differential scanning calorimetry. *Journal of Agricultural and Food Chemistry*, 42(6), 1276-1280.
- Humphreys, D. T., Carver, J. A., Easterbrook-Smith, S. B., & Wilson, M. R. (1999). Clusterin has chaperone-like activity similar to that of small heat shock proteins. *Journal of Biological Chemistry*, 274(11), 6875-6881.
- Iametti, S., Cairoli, S., de Gregori, B., & Bonomi, F. (1995). Modifications of high-order structures upon heating of β -lactoglobulin: Dependence on the protein concentration. *Journal of Agricultural and Food Chemistry*, 43(1), 53-58.
- Iametti, S., de Gregori, B., Vecchio, G., & Bonomi, F. (1996). Modifications occur at different structural levels during the heat denaturation of β -lactoglobulin. *European Journal of Biochemistry*, 237(1), 106-112.
- Iametti, S., Scaglioni, L., Mazzini, S., Vecchio, G., et al. (1998). Structural features and reversible association of different quaternary structures of β -lactoglobulin. *Journal of Agricultural and Food Chemistry*, 46(6), 2159-2166.
- Iconomidou, V. A., & Hamodrakas, S. J. (2008). Natural protective amyloids. *Current Protein and Peptide Science*, 9(3), 291-309.
- Iconomidou, V. A., Vriend, G., & Hamodrakas, S. J. (2000). Amyloids protect the silkworm oocyte and embryo. *FEBS Letters*, 479(3), 141-145.
- Ikeda, S., & Morris, V. J. (2002). Fine-stranded and particulate aggregates of heat-denatured whey proteins visualized by atomic force microscopy. *Biomacromolecules*, 3(2), 382-389.

-
-
- Imafidon, G. I., Ng-Kwai-Hang, K. F., Harwalkar, V. R., & MA, C. Y. (1991). Differential scanning calorimetric study of different genetic variants of β -lactoglobulin. *Journal of Dairy Science*, *74*, 2416-2422.
- Inglis, A. S. (1983). Cleavage at aspartic acid. *Methods in Enzymology*, *91*(C), 324-332.
- Jahn, T. R., & Radford, S. E. (2005). The yin and yang of protein folding. *FEBS Journal*, *272*(23), 5962-5970.
- Jameson, G. B., Adams, J. J., & Creamer, L. K. (2002). Flexibility, functionality and hydrophobicity of bovine β -lactoglobulin. *International Dairy Journal*, *12*(4), 319-329.
- Jarrett, J. T., & Lansbury Jr, P. T. (1993). Seeding 'one-dimensional crystallization' of amyloid: A pathogenic mechanism in Alzheimer's disease and scrapie? *Cell*, *73*(6), 1055-1058.
- Jensen, O. N., Podtelejnikov, A. V., & Mann, M. (1997). Identification of the components of simple protein mixtures by high-accuracy peptide mass mapping and database searching. *Analytical Chemistry*, *69*(23), 4741-4750.
- Johnson Jr, W. C. (1990). Protein secondary structure and circular dichroism: A practical guide. *Proteins: Structure, Function and Genetics*, *7*(3), 205-274.
- Johnson Jr., W. C. (1996). Circular dichroism instrumentation in circular dichroism and the conformational analysis of biomolecules. In G. D. Fasman (Ed.), (pp. 636-652). New York, USA: Plenum Press.
- Jung, J. M., Savin, G., Pouzot, M., Schmitt, C., et al. (2008). Structure of heat-induced β -lactoglobulin aggregates and their complexes with sodium-dodecyl sulfate. *Biomacromolecules*, *9*(9), 2477-2486.
- Kalan, E. B., Greenberg, R., & Walter, M. (1965). Studies on β -Lactoglobulins A, B, and C. I. comparison of chemical properties. *Biochemistry*, *4*(6), 991-997.
- Kamiyama, T., Sadahide, Y., Nogusa, Y., & Gekko, K. (1999). Polyol-induced molten globule of cytochrome C: An evidence for stabilization by hydrophobic interaction. *Biochimica et Biophysica Acta, Protein Structure and Molecular Enzymology*, *1434*(1), 44-57.
- Kaushik, J. K., & Bhat, R. (1998). Thermal stability of proteins in aqueous polyol solutions: Role of the surface tension of water in the stabilizing effect of polyols. *Journal of Physical Chemistry B*, *102*(36), 7058-7066.

References

- Kavanagh, G. M., Clark, A. H., & Ross-Murphy, S. B. (2000). Heat-induced gelation of globular proteins: part 3. Molecular studies on low pH β -lactoglobulin gels. *International Journal of Biological Macromolecules*, 28(1), 41-50.
- Kegeles, G. (1979). A shell model for size distribution in micelles. *Journal of Physical Chemistry*, 83(13), 1728-1732.
- Kegeles, G. (1992). The critical micelle condition revisited. *Indian Journal of Biochemistry and Biophysics*, 29(2), 97-102.
- Kehoe, J. J., & Foegeding, E. A. (2011). Interaction between β -casein and whey proteins as a function of pH and salt concentration. *Journal of Agricultural and Food Chemistry*, 59(1), 349-355.
- Kella, N. K., & Kinsella, J. E. (1988). Enhanced thermodynamic stability of β -lactoglobulin at low pH. A possible mechanism. *Biochemical Journal*, 255(1), 113-118.
- Kelly, S. M., Jess, T. J., & Price, N. C. (2005). How to study proteins by circular dichroism. *Biochimica et Biophysica Acta - Proteins and Proteomics*, 1751(2), 119-139.
- Kelly, S. M., & Price, N. C. (1997). The application of circular dichroism to studies of protein folding and unfolding. *Biochimica et Biophysica Acta - Protein Structure and Molecular Enzymology*, 1338(2), 161-185.
- Khurana, R., Coleman, C., Ionescu-Zanetti, C., Carter, S. A., et al. (2005). Mechanism of thioflavin T binding to amyloid fibrils. *Journal of Structural Biology*, 151(3), 229-238.
- Kim, W., & Hecht, M. H. (2006). Generic hydrophobic residues are sufficient to promote aggregation of the Alzheimer's A β 42 peptide. *Proceedings of the National Academy of Sciences of the United States of America*, 103(43), 15824-15829.
- Kinter, M., & Sherman, N. E. (2000). *Protein sequencing and identification using tandem mass spectrometry*. Toronto, Canada: A John Wiley & Sons Inc.
- Kita, Y., Arakawa, T., Lin, T. Y., & Timasheff, S. N. (1994). Contribution of the surface free energy perturbation to protein-solvent interactions. *Biochemistry*, 33(50), 15178-15189.

-
-
- Kontopidis, G., Holt, C., & Sawyer, L. (2002). The ligand-binding site of bovine β -lactoglobulin: Evidence for a function? *Journal of Molecular Biology*, *318*(4), 1043-1055.
- Koudelka, T., Hoffmann, P., & Carver, J. A. (2009). Dephosphorylation of α _S- and β -caseins and its effect on chaperone activity: A structural and functional investigation. *Journal of Agricultural and Food Chemistry*, *57*(13), 5956-5964.
- Krebs, M. R. H., Bromley, E. H. C., & Donald, A. M. (2005). The binding of thioflavin-T to amyloid fibrils: localisation and implications. *Journal of Structural Biology*, *149*(1), 30-37.
- Krebs, M. R. H., Morozova-Roche, L. A., Daniel, K., Robinson, C. V., et al. (2004). Observation of sequence specificity in the seeding of protein amyloid fibrils. *Protein Science*, *13*(7), 1933-1938.
- Kroes-Nijboer, A., Sawalha, H., Venema, P., Bot, A., et al. (2012). Stability of aqueous food grade fibrillar systems against pH change. *Faraday Discussions*, *158*, 125-138.
- Kroes-Nijboer, A., Venema, P., Baptist, H., & van der Linden, E. (2010). Fracture of protein fibrils as induced by elongational flow. *Langmuir*, *26*(16), 13097-13101.
- Kroes-Nijboer, A., Venema, P., Bouman, J., & van der Linden, E. (2009). The critical aggregation concentration of β -lactoglobulin-based fibril formation. *Food Biophysics*, *4*(2), 59-63.
- Kroes-Nijboer, A., Venema, P., Bouman, J., & van der Linden, E. (2011). Influence of protein hydrolysis on the growth kinetics of β -lg fibrils. *Langmuir*, *27*(10), 5753-5761.
- Kuhn, L. A., Swanson, C. A., Pique, M. E., Tainer, J. A., et al. (1995). Atomic and residue hydrophilicity in the context of folded protein structures. *Proteins: Structure, Function and Genetics*, *23*(4), 536-547.
- Kulmyrzaev, A., Bryant, C., & McClements, D. J. (2000a). Influence of sucrose on the thermal denaturation, gelation, and emulsion stabilization of whey proteins. *Journal of Agricultural and Food Chemistry*, *48*(5), 1593-1597.
- Kulmyrzaev, A., Cancelliere, C., & McClements, D. J. (2000b). Influence of sucrose on cold gelation of heat-denatured whey protein isolate. *Journal of the Science of Food and Agriculture*, *80*(9), 1314-1318.
-

References

- Kuwata, K., Shastry, R., Cheng, H., Hoshino, M., et al. (2001). Structural and kinetic characterization of early folding events in β -lactoglobulin. *Nature Structural Biology*, 8(2), 151-155.
- Kyte, J., & Doolittle, R. F. (1982). A simple method for displaying the hydropathic character of a protein. *Journal of Molecular Biology*, 157(1), 105-132.
- Langton, M., & Hermansson, A. M. (1992). Fine-stranded and particulate gels of β -lactoglobulin and whey-protein at varying pH. *Food Hydrocolloids*, 5(6), 523-539.
- Lara, C., Adamcik, J., Jordens, S., & Mezzenga, R. (2011). General self-assembly mechanism converting hydrolyzed globular proteins into giant multistranded amyloid ribbons. *Biomacromolecules*, 12(5), 1868-1875.
- Lasse, M. (2013). *Does the protein aggregation state affect the digestibility and safety of foods?* (Ph.D Biochemistry), University of Canterbury, Christchurch
- Le Bon, C., Durand, D., & Nicolai, T. (2002). Influence of genetic variation on the aggregation of heat-denatured β -lactoglobulin. *International Dairy Journal*, 12(8), 671-678.
- Leach, S. J. (1956). *The kinetics and mechanism of aspartic acid liberation from proteins*. Paper presented at the International Wool Textile Research Conference, Australia.
- Leclerc, E., & Calmettes, P. (1997a). Interactions in micellar solutions of β -casein. *Physica B: Condensed Matter*, 234-236, 207-209.
- Leclerc, E., & Calmettes, P. (1997b). Structure of β -casein micelles. *Physica B: Condensed Matter*, 241-243, 1141-1143.
- Lee, D., Park, C. W., Paik, S. R., & Choi, K. Y. (2009). The modification of α -synuclein by dicarbonyl compounds inhibits its fibril-forming process. *Biochimica et Biophysica Acta, Proteins and Proteomics*, 1794(3), 421-430.
- LeVine III, H. (1993). Thioflavine T interaction with synthetic Alzheimer's disease β -amyloid peptides: Detection of amyloid aggregation in solution. *Protein Science*, 2(3), 404-410.
- Liu, G., & Zhong, Q. (2013a). Dispersible and thermal stable nanofibrils derived from glycosylated whey protein. *Biomacromolecules*, 14(7), 2146-2153.
- Liu, G., & Zhong, Q. (2013b). Thermal aggregation properties of whey protein glycosylated with various saccharides. *Food Hydrocolloids*, 32(1), 87-96.

-
-
- Lorenzo, A., & Yankner, B. A. (1994). β -Amyloid neurotoxicity requires fibril formation and is inhibited by Congo red. *Proceedings of the National Academy of Sciences of the United States of America*, *91*(25), 12243-12247.
- Loske, C., Gerdemann, A., Schepl, W., Wycislo, M., et al. (2000). Transition metal-mediated glycooxidation accelerates cross-linking of β - amyloid peptide. *European Journal of Biochemistry*, *267*(13), 4171-4178.
- Loveday, S. M., Su, J., Rao, M. A., Anema, S. G., et al. (2011a). Effect of calcium on the morphology and functionality of whey protein nanofibrils. *Biomacromolecules*, *12*(10), 3780-3788.
- Loveday, S. M., Su, J., Rao, M. A., Anema, S. G., et al. (2012a). Whey protein nanofibrils: Kinetic, rheological and morphological effects of group IA and IIA cations. *International Dairy Journal*, *26*(2), 133-140.
- Loveday, S. M., Su, J., Rao, M. A., Anema, S. G., et al. (2012b). Whey protein nanofibrils: The environment-morphology-functionality relationship in lyophilization, rehydration, and seeding. *Journal of Agricultural and Food Chemistry*, *60*(20), 5229-5236.
- Loveday, S. M., Wang, X. L., Rao, M. A., Anema, S. G., et al. (2010). Tuning the properties of β -lactoglobulin nanofibrils with pH, NaCl and CaCl₂. *International Dairy Journal*, *20*(9), 571-579.
- Loveday, S. M., Wang, X. L., Rao, M. A., Anema, S. G., et al. (2011b). Effect of pH, NaCl, CaCl₂ and temperature on self-assembly of β -lactoglobulin into nanofibrils: A central composite design study. *Journal of Agricultural and Food Chemistry*, *59*(15), 8467-8474.
- Loveday, S. M., Wang, X. L., Rao, M. A., Anema, S. G., et al. (2012c). β -Lactoglobulin nanofibrils: Effect of temperature on fibril formation kinetics, fibril morphology and the rheological properties of fibril dispersions. *Food Hydrocolloids*, *27*(1), 242-249.
- Ma, B., Xie, J., Wei, L., & Li, W. (2013). Macromolecular crowding modulates the kinetics and morphology of amyloid self-assembly by β -lactoglobulin. *International Journal of Biological Macromolecules*, *53*, 82-87.
- MacArthur, M. W., & Thornton, J. M. (1991). Influence of proline residues on protein conformation. *Journal of Molecular Biology*, *218*(2), 397-412.
-

References

- Mailliart, P., & Ribadeau-Dumas, B. (1988). Preparation of β -lactoglobulin and β -lactoglobulin free proteins from whey retentate by NaCl salting out at low pH. *Journal of Food Science*, 53(3), 743-&.
- Makin, O. S., Atkins, E., Sikorski, P., Johansson, J., et al. (2005). Molecular basis for amyloid fibril formation and stability. *Proceedings of the National Academy of Sciences of the United States of America*, 102(2), 315-320.
- Manderson, G. A. (1998). *The effect of heat on the structure and aggregation behaviour of bovine β -lactoglobulin A, B, and C*. (PhD Biochemistry), Massey University, Palmerston North, New Zealand.
- Manderson, G. A., Creamer, L. K., & Hardman, M. J. (1999). Effect of heat treatment on the circular dichroism spectra of bovine β -lactoglobulin A, B, and C. *Journal of Agricultural and Food Chemistry*, 47(11), 4557-4567.
- Manderson, G. A., Hardman, M. J., & Creamer, L. K. (1998). Effect of heat treatment on the conformation and aggregation of β -lactoglobulin A, B, and C. *Journal of Agricultural and Food Chemistry*, 46(12), 5052-5061.
- Mann, M., Hendrickson, R. C., & Pandey, A. (2001) Analysis of proteins and proteomes by mass spectrometry. *Vol. 70. Annual Review of Biochemistry* (pp. 437-473).
- Matrix science help: Peptide Fragmentation.). Retrieved 01.07.2014, 2014, from http://www.matrixscience.com/help/fragmentation_help.html
- Matsudomi, N., Kanda, Y., Yoshika, Y., & Moriwaki, H. (2004). Ability of α_s -casein to suppress the heat aggregation of ovotransferrin. *Journal of Agricultural and Food Chemistry*, 52(15), 4882-4886.
- Matsuura, J. E., & Manning, M. C. (1994). Heat-induced gel formation of β -lactoglobulin: A study on the secondary and tertiary structure as followed by circular dichroism spectroscopy. *Journal of Agricultural and Food Chemistry*, 42(8), 1650-1656.
- McClements, D. J. (2002). Modulation of globular protein functionality by weakly interacting cosolvents. *Critical Reviews in Food Science and Nutrition*, 42(5), 417-471.
- McKenzie, H. A. (1971). *β -Lactoglobulins*. New York: Academic Press.
- McKenzie, H. A., & Sawyer, W. H. (1967). Effect of pH on β -lactoglobulins. *Nature*, 214(5093), 1101-1104.

-
-
- McSwiney, M., Singh, H., Campanella, O., & Creamer, L. K. (1994). Thermal gelation and denaturation of bovine β -lactoglobulins A and B. *Journal of Dairy Research*, *61*(2), 221-232.
- Medrano, A., Abirached, C., Panizzolo, L., Moyna, P., et al. (2009). The effect of glycation on foam and structural properties of β -lactoglobulin. *Food Chemistry*, *113*(1), 127-133.
- Meltretter, J., Wust, J., & Pischetsrieder, M. (2013). Comprehensive analysis of nonenzymatic post-translational β -lactoglobulin modifications in processed milk by ultrahigh-performance liquid chromatography-tandem mass spectrometry. *Journal of Agricultural and Food Chemistry*, *61*(28), 6971-6981.
- Mercadante, D., Melton, L. D., Norris, G. E., Loo, T. S., et al. (2012). Bovine β -lactoglobulin is dimeric under imitative physiological conditions: Dissociation equilibrium and rate constants over the pH range of 2.5-7.5. *Biophysical Journal*, *103*(2), 303-312.
- Merril, C. R., Goldman, D., Sedman, S. A., & Ebert, M. H. (1981). Ultrasensitive stain for proteins in polyacrylamide gels shows regional variation in cerebrospinal fluid proteins. *Science*, *211*(4489), 1437-1438.
- Mikheeva, L. M., Grinberg, N. V., Grinberg, V. Y., Khokhlov, A. R., et al. (2003). Thermodynamics of micellization of bovine β -casein studied by high-sensitivity differential scanning calorimetry. *Langmuir*, *19*(7), 2913-2921.
- Mills, O. E. (1976). Effect of temperature on tryptophan fluorescence of β -lactoglobulin B. *Biochimica et Biophysica Acta*, *434*(2), 324-332.
- Minton, A. P. (1997). Influence of excluded volume upon macromolecular structure and associations in 'crowded' media. *Current Opinion in Biotechnology*, *8*(1), 65-69.
- Mishra, R., Sorgjerd, K., Nystrom, S., Nordigarden, A., et al. (2007). Lysozyme amyloidogenesis is accelerated by specific nicking and fragmentation but decelerated by intact protein binding and conversion. *Journal of Molecular Biology*, *366*(3), 1029-1044.
- Moitzi, C., Portnaya, I., Glatter, O., Ramon, O., et al. (2008). Effect of temperature on self-assembly of bovine β -casein above and below isoelectric pH. Structural analysis by cryogenic-transmission electron microscopy and small-angle X-ray scattering. *Langmuir*, *24*(7), 3020-3029.
-

References

- Molinari, H., Ragona, L., Varani, L., Musco, G., et al. (1996). Partially folded structure of monomeric bovine β -lactoglobulin. *FEBS Letters*, 381(3), 237-243.
- Monaco, H. L., Zanotti, G., Spadon, P., Bolognesi, M., et al. (1987). Crystal structure of the trigonal form of bovine β -lactoglobulin and of its complex with retinol at 2.5 Å resolution. *Journal of Molecular Biology*, 197(4), 695-706.
- Morgan, F., Bouhallab, S., Molle, D., Henry, G., et al. (1998). Lactolation of β -lactoglobulin monitored by electrospray ionisation mass spectrometry. *International Dairy Journal*, 8(2), 95-98.
- Morgan, F., Leonil, J., Molle, D., & Bouhallab, S. (1997). Nonenzymatic lactosylation of bovine β -lactoglobulin under mild heat treatment leads to structural heterogeneity of the glycoforms. *Biochemical and Biophysical Research Communications*, 236(2), 413-417.
- Morgan, F., Leonil, J., Molle, D., & Bouhallab, S. (1999a). Modification of bovine β -lactoglobulin by glycation in a powdered state or in an aqueous solution: Effect on association behavior and protein conformation. *Journal of Agricultural and Food Chemistry*, 47(1), 83-91.
- Morgan, F., Molle, D., Henry, G., Venien, A., et al. (1999b). Glycation of bovine β -lactoglobulin: Effect on the protein structure. *International Journal of Food Science and Technology*, 34(5-6), 429-435.
- Morgan, P. E., Treweek, T. M., Lindner, R. A., Price, W. E., et al. (2005). Casein proteins as molecular chaperones. *Journal of Agricultural and Food Chemistry*, 53(7), 2670-2683.
- Morinaga, A., Hasegawa, K., Nomura, R., Ookoshi, T., et al. (2010). Critical role of interfaces and agitation on the nucleation of A β amyloid fibrils at low concentrations of A β monomers. *Biochimica et Biophysica Acta - Proteins and Proteomics*, 1804(4), 986-995.
- Morris, A. M., Watzky, M. A., Agar, J. N., & Finke, R. G. (2008). Fitting neurological protein aggregation kinetic data via a 2-step, minimal/"Ockham's razor" model: The Finke-Watzky mechanism of nucleation followed by autocatalytic surface growth. *Biochemistry*, 47(8), 2413-2427.

-
-
- Morris, A. M., Watzky, M. A., & Finke, R. G. (2009). Protein aggregation kinetics, mechanism, and curve-fitting: A review of the literature. *Biochimica et Biophysica Acta - Proteins and Proteomics*, 1794(3), 375-397.
- Muchowski, P. J., & Wacker, J. L. (2005). Modulation of neurodegeneration by molecular chaperones. *Nature Reviews Neuroscience*, 6(1), 11-22.
- Mudgal, P., Daubert, C. R., Clare, D. A., & Foegeding, E. A. (2011). Effect of disulfide interactions and hydrolysis on the thermal aggregation of β -lactoglobulin. *Journal of Agricultural and Food Chemistry*, 59(5), 1491-1497.
- Mudgal, P., Daubert, C. R., & Foegeding, E. A. (2009). Cold-set thickening mechanism of β -lactoglobulin at low pH: concentration effects. *Food Hydrocolloids*, 23(7), 1762-1770.
- Mulsow, B. B., Jacob, M., & Henle, T. (2009). Studies on the impact of glycation on the denaturation of whey proteins. *European Food Research and Technology*, 228(4), 643-649.
- Munialo, C. D., de Jongh, H. H. J., Broersen, K., van der Linden, E., et al. (2013). Modulation of the gelation efficiency of fibrillar and spherical aggregates by means of thiolation. *Journal of Agricultural and Food Chemistry*, 61(47), 11628-11635.
- Munishkina, L. A., Ahmad, A., Fink, A. L., & Uversky, V. N. (2008). Guiding protein aggregation with macromolecular crowding. *Biochemistry*, 47(34), 8993-9006.
- Nacka, F., Chobert, J. M., Burova, T., Leonil, J., et al. (1998). Induction of new physicochemical and functional properties by the glycosylation of whey proteins. *Journal of Protein Chemistry*, 17(5), 495-503.
- Naiki, H., Higuchi, K., Hosokawa, M., & Takeda, T. (1989). Fluorometric determination of amyloid fibrils in vitro using the fluorescent dye, thioflavine T. *Analytical Biochemistry*, 177(2), 244-249.
- Nelson, R., Sawaya, M. R., Balbirnie, M., Madsen, A. Ø., et al. (2005). Structure of the cross- β spine of amyloid-like fibrils. *Nature*, 435(7043), 773-778.
- Nicolai, T., & Durand, D. (2013). Controlled food protein aggregation for new functionality. *Current Opinion in Colloid and Interface Science*, 18(4), 249-256.

References

- Nielsen, B. T., Singh, H., & Latham, J. M. (1996). Aggregation of bovine β -Lactoglobulins A and B on heating at 75°C. *International Dairy Journal*, 6(5), 519-527.
- Nilsson, M. R. (2004). Techniques to study amyloid fibril formation *in vitro*. *Methods*, 34(1), 151-160.
- O'Brien, J. (Ed.). (1995). *Heat-induced changes in lactose: isomerization, degradation, Maillard browning*. Brussels, Belgium International Dairy Federation (IDF).
- O'Connell, J. E., Grinberg, V. Y., & de Kruijff, C. G. (2003). Association behavior of β -casein. *Journal of Colloid and Interface Science*, 258(1), 33-39.
- O'Kennedy, B. T., & Mounsey, J. S. (2006). Control of heat-induced aggregation of whey proteins using casein. *Journal of Agricultural and Food Chemistry*, 54(15), 5637-5642.
- Oborocanu, D., Wang, L. Z., Brodkorb, A., Magner, E., et al. (2010). Characterization of β -lactoglobulin fibrillar assembly using atomic force microscopy, polyacrylamide gel electrophoresis, and *in situ* fourier transform infrared spectroscopy. *Journal of Agricultural and Food Chemistry*, 58(6), 3667-3673.
- Obrenovich, M. E., & Monnier, V. M. (2004). Glycation stimulates amyloid formation. *Science of Aging Knowledge Environment*, 2004(2), pe3. <Go to ISI>://MEDLINE:14724325
- Oliveira, L. M., Lages, A., Gomes, R. A., Neves, H., et al. (2011). Insulin glycation by methylglyoxal results in native-like aggregation and inhibition of fibril formation. *BMC Biochemistry*, 12(1).
- Oliyai, C., & Borchardt, R. T. (1993). Chemical pathways of peptide degradation. IV. Pathways, kinetics, and mechanism of degradation of an aspartyl residue in a model hexapeptide. *Pharmaceutical Research*, 10(1), 95-102.
- Otte, J., Zakora, M., & Qvist, K. B. (2000). Involvement of disulfide bands in bovine β -lactoglobulin B gels set thermally at various pH. *Journal of Food Science*, 65(3), 384-389.
- Ow, S. Y., & Dunstan, D. E. (2013). The effect of concentration, temperature and stirring on hen egg white lysozyme amyloid formation. *Soft Matter*, 9(40), 9692-9701.

-
-
- Papiz, M. Z., Sawyer, L., & Eliopoulos, E. E. (1986). The structure of β -lactoglobulin and its similarity to plasma retinol-binding protein. *Nature*, 324(6095), 383-385.
- Partridge, S. M., & Davis, H. F. (1950). Preferential release of aspartic acid during the hydrolysis of proteins. *Nature*, 165(4185), 62-63.
- Payens, T. A. J., & Van Markwijk, B. W. (1963). Some features of the association of β -casein. *Biochimica et Biophysica Acta*, 71(C), 517-530.
- Pedersen, K. O. (1936). Ultracentrifugal and electrophoretic studies on the milk proteins. *Biochemical Journal*, 30, 961-970.
- Pepys, M. B., Hawkins, P. N., Booth, D. R., Vigushin, D. M., et al. (1993). Human lysozyme gene mutations cause hereditary systemic amyloidosis. *Nature*, 362(6420), 553-557.
- Peram, M. R., Loveday, S. M., Ye, A., & Singh, H. (2013). *In vitro* gastric digestion of heat-induced aggregates of β -lactoglobulin. *Journal of Dairy Science*, 96(1), 63-74.
- Perez, M. D., Diaz de Villegas, C., Sanchez, L., Aranada, P., et al. (1989). Interaction of fatty acids with β -lactoglobulin and albumin from ruminant milk. *Journal of Biochemistry*, 106(6), 1094-1097.
- Perkins, D. N., Pappin, D. J. C., Creasy, D. M., & Cottrell, J. S. (1999). Probability-based protein identification by searching sequence databases using mass spectrometry data. *Electrophoresis*, 20(18), 3551-3567.
- Pervaiz, S., & Brew, K. (1985). Homology of β -lactoglobulin, serum retinol-binding protein, and protein HC. *Science*, 228(4697), 335-337.
- Politi, R., & Harries, D. (2010). Enthalpically driven peptide stabilization by protective osmolytes. *Chemical Communications*, 46(35), 6449-6451.
- Porat, Y., Abramowitz, A., & Gazit, E. (2006). Inhibition of amyloid fibril formation by polyphenols: Structural similarity and aromatic interactions as a common inhibition mechanism. *Chemical Biology and Drug Design*, 67(1), 27-37.
- Portnaya, I., Ben-Shoshan, E., Cogan, U., Khalfin, R., et al. (2008). Self-assembly of bovine β -casein below the isoelectric pH. *Journal of Agricultural and Food Chemistry*, 56(6), 2192-2198.
- Portnaya, I., Cogan, U., Livney, Y. D., Ramon, O., et al. (2006). Micellization of bovine β -casein studied by isothermal titration microcalorimetry and

References

- cryogenic transmission electron microscopy. *Journal of Agricultural and Food Chemistry*, 54(15), 5555-5561.
- Prabakaran, S., & Damodaran, S. (1997). Thermal unfolding of β -lactoglobulin: Characterization of initial unfolding events responsible for heat-induced aggregation. *Journal of Agricultural and Food Chemistry*, 45(11), 4303-4308.
- Pratim Bose, P., Chatterjee, U., Xie, L., Johansson, J., et al. (2010). Effects of Congo red on A β 1-40 fibril formation process and morphology. *ACS Chemical Neuroscience*, 1(4), 315-324.
- Privalov, P. L., & Makhatadze, G. I. (1993). Contribution of hydration to protein folding thermodynamics. II. The entropy and Gibbs energy of hydration. *Journal of Molecular Biology*, 232(2), 660-679.
- Provencher, S. W., & Glockner, J. (1981). Estimation of globular protein secondary structure from circular dichroism. *Biochemistry*, 20(1), 33-37.
- Qi, P. X., Wickham, E. D., & Farrell Jr, H. M. (2004). Thermal and alkaline denaturation of bovine β -casein. *Protein Journal*, 23(6), 389-402.
- Qi, X. L., Holt, C., McNulty, D., Clarke, D. T., et al. (1997). Effect of temperature on the secondary structure of β -lactoglobulin at pH 6.7, as determined by CD and IR spectroscopy: a test of the molten globule hypothesis. *Biochemical Journal*, 324, 341-346.
- Qian, M., Jun-Bao, F., Zheng, Z., Bing-Rui, Z., et al. (2012). The contrasting effect of macromolecular crowding on amyloid fibril formation. *PLoS One*, 7(4), 1-14.
- Qin, B. Y., Bewley, M. C., Creamer, L. K., Baker, E. N., et al. (1999). Functional implications of structural differences between variants A and B of bovine β -lactoglobulin. *Protein Science*, 8(1), 75-83.
- Qin, B. Y., Bewley, M. C., Creamer, L. K., Baker, H. M., et al. (1998b). Structural basis of the tanford transition of bovine β -lactoglobulin. *Biochemistry*, 37(40), 14014-14023.
- Qin, B. Y., Creamer, L. K., Baker, E. N., & Jameson, G. B. (1998a). 12-Bromododecanoic acid binds inside the calyx of bovine β -lactoglobulin. *FEBS Letters*, 438(3), 272-278.

-
-
- Ragona, L., Pusterla, F., Zetta, L., Monaco, H. L., et al. (1997). Identification of a conserved hydrophobic cluster in partially folded bovine β -lactoglobulin at pH 2. *Folding and Design*, 2(5), 281-290.
- Ralston, G. B. (1990). Effects of "crowding" in protein solutions. *Journal of Chemical Education*, 67(10), 857-860.
- Rao, S. P., Meade, S. J., Healy, J. P., Sutton, K. H., et al. (2012). Amyloid fibrils as functionalizable components of nanocomposite materials. *Biotechnology Progress*, 28(1), 248-256.
- Rasmussen, P., Barbiroli, A., Bonomi, F., Faoro, F., et al. (2007). Formation of structured polymers upon controlled denaturation of β -lactoglobulin with different chaotropes. *Biopolymers*, 86(1), 57-72.
- Raynes, J. K., & Gerrard, J. A. (2012). Amyloid fibrils as bionanomaterials. In B. Rehm (Ed.), *Bionanotechnology: Biological self-assembly and its applications* (pp. 83-106). Norfolk, UK: Horizon Scientific Press.
- Raynes, J. K., Pearce, F. G., Meade, S. J., & Gerrard, J. A. (2011). Immobilization of organophosphate hydrolase on an amyloid fibril nanoscaffold: Towards bioremediation and chemical detoxification. *Biotechnology Progress*, 27(2), 360-367.
- Reches, M., & Gazit, E. (2003). Casting metal nanowires within discrete self-assembled peptide nanotubes. *Science*, 300(5619), 625-627.
- Reddy, P. V., Obrenovich, M. E., Atwood, C. S., Perry, G., et al. (2002). Involvement of Maillard reactions in Alzheimer disease. *Neurotoxicity Research*, 4(3), 191-209.
- Renard, D., & Lefebvre, J. (1992). Gelation of globular proteins: effect of pH and ionic strength on the critical concentration for gel formation. A simple model and its application to β -lactoglobulin heat-induced gelation. *International Journal of Biological Macromolecules*, 14(5), 287-291.
- Renard, D., Lefebvre, J., Griffin, M. C. A., & Griffin, W. G. (1998). Effects of pH and salt environment on the association of β -lactoglobulin revealed by intrinsic fluorescence studies. *International Journal of Biological Macromolecules*, 22(1), 41-49.
- Reynolds, J. A., & Tanford, C. (1970). Gross conformation of protein-sodium dodecyl sulfate complexes. *Journal of Biological Chemistry*, 245(19), 5161-5166.
-

References

- Rezaei-Ghaleh, N., Ramshini, H., Ebrahim-Habibi, A., Moosavi-Movahedi, A. A., et al. (2008). Thermal aggregation of α -chymotrypsin: Role of hydrophobic and electrostatic interactions. *Biophysical Chemistry*, 132(1), 23-32.
- Ribadeau Dumas, B., Brignon, G., Grosclaude, F., & Mercier, J. C. (1972). Primary structure of bovine β -casein. Complete sequence. *European Journal of Biochemistry*, 25(3), 505-514.
- Ribeiro, A. C. F., Ortona, O., Simões, S. M. N., Santos, C. I. A. V., et al. (2006). Binary mutual diffusion coefficients of aqueous solutions of sucrose, lactose, glucose, and fructose in the temperature range from (298.15 to 328.15) K. *Journal of Chemical and Engineering Data*, 51(5), 1836-1840.
- Rochet, J. C., & Lansbury Jr, P. T. (2000). Amyloid fibrillogenesis: Themes and variations. *Current Opinion in Structural Biology*, 10(1), 60-68.
- Roefs, S. P. F. M., & de Kruif, K. G. (1994). A model for the denaturation and aggregation of β -lactoglobulin. *European Journal of Biochemistry*, 226(3), 883-889.
- Rogers, S. S., Venema, P., van der Ploeg, J. P. M., Sagis, L. M. C., et al. (2005). Electric birefringence study of an amyloid fibril system: The short end of the length distribution. *European Physical Journal E*, 18(2), 207-217.
- Romero, C. M., Lozano, J. M., Sancho, J., & Giraldo, G. I. (2007). Thermal stability of β -lactoglobulin in the presence of aqueous solution of alcohols and polyols. *International Journal of Biological Macromolecules*, 40(5), 423-428.
- Ruhs, P. A., Scheuble, N., Windhab, E. J., Mezzenga, R., et al. (2012). Simultaneous control of pH and ionic strength during interfacial rheology of β -lactoglobulin fibrils adsorbed at liquid/liquid interfaces. *Langmuir*, 28(34), 12536-12543.
- Sagis, L. M. C., de Ruiter, R., Rossier Miranda, F. J., de Ruiter, J., et al. (2008). Polymer microcapsules with a fiber-reinforced nanocomposite shell. *Langmuir*, 24(5), 1608-1612.
- Sakai, K., Sakurai, K., Sakai, M., Hoshino, M., et al. (2000). Conformation and stability of thiol-modified bovine β -lactoglobulin. *Protein Science*, 9(9), 1719-1729.
- Sakurai, K., Oobatake, M., & Goto, Y. (2001). Salt-dependent monomer-dimer equilibrium of bovine β -lactoglobulin at pH 3. *Protein Science*, 10(11), 2325-2335.

-
-
- Sawyer, L. (2003). *β-lactoglobulin* (3 ed. Vol. 1). New York: Kluwer Academic/Plenum Publishers
- Schagger, H., & von Jagow, G. (1987). Tricine-sodium dodecyl sulfate-polyacrylamide gel electrophoresis for the separation of proteins in the range from 1 to 100 kDa. *Analytical Biochemistry*, 166(2), 368-379.
- Scheibel, T., Parthasarathy, R., Sawicki, G., Lin, X. M., et al. (2003). Conducting nanowires built by controlled self-assembly of amyloid fibers and selective metal deposition. *Proceedings of the National Academy of Sciences of the United States of America*, 100(8), 4527-4532.
- Schellman, J. A. (1997). Temperature, stability, and the hydrophobic interaction. *Biophysical Journal*, 73(6), 2960-2964.
- Schmidt, D. G. (1982). Association of casein and casein micelle structure. In P. F. Fox (Ed.), *Developments in Dairy Chemistry* (Vol. 1, pp. 61-86). London: Elsevier Applied Science.
- Schmidt, D. G., & Payens, T. A. J. (1972). The evaluation of positive and negative contributions to the second virial coefficient of some milk proteins. *Journal of Colloid And Interface Science*, 39(3), 655-662.
- Schokker, E. P., Singh, H., Pinder, D. N., & Creamer, L. K. (2000). Heat-induced aggregation of β-lactoglobulin AB at pH 2.5 as influenced by ionic strength and protein concentration. *International Dairy Journal*, 10(4), 233-240.
- Schokker, E. P., Singh, H., Pinder, D. N., Norris, G. E., et al. (1999). Characterization of intermediates formed during heat-induced aggregation of β-lactoglobulin AB at neutral pH. *International Dairy Journal*, 9(11), 791-800.
- Serpell, L. C. (2000). Alzheimer's amyloid fibrils: Structure and assembly. *Biochimica et Biophysica Acta - Molecular Basis of Disease*, 1502(1), 16-30.
- Shimada, K., & Cheftel, J. C. (1989). Sulfhydryl-group disulfide bond interchange reactions during heat-induced gelation of whey-protein isolate. *Journal of Agricultural and Food Chemistry*, 37(1), 161-168.
- Singh, L. R., Poddar, N. K., Dar, T. A., Kumar, R., et al. (2011). Protein and DNA destabilization by osmolytes: The other side of the coin. *Life Sciences*, 88(3-4), 117-125.
-

References

- Soskic, V., & Godovac-Zimmermann, J. (2001). Improvement of an in-gel tryptic digestion method for matrix-assisted laser desorption/ionization-time of flight mass spectrometry peptide mapping by use of volatile solubilizing agents. *Proteomics*, 1(11), 1364-1367.
- Sreerama, N., & Woody, R. W. (2004) Computation and analysis of protein circular dichroism spectra. *Vol. 383. Methods in Enzymology* (pp. 318-351).
- Storm, C., Pastore, J. J., MacKintosh, F. C., Lubensky, T. C., et al. (2005). Nonlinear elasticity in biological gels. *Nature*, 435(7039), 191-194.
- Street, A. G., & Mayo, S. L. (1999). Intrinsic β -sheet propensities result from van der Waals interactions between side chains and the local backbone. *Proceedings of the National Academy of Sciences of the United States of America*, 96(16), 9074-9076.
- Strickland, E. H. (1974). Aromatic contributions to circular dichroism spectra of proteins. *Critical Reviews in Biochemistry*, 2(1), 113-175.
- Stryer, L. (1995). *Biochemistry* (4 ed.). New York, USA: W. H. Freeman and Company.
- Sukenik, S., & Harries, D. (2012). Insights into the disparate action of osmolytes and macromolecular crowders on amyloid formation. *Prion*, 6(1), 26-31.
- Sukenik, S., Politi, R., Ziserman, L., Danino, D., et al. (2011). Crowding alone cannot account for cosolute effect on amyloid aggregation. *PLoS One*, 6(1).
- Sullivan, R. A., Fitzpatrick, M. M., Stanton, E. K., Annino, R., et al. (1955). The influence of temperature and electrolytes upon the apparent size and shape of α - and β -casein. *Archives of Biochemistry and Biophysics*, 55(2), 455-468.
- Sunde, M., Serpell, L. C., Bartlam, M., Fraser, P. E., et al. (1997). Common core structure of amyloid fibrils by synchrotron X-ray diffraction. *Journal of Molecular Biology*, 273(3), 729-739.
- Swaigood, H. E. (1982a). *Chemistry of milk protein* (Vol. 1). London: Elsevier Applied Science.
- Swaigood, H. E. (1982b). Chemistry of milk protein. In P. F. Fox (Ed.), *Developments in Dairy Chemistry* (Vol. 1, pp. 1-59). London: Elsevier Applied Science.
- Swaigood, H. E. (1993). Review and update of casein chemistry. *Journal of Dairy Science*, 76(10), 3054-3061.

-
-
- Synge, R. L. (1945). The kinetics of low temperature acid hydrolysis of gramicidin and of some related dipeptides. *Biochemical journal*, 39(4), 351-355.
- Takase, K., Niki, R., & Arima, S. (1980). A sedimentation equilibrium study of the temperature-dependent association of bovine β -casein. *Biochimica et Biophysica Acta- Protein Structure*, 622(1), 1-8.
- Tal, M., Silberstein, A., & Nusser, E. (1985). Why does Coomassie Brilliant Blue R interact differently with different proteins? A partial answer. *Journal of Biological Chemistry*, 260(18), 9976-9980.
- Tanaka, M., Chien, P., Yonekura, K., & Weissman, J. S. (2005). Mechanism of cross-species prion transmission: An infectious conformation compatible with two highly divergent yeast prion proteins. *Cell*, 121(1), 49-62.
- Tanford, C. (1991). *The hydrophobic effect: Formation of micelles and biological membranes* (2nd ed.). Malabar, FL: Kreiger Publishing Company.
- Tanford, C., Bunville, L. G., & Nozaki, Y. (1959). The reversible transformation of β -lactoglobulin at pH 7.51. *Journal of the American Chemical Society*, 81(15), 4032-4036.
- Taulier, N., & Chalikian, T. V. (2001). Characterization of pH-induced transitions of β -lactoglobulin: Ultrasonic, densimetric, and spectroscopic studies. *Journal of Molecular Biology*, 314(4), 873-889.
- Thompson, M. P., & Pepper, L. (1964). Genetic polymorphism in caseins of cows milk.4. Isolation and properties of β -caseins A B and C. *Journal of Dairy Science*, 47(6), 633-&.
- Thorn, D. C., Meehan, S., Sunde, M., Rekas, A., et al. (2005). Amyloid fibril formation by bovine milk κ -casein and its inhibition by the molecular chaperones α_s - and β -casein. *Biochemistry*, 44(51), 17027-17036.
- Thresher, W., & Hill, J. P. (1997). Thermodynamic Characterization of β -Lactoglobulin A, B and C Subunit Interactions Using Analytical Affinity Chromatography *Proceedings of the IDF Seminar "Milk Protein Polymorphism II"* (pp. 189-193). Brussels, Belgium International Dairy Federation.
- Timasheff, S. N. (1993). The control of protein stability and association by weak-interactions with water - how do solvents affect these processes. *Annual Review of Biophysics and Biomolecular Structure*, 22, 67-97.

References

- Timasheff, S. N. (1998). Control of protein stability and reactions by weakly interacting cosolvents: The simplicity of the complicated. *Advances in Protein Chemistry, Vol 51, 51*, 355-432.
- Tiwari, A., & Bhat, R. (2006). Stabilization of yeast hexokinase A by polyol osmolytes: Correlation with the physicochemical properties of aqueous solutions. *Biophysical Chemistry, 124*(2), 90-99.
- Tjernberg, L., Hosiya, W., Bark, N., Thyberg, J., et al. (2002). Charge attraction and β propensity are necessary for amyloid fibril formation from tetrapeptides. *Journal of Biological Chemistry, 277*(45), 43243-43246.
- Tompa, P. (2002). Intrinsically unstructured proteins. *Trends in Biochemical Sciences, 27*(10), 527-533.
- Townend, R., Herskovits, T. T., Timasheff, S. N., & Gorbunoff, M. J. (1969). The state of amino acid residues in β -lactoglobulin. *Archives of Biochemistry and Biophysics, 129*(2), 567-580.
- Townend, R., Weinberger, L., & Timasheff, S. N. (1960). Molecular interactions in β -lactoglobulin. IV. The dissociation of β -lactoglobulin below pH 3.5. *Journal of the American Chemical Society, 82*(12), 3175-3179.
- Tracz, S. M., Abedini, A., Driscoll, M., & Raleigh, D. P. (2004). Role of aromatic interactions in amyloid formation by peptides derived from human amylin. *Biochemistry, 43*(50), 15901-15908.
- Trovato, A., Seno, F., & Tosatto, S. C. E. (2007). The PASRA Server for Protein Aggregation Prediction. *Protein Engineering, Design and Selection, 20*(10), 521-523.
- Tsung, C. M., & Fraenkel-Conrat, H. (1965). Preferential release of aspartic acid by dilute acid treatment of tryptic peptides. *Biochemistry, 4*(5), 793-801.
- Uhrinova, S., Smith, M. H., Jameson, G. B., Uhrin, D., et al. (2000). Structural changes accompanying pH-induced dissociation of the β -lactoglobulin dimer. *Biochemistry, 39*(13), 3565-3574.
- Uversky, V. N., & Fink, A. L. (2004). Conformational constraints for amyloid fibrillation: The importance of being unfolded. *Biochimica et Biophysica Acta, Proteins and Proteomics, 1698*(2), 131-153.
- Vagenende, V., Yap, M. G. S., & Trout, B. L. (2009). Mechanisms of protein stabilization and prevention of protein aggregation by glycerol. *Biochemistry, 48*(46), 11084-11096.

-
-
- van Teeffelen, A. M. M., Broersen, K., & de Jongh, H. H. J. (2005). Glucosylation of β -lactoglobulin lowers the heat capacity change of unfolding; a unique way to affect protein thermodynamics. *Protein Science*, *14*(8), 2187-2194.
- Vassar, P. S., & Culling, C. F. (1959). Fluorescent stains, with special reference to amyloid and connective tissues. *Archives of Pathology*, *68*, 487-498.
- Veerman, C., Baptist, H., Sagis, L. M. C., & van der Linden, E. (2003a). A new multistep Ca^{2+} -induced cold gelation process for β -lactoglobulin. *Journal of Agricultural and Food Chemistry*, *51*(13), 3880-3885.
- Veerman, C., de Schiffart, G., Sagis, L. M. C., & van der Linden, E. (2003b). Irreversible self-assembly of ovalbumin into fibrils and the resulting network rheology. *International Journal of Biological Macromolecules*, *33*(1-3), 121-127.
- Veerman, C., Ruis, H., Sagis, L. M. C., & van der Linden, E. (2002). Effect of electrostatic interactions on the percolation concentration of fibrillar beta-lactoglobulin gels. *Biomacromolecules*, *3*(4), 869-873.
- Veerman, C., Sagis, L. M. C., Heck, J., & van der Linden, E. (2003c). Mesostructure of fibrillar bovine serum albumin gels. *International Journal of Biological Macromolecules*, *31*(4-5), 139-146.
- Verheul, M., Pedersen, J. S., Roefs, S. P. F. M., & de Kruif, K. G. (1999). Association behavior of native β -lactoglobulin. *Biopolymers*, *49*(1), 11-20.
- Wang, X. L. (2009). *Effects of environmental factors on heat-induced β -lactoglobulin fibril formation*. (MSc. Food Technology), Massey University, Palmerston North, New Zealand.
- Waterhouse, S. H., & Gerrard, J. A. (2004). Amyloid fibrils in bionanotechnology. *Australian Journal of Chemistry*, *57*(6), 519-523.
- Watzky, M. A., & Finke, R. G. (1997). Transition metal nanocluster formation kinetic and mechanistic studies. A new mechanism when hydrogen is the reductant: slow, continuous nucleation and fast autocatalytic surface growth. *Journal of the American Chemical Society*, *119*(43), 10382-10400.
- Weber, K., & Osborn, M. (1969). Reliability of molecular weight determinations by dodecyl sulfate-polyacrylamide gel electrophoresis. *Journal of Biological Chemistry*, *244*(16), 4406-&.

References

- West, M. W., Wang, W., Patterson, J., Mancias, J. D., et al. (1999). *De novo* amyloid proteins from designed combinatorial libraries. *Proceedings of the National Academy of Sciences of the United States of America*, 96(20), 11211-11216.
- Westermarck, P., Benson, M. D., Buxbaum, J. N., Cohen, A. S., et al. (2005). Amyloid: Toward terminology clarification: Report from the Nomenclature Committee of the International Society Of Amyloidosis. *Amyloid*, 12(1), 1-4.
- Woody, R. W. (1978). Aromatic side-chain contributions to far ultraviolet circular-dichroism of peptides and proteins. *Biopolymers*, 17(6), 1451-1467.
- Woody, R. W. (1995). Circular-dichroism. *Methods in Enzymology*, 246, 34-71.
- Wu, C. Y., Chen, S. T., Chiou, S. H., & Wang, K. T. (1992). Specific peptide-bond cleavage by microwave irradiation in weak acid solution. *Journal of Protein Chemistry*, 11(1), 45-50.
- Xie, G., & Timasheff, S. N. (1997a). Mechanism of the stabilization of ribonuclease A by sorbitol: Preferential hydration is greater for the denatured than for the native protein. *Protein Science*, 6(1), 211-221.
- Xie, G., & Timasheff, S. N. (1997b). Temperature dependence of the preferential interactions of ribonuclease A in aqueous co-solvent systems: Thermodynamic analysis. *Protein Science*, 6(1), 222-232.
- Xiong, H., Buckwalter, B. L., Shieh, H. M., & Hecht, M. H. (1995). Periodicity of polar and nonpolar amino acids is the major determinant of secondary structure in self-assembling oligomeric peptides. *Proceedings of the National Academy of Sciences of the United States of America*, 92(14), 6349-6353.
- Yang, D. S., Yip, C. M., Huang, T. H. J., Chakrabarty, A., et al. (1999). Manipulating the Amyloid- β Aggregation Pathway with Chemical Chaperones. *Journal of Biological Chemistry*, 274(46), 32970-32974.
- Yang, J. T., Wu, C. S. C., & Martinez, H. M. (1986) Calculation of protein conformation from circular dichroism. *Vol. 130. Methods in Enzymology* (pp. 208-269).
- Yong, Y. H., & Foegeding, E. A. (2008). Effects of caseins on thermal stability of bovine β -lactoglobulin. *Journal of Agricultural and Food Chemistry*, 56(21), 10352-10358.
- Yong, Y. H., & Foegeding, E. A. (2010). Caseins: Utilizing molecular chaperone properties to control protein aggregation in foods. *Journal of Agricultural and Food Chemistry*, 58(2), 685-693.

- Yousefi, R., Schutskaya, Y. Y., Zimny, J., Gaudin, J. C., et al. (2009). Chaperone-like activities of different molecular forms of β -casein. Importance of polarity of N-terminal hydrophilic domain. *Biopolymers*, *91*(8), 623-632.
- Zappone, B., de Santo, M. P., Labate, C., Rizzuti, B., et al. (2013). Catalytic activity of copper ions in the amyloid fibrillation of β -lactoglobulin. *Soft Matter*, *9*(8), 2412-2419.
- Zhang, X. F., Fu, X. M., Zhang, H., Liu, C., et al. (2005). Chaperone-like activity of β -casein. *International Journal of Biochemistry & Cell Biology*, *37*(6), 1232-1240.
- Zimmerman, S. B., & Minton, A. P. (1993). Macromolecular crowding: Biochemical, biophysical, and physiological consequences. *Annual Review of Biophysics and Biomolecular Structure*, *22*, 27-65.
- Zuniga, R. N., Tolkach, A., Kulozik, U., & Aguilera, J. M. (2010). Kinetics of formation and physicochemical characterization of thermally-induced β -lactoglobulin aggregates. *Journal of Food Science*, *75*(5), E261-E268.

11. Annexures

11.1 Calculation of standard deviations for kinetic parameters

The parameters t_{lag} , $(df/dt)_{max}$ and $t_{1/2 \ max}$ are functions of α , β , and γ , whose variances are known from the nonlinear regression calculation. Calculating variances for functions $f(\alpha, \beta, \gamma)$ requires the following approach:

$$\mathbf{X} \equiv [\alpha \quad \beta \quad \gamma]$$

$$V(f(\mathbf{X})) = (\mathbf{f}')^T V(\mathbf{X}) \mathbf{f}'$$

where $\mathbf{f}' = \left[\frac{\partial f}{\partial \alpha} \quad \frac{\partial f}{\partial \beta} \quad \frac{\partial f}{\partial \gamma} \right]$ and the covariance matrix

$$V(\mathbf{X}) = \begin{bmatrix} \sigma_{\alpha}^2 & \sigma_{\alpha\beta} & \sigma_{\alpha\gamma} \\ \sigma_{\alpha\beta} & \sigma_{\beta}^2 & \sigma_{\beta\gamma} \\ \sigma_{\alpha\gamma} & \sigma_{\beta\gamma} & \sigma_{\gamma}^2 \end{bmatrix}$$

All calculations were done in Microsoft Excel, and variances were converted to standard deviations by taking the square root. Tables in the text show standard deviations in brackets.

11.2.1 Computation of partial derivatives.

(1) t_{lag}

$$\begin{aligned} t_{lag} &= \frac{1}{\beta + \alpha\gamma} \left(\ln \left(\frac{\alpha\gamma}{\beta} \right) - 4 \frac{\alpha\gamma}{\beta + \alpha\gamma} + 2 \right) \\ &= \left[\frac{1}{\beta + \alpha\gamma} \times \ln \left(\frac{\alpha\gamma}{\beta} \right) \right] - \left[4 \frac{\alpha\gamma}{(\beta + \alpha\gamma)^2} \right] + \left[\frac{2}{\beta + \alpha\gamma} \right] \dots \dots \dots (11.1) \end{aligned}$$

To simplify calculations new constants are defined:

$$P \equiv \left[\frac{1}{\beta + \alpha\gamma} \times \ln \left(\frac{\alpha\gamma}{\beta} \right) \right] \quad Q \equiv \left[4 \frac{\alpha\gamma}{(\beta + \alpha\gamma)^2} \right] \quad R \equiv \left[\frac{2}{\beta + \alpha\gamma} \right]$$

Differentiating with respect to α :

$$\begin{aligned} \left(\frac{\partial P}{\partial \alpha} \right)_{\beta, \gamma} &= \frac{\partial}{\partial \alpha} \left[\frac{1}{\beta + \alpha\gamma} \times \ln \left(\frac{\alpha\gamma}{\beta} \right) \right] \\ &= \left\{ \ln \left(\frac{\alpha\gamma}{\beta} \right) \times \frac{\partial}{\partial \alpha} \left(\frac{1}{\beta + \alpha\gamma} \right) \right\} + \left\{ \left(\frac{1}{\beta + \alpha\gamma} \right) \times \left[\frac{\partial}{\partial \alpha} \ln \left(\frac{\alpha\gamma}{\beta} \right) \right] \right\} \\ &= \left[\ln \left(\frac{\alpha\gamma}{\beta} \right) \times \left(\frac{-\gamma}{(\beta + \alpha\gamma)^2} \right) \right] + \left[\left(\frac{1}{\beta + \alpha\gamma} \right) \times \left(\frac{\beta}{\alpha\gamma} \times \frac{\gamma}{\beta} \right) \right] \\ &= \left[\ln \left(\frac{\alpha\gamma}{\beta} \right) \times \left(\frac{-\gamma}{(\beta + \alpha\gamma)^2} \right) \right] + \left[\left(\frac{1}{\alpha(\beta + \alpha\gamma)} \right) \right] \\ &= \frac{-\alpha\gamma \ln \left(\frac{\alpha\gamma}{\beta} \right) + (\beta + \alpha\gamma)}{\alpha(\beta + \alpha\gamma)^2} \dots\dots\dots (11.2) \end{aligned}$$

$$\begin{aligned} \left(\frac{\partial Q}{\partial \alpha} \right)_{\beta, \gamma} &= \frac{\partial}{\partial \alpha} \left[4 \frac{\alpha\gamma}{(\beta + \alpha\gamma)^2} \right] \\ &= \frac{\partial}{\partial \alpha} [4 \alpha\gamma (\beta + \alpha\gamma)^{-2}] \\ &= \left[(\beta + \alpha\gamma)^{-2} \times \frac{\partial}{\partial \alpha} (4 \alpha\gamma) \right] + \left[4 \alpha\gamma \times \frac{\partial}{\partial \alpha} (\beta + \alpha\gamma)^{-2} \right] \\ &= [(4 \gamma) \times (\beta + \alpha\gamma)^{-2}] + [-8 \alpha\gamma^2 \times (\beta + \alpha\gamma)^{-3}] \\ &= \frac{4 \gamma(\beta + \alpha\gamma) - 8 \alpha\gamma^2}{(\beta + \alpha\gamma)^3} \dots\dots\dots (11.3) \end{aligned}$$

$$\begin{aligned} \left(\frac{\partial R}{\partial \alpha} \right)_{\beta, \gamma} &= \frac{\partial}{\partial \alpha} \left(\frac{2}{\beta + \alpha\gamma} \right) \\ &= \left(\frac{-2}{(\beta + \alpha\gamma)^2} \times \gamma \right) \dots\dots\dots (11.4) \end{aligned}$$

Combining equations 11.2, 11.3 and 11.4:

$$\left(\frac{\partial t_{lag}}{\partial \alpha}\right)_{\beta, \gamma} = \left[\frac{-\alpha \gamma \ln\left(\frac{\alpha \gamma}{\beta}\right) + (\beta + \alpha \gamma)}{\alpha(\beta + \alpha \gamma)^2} \right] - \left[\frac{4 \gamma(\beta + \alpha \gamma) - 8 \alpha \gamma^2}{(\beta + \alpha \gamma)^3} \right] + \left[\frac{-2 \gamma}{(\beta + \alpha \gamma)^2} \right] \dots (11.5)$$

Differentiating with respect to β :

$$\begin{aligned} \left(\frac{\partial P}{\partial \beta}\right)_{\alpha, \gamma} &= \frac{\partial}{\partial \beta} \left[\frac{1}{\beta + \alpha \gamma} \times \ln\left(\frac{\alpha \gamma}{\beta}\right) \right] \\ &= \left\{ \ln\left(\frac{\alpha \gamma}{\beta}\right) \times \frac{\partial}{\partial \beta} \left(\frac{1}{\beta + \alpha \gamma}\right) \right\} + \left\{ \left(\frac{1}{\beta + \alpha \gamma}\right) \times \left[\frac{\partial}{\partial \beta} \ln\left(\frac{\alpha \gamma}{\beta}\right) \right] \right\} \\ &= \left\{ \ln\left(\frac{\alpha \gamma}{\beta}\right) \times \left(\frac{-1}{(\beta + \alpha \gamma)^2}\right) \right\} + \left\{ \left(\frac{1}{\beta + \alpha \gamma}\right) \times \left[\frac{\beta}{\alpha \gamma} \times \frac{-\alpha \gamma}{\beta^2} \right] \right\} \\ &= \left(\frac{-\ln\left(\frac{\alpha \gamma}{\beta}\right)}{(\beta + \alpha \gamma)^2} \right) - \left(\frac{1}{\beta(\beta + \alpha \gamma)} \right) \\ &= \frac{-\beta \ln\left(\frac{\alpha \gamma}{\beta}\right) - (\beta + \alpha \gamma)}{\beta(\beta + \alpha \gamma)^2} \dots (11.6) \end{aligned}$$

$$\begin{aligned} \left(\frac{\partial Q}{\partial \beta}\right)_{\alpha, \gamma} &= \frac{\partial}{\partial \beta} \left[4 \frac{\alpha \gamma}{(\beta + \alpha \gamma)^2} \right] \\ &= \left[(\beta + \alpha \gamma)^{-2} \times \frac{\partial}{\partial \beta} (4 \alpha \gamma) \right] + \left[4 \alpha \gamma \times \frac{\partial}{\partial \beta} (\beta + \alpha \gamma)^{-2} \right] \\ &= [0] + [-8 \alpha \gamma \times (\beta + \alpha \gamma)^{-3}] \\ &= \frac{-8 \alpha \gamma}{(\beta + \alpha \gamma)^3} \dots (11.7) \end{aligned}$$

$$\begin{aligned} \left(\frac{\partial R}{\partial \beta}\right)_{\alpha, \gamma} &= \frac{\partial}{\partial \beta} \left(\frac{2}{\beta + \alpha \gamma} \right) \\ &= \left(\frac{-2}{(\beta + \alpha \gamma)^2} \times 1 \right) \dots (11.8) \end{aligned}$$

Combining equations 11.6, 11.7 and 11.8

$$\frac{\partial t_{lag}}{\partial \beta} = \left[\frac{-\beta \ln\left(\frac{\alpha \gamma}{\beta}\right) - (\beta + \alpha \gamma)}{\beta(\beta + \alpha \gamma)^2} \right] - \left[\frac{-8 \alpha \gamma}{(\beta + \alpha \gamma)^3} \right] + \left[\frac{-2}{(\beta + \alpha \gamma)^2} \right] \dots (11.9)$$

Differentiating with respect to γ :

$$\begin{aligned}
 \left(\frac{\partial P}{\partial \gamma}\right)_{\alpha, \beta} &= \frac{\partial}{\partial \gamma} \left[\frac{1}{\beta + \alpha \gamma} \times \ln \left(\frac{\alpha \gamma}{\beta} \right) \right] \\
 &= \left\{ \ln \left(\frac{\alpha \gamma}{\beta} \right) \times \frac{\partial}{\partial \gamma} \left(\frac{1}{\beta + \alpha \gamma} \right) \right\} + \left\{ \left(\frac{1}{\beta + \alpha \gamma} \right) \times \left[\frac{\partial}{\partial \gamma} \ln \left(\frac{\alpha \gamma}{\beta} \right) \right] \right\} \\
 &= \left\{ \left(\frac{-\alpha}{(\beta + \alpha \gamma)^2} \right) \times \ln \left(\frac{\alpha \gamma}{\beta} \right) \right\} + \left\{ \left(\frac{1}{\beta + \alpha \gamma} \right) \times \left[\frac{\beta}{\alpha \gamma} \times \frac{\alpha}{\beta} \right] \right\} \\
 &= \left(\frac{-\alpha \ln \left(\frac{\alpha \gamma}{\beta} \right)}{(\beta + \alpha \gamma)^2} \right) + \frac{1}{\gamma(\beta + \alpha \gamma)} \\
 &= \frac{-\alpha \gamma \ln \left(\frac{\alpha \gamma}{\beta} \right) + (\beta + \alpha \gamma)}{\gamma(\beta + \alpha \gamma)^2} \dots\dots\dots(11.10)
 \end{aligned}$$

$$\begin{aligned}
 \left(\frac{\partial Q}{\partial \gamma}\right)_{\alpha, \beta} &= \frac{\partial}{\partial \gamma} \left[4 \frac{\alpha \gamma}{(\beta + \alpha \gamma)^2} \right] \\
 &= \left[\frac{\partial}{\partial \gamma} (4 \alpha \gamma) \times (\beta + \alpha \gamma)^{-2} \right] + \left[4 \alpha \gamma \times \frac{\partial}{\partial \gamma} (\beta + \alpha \gamma)^{-2} \right] \\
 &= [4\alpha (\beta + \alpha \gamma)^{-2}] + [-8 \alpha \gamma \times (\beta + \alpha \gamma)^{-3} \times \alpha] \\
 &= \frac{4\alpha}{(\beta + \alpha \gamma)^2} - \frac{8 \alpha^2 \gamma}{(\beta + \alpha \gamma)^3} \\
 &= \frac{4\alpha (\beta + \alpha \gamma) - 8 \alpha^2 \gamma}{(\beta + \alpha \gamma)^3} \dots\dots\dots(11.11)
 \end{aligned}$$

$$\begin{aligned}
 \left(\frac{\partial R}{\partial \gamma}\right)_{\alpha, \beta} &= \frac{\partial}{\partial \gamma} \left(\frac{2}{\beta + \alpha \gamma} \right) \\
 &= \frac{-2\alpha}{(\beta + \alpha \gamma)^2} \dots\dots\dots(11.12)
 \end{aligned}$$

Combining equations 11.10, 11.11 and 11.12

$$\left(\frac{\partial t_{lag}}{\partial \gamma}\right)_{\alpha, \beta} = \left[\frac{-\alpha \gamma \ln\left(\frac{\alpha \gamma}{\beta}\right) + (\beta + \alpha \gamma)}{\gamma(\beta + \alpha \gamma)^2} \right] - \left[\frac{4\alpha(\beta + \alpha \gamma) - 8\alpha^2 \gamma}{(\beta + \alpha \gamma)^3} \right] - \left[\frac{2\alpha}{(\beta + \alpha \gamma)^2} \right] \dots (A13)$$

$$(2) \left(\frac{df}{dt}\right)_{max}$$

Original equation for $\left(\frac{df}{dt}\right)_{max}$ is given by

$$\left(\frac{df}{dt}\right)_{max} = \frac{\left(\frac{\beta}{\gamma} + \alpha\right)(\beta + \alpha \gamma)}{4} \dots (11.14)$$

Differentiating with respect to α :

$$\begin{aligned} \left(\frac{\partial \left(\frac{df}{dt}\right)_{max}}{\partial \alpha}\right)_{\beta, \gamma} &= \frac{\partial}{\partial \alpha} \left[\frac{\left(\frac{\beta}{\gamma} + \alpha\right)(\beta + \alpha \gamma)}{4} \right] \\ &= \frac{1}{4} \left[\frac{\partial}{\partial \alpha} \left(\frac{\beta^2}{\gamma} + 2\alpha\beta + \gamma\alpha^2 \right) \right] \\ &= \frac{(\beta + \gamma\alpha)}{2} \dots (11.15) \end{aligned}$$

Differentiating with respect to β :

$$\begin{aligned} \left(\frac{\partial \left(\frac{df}{dt}\right)_{max}}{\partial \beta}\right)_{\alpha, \gamma} &= \frac{1}{4} \left[\frac{\partial}{\partial \beta} \left(\frac{\beta^2}{\gamma} + 2\alpha\beta + \gamma\alpha^2 \right) \right] \\ &= \frac{1}{4} \left[\left(\frac{2\beta}{\gamma} + 2\alpha \right) \right] \\ &= \frac{\beta + \alpha \gamma}{2\gamma} \dots (11.16) \end{aligned}$$

Differentiating with respect to γ :

$$\begin{aligned} \left(\frac{\partial \left(\frac{df}{dt} \right)_{max}}{\partial \gamma} \right)_{\alpha, \beta} &= \frac{1}{4} \left[\frac{\partial}{\partial \gamma} \left(\frac{\beta^2}{\gamma} + 2\alpha\beta + \gamma\alpha^2 \right) \right] \\ &= \frac{1}{4} \left[\left(\frac{-\beta^2}{\gamma^2} + \alpha^2 \right) \right] \\ &= \left(\frac{-\beta^2 + \alpha^2 \gamma^2}{4\gamma^2} \right) \dots \dots \dots (11.17) \end{aligned}$$

(3) $t_{1/2 max}$

Original expression of $t_{1/2 max}$ is shown below in Equation 19

$$t_{1/2 max} = \frac{\ln\left(2 + \frac{\alpha\gamma}{\beta}\right)}{(\beta + \alpha\gamma)} \dots \dots \dots (11.18)$$

Differentiating with respect to α :

$$\begin{aligned} \left(\frac{\partial t_{1/2 max}}{\partial \alpha} \right)_{\beta, \gamma} &= \frac{\partial}{\partial \alpha} \left[\frac{\ln\left(2 + \frac{\alpha\gamma}{\beta}\right)}{(\beta + \alpha\gamma)} \right] \\ &= \frac{\partial}{\partial \alpha} \left[\ln\left(2 + \frac{\alpha\gamma}{\beta}\right) (\beta + \alpha\gamma)^{-1} \right] \\ &= \left[\ln\left(2 + \frac{\alpha\gamma}{\beta}\right) \frac{\partial}{\partial \alpha} (\beta + \alpha\gamma)^{-1} \right] + \left[\left\{ \frac{\partial}{\partial \alpha} \ln\left(2 + \frac{\alpha\gamma}{\beta}\right) \right\} (\beta + \alpha\gamma)^{-1} \right] \\ &= \left[\frac{-\gamma \ln\left(2 + \frac{\alpha\gamma}{\beta}\right)}{(\beta + \alpha\gamma)^2} \right] + \left[\left\{ \frac{1}{\left(2 + \frac{\alpha\gamma}{\beta}\right)} \times \left(0 + \frac{\gamma}{\beta}\right) \right\} (\beta + \alpha\gamma)^{-1} \right] \\ &= \left[\frac{-\gamma \ln\left(2 + \frac{\alpha\gamma}{\beta}\right)}{(\beta + \alpha\gamma)^2} \right] + \left[\frac{\gamma}{(2\beta + \alpha\gamma)(\beta + \alpha\gamma)} \right] \dots \dots \dots (11.19) \end{aligned}$$

Differentiating with respect to β :

$$\begin{aligned}
 \left(\frac{\partial t_{1/2 \max}}{\partial \beta}\right)_{\alpha, \gamma} &= \frac{\partial}{\partial \beta} \left[\frac{\ln\left(2 + \frac{\alpha\gamma}{\beta}\right)}{(\beta + \alpha\gamma)} \right] \\
 &= \frac{\partial}{\partial \beta} \left[\ln\left(2 + \frac{\alpha\gamma}{\beta}\right) (\beta + \alpha\gamma)^{-1} \right] \\
 &= \left[\ln\left(2 + \frac{\alpha\gamma}{\beta}\right) \times \frac{\partial}{\partial \beta} (\beta + \alpha\gamma)^{-1} \right] \\
 &\quad + \left[(\beta + \alpha\gamma)^{-1} \times \left\{ \frac{\partial}{\partial \beta} \ln\left(2 + \frac{\alpha\gamma}{\beta}\right) \right\} \right] \\
 &= \left[\frac{-\ln\left(2 + \frac{\alpha\gamma}{\beta}\right)}{(\beta + \alpha\gamma)^2} \right] + \left[\left\{ \frac{1}{\left(2 + \frac{\alpha\gamma}{\beta}\right)} \times \left(0 + \frac{-\alpha\gamma}{\beta^2}\right) \right\} (\beta + \alpha\gamma)^{-1} \right] \\
 &= \left[\frac{-\ln\left(2 + \frac{\alpha\gamma}{\beta}\right)}{(\beta + \alpha\gamma)^2} \right] - \left[\frac{\alpha\gamma}{\beta(2\beta + \alpha\gamma)(\beta + \alpha\gamma)} \right] \dots\dots\dots (11.20)
 \end{aligned}$$

Differentiating with respect to γ :

$$\begin{aligned}
 \left(\frac{\partial t_{1/2 \max}}{\partial \gamma}\right)_{\alpha, \beta} &= \frac{\partial}{\partial \gamma} \left[\frac{\ln\left(2 + \frac{\alpha\gamma}{\beta}\right)}{(\beta + \alpha\gamma)} \right] \\
 &= \frac{\partial}{\partial \gamma} \left[\ln\left(2 + \frac{\alpha\gamma}{\beta}\right) (\beta + \alpha\gamma)^{-1} \right] \\
 &= \left[\ln\left(2 + \frac{\alpha\gamma}{\beta}\right) \frac{\partial}{\partial \gamma} (\beta + \alpha\gamma)^{-1} \right] + \left[(\beta + \alpha\gamma)^{-1} \times \left\{ \frac{\partial}{\partial \gamma} \ln\left(2 + \frac{\alpha\gamma}{\beta}\right) \right\} \right] \\
 &= \left[\frac{-\alpha \ln\left(2 + \frac{\alpha\gamma}{\beta}\right)}{(\beta + \alpha\gamma)^2} \right] + \left[\left\{ \frac{1}{\left(2 + \frac{\alpha\gamma}{\beta}\right)} \times \left(0 + \frac{\alpha}{\beta}\right) \right\} (\beta + \alpha\gamma)^{-1} \right] \\
 &= \left[\frac{-\alpha \ln\left(2 + \frac{\alpha\gamma}{\beta}\right)}{(\beta + \alpha\gamma)^2} \right] + \left[\frac{\alpha}{(2\beta + \alpha\gamma)(\beta + \alpha\gamma)} \right] \dots\dots\dots (11.21)
 \end{aligned}$$

11.2 Method development for CD spectroscopy

The sample preparation method and the choice of buffer system are critical for successful interpretation of the results obtained using CD spectroscopy. In this section the different issues encountered during the standardization of the final protocol used in sections 3.3.6.2 and 3.3.6.3 have been listed. This section is divided into two sub-sections: In the first part, experiments which form the basis for the selection of cuvette are described while the second part investigates the presence of chloride ions on the CD spectra of samples.

11.2.1 Selection of cuvette for FUV scans

The CD signals in the FUV region arise by the absorption by the peptide bonds of the polypeptide chain (Gerrard, 2002; Woody, 1995). A typical FUV spectrum of β -Lg consists of a broad negative trough at approximately 217 nm and a positive trough between 190 to 200 nm (Manderson et al., 1999).

For investigating the unfolding of β -Lg at 80 °C, the sample must be heated in the sample holder. In the early work, 1 mm cuvette was used for recording the scans. A typical spectrum in the FUV region when using this cuvette is shown in Figure 11.2.1.(B). The spectra showed a broad trough at 217 nm as expected, but the positive trough between 190-200 nm was not observed.

To determine whether the loss of positive troughs was due to the type of cuvette used, four different cuvettes with path lengths 0.1 mm, 1 mm, 2 mm and 10 mm were used. The scans using all the cuvettes were recorded at 20°C. The β -Lg concentrations were adjusted with respect to the path length of the cell used for the scan.

Annexures

The scans of unheated native β -Lg at pH 2, recorded in cells of different pathlengths are shown in Figure 11.2.1 All spectra recorded using cells of different path lengths showed the characteristic negative trough at 217 nm, in agreement with the known structure, while the trough at 190 nm was distinct only when a 0.1 mm cuvette was used. The spectra when using 1 and 2 mm cuvettes did not have expected absorption in the 180 to 200 nm range while that for a 10 mm cuvette was difficult to interpret in this range.

To investigate whether or not the loss of the positive troughs for 1 and 2 mm cuvettes was not due to the high absorption by the sample, the HT scans of the above spectra were compared (Figure 11.2.2). The HT curves of cuvettes with path lengths 0.1, 1 and 2 mm were very similar, while that of 10 mm cuvette showed high values < 195 nm. The high tension curves suggest that the loss of troughs at 190 nm in Figure 11.2.1, (B) and (C) were unlikely to be from high sample absorption.

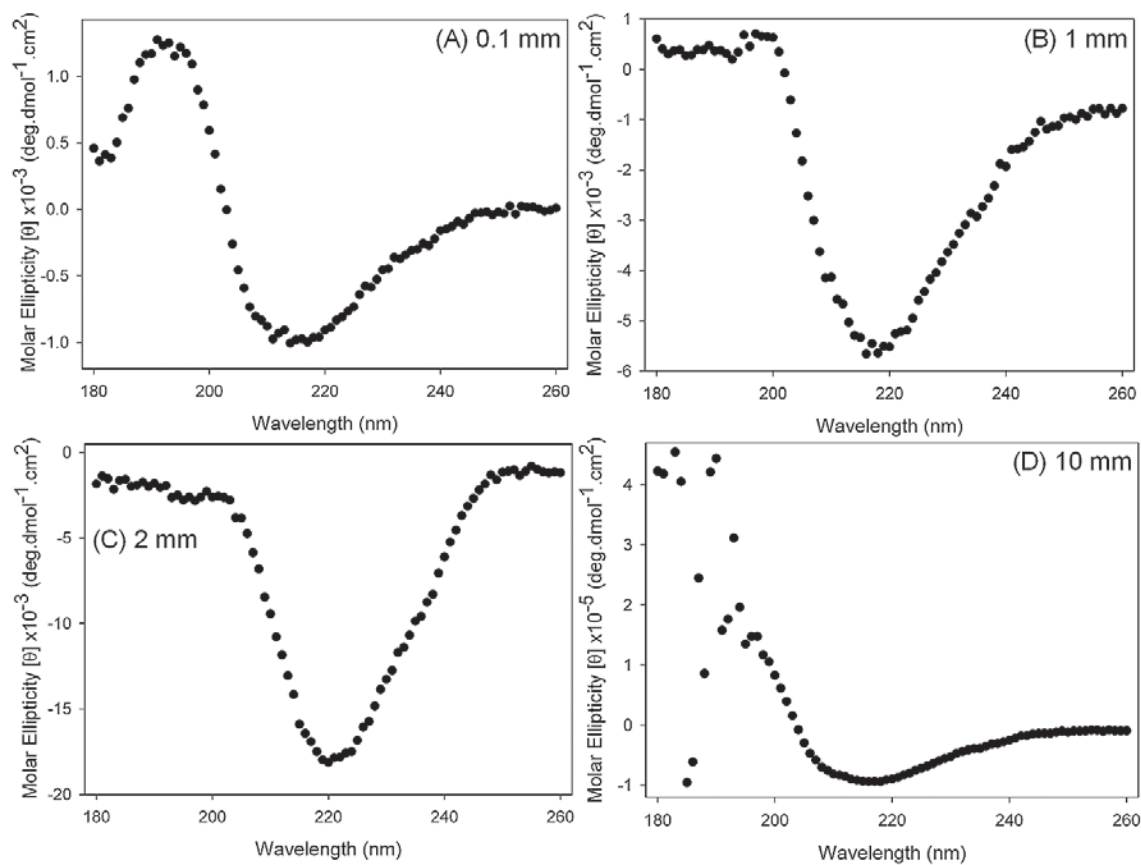


Figure 11.2.1 FUV scans of the unheated β -Lg in cells of different path lengths (A) 0.1 mm, 1 mg/mL; (B) 1 mm, 0.1 mg/mL; (C) 2 mm, 0.15 mg/mL and (D) 10 mm, 0.01 mg/mL. Each spectrum shows un-smoothed and average values from 10 scans at 20°C.

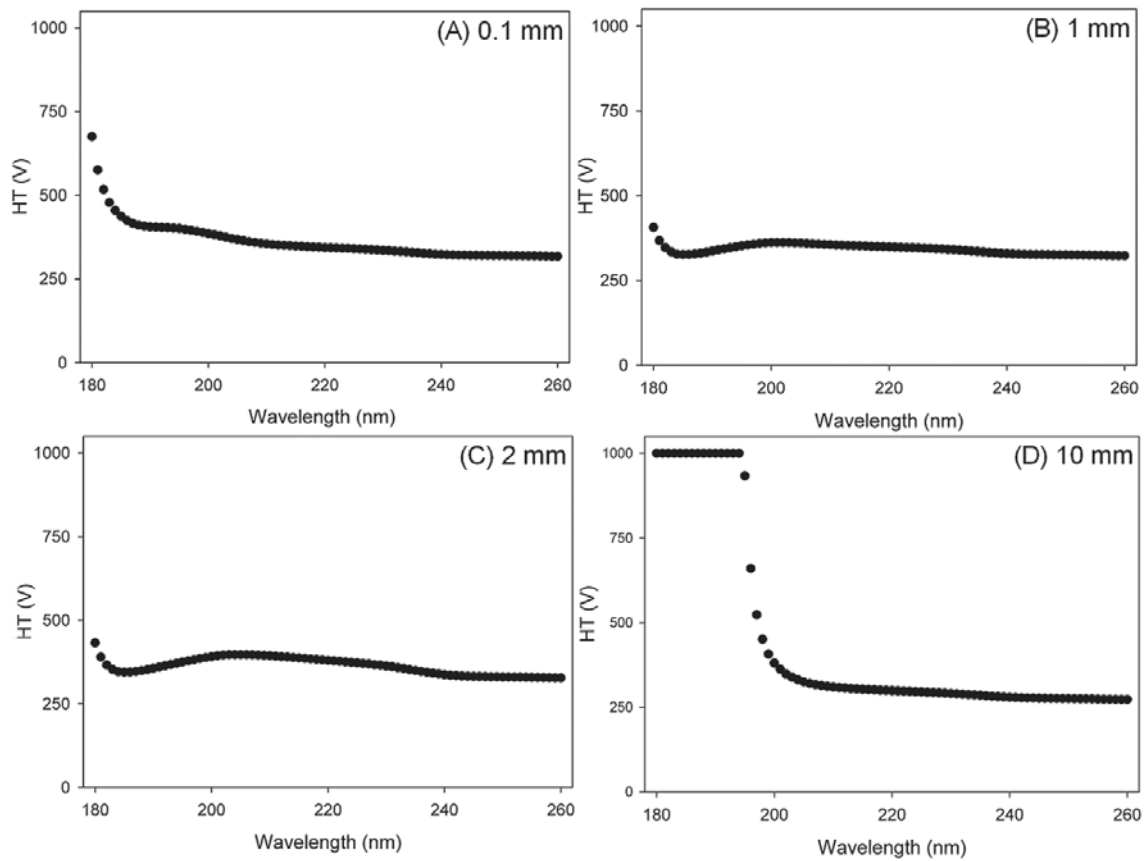


Figure 11.2.2 High Tension curves for the same scans shown in Figure 3.1.1 recorded in cuvettes of different path lengths. The numbers in A to D indicate cell length.

11.2.1 Effect of chloride ions

To determine the origin of the interference at wavelengths <200 nm in the spectra of 10 mm cuvette (Figures 11.2.1 and 11.2.2, D) the spectra of water samples without β -Lg were compared. Figure 11.2.3 shows the spectra of HPLC grade Milli Q water without adjusting pH and after adjusting pH to 2 using 6 M HCl.

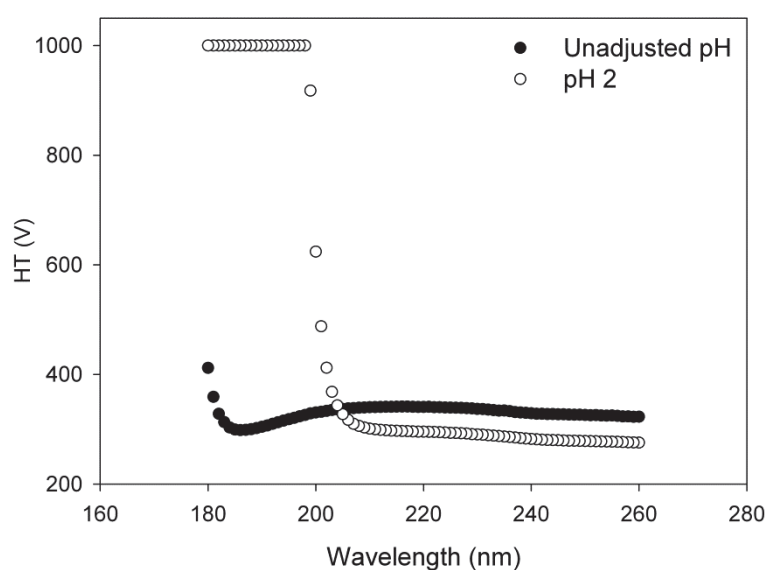


Figure 11.2.3 Comparison of HT curves of Milli Q water spectra before and after adjusting pH to 2 using 6M HCl.

11.2.3 Discussion

From the data in Figures 11.2.1 and 11.2.2, it is clear that the optimum path length for recording FUV scans of the sample is 0.1 mm. This cuvette has an open design requiring the sample to be held in between two separate thin cuvette material slides (Figure 11.2.1). This open design of the sample cell limits its use for specific applications e.g. the open design may result in sample evaporation or leakage during unfolding kinetic studies at high temperatures. The use of sealants to prevent this was not considered since due to their potential instability at higher temperature, difficulties in handling and their effect on the CD signals.

The spectra of 1 and 2 mm were intriguing due to the absence of positive troughs. These are unlikely to arise from the sample since the sample β -Lg sample was used for recording the spectra. The exact reason for this discrepancy is not known. As per the instrument manufacturer, this may result from cuvette-specific effects arising from the differences in the leveling and alignment of these cells in the cell-holder of the instrument.

In comparison, the shape of the FUV spectra recorded using 10 mm cuvette was closer to those obtained by using 0.1 mm cell. However, the samples showed high absorbance in the lower UV range (180-200 nm) due to the chloride ions in the sample which are known to interfere with protein signals in this range (Kelly et al., 2005). Accurate quantification of the spectra using this cuvette is not possible due to unavailability of reliable data in the lower UV range. Based on the data in Figures 3.1.2 and 3.1.3 the cuvette of 10 mm path length was selected for all FUV scans used in the study.

11.3 TEM image of bovine serum albumin solution

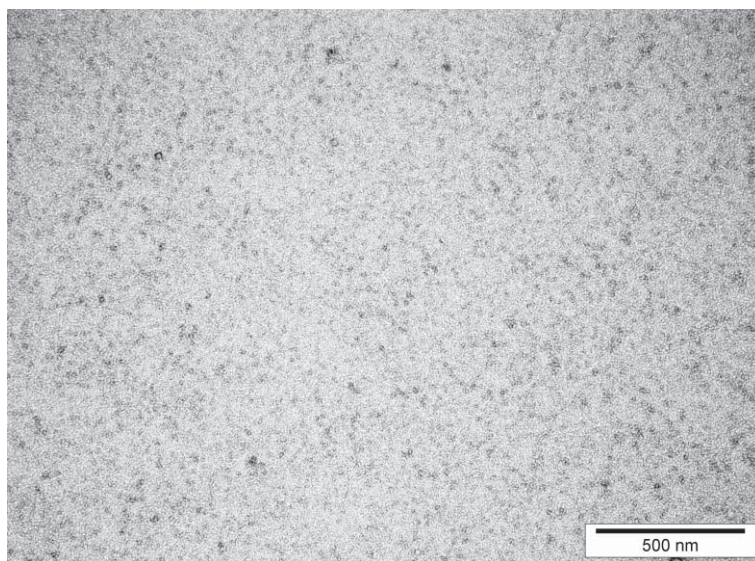


Figure 11.3.1 TEM image of bovine serum albumin solution 0.025% (w/v) solution without any fibrils.

11.4 Proximate composition of salt-extracted β -Lg



MASSEY UNIVERSITY
COLLEGE OF SCIENCES
TE WĀHANGA PŪTAIAO

NUTRITION LABORATORY

TO: Anant Dave

AT: Riddet

SAMPLES: B-
LACTOGLOBULIN

DATE: 22/6/10

TRIAL #: TN10-240

Analysis Report, Final

DATE SAMPLES RECEIVED: 1/6/10

Number of pages in this report: 1

Results are on an as received basis

Sample Name	Protein %	Moisture %	Salt g/100g
B-Lactoglobulin	97.1	3.2	0.166

Nitrogen – protein conversion factor = 6.41

IANZ Approved signatory
Wibha Desai

Methodology

Protein: Leco, total combustion method. AOAC 968.06

Moisture: Convection oven 105 °C, AOAC 930.15, 925.10

Salt: sub-contracted.

Please don't hesitate to contact me if you have any questions.

Please note, although the University has taken all due care in preparing this information in a proper manner, it shall not be liable for any loss or damage incurred by the use of this opinion by persons or organisations.

This report may not be reproduced except in full.

Samples will be discarded one month from date of this report unless otherwise requested by client.

11.5 Peptide sequences in fibrils characterized by in-gel digestion ESI-MS/MS analysis

Table 11.5.1 Peptide sequences of peptide bands A to E (Figure 4.12) in the pellet (12 h) analyzed by ESI-MS/MS after extraction following in-gel digestion with trypsin.

Band	Amino acid sequence of peptides in bands	Seq.	Observed molar mass (Da)	Delta Mass (ppm) ¹	Expect value ²	Ion score
A	(K)VAGTWYSLAMAASDISLLDAQSAPLR(V) ^{a,c}	15-40	2706.3487	-1.46	8.4x10 ⁻¹⁰	131
	(K) IDALNENKVLVL (D) ^b	84-95	1340.7320	-17.20	4.9x10 ⁻⁴	49
B	(K)VAGTWYSLAMAASDISLLDAQSAPLR(V)	15-40	2706.3519	-6.19	4.3x10 ⁻¹⁰	142

Annexures

	V) ^a								11
C	(K)VAGTWYSLAMAASDISLLDAQSAPLR(V)	15-40	2706.3648	-1.41	1.2x10 ⁻⁹	127			
	V) ^{a,c}								
	(M)AASDISLLDAQSAPLR(V)	25-40	1626.8517	-3.69	1.6x10 ⁻²	56			
D	(K)VAGTWYSLAMAASDISLLDAQSAPLR(V)	15-40	2707.3636	0.08	5.5x10 ⁻¹⁰	133			
	V) ^{a,c}								
	(M)AASDISLLDAQSAPLR(V)	25-40	1626.8535	-2.57	2.7x10 ⁻⁵	83			
	(R)VYVEELKPTPE(G)	41-51	1474.7313	-3.16	3.4x10 ⁻³	63			
	(R)VYVEELKPTPEG(D)	41-52	1359.6898	-1.76	2.0x10 ⁻³	64			

Annexures

E	(K)VAGTWYSLAMAASDISLLDAQSAPLR(V) ^{a,c}	15-40	2707.3636	-1.86	4.2×10^{-9}	121
	(R)VYVEELKPTPEGD(L)	41-53	1474.7273	0.94	7.2×10^{-3}	57
	(R)VYVEELKPTPEG(D)	41-52	1359.6935	5.52	5.2×10^{-2}	50

Letters in the parenthesis indicate the amino acids adjacent to the peptides. *a*: de-amidation of glutamine (Q). *b*: Deamination of asparagines (N). *c*: Oxidation of methionine (M). For descriptions of 1 and 2 see footnote for Table 4.3

11.6 ThT fluorescence intensities in heated β -casein samples

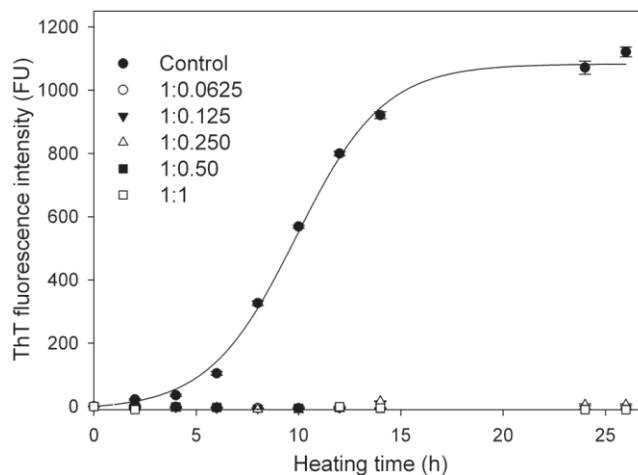


Figure 11.6.1 ThT intensities in β -casein solutions heated at 80°C and pH 2. The control sample of β -Lg without any β -casein is included for comparison. Ratios (β -Lg: β -casein) indicate concentrations (M) of β -casein per mole of β -Lg (for details see Table 8.1, Chapter 8). Error bars represent standard deviations from two separate experiments with two replicates in each. Solid lines represent fit of Equation 3.1.